/
Article / Book Information

（　　）	
Title(English)	Studies on interfacial microenvironments using fluorescent molecules
（　　）	
Author(English)	YUKO HAYASHI
（　　）	：　　　　， ：　　　　　， ：　3511　， ：2001　3　31　， ：　　　， ：
Citation(English)	Degree:Doctor of Science, Conferring organization:　Tokyo Institute of Technology, Report number:　3511　, Conferred date:2001/3/31, Degree Type:Thesis doctor, Examiner:
（　　）	
Type(English)	Doctoral Thesis

Studies on interfacial microenvironments using fluorescent molecules

Chemical Resources Laboratory, Tokyo Institute of Technology

Yuko Hayashi

Contents

Chapter 4   Dicyanoanthracene as a fluorescent probe for studies on microenvironment at silica/fluid interfaces

Chapter 5   Synthesis and fluorescence behavior of calix[4]resorcinarenes possessing pyrenyl group(s)

iv

Chapter 1

General introduction

1-1. Analyses of solid surfaces

Spectroscopic methods have been extensively applied for characterization of solid surfaces including elemental distribution, atomic bonds, atomic configurations, molecular geometries and surface shapes. Predominant methods are listed in Table 1-1.[1-3] They consist of the irradiation of surfaces with an exciting beam to monitor the second beam created from the surfaces. Though the most of them are the methods in vacuum, some enable us to achieve *in-situ* analyses because both probe and sample beams are both of photons. Alternate methods involving microscopes without using exciting beams such as scanning tunneling microscopy (STM), atomic force microscopy (AFM) and so on are used for *in-situ* observation of solid surfaces whose space resolution is of atomic order.[4]

The elucidation of differences in structures and properties between surfaces and bulk layers and of depth profiles of materials plays critical roles in material science and technology. When materials are used for practical applications, the characterizations of topmost surfaces are very important because properties of materials are determined not only by the nature of bulk layers, but also microenvironments including their interfacial regions and depth profiles. For example, corrosion and rust of solids are affected crucially by intermolecular interactions between surface molecules or atoms and contacting atmospheric components. Wettablity depends on molecular level interactions at interfaces between topmost surfaces and fluid layers. Chemical reactivity at solid surfaces in a solution is determined specifically by interactions between surface molecules and solute molecules. Friction and adhesion are phenomena caused by intermolecular interactions between surface residues of a couple of solids.

Performances of composite materials such as fiber-reinforced glasses or plastics as well as polymer alloys are determined not only by bulk's properties but by intermolecular interactions at interfacial regions between two components. Polymer blends or alloys have been widely used commercially on account of their excellent performances and

Table 1-1 Various analytical methods of solid surface

		irradiation beam	observation beam	information
AES	Auger electron spectroscopy	electron	electron	constituent element
EELS	electron energy loss spectroscopy	electron	electron	atom bonding
EPMA(XMA)	electron probe micro analysis	electron	X-ray	elemental distribution
EXAFS	extended X-ray absorption fine structure	X-ray	X-ray	atomic configuration
FEM	field emission microscopy	electric field	electron	atomic configuration
FIM	filed ion microscopy	electric field	ion	atomic configuration
HREELS	high resolution electron energy loss spectroscopy	electron	electron	atom bonding
INS	ion neutralization spectroscopy	ion	electron	atom bonding
IRAS	infrared reflection-absorption spectroscopy	photon	photon	atom bonding
ISS	ion scattering spectroscopy	ion	ion	constituent element, atomic configuration
LEED	low energy electron diffraction	electron	electron	atomic configuration
PAS	photoacoustic spectroscopy	photon	sound	atom bonding
RBS	rutherford backscattering spectroscopy	ion	ion	constituent element
RHEED	reflection high energy electron diffraction	electron	electron	atomic configuration
SAM	scanning Auger microscopy	electron	electron	shape, elemental distribution
SEM	secondaryelectron microscopy	electron	electron	shape
SEM-EDX	SEM - energy dispersive X-ray detector	electron	X-ray	elemental distribution
SERS	surface enhanced Raman spectroscapy	photon	photon	atom bonding
SIMS	secondary ion mass spectroscopy	ion	ion	constituent element
UPS	ultraviolet photoelectron spectroscopy	photon	electron	constituent element, atom bonding
XANES	X-ray absorption near edge structure	X-ray	X-ray	atomic configuration
XPS (ESCA)	X-ray photoelectron spectroscopy	X-ray	electron	elemental distribution, atom bonding,

reliabilities, which are strictly influenced by interfacial structures and properties of component polymers. Polymer blends are produced by molding of melt mixtures of two or more polymers, and most of them have "island-sea" textures. Boundary layers of polymer blends or alloys, in which polymer chains are intertwined as illustrated in Figure 1-1, has specific properties different from original ones of component polymers.[5-7] Despite of a critical role of the boundary regions in displaying practical performances, aspects and structures at these regions have not yet been elucidated in molecular levels.

Interfacial phenomena are also tightly connected with exhibiting versatile functionalities of materials. One of the typical examples is the alignment control of liquid crystals (LCs). It has been known that orientations of LC molecules are actively controlled by photoinduced alterations of chemical properties as well as orientational structures of molecules tethered to substrate surfaces, which are referred to as "command surfaces". For instance, the photoisomerization of azobenzene moieties attached to a surface of a silica plate triggers drastic changes in the orientation a nematic LCs as a consequence of intimate interactions between the surface azobenzene and LC molecules.[8-12] The command surfaces provide versatile modes of the orientational control of LC molecules including the reversible modification of the alignments between homeotropic and planer states, the control of LC directors maintaining homogeneous orientation[10,11] and the control of tilt angles of LC molecules.[12] They are all achieved by photochemical events of functional residues tethered to the topmost surfaces of substrate plates, as shown in Figure 1-2. It should be noted that these kinds of macroscopic phenomena leading to photo-optical effects of LC systems are originated from molecular interactions at interfaces between solid surfaces and LC layers. In this respect, it is highly required to gain detailed information concerning how photosensitive molecules attached to surfaces interact with LC molecules at interfacial regions.

The two representative examples mentioned above suggest the significances of approaches to molecular-level understandings of interactions at interfaces between solids and solid or fluid layers. The following factors may be extracted in order to perform studies on molecular interactions at interfaces. The first is microenvironmental conditions such as polarity of interfacial regions, because the estimation of surface energies at boundary regions gives a clue to reveal relationship between material performances and the
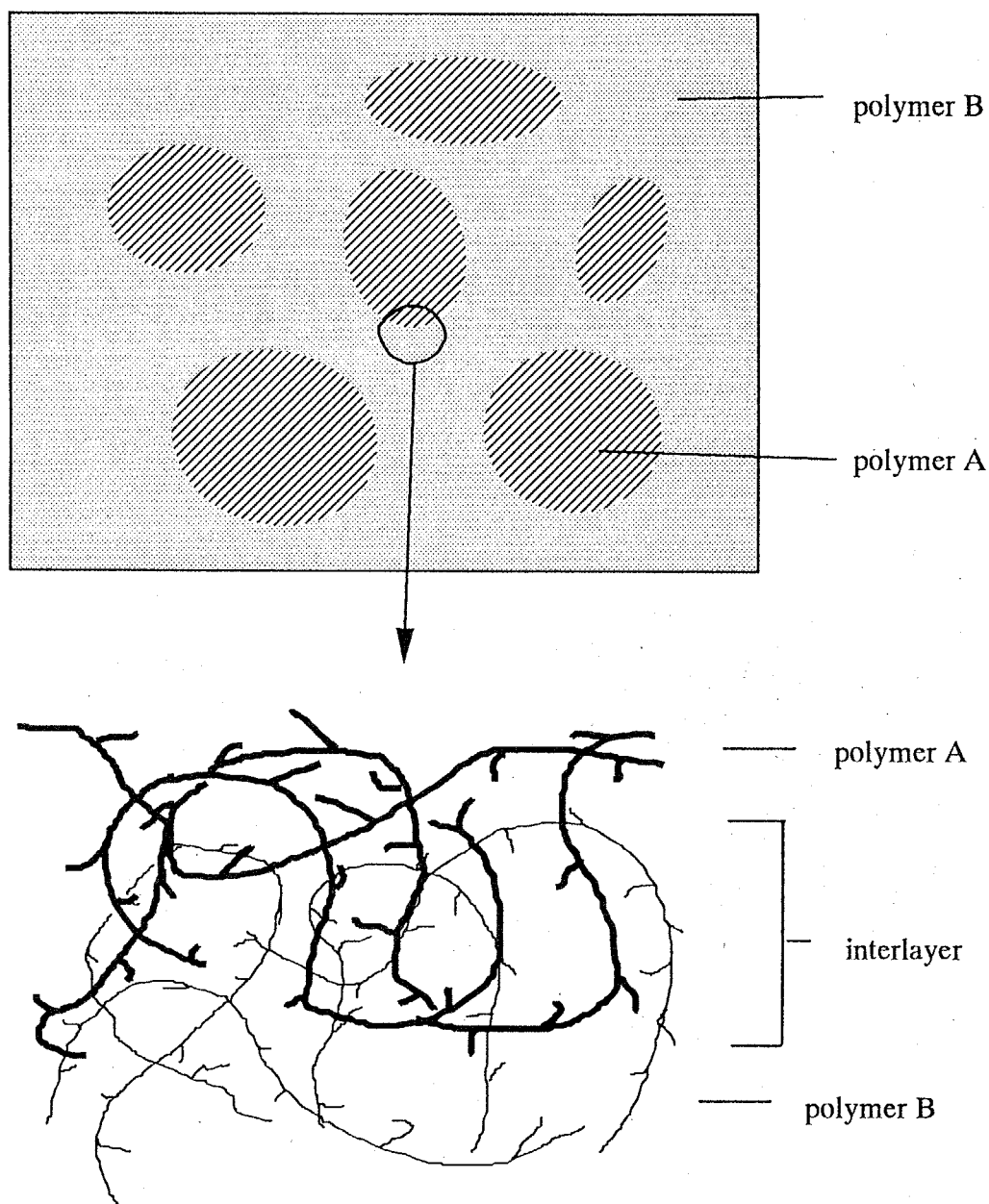
Figure 1-1. "Island-sea structure" of a polymer blend (polymer A and Polymer B)

(a)

liquid crystal

hv1

hv2

photoreactive molecule

(b)

liquid crystal

polarized light

photoreactive molecule

(c)

hv
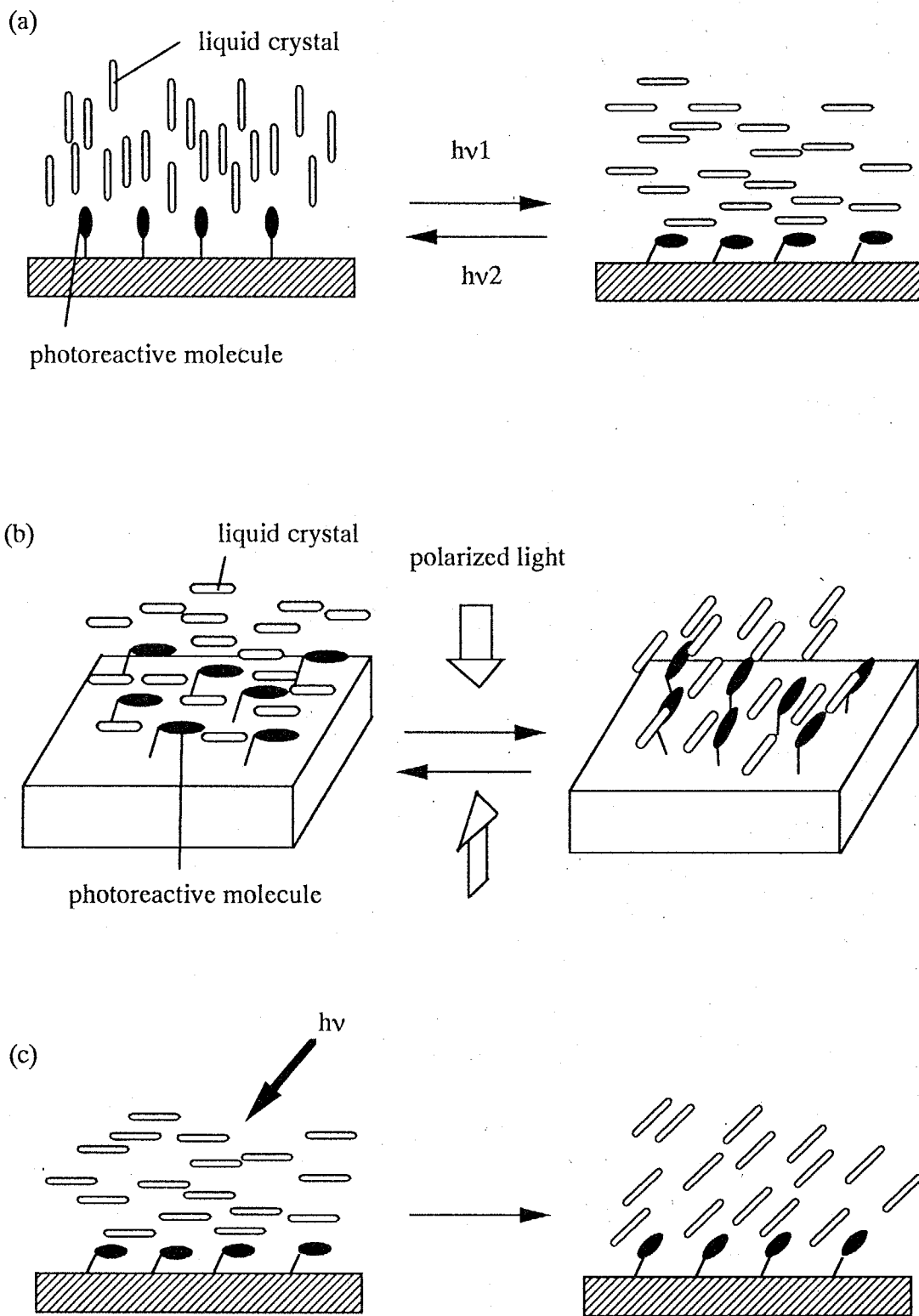
Figure 1-2. "Command surface" (a) homeotropic to planer and planer to homeotropic controlled by light of different wavelength   (b) homogenious planer controlled by linear polarized light (c) tilt angle controll

nature of components. The second consists of the elucidation of molecule-to-molecule interactions at interfaces. They involve conformational orientations of component molecules as a result of interactions, distribution of component molecules, the nature of molecular interactions, dynamics of the interactions and so forth.

In order to obtain information concerning these factors, *in-situ* measurements of interfacial regions in molecular levels are necessary. Furthermore, the measurements should be better done in non-destructive manners, whereas extremely high sensitivity in measurements is a prerequisite condition simply because the concentration of molecules participating in interfacial phenomena is quite small. In this respect, analyses on the basis of interactions of photons with molecules are excellent, since they are non-destructive with high sensitivity and specific to each component molecule owing to the principle of light absorption to give rise to spectroscopic information. Spectroscopic methods applicable to studies on interfaces involve UV-visible absorption spectroscopy, IR absorption spectroscopy, Raman spectroscopy and fluorescence spectroscopy. The have been in fact employed extensively for investigations of ultra-thin layers such as Langmuir-Blodgett films, monolayers deposited on solid surfaces. SFG (sum frequency generation) [13] and SERS (surface enhanced Raman spectroscopy) [14] are suitable for structural elucidation of well-orientated surface molecules, but there is still a problem because of relatively low sensitivity.

The efforts of the present author have been focused on the applicability of the fluorescence spectroscopy to revealing interfacial phenomena to discuss molecular interactions at boundary regions, taking notice of the facts that the fluorescent probe method is highly sensitive and very suitable for studies on microenvironments and intermolecular interactions. In this context, the fluorescent probe method is surveyed in the next section.

1-2. Fluorescence measurements of ultra-thin layers

Spectroscopic properties of fluorescent moieties, which are called sometimes fluorophores, are significantly influenced by the nature of media, where they exist, as a result of interactions of a fluorophore with surrounding molecules at its ground state as well as its excited singlet state. This situation provides the novel way to probe molecular

interactions by using fluorophores because their emission behavior reflects microenvironments consisting of polarity, rigidity, orientation, the nature of non-covalent bonds and so on. In this context, fluorophores as reporter molecules to give information about microenvironmental conditions are called fluorescent probes. Multiple fluorescent probe molecules have been developed so far for specific purposes. Representative studies are shown below to bring the significance of this method into relief.

Fluorescent probe moieties incorporated in Langmuir-Blodgett films as well as self-assembled molecular films (SAMs) give information about microenvironmental conditions in these ultra-thin films. Moreover, when ultra-thin films are divided into small areas to monitor emission intensity of a fluorescent probe at each area, maps of the fluorescence can be obtained to reveal spatial distribution of the molecules.[15-20] In cases where fluorescent probe molecules form aggregates, the mapping of emission of both monomeric and aggregated fluorophore have been performed.[21-24] The fluorescent probe method is also suitable for real time observation of interfacial phenomena. For example, adsorption and desorption of fluorescent molecules on electrodes generated by electric current switching was reported.[25] Because of extremely high sensitivity in fluorescence measurements, the fluorescent probe method was conveniently applied even for monomolecular layers at air/water interface to follow changes in molecular distributions during expansion and compression.[26] Two-dimensional energy transfer [27] and electron transfer [28] in monomolecular layers deposited on solids were also studied by means of the fluorescent probe method. Phase separation of a polymer blend was directly monitored by measuring fluorescence decay time to make an imaging map on the basis of the fact that emission decay time depends on efficiencies of energy transfer from one polymer bearing fluorophore residues to the other polymer with chromophoric residues which are able to absorb the fluorescence.[29]

The present method is also applied to studies on solid surfaces. In case of liquid crystal (LC) cells with alkylated cyanobiphenyls as LC molecules, it was found that the alkyl chain length at *para*-position of cyanobiphenyl determines the dependence of aggregation of the mesogenic molecules on the nature of substrates and deposition conditions of the molecules.[30,31] On account of fluorescence behavior of alkylated cyanobiphenyls as LC molecules, molecular information is obtained about substrate

surfaces covered with the mesogenic molecules. Since cyanobiphenyl as a fluorophore exhibits excimer emission as a result of the formation of a complex between an excited single state molecule and a ground state molecule, thin films of cyanobiphenyls can be figured out by ratios of emission intensity of monomer and the corresponding excimer. As another example, photodimerization process of anthryl groups in SAM on gold to form monolayered photoimages was also studied with fluorescence spectra because monomeric anthracene emits strong fluorescence.[32]

P. de Mayo and W. R. Ware et. al. studied adsorption behavior of fluorescent probe molecules on silica gel to reveal its surface properties.[33-40] It was pointed out by measurements of photochemical reaction rates and fluorescence lifetimes of the probe molecules that a silica gel surface is not homogeneous, but rather comprised of several sites, which memorize preparation conditions of the silica including baking as well as washing with an acid.

M. L. Hunnicutt et. al.[41-47] and J. M. Harris et. al.[48-52] reported fluorescent behavior of pyrenyl derivatives covalently bound on silica gels. Pyrenylalkyldimethylchlorosilanes were reacted with silica gels to measure fractions of excimer emission in monolayers on the silica, leading to the implication of the existence of clusters of pyrene moieties on the silica surface. Measurements of fluorescence lifetime indicate that the co-modification of silica gel with alkylsilane influences the level of aggregation of the pyrene. Exciplex formation between pyrene as a fluorophore and N,N-dimethylaniline, which is also attached to the silica surface, gives novel information about microenvironmental polarity on solid surfaces.[43]

J. K. Thomas et. al. prepared 4-pyrenylbutyltrimethylammonium salt and pyrenylbutyric acid as adsorbents on surfaces of inorganic solids such as clay, calcium oxide, alumina, zeolite, silica and so on.[53-61] Studies on dynamics of pyrene fluorescence, which is sensitive to molecular environments and the nature of solid surfaces, revealed the involvement of inorganic solid surfaces in photophysical quenching of pyrene fluorescence. They also described that the pyrene fluorescence is significantly affected by thin films of polymers coated on solids adsorbing pyrenyl derivatives to suggest that poly(methyl methacrylate) chains interact with silanols on silica surface through hydrogen bond formation. A noteworthy approach was presented by study on picosecond time-

resolved total internal reflection fluorescence to reveal that molecular motions of solute molecules are restricted at a solid/liquid interface.[62-66]

The representative studies cited above support that the fluorescent probe method is very attractive to reveal phenomena at solid/fluid, solid/liquid crystal and solid/solid interfaces. The usefulness of the fluorescence probe technique can be summarized as follows. First, fluorescence can be detected with extremely high sensitivity so that fluorescent probes give information of monolayered or even sub-monolayered films at interfaces. Second, the emission of fluorophores provides versatile molecular information on the basis of the following factors including the dependence of fluorescence wavelength of polarity of media, the formation of excimer as well as exciplex, quenching by appropriate molecules, the effect of fluorescence lifetimes and decay modes on circumstances, the relaxation of orientational direction of fluorophores. Thirdly, fluorescence measurements provide non-destructive approaches to reveal interfacial phenomena, because usually fluorescent probes do not suffer from photodegradation during the measurements.

1-3. Surface modifications with functional groups

The modification of solid surfaces is carried out by adsorption of organic molecules through covalent bonds or non-covalent bonds. One of the typical ways of the covalent bonding is the silylation reacting of molecules bearing silyl units with silanols at a silica surface.[31-52] Structures of silylated surfaces depend on chemical structures of silylating units. Monoalkoxysilanes or monochlorosilanes with one reactive group form molecular layers exhibiting brush- or comb-like structures, whereas polymeric structures with crowded and multilayered films are fabricated when silylating units possess two or three reactive groups such as dialkoxysilanes and trichlorosilanes.[45,46] On the other hand, the adsorption through non-covalent bonds is achieved by coulombic interactions,[53-61] van der Waals forces [33-40] and hydrogen bonds. As one of the examples of non-covalent adsorption, SAMs are formed by adsorption of amphiphilic compounds on gold when a substrate is immersed in a solution of the compounds.[67,68] Because an adsorption force through non-covalent bonds is much weaker when compared with covalent methods, it is convenient to introduce multi-site of polar heads to a single amphiphilic molecule to result

in multi-point adsorption to enhance adsorptivity.

This thesis employs the following two methods to modify a silica surface with fluorescence molecules; silylation as the chemisorption and non-covalent multi-site adsorption. For the latter procedure, calix[4]resorcinarenes (CRAs) derivatives are used here.[69-73]

1-4. Calix[4]resorcinarenes as adsorbates

CRA has a cyclic structure as shown in Figure 1-3(a). CRAs are have been attracting interest from a viewpoint of host-guest chemistry to achieve molecular recognition.[74-79] CRAs are ready prepared by the acid-catalyzed cyclic tetramerization of resorcinol with aldehyde.[80-82] The crown conformer shown in Figure 1-3(b) is the most thermodynamically stable isomer among the others isomers including partial cone alternate and 1,3-partial alternate, leading to good availability.[83-86] Hydrophobic tails at the upper rim of the crown type CRA can be modified by versatile functional groups, whereas eight phenolic OH groups at the upper rim can be also transformed into any functional groups.[69-73]

In the crown conformer, all of four substituents at the methylene bridge linking resorcinol moieties are tethered from the upper rim of the cylindrical structure in the same direction so that it is reasonable to regard the molecules as a fragmented model of two-dimensionally self-assembled monolayers formed on solid surfaces. By immersing silica in a crown-type CRA derivative solution, CRA molecules adsorb on polar surfaces to form a densely packed monolayer through multi-point adsorptivity.[71] Hydrophobic tails of CRA stretch out from solid surfaces owing to its rigid cyclic structure. This situation leads to photoinduced changes of surface properties so that the surface adsorption of a CRA having four azobenzene residues on colloidal silica particles results in the photocontrol of dispensability of the particles in organic solvents.[69] The adsorptivity of CRAs possessing phenolic OH groups, alcoholic OH groups and carboxyls as polar heads has been also studied.[72]

1-5. The outline and purpose of this thesis

The present work has been performed, focusing on the followings. The first is to
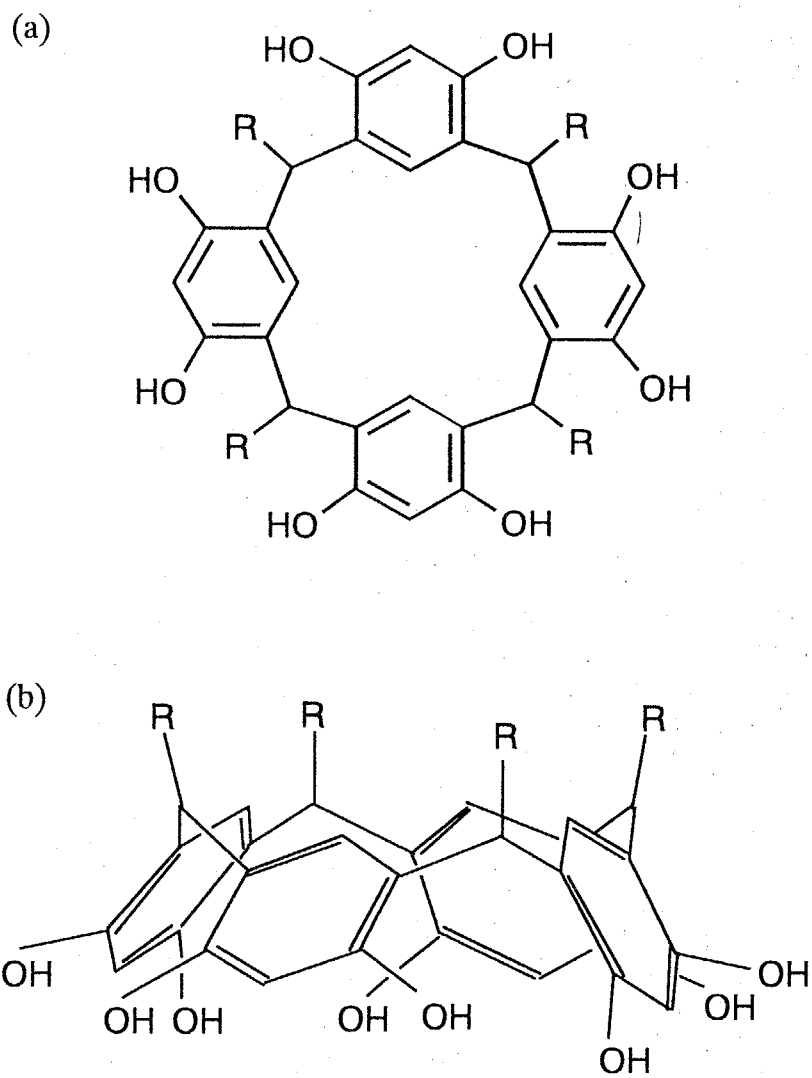
(a)

(b)

Figure 1-3. Structure of calix[4]resorcinarene (a) and steric view of the crown conformer (b)

11

display a model system for command surfaces consisting of photoactive molecular surfaces and liquid crystal layers to reveal microenvironments at boundary regions. The second is to present a model system for interfacial regions between two kinds of polymer solids exemplified by island-sea structures of polymer blends. The last is to provide a method for the modification of hydrophilic surfaces with CRAs to give SAMs with enhanced desorption resistance.

Cyanobiphenyl is a typical mesogenic unit, which emits strong fluorescence and form excimer. In this context, in chapter 2, cyanobiphenyl is adsorbed covalently by silylation to modify a silica plate surface to give a model of a command surface to characterize properties of surface molecules in the presence of a liquid crystal layer in comparison with the same molecules dissolved in a solution.

Based on the results described in chapter 2, chapter 3 deals with the effect of the orientation of surface cyanobiphenyls on the ways to attach the fluorescent moieties. The methods for the introduction of the fluorescent probe molecules are silylation and multi-site adsorption of a CRA, both of which possess cyanobiphenyl unit(s). Fluorescent measurements of surface cyanobiphenyls suggested that molecular reorientation of the fluorophore residues upon contact with a liquid crystal layer is critically influenced by the attachment methods of the surface molecule.

9,10-Dicyanoanthracene was used in chapter 4 as a fluorescent probe to shed light into interfacial interactions between a silica surface and a polymer solution as a model of polymer blend interface. The fluorescent molecules were introduced on silica surfaces through silylation to monitor microenvironmental polarity at a silica surface. The silica plate surface-modified with the fluorophore molecules was also useful for revealing interfacial phenomena between two layers. The first observation was made on exciplex emission between the surface-modified silica plate and a polymer bearing phenanthrene side chains.

Chapter 5 describes the preparation and characterization of novel CRA derivatives possessing different numbers of pyrenyl moieties, aiming at the development of novel fluorescent probe molecules capable of controlling molecular density of the fluorophore in molecular films. Particular interest was focused in this chapter on fluorescence behavior of the CRAs bearing pyrenyl groups in solutions.

Chapter 6 presents a novel system exhibiting exciplex emission at an interface between a colloidal silica surface covered with the CRA with a single pyrene unit and polymethacrylate bearing N,N-dimethylaniline. The emission behavior was markedly influenced by preparative conditions of samples so that the validity of the system as a model for island-sea textures of polymer blends will be discussed.

The major concern of chapter 7 is to propose a novel method to enhance desorption resistance of CRAs onto a silica surface by a photochemical way. Cinnamate groups were introduced to the tail part of CRA as a photodimerizable unit to form SAMs on a silica surface through the multi-site adsorption. UV irradiation of a silica plate modified with the photosensitive SAM resulted in the enhancement of desorption resistance because of intermolecular photodimerization leading to increase adsorption points of one adsorbent.

Chapter 8 describes the summery of the present work.

References

1. K Furuya, *Hyomen*, 1981, **19**, 673.

2. S. Nakamura, *Hyomen*, 1982, **20**, 207.

3. K. Seki, *Hyomen*, 1991, **29**, 460.

4. R. J. Behm, *Atomic Phys.* 1989, **11**, 555.

5. O. Olabisi, L. M. Robeson, and M. T. Shaw, *"Polymer-Polymer Miscibility"*, Academic Press, New York, 1979, Chap. 3

6. T. Inoue and S. Ichihara, *"Polymer Alloy"*, Kyouritsu-shuppan, Tokyo, 1988,

7. T. A. Vilgis and J. Noolandi, *Makromol, Chem., Macromol. Symp.*, 1988, **16**, 225

8. K. Ichimura, *"Photochromic polymers, Polymers as electrooptical and photooptical active media"* ed. by V. Shibaev, Springer-Verlag, 1996, 138.

9. K. Ichimura, Y. Suzuki, T. Seki, A. Hosoki and K. Aoki, *Langmuir*, 1988, **4**, 1214.

10. Y. Kawanishi, T. Tamaki, M. Sakuragi, T. Seki and K. Ichimura, *Langmuir*, 1992, **8**, 2061.

11. K. Ichimura, Y. Akita, H. Akiyama, Y. Hayashi and K. Kudo, *Jpn. J. Appl. Phys.*, 1996, **35**, L996.

12. K. Ichimura, S. Morino and H. Akiyama, *Appl. Phys. Lett.*, 1998, **73**, 92.

13. K. B. Eisenthal, *Chem. Rev.*, 1996, 96, 1343.

14. A. Otto, *Appl. Surf. Sci.*, 1980, **6**, 309.

15. M. Fujihira, H. Monobe, H. Muramatsu and T. Akita, *Ultramicroscopy*, 1995, **57**, 118.

16. H. Fukushima, D. M. Taylor, H. Morgan, H. Ringsdorf and E. Rump, *Thin Solid Films*, 1995, **266**, 289.

17. V. B. Ivanov, J. Behnisch, A. Hollaender, F. Mehdorn and H. Zimmermann, *Surface and Interface Anlysis*, 1996, **24**, 257.

18. T. L. Calvert and D. Leckband, *Langmuir*, 1997, **13**, 6737.

19. J. Buijs, D. W. Britt and V. Hlady, *Langmuir*, 1998, **14**, 335.

20. C. K. Park, F. J. Schmitt, L. Evert, D. K. Schwartz, J. N. Israelachvili and C. M. Knobler, *Langmuir*, 1999, **15**, 202.

21. K. Fujita, Y. Orihashi and A. Itaya, *Thin Solid Films*, 1995, **260**, 98.

22. H. Saijo and M. Shiojiri, *J. Crystal Growth*, 1995, **153**, 31.

23. K. Asaia, T. Watanabe, D. Hiroishia, K. Ishigurea and T. Satoa, *Thin Solid Films*, 1996,

283, 124.

24. E. Mubarekyan and M. Santore, *Langmuir*, 1998, **14**, 1597.

25. D. Bizzotto and B. Pettinger, *Langmuir*, 1999, **15**, 8309.

26. M. Kawaguchi, M. Yamamoto, N. Kurauchi and T. Kato, *Langmuir*, 1999, **15**, 1388.

27. B. Choudhury, A. C. Weedon and J. R. Bolton, *Langmuir*, 1998, **14**, 6199.

28. B. Choudhury, A. C. Weedon and J. R. Bolton, *Langmuir*, 1998, **14**, 6192.

29. J. H. Hsu, P. K. Wei, W. S. Fann, K. R. Chuang and S. A. Chen, *Ultramicroscopy*, 1998, **71**, 263.

30. A. Itaya, K. Watanabe, T. Imamura and H. Miyasaka, *Thin Solid Films*, 1997, **292**, 204.

31. A. Itaya, T. Imamura, M. Hamaguchi, Y. Tsuboi, H. Miyasaka, T. Asahi and H. Masuhara, *Thin Solid Films*, 1997, **311**, 277.

32. M. A. Fox and M. D. Wooten, *Langmuir*, 1997, **13**, 7099.

33. K. Hara, P. de Mayo, W. R. Ware, W. A. C. Weeden, G. S. K. Wong and K. C. Wu, *Chem. Phys. Lett.*, 1980, **69**, 105.

34. R. K. Bauer, R. Borenstein, P. de Mayo, K. Okada, M. Rafalska, W. R. Ware and K. C. Wu, *J. Am. Chem. Soc.*, 1982, **104**, 4635.

35. R. K. Bauer, P. de Mayo, W. R. Ware and K. C. Wu, *J. Phys. Chem.*, 1982, **86**, 3781.

36. R. K. Bauer, P. de Mayo, K. Okada, W. R. Ware and K. C. Wu, *J. Phys. Chem.*, 1983, **87**, 460.

37. R. K. Bauer, P. de Mayo, L. V. Natarajan and W. R. Ware, *Can. J. Chem.*, 1984, **62**, 1279.

38. P. de Mayo, L. V. Natarajan and W. R. Ware, *Chem. Phys. Lett.*, 1984, **107**, 187.

39. P. de Mayo, L. V. Natarajan and W. R. Ware, *J. Phys. Chem.*, 1985, **89**, 3526.

40. P. de Mayo, L. V. Natarajan and W. R. Ware, *ACS Symp. Ser.*, 1985, **278**, 1.

41. C. H. Lochmüller, A. S. Colborn, M. L. Hunnicutt and J. M. Harris, *Anal. Chem.*, 1983, **55**, 1344.

42. C. H. Lochmüller, A. S. Colborn, M. L. Hunnicuttand and J. M. Harris, *J. Am. Chem. Soc.*, 1984, **106**, 4077.

43. C. H. Lochmüller, M. T. Kersey and M. L. Hunnicutt, *Anal. Chim. Acta*, 1985, **175**, 267.

44. C. H. Lochmüller and M. J. Hunnicutt, *J. Phys. Chem.*, 1986, **90**, 4318.

45. C. H. Lochmüller, M. M. Thompson and M. T. Kersey, *Anal. Chem.*, 1987, **59**, 263.

46. C. H. Lochmüller and M. T. Kersey, *Anal. Chem.*, 1988, **60**, 1910.

47. C. H. Lochmüller and M. T. Kersey, *Langmuir*, 1988, **4**, 572.

48. M. L. Hunnicutt, J. M. Harris and C. H. Lochmüller, *J. Phys. Chem.*, 1985, **89**, 5246.

49. A. L. Wong, J. M. Harris and D. B. Marshall, *Can. J. Phys.*, 1990, **68**, 1027.

50. A. L. Wong, M. L. Hunnicutt and J. M. Harris, *J. Phys. Chem.*, 1991, **95**, 4489.

51. A. L. Wong and J. M. Harris, *J. Phys. Chem.*, 1991, **95**, 5895.

52. A. L. Wong, M. L. Hunnicutt and J. M. Harris, *Anal. Chem.*, 1991, **63**, 1076.

53. R. A. DellaGuardia and J. K. Thomas, *J. Phys. Chem.*, 1983, **87**, 3550.

54. P. Hite, R. Kransansky and J. K. Thomas, *J. Phys. Chem.*, 1986, **90**, 5795.

55. S. Pankasem and J. K. Thomas, *J. Colloid Interface Sci.*, 1988, **126**, 231.

56. J. Wheeler and J. K. Thomas, *Langmuir*, 1988, **4**, 543.

57. R. Kransansky, K. Koike and J. K. Thomas, *J. Phys. Chem.*, 1990, **94**, 4521.

58. S. Pankasem and J. K. Thomas, *J. Phys. Chem.*, 1991, **95**, 7385.

59. M. A. Marro and J. K. Thomas, J. K. *J. Photochem. Photobio.*, 1993, **A72**, 251.

60. X. Liu and J. K. Thomas, *Langmuir*, 1993, **9**, 727.

61. E. H. Ellison and J. K. Thomas, *Langmuir*, 1996, **12**, 1870.

62. A. Itaya, *Hyomen*, 1992, **30**, 138.

63. M. Yanagimachi, N. Tamai and H. Masuhara, *Chem. Phys. Lett.*, 1992, **200**, 469.

64. M. Yanagimachi, N. Tamai and H. Masuhara, *Chem. Phys. Lett.*, 1993, **201**, 115.

65. S. Hamai, N. Tamai, and H. Masuhara, *Chem. Lett.*, 1993, 1105.

66. S. Hamai, N. Tamai and H. Masuhara, *Chem. Phys. Lett.*, 1993, **213**, 407.

67. H. Schneider, D. Guttes and U. Schneider, *Angew. Chem. Int. Ed. Engl.*, 1986, **25**, 647.

68. W. Li, V. Lynch, H. Thompson and M. A. Fox, *J Am. Chem. Soc.*, 1997, **119**, 7211.

69. M. Ueda, N. Fukushima and K. Ichimura, *J. Mater. Chem.*, 1995, **5**, 1007.

70. M. Ueda, N. Fukushima, K. Kudo and K. Ichimura, *J. Mater. Chem.* 1997, **7**, 641.

71. K. Ichimura, N. Fukushima, M. Fujimaki, S. Kawahara, Y. Matsuzawa, Y. Hayashi and K. Kudo, *Langmuir*, 1997, **13**, 6780.

72. E. Kurita, N. Fukushima, M. Fujimaki, Y. Matsuzawa, K. Kudo and K. Ichimura, *J. Mater. Chem.*, 1998, **8**, 397.

73. M. Fujimaki, S. Kawahara, Y. Matsuzawa, E. Kurita, Y. Hayashi and K. Ichimura,

Langmuir, 1998, **14**, 4495.

74. H. Schneider, D. Guttes and U. Schneider, *Angew. Chem. Int. Ed. Engl.*, 1986, **25**, 647.

75. B. Dhawan, S. I. Chen and C. D. Guttes, *Macromol. Chem.* 1987, **188**, 921.

76. Y. Aoyama, Y. Tanaka and S. Sugahara, *J. Am. Chem. Soc.*, 1989, **111**, 5397.

77. K. Kurihara, K. Ohta, Y. Tanaka, Y. Aoyama and Y. Kunitake, *Thin Solid Films*, 1989, **179**, 21.

78. K. Kurihara, K. Ohta, Y. Tanaka, Y. Aoyama and Y. Kunitake, *J. Am. Chem. Soc.*, 1991, **113**, 444.

79. D. Cram, *Nature*, 1992, **356**, 29.

80. J. B. Niederl and H. J. Vogel, *J. Am. Chem. Soc.*, 1940, **62**, 2512.

81. C. D. Guttes, B. Dhawan, K. H. No and R. Muthukrishnan, *J. Am. Chem. Soc.*, 1981, **103**, 3782.

82. H. Schneider, C. D. Guttes and U. Schneider, *Angew. Chem. Int. Ed. Engl.*, 1986, **25**, 647.

83. A. G. S. Hogberg, *J. Org. Chem.*, 1980, **45**, 4498.

84. A. G. S. Hogberg, *J. Am. Chem. Soc.*, 1980, **102**, 6046

85. L. Abis, E. Dalcanale, A. Du vosel and S .Spera, *J. Org. Chem.*, 1988, **53**, 5475.

86. A. G. S. Hogberg, *J. Am. Chem. Sci.*, 1989, **111**, 5397.

Chapter 2

Fluorescence behavior of cyanobiphenyl groups chemisorbed on a silica surface in the presence of liquid crystals

2-1. Introduction

In this chapter, a binary system consisting of a silica plate surface-modified with fluorescent probe molecules and a liquid crystal (LC) layer is designed to reveal microenvironments and interfacial molecular interactions of the solid surface molecule with LCs, to present a model system for "command surfaces", which are active for the photocontrol of LC alignment, as discussed in chapter 1.[1-6] The working principle of the command surfaces has been interpreted as a result of the specific interaction of surface photoisomerizable units like azobenzenes with nearest neighbor liquid crystal molecules. The reorientation of mesophasic molecules is triggered by the photoinduced structural change of surface molecules to lead to the alignment alteration of the whole mesophase layer. This interpretation coincides with a previous report that a substrate surface can impose the orientation of the whole liquid crystal phase without any orienting field.[7,8] The molecular orientation of liquid crystals at a boundary region has been elucidated by means of second harmonic generation spectroscopy which gives precious information on the molecular orientation of liquid crystals on solid surfaces.[9-11] However, dynamic processes of conformational change of surface molecules upon contact with liquid crystal molecules have not yet been revealed except the alteration of electronic absorption spectra of monolayer surface azobenzenes upon contact with liquid crystals.[12]

The strategy to obtain information concerning molecular interactions of surface residues with mesophasic molecules is based on the modification of a substrate surface with a fluorescent probe to detect the perturbation of its emission upon contact with liquid crystals. In this chapter, cyanobiphenyl moiety is employed as a fluorophore to bind covalently on a silica surface to show the specific molecular interaction with liquid crystal molecules at an interface by means of steady state fluorescence measurement. Since some cyanobiphenyl derivatives with long carbon chain are liquid crystals themselves, the

solid surface cyanobiphenyl units with nematic liquid crystals are considered to behave like as "command surface".

For the modification of a silica surface, N-(3-dimethylethoxysilylpropyl)-6-(4-cyanobiphenyl-4'-oxy)hexanamide was prepared to obtain information about molecular interactions between surface moieties and liquid crystal molecules by monitoring changes in emission ratios of monomer and excimer of the cyanobiphenyl. To prove the advantage of cyanobiphenyl moiety as a probe for interfacial microenvironment, a compound whose fluorescent unit is 1-pyrenyl group was also prepared.

2-2. Experimental

2-2-1. Materials

N-(3-dimethylethoxysilylpropyl)-6-(4- cyanobiphenyl-4'-oxy)hexanamide (**1**) was synthesized as shown in Scheme 2-1. Two model compounds are also shown in the same scheme. Nematic liquid crystals were kindly donated by Rodic Co., and their structures are shown in Table 2-1. *N*-(3-Dimethylethoxysilylpropyl)-3-(1-pyrenyl)propanamide (**4**) was also synthesized as shown in Scheme 2-1. 1-Pyrenebutyric acid is commercial available (Aldrich Chemical Company, Inc.).

6-(4-Cyanobiphenyl-4'-oxy)hexanoic acid

A solution of 4-cyano-4'-hydroxybiphenyl (1.00 g, 5.13 mmol) and tetrahydropyranyl 6-bromohexanoate (1.50 g, 5.38 mmol) was stirred at 80 °C for 4 hours in the presence of potassium carbonate (1.06 g, 7.67 mmol), followed by adding water to obtain white precipitates which were dissolved in THF to be subjected to the hydrolysis with 6 N hydrochloric acid. After evaporating the solvent, residual crystals were recrystallized from ethyl acetate to give the acid.

mp = 170-171 °C
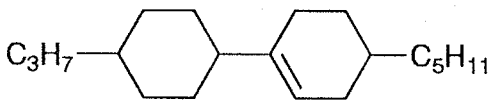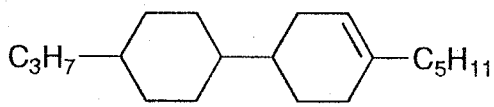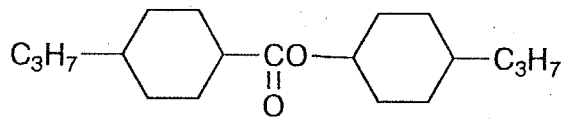
N-(3-Dimethylethoxysilylpropyl)-6-(4-cyanobiphenyl-4'-oxy)hexanamide (**1**)

6-(4-Cyanobiphenyl-4'-oxy)hexanoic acid (81.3 mg, 0.26 mmol) was treated with
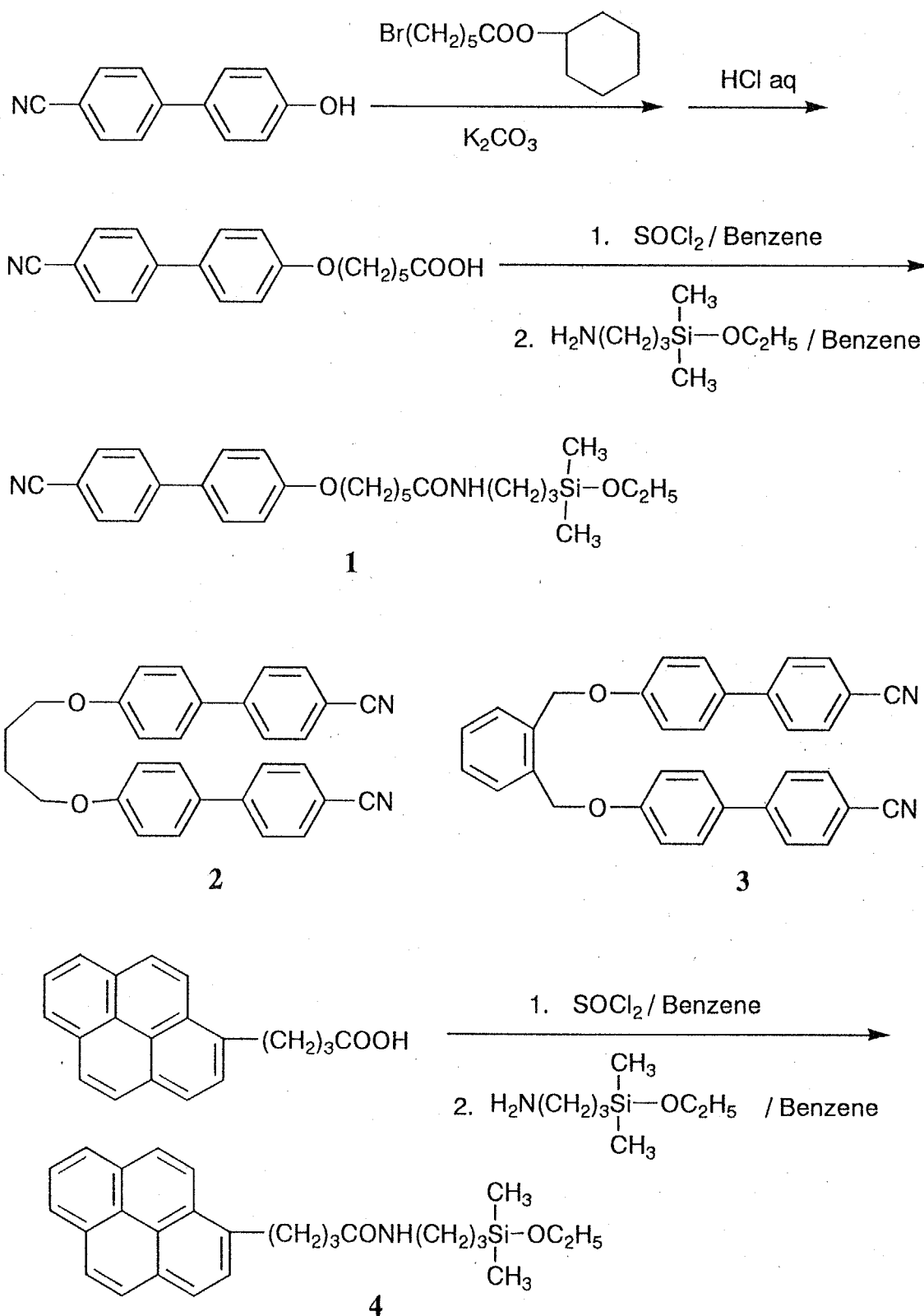
Scheme 2-1 Syntheses and structures of **1**, **2**, **3** and **4**

Table 2-1 T_{NI} and the structures of liquid crystals used in Chapter 2

	LC1	LC2
T_{NI} / ^{O}C	26.6	31.8
C$_3$H$_7$—⬡—⬡—C$_5$H$_{11}$	40%	10%
C$_3$H$_7$—⬡—⬡—C$_5$H$_{11}$	60%	15%
C$_3$H$_7$—⬡—CO—O—⬡—C$_3$H$_7$		75%

thionyl chloride in benzene in the presence of a catalytic amount of DMF to convert into the corresponding acid chloride. The acid chloride and freshly distilled 3-aminopropyldimethylethoxysilane (44.1 mg, 0.27 mmol) was stirred in benzene at room temperature for 1 hour in the presence of a slightly excess amount of triethylamine. After removal of the amine hydrochloride, the solvent was evaporated, and a residual mass was purified by column chromatography on silica gel using ethyl acetate as an eluent and recrystallized from a mixture of petroleum ether and chloroform to yield white powders in a 9 % yield.

mp = 79-80 °C

Elemental Anal. for $C_{26}H_{36}N_2O_3Si$:   Calcd. C: 68.99, H: 8.02, N: 6.19%.

Found C: 69.07, H: 8.14, N: 6.26%.

A hydrolyzed product as white needle-like crystals of mp 126 - 127 °C was isolated as a main product in a 30 % yield, and the structure was revealed by the absence of ethoxy group in their NMR spectra.

Elemental Anal. for $C_{48}H_{62}N_4O_5Si_2$ as the condensation product:

Calcd. C: 69.36, H: 7.52, N: 6.74%.

Found C: 69.55, H: 7.28, N: 6.54%.

The condensation of 6-(4-cyanobiphenyl-4'-oxy)hexanoic acid with 3-aminopropyldimethylethoxysilane with the aid of dicyclohexylcarbodiimide yielded no desired product, but exclusively the hydrolyzed product in 40 - 60 %.

1,3-Bis(4-cyanobiphenyl-4'-oxymethyl)propane (2)

This was synthesized by the Williamson's reaction of 4-cyano-4'-hydroxybiphenyl and 1,3-dibromopropane. White crystals exhibiting nematic phase at elevated temperatures were obtained by recrystallization from benzene.

mp = 155 - 156 °C

T_{NI} = 174 °C

Elemental Anal. for $C_{29}H_{22}N_2O_2$:   Calcd. C: 80.91, H: 5.15, N: 6.50%.

Found C: 81.18, H: 5.17, N: 6.47%.

1,2-Bis(4-cyanobiphenyl-4'-oxymethyl)benzene (3)

This was also synthesized by the Williamson's reaction of 4-cyano-4'-hydroxybiphenyl and 1,2-dibromomethylbenzene. Recrystallization from ethanol gave the purpose white crystals.

mp = 197-198 °C

Elemental Anal. for $C_{34}H_{24}N_2O_2$:   Calcd. C: 82.91, H: 4.91, N: 5.68%.

Found C: 82.97, H: 4.99, N: 5.60%.

N-(3-Dimethylethoxysilylpropyl)-3-(1-pyrenyl)propanamide (4)

This was synthesized with 1-pyrenebutyric acid chloride and 3-aminopropyldimethylethoxysilane in the same way as that for 1.   Yield was 25 %.

mp = 70-71 °C

Elemental Anal. for $C_{27}H_{33}NO_2Si$:   Calcd. C: 75.13, H: 7.71, N: 3.24%.

Found C: 75.07, H: 7.71, N: 3.33%.

2-2-2. Surface modification

A fused silica plate (9 mm × 30 mm) was washed ultrasonically in acetone, conc. nitric acid, saturated aqueous solution of sodium bicarbonate and water for 15 min each. The plate was subsequently immersed in a 0.05 wt% (1×10^{-3} mol/l) ethanol solution of the cyanobiphenyl silylating reagent (1) or the pyrenyl silylating reagent (4) for 20 min and baked at 120 °C for 20 min, followed by three-fold ultrasonical washings in THF for 10 min until no fluorescence was detected from washings.

An average density of the surface CB was estimated to be around 0.82 molecules/nm^2 by an absorbance at λmax of 296 nm using the molar absorption coefficient ($\varepsilon = 2.9 \times 10^4$ l/mol•cm) of 6-(4-cyanobiphenyl-4'-oxy)hexanoic acid at 296 nm in ethanol. A contact angle for water of the plate was increased by the modification with the reagent from 12° to 45°.

An amount of the surface pyrene was estimated in the same way as for CB. With an absorbance at λmax of 345nm of the pyrene on a plate and the molar absorption coefficient ($\varepsilon = 4.5 \times 10^4$ l/mol•cm) of the pyrenyl silylation reagent at 344 nm in THF, an average density of pyrene on a plate was estimated to be about 0.34 molecules/nm^2. A contact angle for water on the plate was increased by the modification with the reagent

23

from 12° to 6°, supporting the introduction of the hydrophobic units on the surface.

2-2-3. Measurements

Absorption and fluorescence spectra were taken on a Hitachi UV-320 and a Hitachi F-4010, respectively. The fluorescence spectra of a fused silica plate were measured with a film-measuring attachment. The excitation wavelength for fluorescence measurement was 296 nm. All the spectra of plates shown in this paper were subtracted those of blank washed fused silica plates.

2-3. Results and discussions

2-3-1. Molecular design and synthesis of a cyanobiphenyl derivative

Cyanobiphenyl (CB) unit is a suitable fluorophore for the present purpose because of the following features. First, CB itself is one of the typical mesogens and assumed to interact intimately with liquid crystal molecules. Second, CB displays excimer fluorescence at the longer wavelength like a shoulder to afford information about the molecular interaction between surface-bound CB and liquid crystals by measuring a ratio of the excimer and the monomer fluorescence of CB. Third, the fluorescence of CB is affected by solvent polarity to be able to probe microenvironmental polarity on substrate surfaces.

In order to bind CB unit covalently to a silica surface, a silyl residue was introduced to the moiety through a spacer. Dimethylethoxysilyl group was employed here to cap silanol groups separately on the surface since there is a possibility to cover the surface with a polysiloxane substituted with CB when triethoxysilyl residue is introduced.

2-3-2. Fluorescence in solutions

Prior to determining fluorescence behaviors of CB covalently bound on a fused silica plate, the solution fluorescence of the silylating reagent (**1**) was examined. The spectral shape did not depend on the concentration in the range of 10^{-7} - 5×10^{-4} mol/l, showing no excimer formation in these concentrations. The monomer fluorescence

showed a marked red shift in polar solvents. There is a linear relationship between emission wavenumber maximum and the solvent polarity parameter, $E_T(30)$ [17], as plotted in Figure 2-1.

Fluorescence spectra of the CB (1) in liquid crystals filled in a quartz cell with a 100 μm thickness were also measured. Nematic liquid crystals used here are UV-transparent and of lower polarity. The structures of liquid crystals are shown in Table 2-1. LC1 is a binary mixture of cyclohexylcyclohexanes while a cyclohexanecarboxylate is mixed with LC1 to afford LC2. The emission spectrum of the CB in non-polar LC1 was quite the same as that in cyclohexane and the fluorescence in LC2 resembled that in a 3 : 1 mixture of cyclohexane and ethyl acetate, reflecting the contribution of the polar ester component as shown in Figure 2-2 and 2-3 respectively. These facts show that the monomeric fluorescence spectral maxima and shapes depend on only the polarity around the fluorescent species.

2-3-3. Fluorescence at an interface

The fluorescence spectra of CB chemisorbed on a plate were red-shifted when the plate was immersed in solvents as compared with that of CB dissolved in the corresponding solvents. The red-shift reached 28nm in cyclohexane as shown in Figure 2-4, suggesting that the polar nature of microenvironment surrounding CB units on the surface was much higher than that in bulk solvent. This may arise from residual surface silanols and water molecules adsorbed on the fused silica surface.[13-16]

If the fluorescence of CB units at an interface between a fused silica plate and cyclohexane is identical with monomeric CB species, a spectral shape of the former should be identify with that of CB dissolved in a polar solvent. Figure 2-4 also shows a fluorescence spectrum of the monomeric CB (1) dissolved in methanol and spectra of a surface-modified fused silica plate immersed in cyclohexane and 1 in cyclohexane. Whereas the emission maxima of 1 in methanol appears exactly at the same wavelength as that of the surface CB in contact with cyclohexane within an experimental error (0.5 nm), the spectral shape differs from each other; the spectrum of the surface CB exposed to cyclohexane is much broader at long wavelength region. This means that the fluorescence of the interfacial CB units comes not only from monomeric, but also from
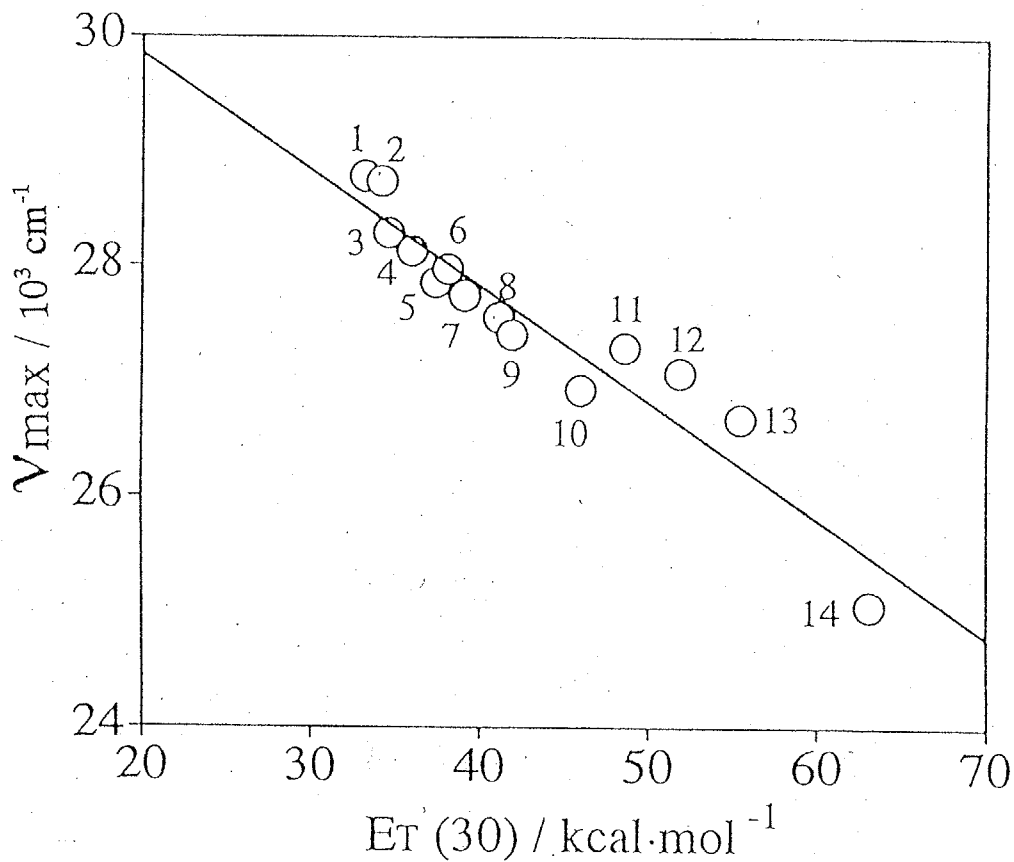
Figure 2-1. The correlation between λmax of **1** and $E_T(30)$ of the solvent; 1: cyclohexane, 2: cyclohexene, 3: diethylether, 4: 1,4-dioxane, 5: tetrahydrofuran, 6: ethyl acetate, 7: chloroform, 8: dichloromethane, 9: 1,2-dichloroethane, 10: acetonitrile, 11: 2-propanol, 12: ethanol, 13: methanol and 14: water
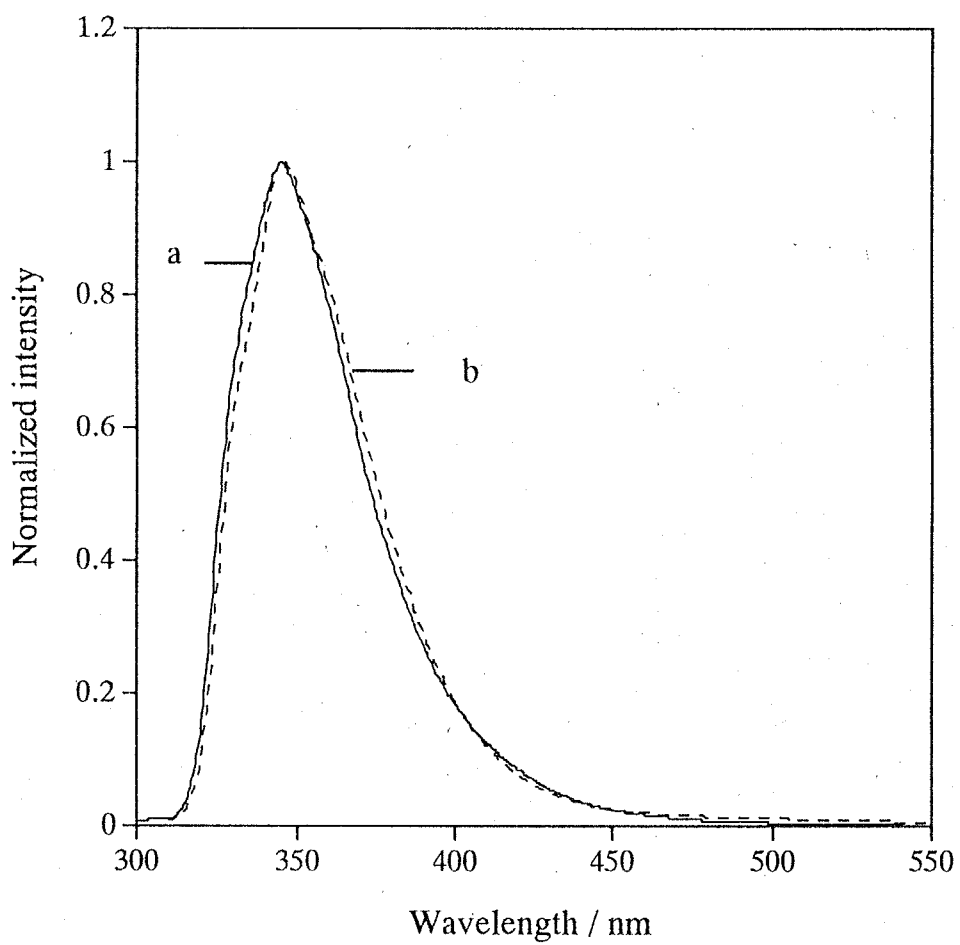
Figure 2-2. The fluorescence spectra of **1** dissolved in cyclohexane (a) and LC1(b).
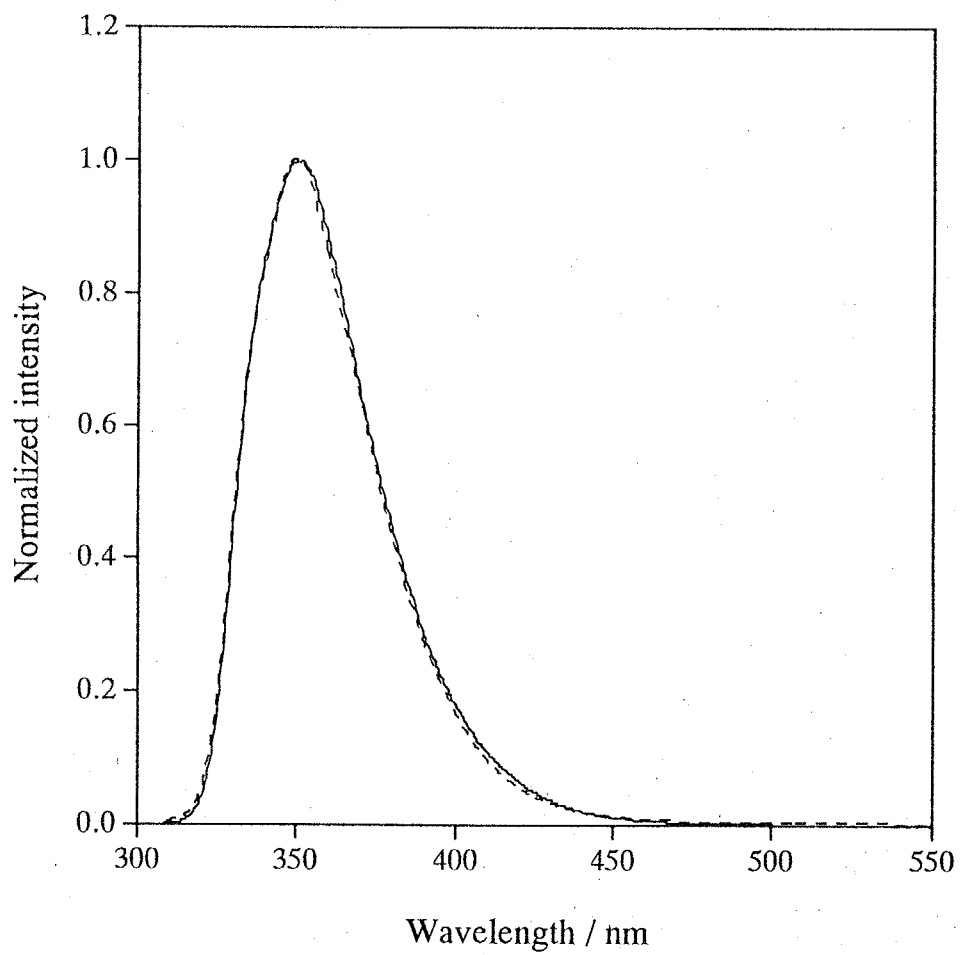
Figure 2-3. The fluorescence spectra **1** dissolved in 3:1 mixture of cyclohexane and ethyl acetate (solid line) and in LC2 (broken line).
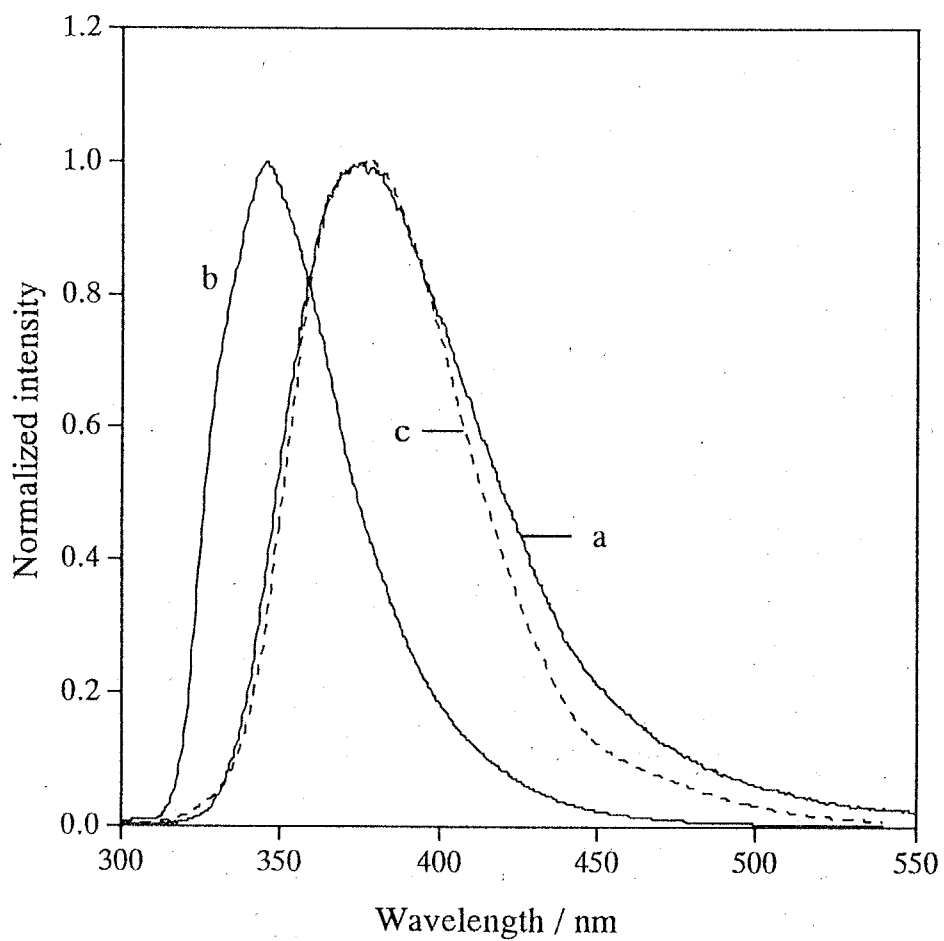
Figure 2-4. The fluorescence spectra of a CB-modified fused silica plate immersed in cyclohexane (a) and 1 dissolved in cyclohexane (b) and in methanol (c).

excimer. Some literatures pointed out the existence of an excimer for a highly concentrated solution of 4-cyano-4'-alkyloxybiphenyl [17,18] and a solution of polyacrylate with CB side chains through a polymethylene spacer.[19,20]

The excimers reported so far display a broad spectral band with a red-shift. According to these literatures, cyanobiphenyl excimer is assigned to head-to-tail type. To check head-to-head type configuration for the excimer, fluorescent spectra of 1×10^{-6} mol/l solutions of **2** and **3** were compared to each other. As shown in Figure 2-5, a shoulder was observed for **3** at a longer wavelength region in ethanol when compared with **2**, being ascribable to head-to-head type excimer due to the geometrical situation. This emission was similar to head-to-tail type excimer emission in the literatures. A spectral shape of CB on a silica plate exposed to cyclohexane was very similar to that of the excimer shown in Figure 2-5. This suggests the formation of an excimer of the CB on the silica. Since it was hard to estimate the microenvironmental polarity at the interface between a fused silica plate and a cyclohexane layer, no exact evaluation of an emission shape of monomeric CB at the interface was successful and prevented us from the calculation of the surface excimer emission. Further studies are required for revealing details of the excimer formation on a silica surface. Since a few of CB units were stripped from a fused silica plate during UV light for longer than 10 min with a Xe lamp for fluorescence measurements, the dynamic fluorescent measurement which takes more than an hour could not be carried out.

The fluorescence maximum of CB on a fused silica plate immersed in a 3:1 mixed solvent of cyclohexane and ethyl acetate was 20 nm red-shifted when compared with CB dissolved in the same mixed solvent having a polarity similar to that of LC2 as shown in Figure 2-6. The fluorescence maximum of CB on the surface appeared at 370 nm, which is the same in an experimental error as that of CB in ethanol. However, the spectral shape of the surface CB in contact with the mixed solvent was broader at the long wavelength region than that of an ethanol homogeneous solution. These facts show that there exists probably a CB excimer at the interface and that the polarity at the interface between a silica surface and the mixed solvent phase is much higher than that of bulk solvent.
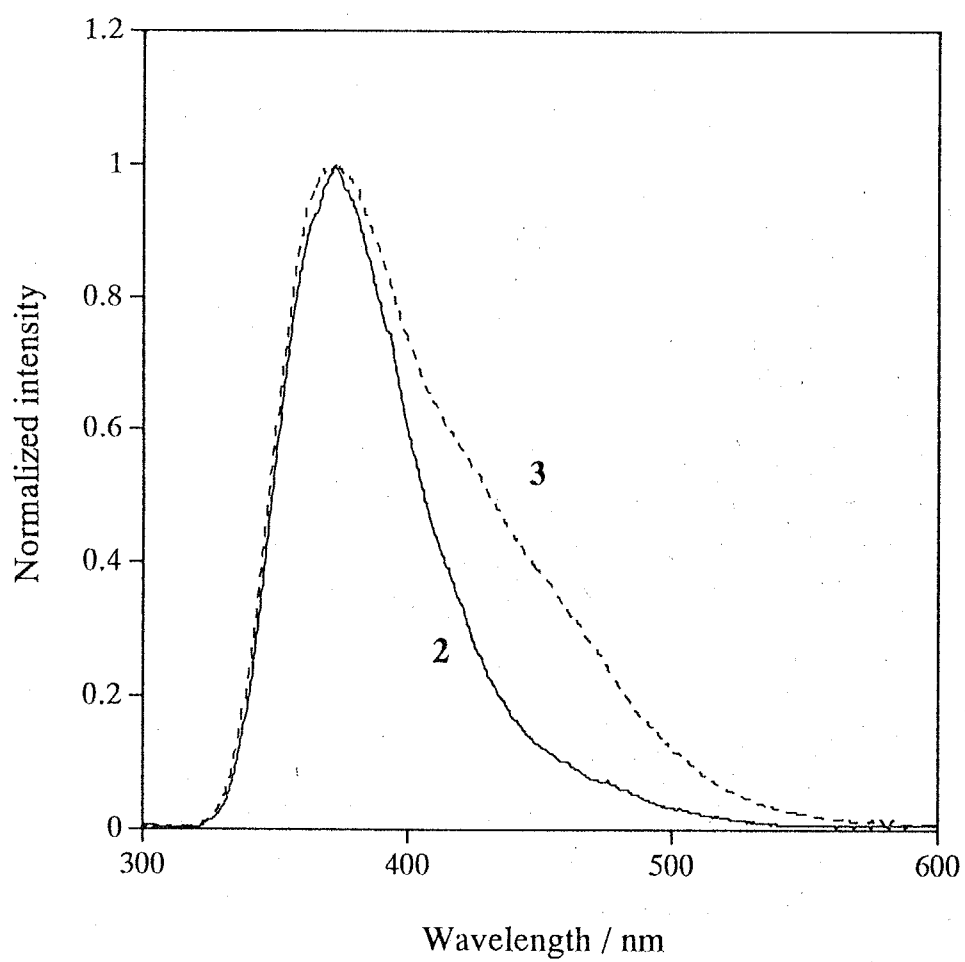
Figure 2-5. The fluorescence spectra of 5×10^{-4} mol/dm^3 ethanol solution of **2** (solid line) and **3** (broken line).
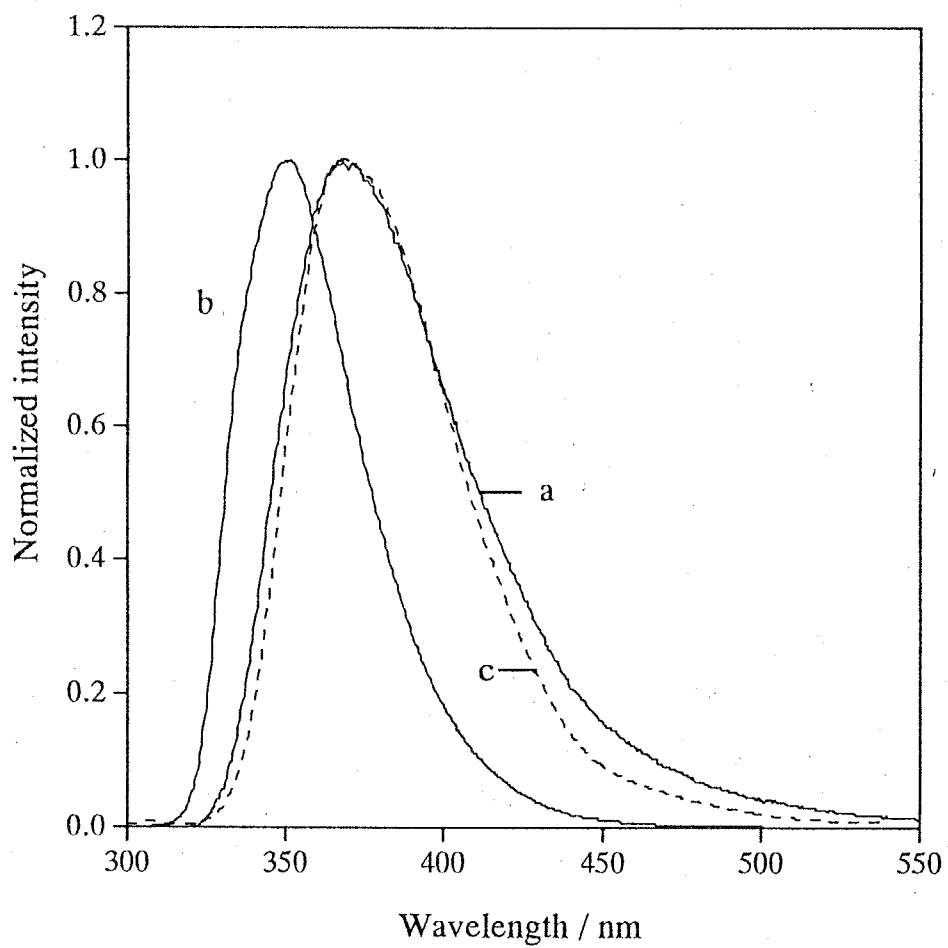
. Figure 2-6. The fluorescence spectra of a CB-modified fused silica plate

immersed in 3:1 mixture of cyclohexane and ethyl acetate (a) and 1

dissolved in the mixture (b) and in ethanol (c).

2-3-4. Fluorescence of surface CB in contact with liquid crystals

Since both sides of a fused silica plate were modified with CB in the present procedure, the following double-layered cell was assembled to measure the fluorescence spectrum of CB at the interface between a fused silica plate and a liquid crystal layer. A nematic liquid crystal with 5 μm spherical spacers was put on both surfaces of the CB-modified plate, and each side was covered with a fused silica plate. The alignment was in a planar mode for both nematic LC1 and LC2, as determined by polarized light microscopic observation. In order to subtract a background fluorescence spectrum from an observed one, a double-layered liquid crystal cell as a reference was fabricated in a similar fashion with the use of an untreated fused silica plate instead of a surface-modified fused silica plate.

Figure 2-7 shows the fluorescence spectra of a double-layered cell filled in with LC1 and an LC1 solution of 1. Just as in the case of the observation in cyclohexane, a red shift was induced in the emission maximum of CB attached onto a surface although the shift value of 17 nm was considerably smaller than that in cyclohexane (28 nm). A spectrum of 1 dissolved in 1,2-dichloroethane, which results in the same λmax within an experimental error (0.5 nm), is also illustrated in Figure 2-7. It should be stressed here that both spectra of the surface CB exposed to an LC1 layer and the CB in a solution of dichloroethane are quite superimposed on each other, indicating that the fluorophore units exist as a monomeric form without excimer formation and the red-shift was occurred only by higher micropolarity around interfacial CB units than that of bulk LC1. In this system, a few of CB units were also stripped from a fused silica plate during UV light irradiation for long time with Xe lamp of fluorescence equipment, the dynamic fluorescent measurement witch would be make an excimer existence clear could not be carried out.

Distinct characteristics of the emission of surface-bound CB in contact with cyclohexane and LC1 are two-fold; the emission maximum and the spectral shape particularly at a longer wavelength region. First, the red-shift of the surface emission of CB is markedly reduced for LC1 in comparison with that in cyclohexane although the polarity of both solvents is not different from each other (Figure 2-2). As suggested above, CB groups on a surface interact rather intensively with highly polar silanol
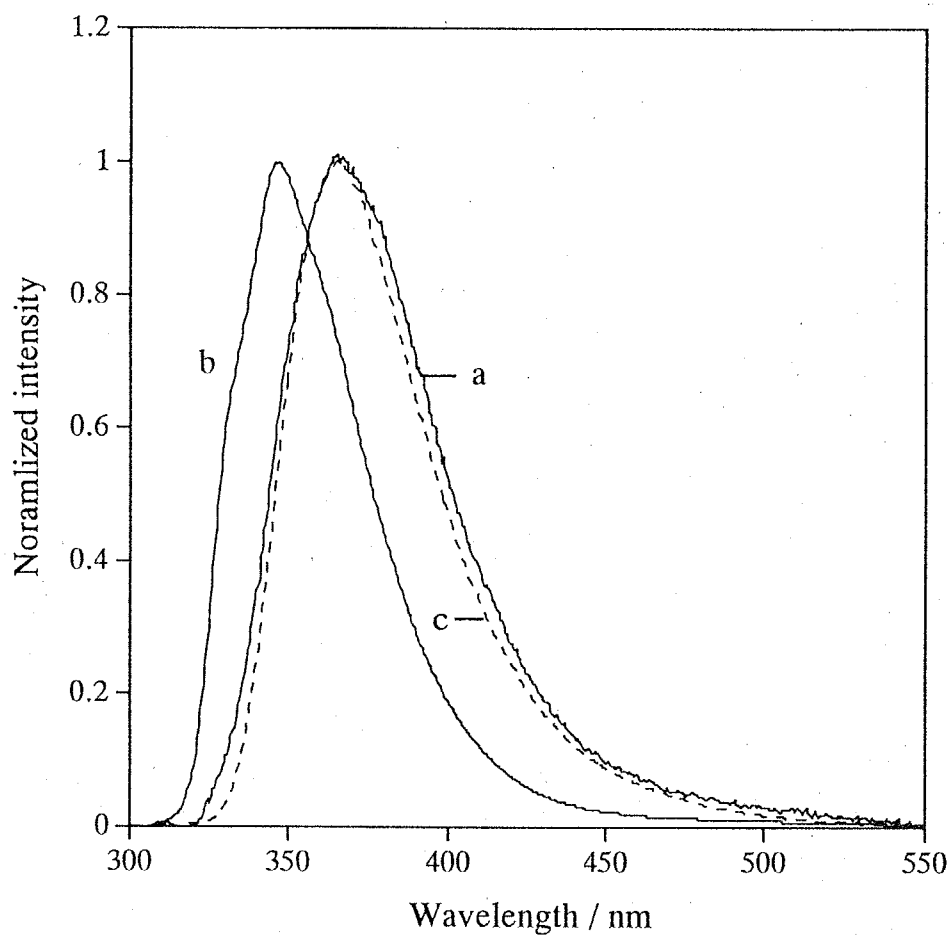
Figure 2-7. The fluorescence spectra of a CB-modified fused silica plate covered with LC1 (a) and **1** dissolved in LC1 (b) and in 1,2-dichloroethane (c).

residues and/or adsorbed water molecules when the plate is immersed in non-polar cyclohexane. It follows that the decrease in the red shift for LC1 is reasonably ascribable to a specific molecular interaction of CB units having a mesogenic nature with liquid crystal molecules at an interface. That is, the fluorophore units adhering on a silica surface are capable of interacting with liquid crystal molecules to lead to molecular aggregates. This gives rise to the situation that CB units are surrounded by non-polar mesogenic molecules. The fact that the emission maximum of the surface CB in contact with LC1 is still subjected to the red shift implies that the fluorophore units are not completely surrounded by non-polar mesophasic molecules. The microenvironmental polarity of the surface CB is still affected by the highly polar nature of a silica surface. This may lead to the assumption that the CB holds an intimate interaction with a surface so that the perpendicular reorientation of the molecular axis of CB is inhibited to lead to a planar alignment.

This interpretation is strongly supported by the second point; no emission band at a longer wavelength region appears when the CB-modified plate is wetted with LC1 although there is a shoulder at a longer wavelength region when exposed to cyclohexane. It is very likely that the specific interaction with LC1 molecules at an interface brings about the suppression of the excimer formation. It has been reported that wall-mediated formation of a birefringent thin layer of mesophase at an interface is not destroyed even above T_{NI} although a thickness of the ordered layer is dependent on a difference between a experiment temperature and T_{NI}.[21,22] This suggests that the encounter of an excited CB with ground state CB is strongly prohibited within the short life time of the excited singlet state owing to the higher ordered structure of the boundary mesophase layer. The transition temperature between nematic and isotropic phases (T_{NI}) of LC1 is 26.6 °C. The fluorescence measurement was carried out at 20 °C and 40 °C, and no alteration of both the shape and λmax of the fluorescence spectrum were observed. This supports unequivocally that the specific molecular interaction between the surface CB molecules and liquid crystal molecules is not influenced by the phase change of a bulk mesophase at all.

The fluorescent spectral shape of a LC2 cell with CB surface-bound silica plates resembles that of CB dissolved in 2-propanol and is indicative of no excimer formation as

shown in Figure 2-8.   The above-mentioned specific molecular interaction at a boundary region exists not only for LC1, but also for LC2.

2-3-5. A pyrene derivative as a photoprobe

Pyrene has been used extensively to probe microenvironments since the fluorescence maximum between the monomer and the excimer is enough separated. This photoprobe was applied to monitor the behavior of liquid crystals on a substrate surface.   *N*-(3-dimethylethoxysilylpropyl)-3-(1-pyrenyl)propanamide (**4**) was prepared and used for the surface modification of a silica plate.

Fluorescent spectra of a pyrene-modified silica plate immersed in cyclohexane and LC1 are shown in Figure 2-9.   Fluorescence intensity ratio of excimer to monomer for LC1 was almost the same as that for cyclohexane.   This reveals that LC1 molecules do not go into the bush of pyrene groups on a silica surface and cannot suppress the excimer formation.   This is in marked contrast to the case of CB stated above.   This difference arises surely from whether fluorescent probe has mesogenic nature and stresses the novelty of CB as a photoprobe for studies on interfacial events of liquid crystals.
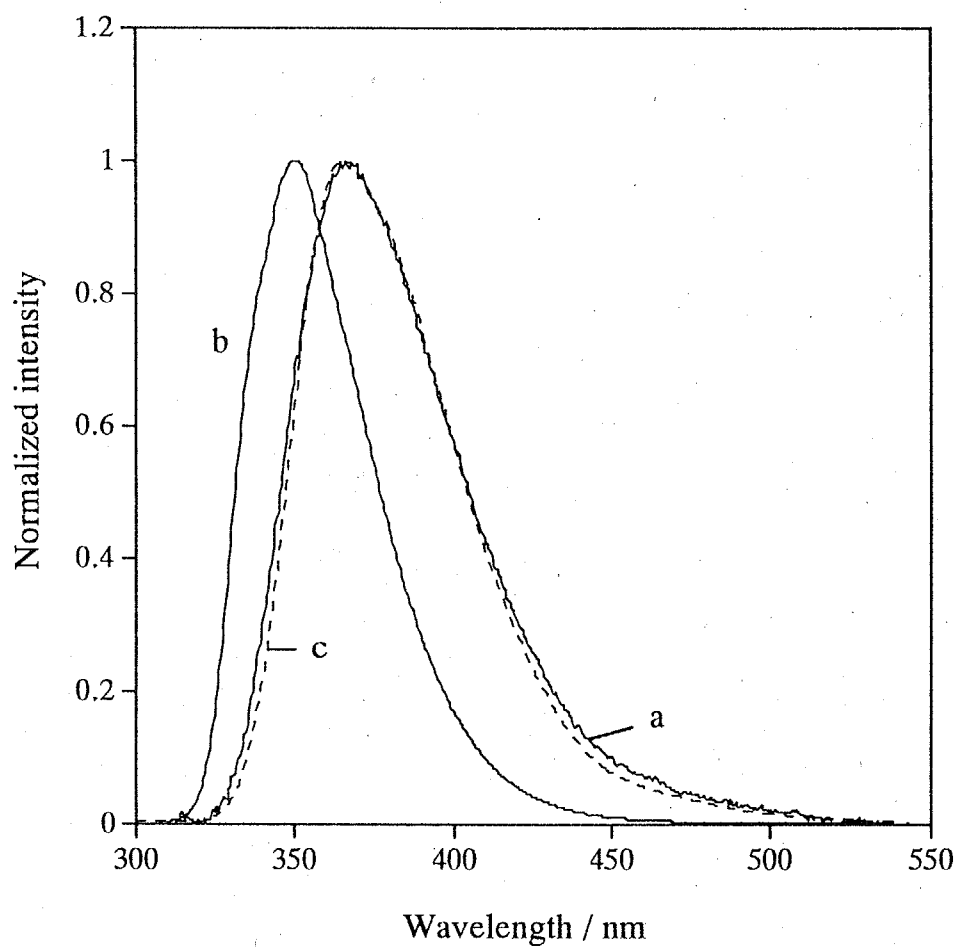
Figure 2-8. The fluorescence spectra of a CB-modified fused silica plate

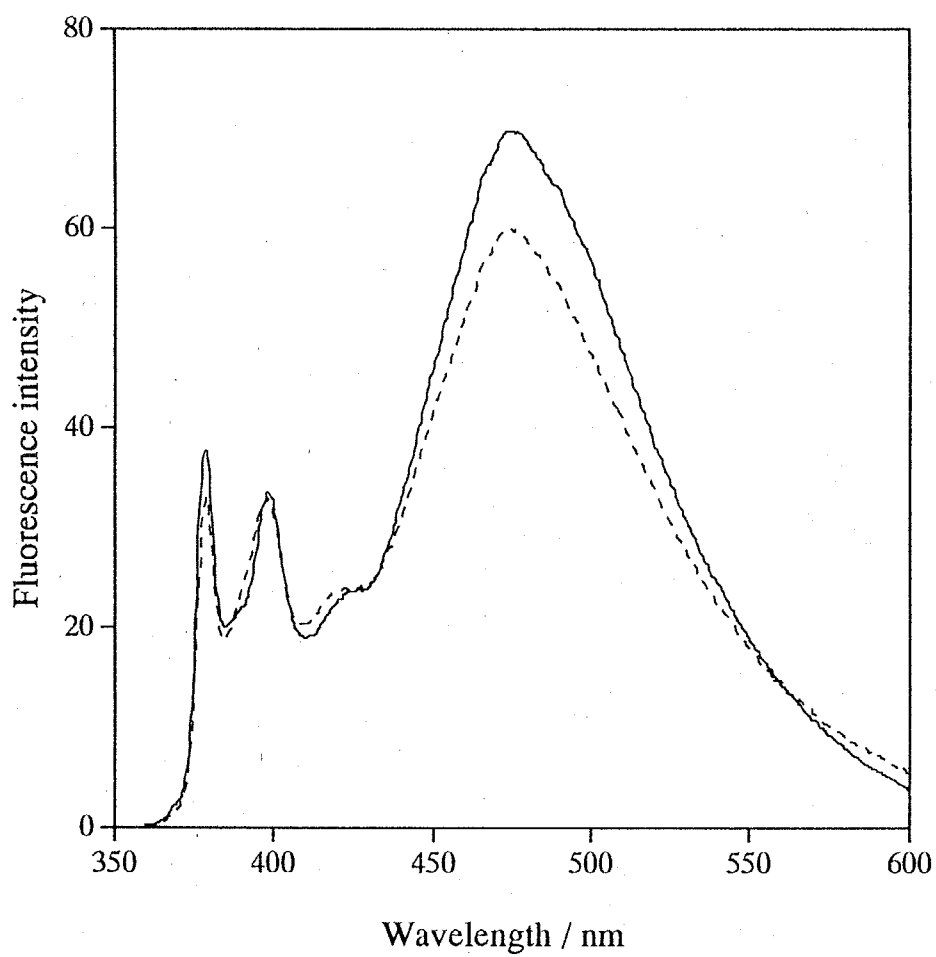covered with LC2 (a) and **1** dissolved in LC2 (b) and in propanol (c).

Figure 2-9 The fluorescece spectra of pyrene-modified fused silica plate immersed in cyclohexane (solid line) and in LC1 (broken line).

2-4. Conclusions

The steady state fluorescent measurement is a simple and novel tool to evaluate molecular interactions at interfaces between a solid and a fluid layer as well as a liquid crystal layer. CB moiety can act as a prominent fluorescence probe to estimate microenvironmental polarity because of the linear dependence of the emission maximum on solvent polarity. CB groups attached onto a fused silica plate exhibited a considerable red shift in fluorescence when the plate was immersed in non-polar cyclohexane. This anomalous red shift results from intimate interactions of the surface CB with a highly polar silica surface. A CB-modified plate also displayed an emission band at a longer wavelength region, implying the formation of an excimer of CB on the surface.

Owing to the mesogenic nature of CB, the surface fluorophore exhibited a characteristic emission when a surface-modified plate was covered with nematic liquid crystals. In contrast to the case of cyclohexane, the red shift was reduced markedly although the polarity of the liquid crystals is not far from that of cyclohexane. Furthermore, the emission band at longer wavelengths was completely lost to be superimposed on that of monomeric emission band. These emissive behavior of the surface CB in contact with a liquid crystal layer supports that there is specific molecular interactions between CB units and liquid crystal molecules at an interface. Such a phenomenon was not observed when a pyrene was employed as a surface photoprobe. Moreover, CB emission in the presence of liquid crystals was not influenced by temperatures below and above T_{NI}. These observations are all in line with previous reports based on experimental results as well as theoretical considerations that a substrate surface is covered with a birefringent thin layer even though the bulk mesophase is converted into an isotropic phase by heating.

References

1. K. Ichimura, Y. Suzuki, T. Seki, A. Hosoki and K. Aoki, *Langmuir*, 1988, **4**, 1214.

2. Y. Kawanishi, T. Tamaki, M. Sakuragi, T. Seki and K. Ichimura, *Langmuir*, 1992, **8**, 2061.

3. K. Ichimura, Y. Hayashi, Y. Kawanishi, T. Seki, T. Tamaki and N. Ishizuki, *Langmuir*, 1993, **9**, 857.

4. K. Ichimura, Y. Hayashi, H. Akiyama, T. Ikeda and N. Ishizuki, *Appl. Phys. Lett.*, 1993, **63**, 449.

5. K. Ichimura, "*Photochromic polymers, Polymers as electrooptical and photooptical active media*" ed. by V. Shibaev, Springer-Verlag, 1996, 138.

6. K. Ichimura, S. Morino and H. Akiyama, *Appl. Phys. Lett.*, 1998, **73**, 92.

7. B. Jérôme, *Rep. Prog. Phys.*, 1991, **54**, 391.,

8. B. Jérôme, *Mol. Cryst. Liq. Cryst.*, 1992, **212**, 2.

9. C. S. Mullin, P. Guyot-Sionnest and Y. Shen, *R. Phys. Rev.*, 1989, **A39**, 3745.

10. M. Barmentlo, F. R. Hoekstra, N. P. Willard and R. W. Hollering, *J. Phys. Rev.*, 1991, **A43**, 5740.

11. T. Sakuhara, E. Tomita, H. Nakahara and K. Fukuda, *Thin Solid Films*, 1992, **209**, 269.

12. Y. Kawanishi, T. Tamaki and K. Ichimura, *ACS. Symp. Ser.*, 1994, **537**, 453.

13. J. C. W. Frazer, W. A. Patrick and H. E. Smith, *J. Phys. Chem.*, 1927, **31**, 897.

14. J. H. Frazer, *Phys. Rev.*, 1929, **33**, 97.

15. R. I. Razouk and A. S. Salem, *J. Phys. Chem.*, 1948, **52**, 1208.

16. K. Kiler, K J. H. Shen and A. C. Zettlemoyer *J. Phys. Chem.*, 1973, **77**, 1458.

17. N. Tamai, I. Yamazaki, H. Masuhara and N. Mataga, *Chem. Phys. Lett.*, 1984, **104**, 485.

18. T. Ikeda, S. Kurihara and S. Tazuke, *J. Phys. Chem.*, 1990, **94**, 6550.

19. S. Kurihara, T. Ikeda and S. Tazuke, *Macromolecules*, 1991, **24**, 627.

20. S. Kurihara, T. Ikeda and S. Tazuke, *Macromolecules*, 1993, **26**, 1590.

21. K. Miyano, *Phys. Rev. Lett.*, 1979, **43**, 51.

22. K. Miyano, *J. Chem. Phys.*, 1979, **71**, 4108.

Chapter 3

Effect of chemisorption methods on fluorescence behavior of cyanobiphenyl units attached to silica surfaces

3-1. Introduction

Surface-mediated alignment control of liquid crystals (LCs) achieved by command surfaces is based on photoinduced changes not only of chemical structures, but also orientation of axis of surface molecules.[1,2] Consequently, conformations of command molecules play a significant role in the LC photoalignment so that the effect of how to attach the command molecules on efficiencies of controllability of LC alignment is an interesting subject in order to optimize this technique for practical applications. In chapter 2, cyanobiphenyl (CB) residues as a fluorescent probe for revealing interfacial interactions between surface molecules and LC molecules were tethered to a silica surface through silylation to assemble a model system for command surfaces. But the work was done without any consideration of conformational effects on the interactions at a boundary region. Because CB units were introduced to a silica surface through a flexible long alkyl chain through silylation, the orientation of the CB is not controllable and randomly distributed. In order to present an approach to construct a model system to elucidate effects of the ways to link command molecules on substrate surfaces,[3-7] crown isomer of calix[4]resorcinarene (CRA) derivatives substituted with CB units are employed in this chapter for the surface modification of a substrate surface with the fluorescent probe.

As mentioned in chapter 1, the crown isomer of CRA, which has eight polar groups at the upper rim and hydrophobic tails at the lower one,[8,9] is the most thermodynamically stable isomer among the others among other isomers.[10-12] It has been shown that immersion of a fused silica plate in dilute solutions of CRA derivatives results in effective adsorption of the cyclic molecules to form self-assembled molecular films (SAMs) with high packing density owing to the multi-point adsorptivity through hydrogen bonds between polar arrays of CRA and residual silanols on a silica surface. It has been also suggested that hydrophobic tails of CRA are stretched out perpendicularly in respect to a

substrate surface because of the rigidity of the CRA framework.[8,11]

The purpose of this chapter is in this context to review the contribution of restricted orientation of the fluorescent probe attached through CRA unit in intermolecular interactions between the surface CB and fluid as well LC molecules. The results will be discussed also based on the comparison of those for chemisorbed CB through silylation, taking note to differences in the flexibility of spacers. Since it has been revealed that CRA possessing eight carboxymethylated groups adsorbs firmly on a fused silica surface through hydrogen bonds,[13] octacarboxymethylated CRA (CRA-CM) bearing CB units is used in this chapter. Another CB compound to combine a silica surface by silylation through an alkyl chain, whose length was same as that between CB and CRA skeleton of CB-CRA-CM above mentioned, was also prepared to reveal the effect of linkage methods between CB and silica surface.

3-2. Experiment

3-2-1. Materials

Cyclohexane was of a spectroscopy grade purchased from Tokyo Kasei and used as received. Nematic liquid crystals used in this chapter are the same as that shown in chapter 2.

2,8,14,20-Tetra(4'-cyanobiphenyl-4-oxypropyl)-4,6,10,12,16,18,22,24-octa(carboxymetoxy)-calix[4]resorcinarene (5), which is CB-CRA-CM mentioned in 3-1, and 3-(4'-Cyanobiphenyloxy-4)propyldimethylethoxysilane (6) were synthesized as shown in Schemes 3-1 and 3-2 respectively. 2,8,14,20-Tetra(3-iodopropyl)-4,6,10,12,16,18,22,24-octa(ethoxycarbonyloxymethoxy)-calix[4]resorcinarene (7) was prepared according to the literature.[7] Monomer model and dimer model compounds (9 and 10) were also synthesized by the routes shown in Scheme 3-2.

<u>2,8,14,20-tetra(4'-cyanobiphenyl-4-oxypropyl)-4,6,10,12,16,18,22,24-octa(ethoxycarbonyl-oxymethoxy)calix[4]resorcinarene (8)</u>

4-Cyano-4'-hydroxybiphenyl (49 mg, 2.5×10^{-5} mol) and K_2CO_3 (43 mg, 3.1×10^{-5}
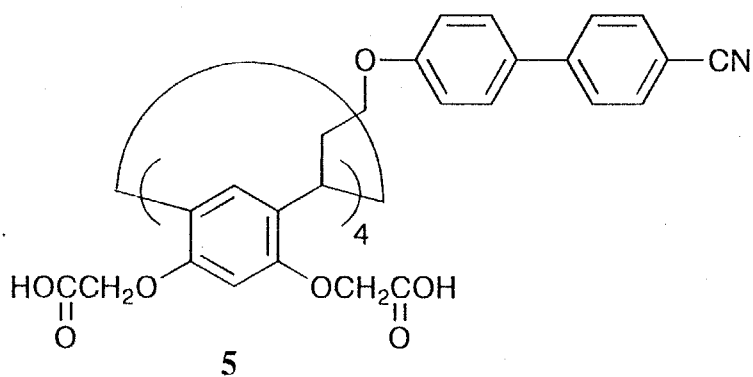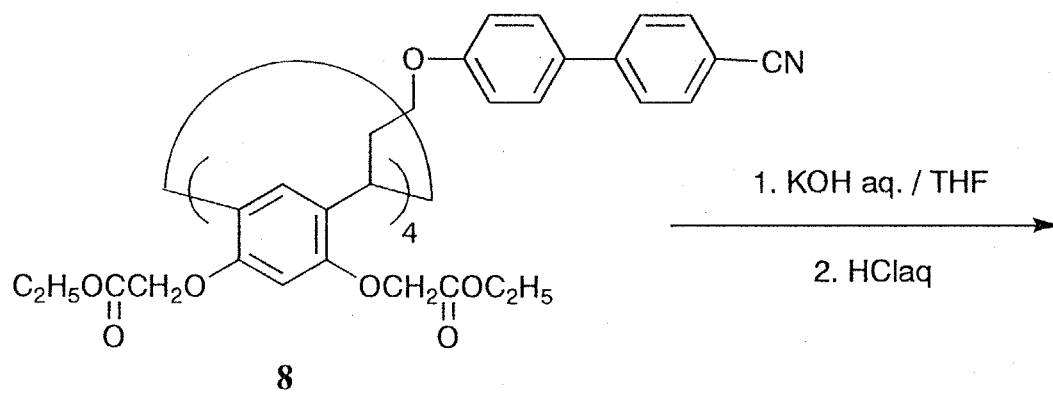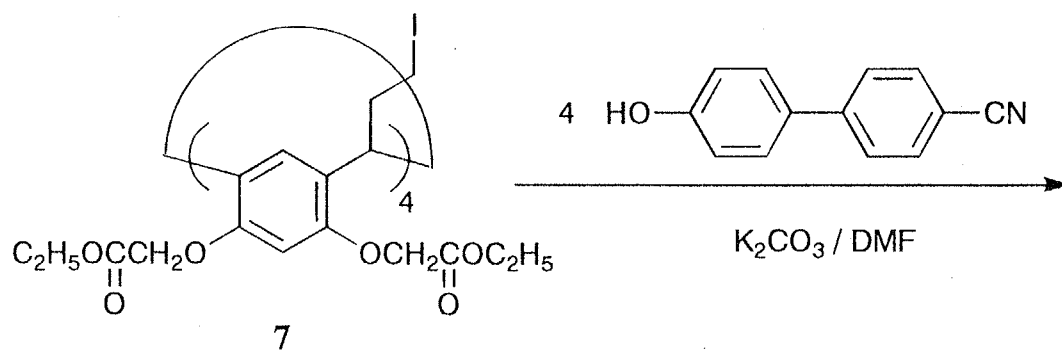
Scheme 3-1 Synthesis of **5**
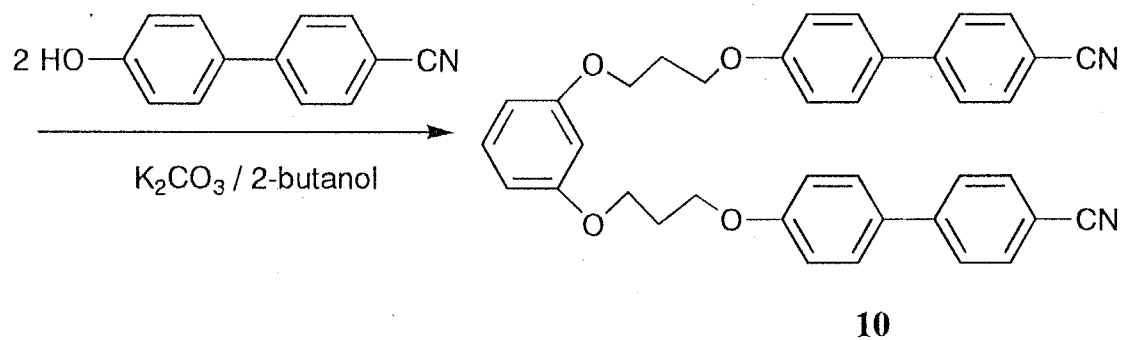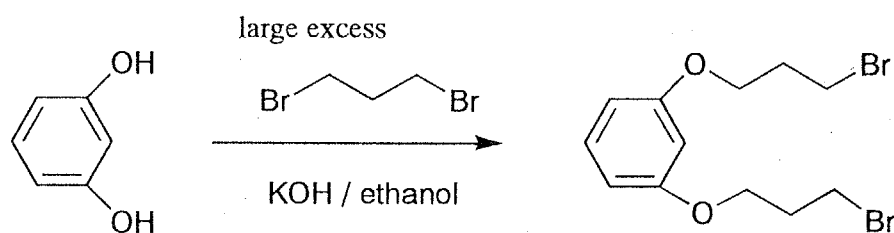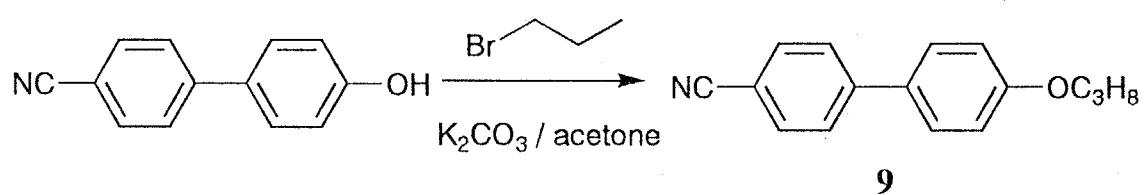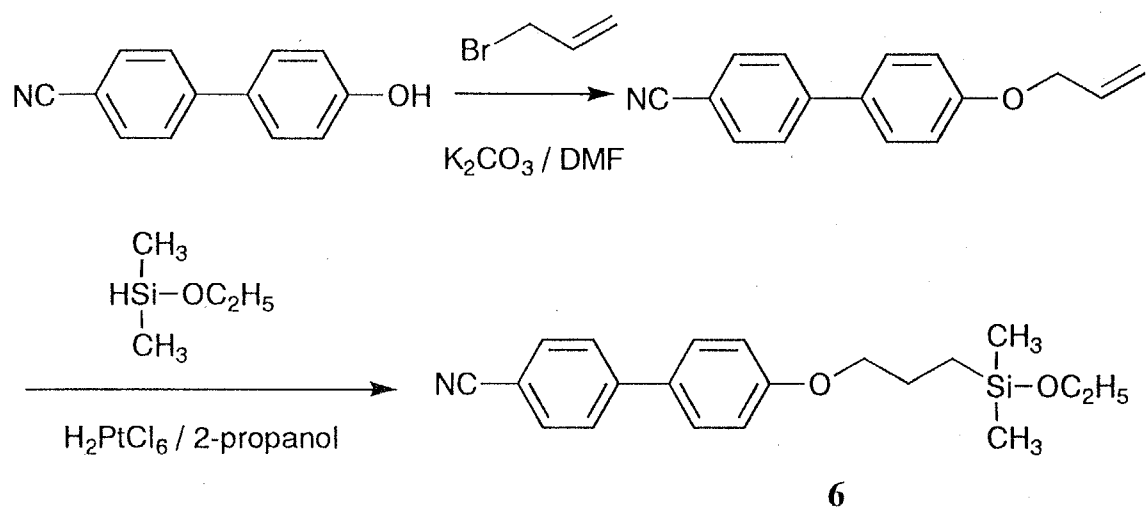
Scheme 3-2 Synthesis of **6**, **9** and **10**

44

mol) were added to a DMF solution of **7** (100 mg, 5.4×10^{-5} mol / 2 ml). The mixture was stirred overnight at room temperature, followed by a conventional workup. The desired compound, **8**, was purified by column chromatography (SiO_2, ethyl acetate:hexane = 1:1) and recrystallization from 2-propanol. Yield was 72 %.

mp = 80 - 81 °C

^{1}H-NMR (in $CDCl_3$):

δ (ppm) = 1.26 ppm (t, J = 7 Hz, 24H, CH_3), 1.7-2.3 (br, 16H, CH_2CH_2CH), 3.9-4.1 (br, 16H, OCH_2CH_2), 4.20 (q, J = 7 Hz 16H, CH_2CH_3), 4.28 (s, 16H, OCH_2CO), 4.6-4.9 (br, 4H, CH), 6.23 (s, 4H, Ar of CRA), 6.76 (s, 4H, Ar of CRA), 6.88 (d, J = 9 Hz, 8H, Ar of CB), 7.39 (d, J = 9 Hz, 8H, Ar of CB), 7.56 (s, 16H, Ar of CB)

Elemental Anal. for $C_{124}H_{124}N_4O_{28}$: Calcd. C: 70.30, H: 5.90, N: 2.64%.

Found C: 70.21, H: 5.85, N: 2.57%.

2,8,14,20-Tetra(4'-cyanobiphenyl-4-oxypropyl)-4,6,10,12,16,18,22,24-octa(carboxymetoxy)-calix[4]resorcinarene (5)

A mixture of a THF solution of **8** (40 mg, 1.0×10^{-5} mol / 5 ml) and an aqueous solution of KOH (120 mg, 2.2×10^{-3} mol / 5 ml) was stirred for 1 hr at room temperature. After addition of ether, the aqueous phase was separated and acidified with dilute hydrochloric acid to precipitate a white solid, which was centrifuged for isolation. A THF solution of the solid was treated with charcoal to give the product in a 63% yield.

mp = 211 - 213 °C

^{1}H-NMR (in DMSO-d_6):

δ (ppm) = 1.6-1.8 ppm (br, 8H, CH_2CH_2CH), 1.9-2.1 (br, 8H, CH_2CH_2CH), 3.9-4.1 (br, 16H, OCH_2CH_2), 4.28, 4.37, 4.49 and 4.58 (s each, 16H(1:2:2:1), OCH_2COO), 4.6-4.8 (br, 4H, CH), 6.49 (s, 4H, Ar of CRA), 6.76 (s, 4H, Ar of CRA), 6.84 (d, J = 9 Hz, 8H, Ar of CB), 7.46 (d, J = 9 Hz, 8H, Ar of CB), 7.61 (d, J = 8 Hz, 8H, Ar of CB), 7.74 (d, J = 8 Hz, 8H, Ar of CB)

Elemental Anal. for $C_{108}H_{92}N_4O_{28}$: Calcd. C: 68.49, H: 4.90, N: 2.96%.

Found C: 66.41, H: 6.13, N: 2.27%.

4-Cyano-4'-(2-propenyloxy)biphenyl

3-Bromopropene (1.65 g, 13.7 mmol) and 1.40g of K_2CO_3 (10.1 mmol) were added to a DMF solution of 4-cyano-4'-hydroxybiphenyl (1.45 g, 7.43 mmol / 100 ml), and the mixture was stirred for 2 hours at 120 °C. A solid was purified by column chromatography (SiO_2, chloroform) and recrystallization from methanol to give the desired product in a 32 % yield.

mp = 84.0 - 84.5 °C

Elemental Anal. for $C_{16}H_{13}NO$:　Calcd. C: 81.68, H: 5.57, N: 5.96%.

Found C: 81.59, H: 5.41, N: 6.12%.

3-(4'-Cyanobiphenyloxy-4)propyldimethylethoxysilane (6)

Dimethylethoxysilane (0.21 g, 2.0 mmol) was added dropwise to a mixture of toluene solution of 4-cyano-4'-(2-propenyloxy)biphenyl (0.25 g, 1.0 mmol / 2 ml) and 0.3 ml of a solution of H_2PtCl_6 in 2-propanol (0.02 mol/l). The solution was stirred for 6 hours at 120 °C. 6 as an oily substance was purified by column chromatography (SiO_2, toluene).

^{1}H-NMR (in $CDCl_3$):

δ (ppm) = 0.12 ppm (s, 6H, CH_3Si), 0.6-1.0 (m, 2H, CH_2Si), 1.16 (t, J = 7 Hz, 3H, CH_3), 1.6-2.1 (m, 2H, $CH_2CH_2CH_2$), 3.69 (q, J = 7 Hz 2H, CH_2CH_3), 3.97 (t, 2H, OCH_2CH_2), 6.98 (d, J = 9 Hz, 2H, Ar), 7.52 (d, J = 9 Hz, 2H, Ar), 7.66 (s, 4H, Ar)

Elemental Anal. for $C_{20}H_{25}NO_2Si$:　Calcd. C: 70.76, H: 7.42, N: 4.12%.

Found C: 71.02, H: 7.16, N: 4.38%.

4-Cyano-4'-propoxybiphenyl (9)

Propyl bromide (230 mg, 1.87 mmol) and 200 mg of K_2CO_3 (1.45 mmol) was added to a solution of 4-cyano-4'-hydroxybiphenyl (150 mg, 0.77 mmol) in acetone (30 ml). After the solution was refluxed for 10 hours, precipitates were removed by filtration, followed by evaporation of excess propyl bromide. The desired product was obtained as a white solid and recrystallized from methanol. A yield was 52 %

mp = 74.5 - 75.0 °C

Elemental Anal. for $C_{16}H_{15}NO$:　Calcd. C: 80.98, H: 6.37, N: 5.90%.

Found C: 81.22, H: 6.42, N: 5.71%.

1,2-Bis(3-bromopropoxy)benzene

To an ethanol solution of resorcinol (5.00 g, 0.0455 mol) was added 1,3-dibromopropane (75.0 g, 0.373 mol) and potassium hydroxide (8.57 g, 0.159 mol), and the mixture was refluxed for 5 hours.　After ethanol was evaporated, diethyl ether and water was added, and an ethereal layer was washed with water.　Evaporation of the solvent and unreacted 1,3-dibromopropane gave a pale brownish oil, which was subjected to silica gel column chromatography using a mixture of ethyl acetate and hexane (1/3) as an eluent to give white crystals of 1,2-bis(3-bromopropoxy)benzene in a 47.3 % yield after recrystallization from benzene-hexane.

mp = 63 - 64 °C

Elemental Anal. for $C_{12}H_{16}O_2Br_2$:　Calcd. C: 40.94, H: 4.58, Br: 45.39%

Found C: 42.56, H: 4.51, Br: 45.59%

1,4-Bis[3-(4'-cyanobiphenyloxy-4)propoxyl]benzene (10)

10 was also synthesized by the Williamson's reaction of 0.40g of 4-cyano-4'-hydroxybiphenyl (2.0×10^{-3} mol) with 0.32 g of 1,2-bis(3-bromopropoxy)benzene (9.1×10^{-4} mol) in the presence of 0.23 g of K_2CO_3 (1.7×10^{-3} mol) in 50 ml of 2-butanal under reflux for 6 hours.　The compound was purified by column chromatography (SiO_2, ethyl acetate : hexane = 1:3) and recrystallization from benzene - hexane.　A yield was 51 %

mp = 143.2 - 144.0 °C

Elemental Anal. for $C_{38}H_{32}N_2O_4$:　Calcd. C: 78.60, H: 5.55, N: 4.82%.

Found C: 78.32, H: 5.41, N: 4.97%.

3-2-2. Adsorption experiments

Fused silica plates (9 mm × 30 mm × 1 mm) were washed in acetone, a sodium hydroxide aqueous solution, nitric acid and sodium hydrogencarbonate aqueous solution ultrasonically, followed by washing with pure water after every step.　Fused silica plate were immersed in a THF solution of 6 in a concentration of 5×10^{-4} mol/dm^3 and heated at

47

100 °C for 20 min after washing with THF.   The preparation of a plate surface-modified with **5** (CB-CRA plate) was performed by immersion of a silica plate in a 1×10^{-5} mol/l THF solution of **5**, followed by washing with acetone ultrasonically.

3-2-3. Partial desorption of **5**

A silica plate modified with **5** from CB-CRA according to the above-mentioned procedure was subjected ultrasonical treatment in methanol for 10min, followed by washing with acetone.

3-2-4. Assembly of liquid crystal cells

A drop of a liquid crystal was put on a CB-modified plate, which was covered with a silica plate modified with lecithin, to fabricate a cell fixed with clips.

3-2-5. Physical measurements

Absorption and fluorescence spectra were taken on a HITACHI UV320 spectrometer and an F4000 fluorospectrometer, respectively.   The excitation wavelength of fluorescence spectra was 300 nm.

3-3. Results and discussions

3-3-1 Sample preparation

A crown isomer of calix[4]resorcinarene (CRA) possessing four cyanobiphenyl (CB) groups at the lower rim and eight carboxyl acid units at the upper rim, 2,8,14,20-tetra(4'-cyanobiphenyl-4-oxypropyl)-4,6,10,12,16,18,22,24-octa(carboxymethoxy)calix[4]-resorcinarene (**5**), was prepared as a CRA-CM adsorbate, as shown in Scheme 3-1.   The Williamson's reaction of the iodopropyl derivative of CRA-CM (**7**)[7] with 4-cyano-4'-hydroxybiphenyl gave the corresponding octaester (**8**), which was subjected to alkaline hydrolysis.   4-Cyano-4'-propoxybiphenyl (**9**) as a monomer model compound and 1,4-bis[3-(4'-cyanobiphenyloxy-4)propoxyl]benzene (**10**) as a dimer model compound were also synthesized.   **10** has two CB units, which are linked to benzene ring at *meta-*

positions through propyloxy spacer in a manner similar to 5 and 8. For comparative studies, 3-(4'-cyanobiphenyloxy-4)propyldimethylethoxysilane (6) was synthesized for the chemisorption of CB unit on a silica surface.

3-3-2. Fluorescence of cyanobiphenyl derivatives in solutions

Fluorescence spectra of the model compounds (9 and 10) and the octaester of 5 (8) were taken in cyclohexane and THF are shown in Figures 3-1 and 3-2. The concentrations were low enough to eliminate the possibility to form intermolecular excimer. The dimer model (10) displayed excimer fluorescence in less polar cyclohexane, whereas a fluorescence spectrum was almost identical with that of the monomer model compound (9) in more polar THF. These facts mean that it is profitable for two CB linked to10 to be close in cyclohexane and far in THF in which 10 was well solvated. In other words, solvation of THF results in the separation of the two fluorophoric units to suppress intramolecular excimer formation. On the other hand, 8 showed an emission band at a longer wavelength region in both solvents. The fluorescence of 8 in cyclohexane was almost the same as that of the dimer model (10), which shows intramolecular excimer emission. A shoulder was observed at a longer wavelength region even in THF of 8, in contrast to fluorescence of 8 and 10 in THF, possessing solely monomer emission. This is because CB units of 8 are positioned close to each other even in a polar solvent, reflecting the restricted conformation.

3-3-3. Fluorescence of CB moieties on a silica surface

The surface modification of a silica plate with 5 was conveniently carried out by dipping a silica plate in a dilute solution of 5 through multi-site hydrogen bonds between COOH groups of the macrocyclic amphiphile and surface silanols of silica.[7,13] The surface density of CB on the plate was estimated to be 1.8 units/nm^2 spectroscopically. Because the molecule has four CB units, this density corresponds to an occupied area of 2.2 nm^2/molecule for a CB-modified CRA-CM molecule. This value is in line with the other CRA-CM derivatives,[7,10] supporting that the molecular packing is determined specifically by the base areas of CRA-CM skeleton. The plate thus prepared is abbreviated a CB-CRA plate.
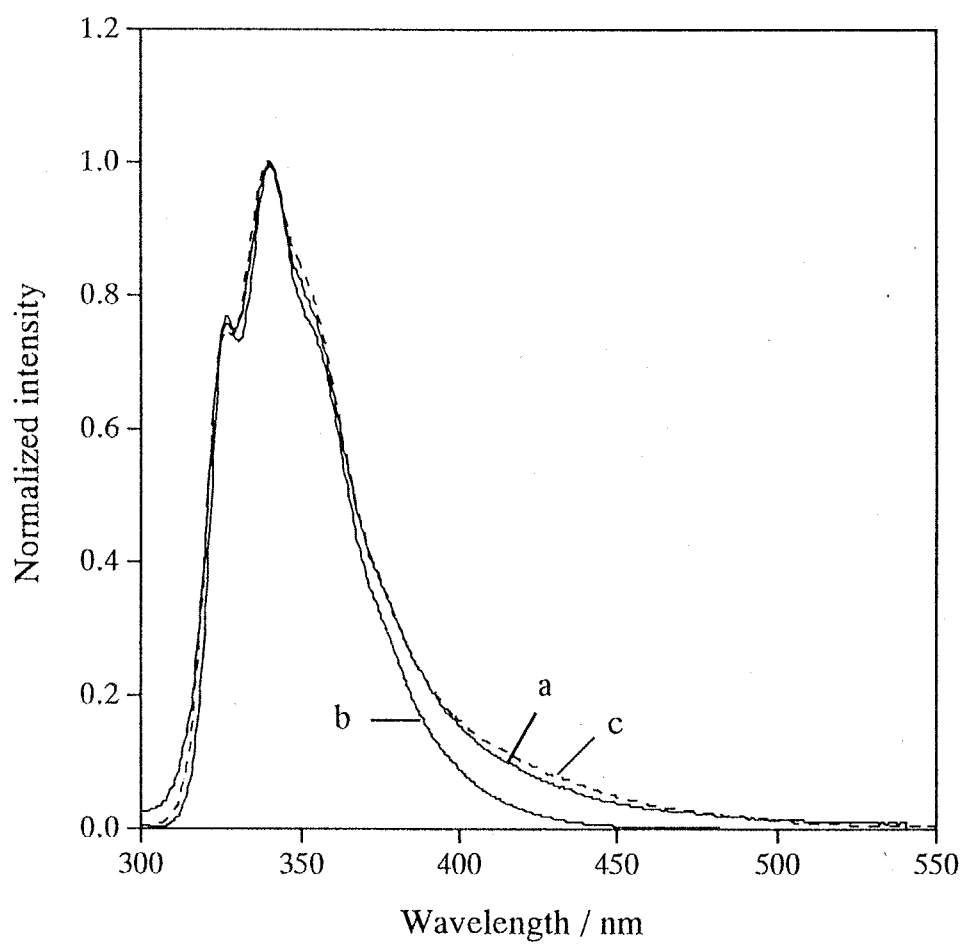
Figure 3-1 Fluorescent spectra of ethyl ester CRA (**8**) (a, solid line) and

model compounds (**9** (b) and **10** (c, broken line)) in cyclohexane solutions
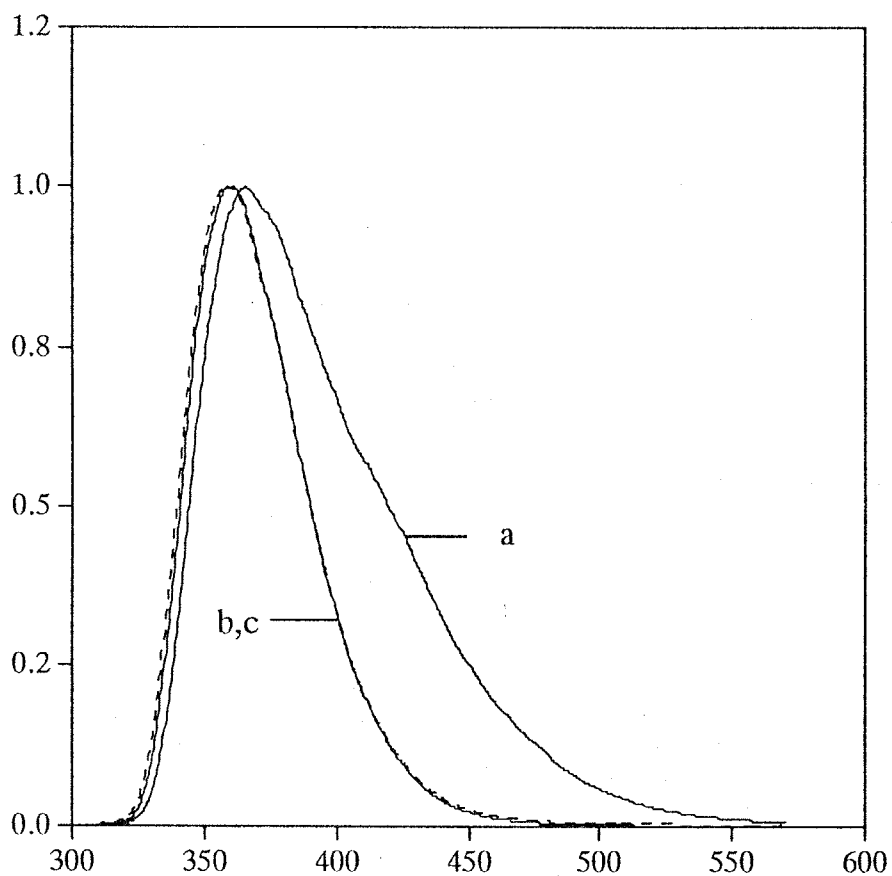
Figure 3-2 Fluorescent spectra of ethyl ester CRA (**8**) (a) and model

compounds (**9** (b, solid line) and **10** (c, broken line)) in THF solutions

6 was chemisorbed on a fused silica plate through O-Si-O bonds according to the conventional procedure.[14] The density of CB was 1.9 molecules/nm^2. Note that this value is not far from the density of residual silanols on a silica surface, suggesting efficient coverage of a silica surface by the silylation.[15-16] The plate treated with 6 is abbreviated as CB-SiMe2 plate for further discussion.

Fluorescence spectra of both modified silica plates are shown in Figure 3-3. It is worthy to note that fluorescent intensity of CB-CRA plate is extremely weaker when compared with CB-SiMe2 plate; the former was one twenty fourth (1/24) of the latter in the intensity, whereas adsorbed amounts of CB units were not far from each other. It is hard to explain such marked fluorescence quenching for the CB-CRA plate, but it is likely that CB is packed so densely on the plate that energy migration followed by non-radiative deactivation occurs efficiently. In order to check this assumption, the loading of the CB on a CB-CRA plate was reduced by treatment with methanol to cause partial desorption of 5. A UV absorption spectrum shown in Figure 3-4 indicates that an amount of CB adsorbed on the plate is reduced approximately by half. λmax of the plate treated with methanol suffers from a slightly red-shift, suggesting the reduction of interactions between the CB units at ground state. On the other hand, the fluorescent intensity of the plate of the low loading of CB was almost twice of the CB-CRA plate before washing with methanol, whereas a shoulder at a long wavelength region disappears for the plate with the low CB loading. These results are in line with the above-mentioned assumption that the fluorescence quenching for the CB-CRA plate comes from the high density of CB units on a surface.

The fluorescent maximum appears at 367 nm for the CB-CRA plate, while the CB-SiMe2 plate has the maximum at 378 nm, suggesting that micropolarity around the CB on the former plate is higher than that of the latter, as discussed in chapter 2. This situation implies that the CB of the CB-SiMe2 plate lies much closer to a polar silica surface of fused silica probably because of the flexible spacer chain. There is a slight difference in the spectral shape between the two plates. A shoulder exists at long wavelength region for CB-CRA plate, suggesting the partial formation of excimer.
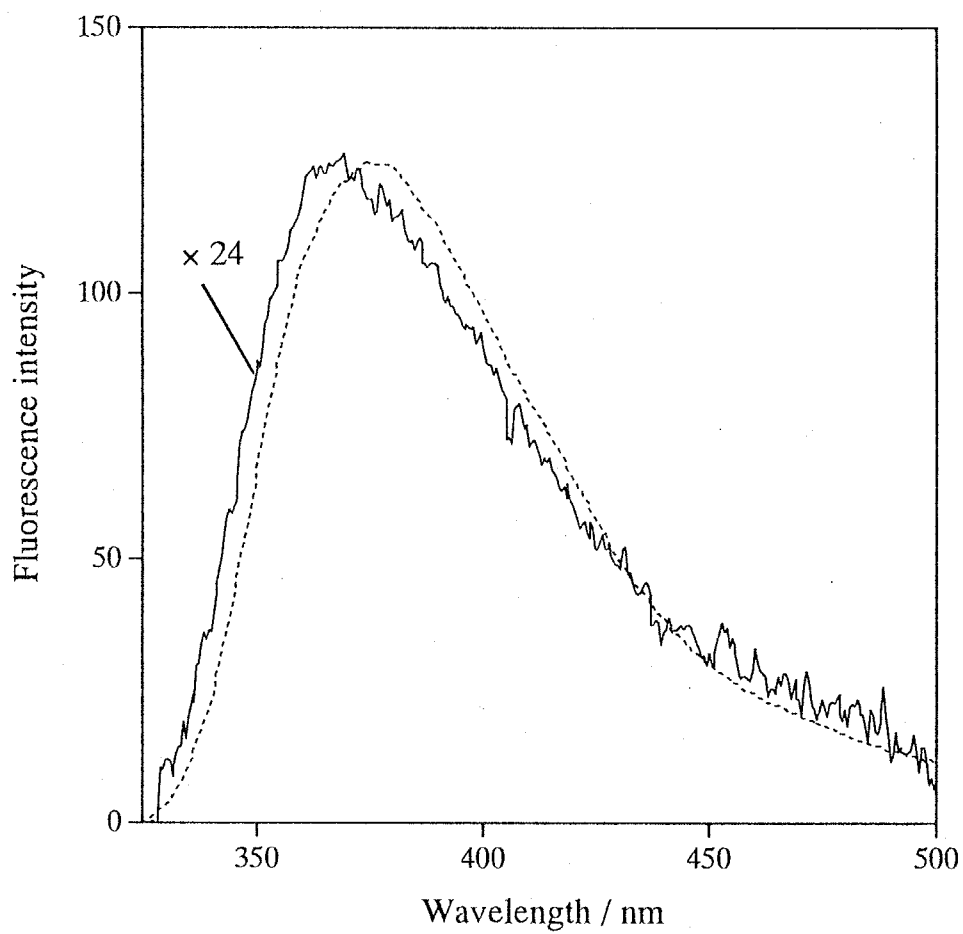
Figure 3-3 Fluorescent spectra of CB-CRA plate (solid line) and

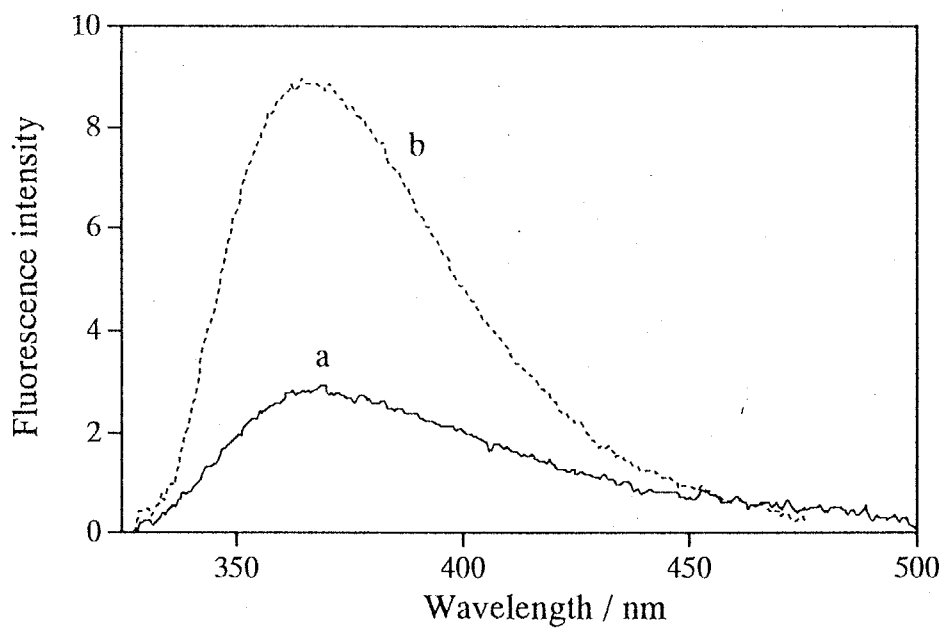CB-SiMe2 plate (dot line) in air atmosphere
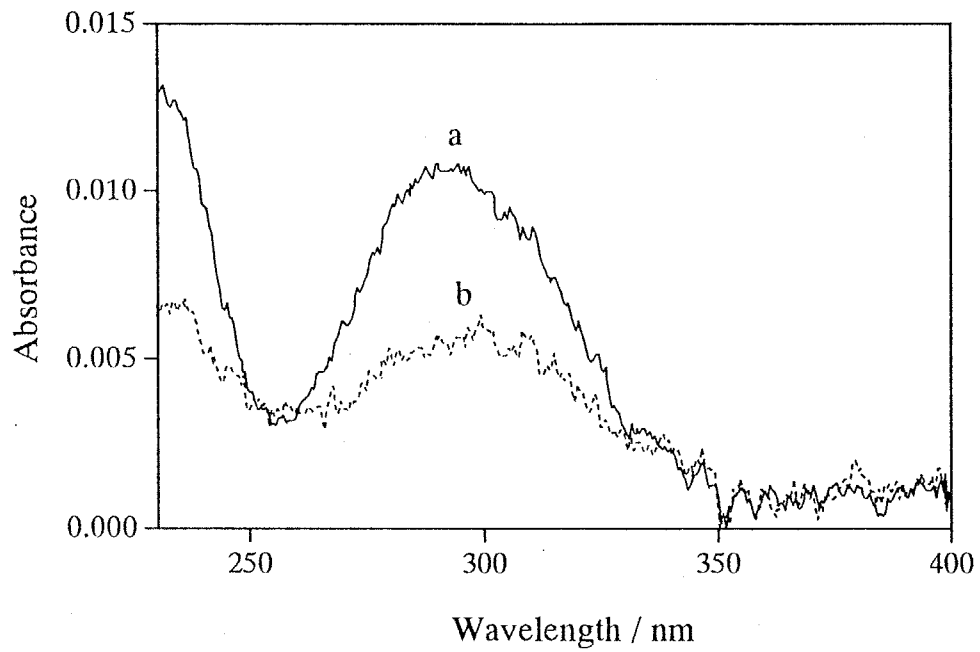
Figure 3-4　Absorption and fluorescent spectra of thinned CB-CRA

plate (b, dot line) compared with original CB-CRA plate (a, solid line)

in air atmosphere

3-3-4. Fluorescence of CB-modified silica plates exposed to cyclohexane

Figure 3-5 shows fluorescence spectra of the both plates immersed in cyclohexane. Whereas the emission intensity of a CB-CRA plate is still weaker than that of a CB-SiMe2 plate, relative intensity of the former is partially recovered. The intensity is three times larger when compared with the fluorescence measured in the air. The fluorescent maximum was blue shifted up to 355 nm, while a shoulder in a long wavelength region disappears as a result of the exposure to the solvent, implying a significant role of cyclohexane molecules as a diluent. Consequently, the enhancement of fluorescence induced by the exposure to cyclohexane is originated from the suppression of direct molecular interactions between CB units due to the dilution effect of solvent molecules, likely leading to a decrease in fractions of energy migration path and non-radiative deactivation. The blue-shift and disappearance of shoulder imply that the polarity around CB units become lower and ratio of excimer did not form because relative position of CB each other. On the other hand, a fluorescence spectrum of a CB-SiMe2 plate was essentially not altered by the exposure to cyclohexane, indicative of no marked dilution effect of the solvent.

3-3-5. Fluorescence of CB-modified silica plates in contact with a liquid crystal

Fluorescence spectra of CB-modified plates were taken after wetting with a nematic liquid crystal with polarity similar to that of cyclohexane. As shown in Figure 3-6, the fluorescent intensity of CB-SiMe2 plate was one sixth (1/6) compared with CB-CRA plate in liquid crystal. The spectral shape of CB-CRA plate was essentially the same as that taken in cyclohexane, suggesting that molecular interactions between liquid crystal molecules and CB units on the CB-CRA plate are similar to those between cyclohexane and the CB. In contrast to the CB-CRA plate, a CB-SiMe2 plate wetted with the liquid crystal displayed a blue shift of the fluorescence maximum from 378 nm to 372 nm, while a shoulder at a long wavelength region decreased. As mentioned just above, cyclohexane exhibits no role in fluorescence behavior of the CB on the CB-SiMe2 plate. In a contrast, liquid crystal molecules show the significant effect on the fluorescent behavior, indicating a specific interaction of the mesogenic molecules with mesogenic CB units even on the CB-SiMe2.
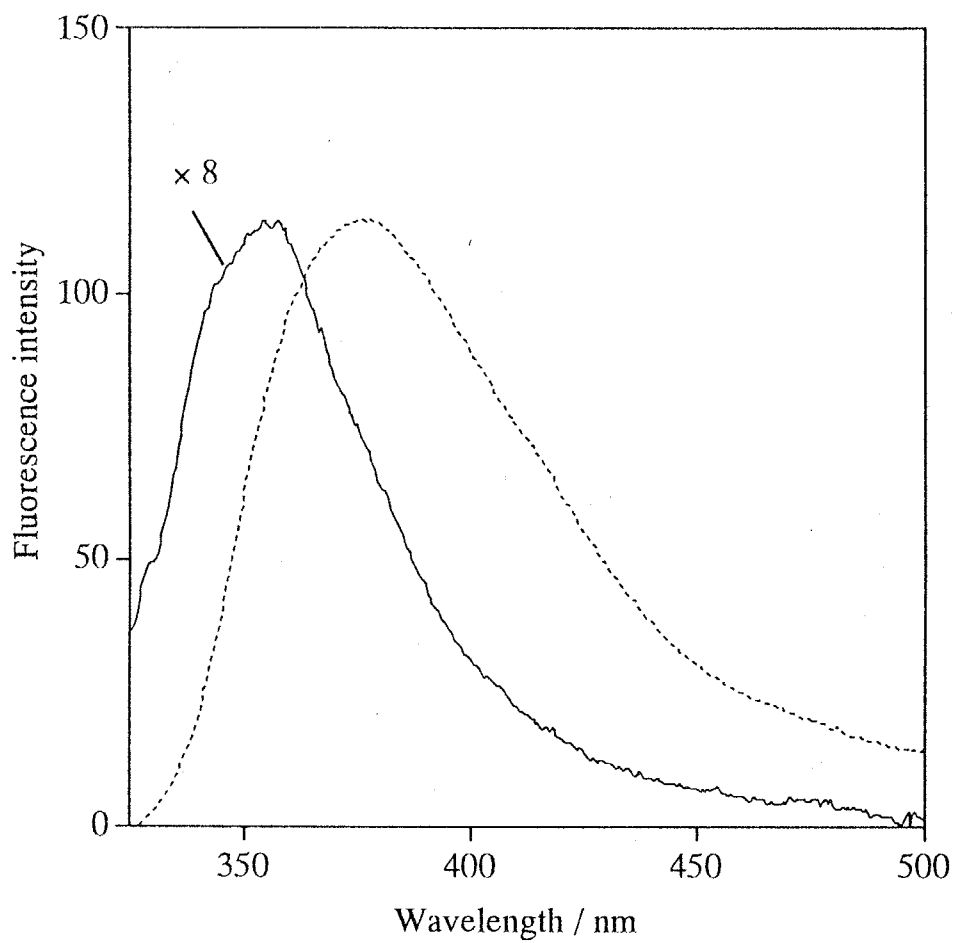
Figure 3-5 Fluorescent spectra of CB-CRA plate (solid line) and CB-SiMe2 plate (dot line) immersed in cyclohexane

Fluorescence spectra shown in Figure 3-6 indicate also that the microenvironmental polarity around the CB units on a CB-CRA plate is still much lower than that on CB-SiMe2 plate even the effective interactions of the less polar liquid crystal. The interplay among the CB units on the CB-CRA is still maintained owing dense packing to cause energy migration and the subsequent non-irradiation deactivation more effectively, when compared the CB-SiMe2 plate.

Figure 3-7 shows fluorescence spectra of both CB-modified plates as a function of time after the contact the liquid. The fluorescent intensity of the CB on a CB-SiMe2 plate decreased gradually and markedly, whereas no change was observed for a CB-CRA. These results show that specific interactions of the CB residues with liquid crystal molecules occurs very slowly on the CB-SiMe2 plate, while intermolecular interactions for the CB-CRA/liquid crystal system are complete before the measurement. The intermolecular interactions of the CB with liquid crystal molecules on the former plate result in the conformational rearrangement of the fluorescent moieties to cause the enhancement of efficiencies of energy migration and non-irradiation deactivation leading to fluorescence self-quenching. This kind of contrastive behavior between the two CB-modified plates reflects evidently the difference in the level of conformational restriction of the spacers linking the CB on a silica surface.

In order to obtain further information about the effect of chemisorption methods on interactions of the CB with liquid crystals, liquid crystal cells were assembled by sandwiching the nematics between a CB-modified plate and a lecithin-treated silica plate. The modification with lecithin gives rise homeotropic (perpendicular) alignment of liquid crystals so that liquid crystal alignment in the hybrid cells is determined solely by the CB-modified plate. When a CB-CRA plate was used, a random parallel texture just after the cell assembly was transformed into homeotropic alignment, as visualized by polarized micrographs shown in Figure 3-8 (a and b). A CB-SiMe2 plate resulted also in random parallel alignment after the cell assembly. The alignment was changed only partially into homeotropic one even after prolonged storage for a month at room temperature (Figure 3-8 (c and d)). The results disclose clear-cut dependence of liquid crystal alignment on the nature of spacers.
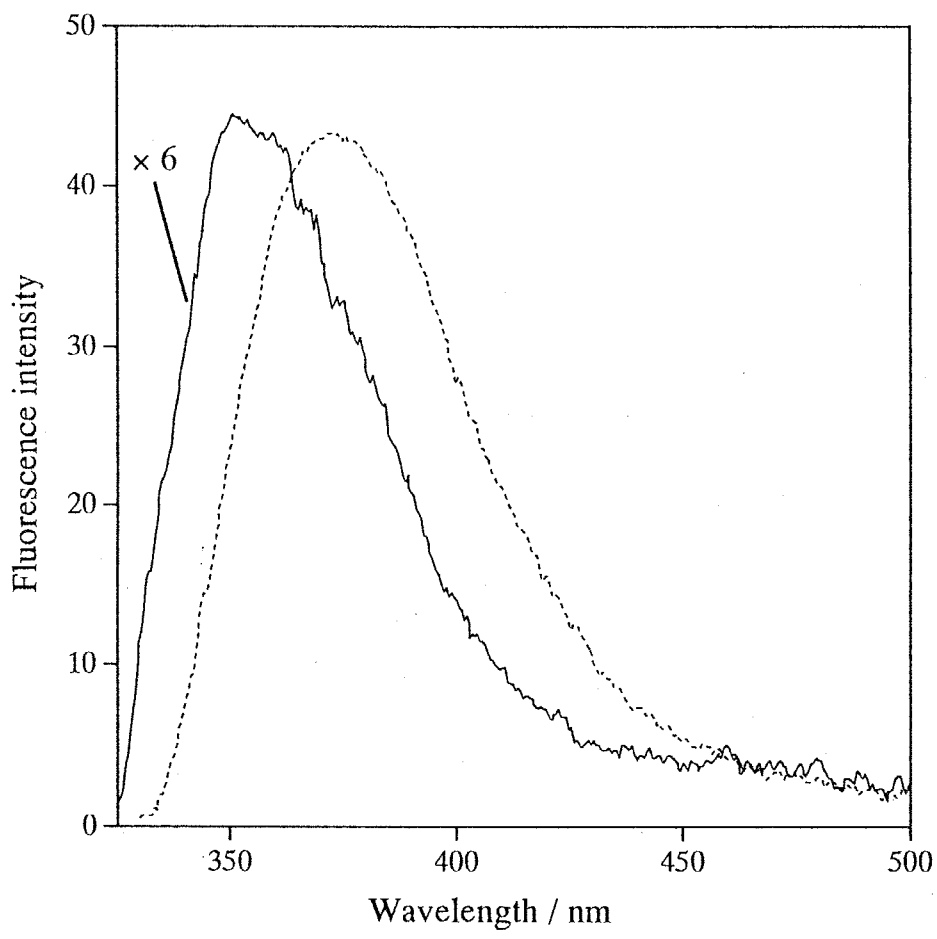
Figure 3-6 Fluorescent spectra of CB-CRA plate (solid line) and

CB-SiMe2 plate (dot line) immersed in the liquid crystal
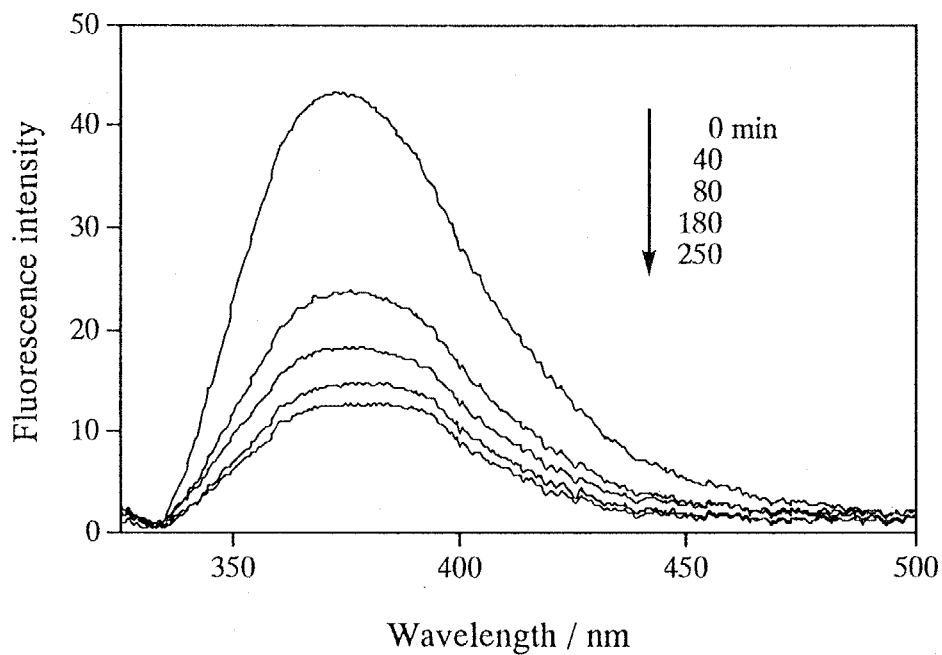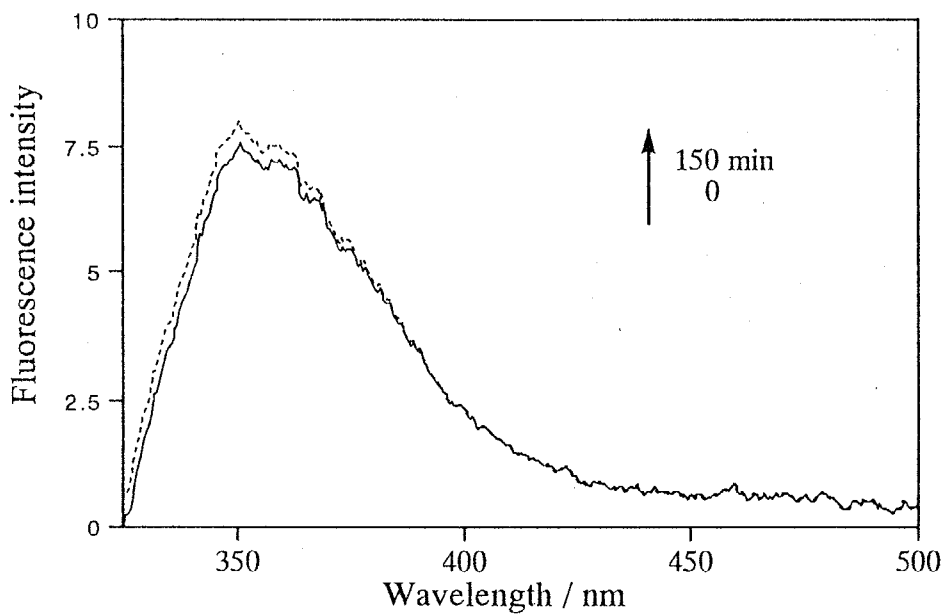
Figure 3-7 Time dependence of fluorescent spectra of CB-CRA plate

(upper) and CB-SiMe2 plate (lower) after immersing in the liquid crystal

(a)   (b)

(c)   (d)
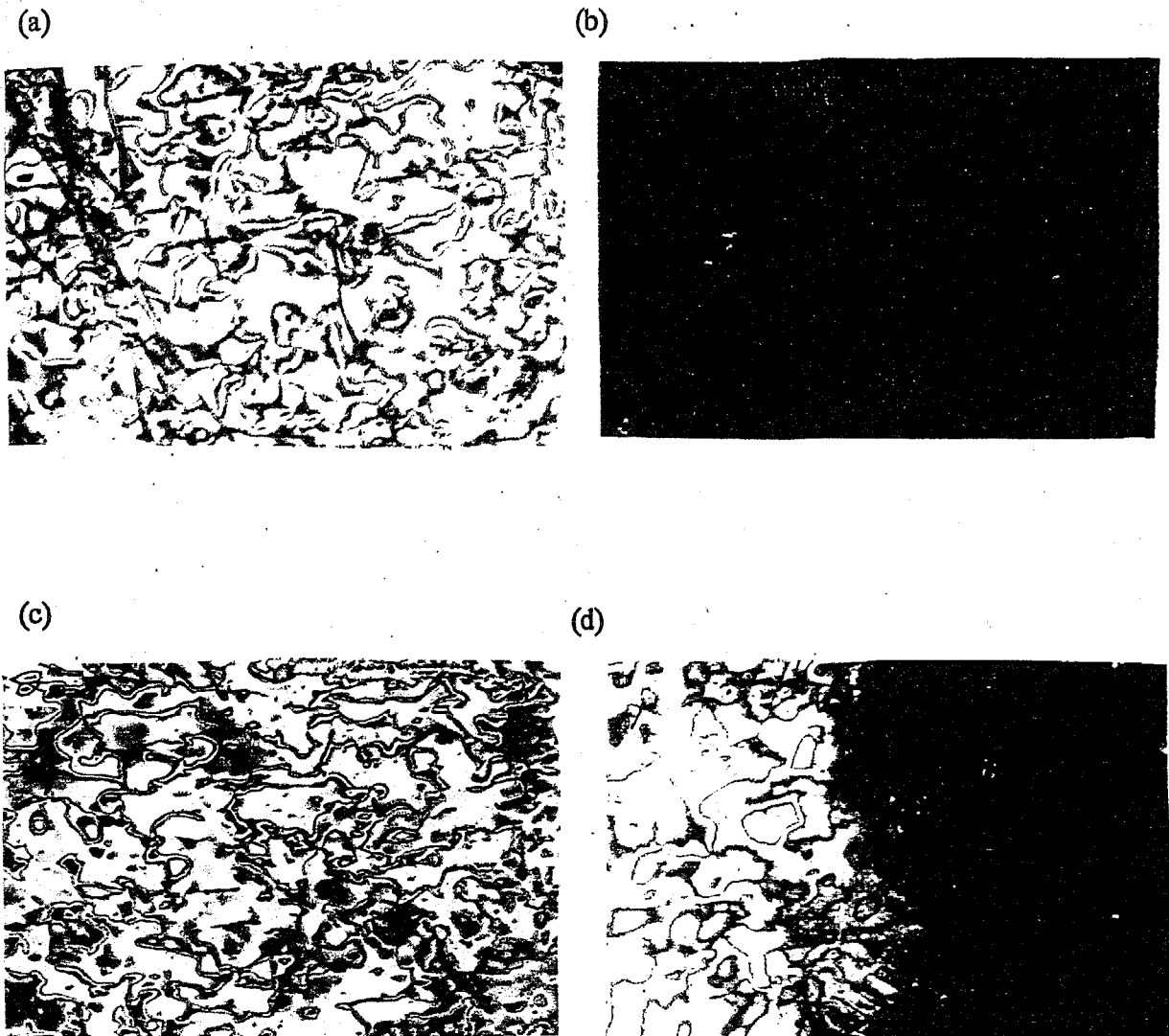
Figure 3-8 Polarized micrographs of liquid crystal celles with a CB-CRA plate
(a, b) or a CB-SiMe2 plate (c, d) and a lecithin-modified plate. Just after (a, c)
and 3 hours after (b, d) preparation of the cell.

(a) planer, (b) homeotropic, (c) planer, (d) partial planer and partial homeortopic

3-3-6. Microenvironments of CB moieties at interfaces

Based on the results shown above, pictures illustrating dynamic aspects of the surface CB units are shown in Figure 3-9. At an air/solid interface, the CB of a CB-CRA plate with a dense packing of the CRA base skeleton is forced to be stretched out from a surface owing to the rigidity of the cyclic skeleton so that intimate molecular interactions among CB moieties are generated. This situation results in efficient migration of single state energy, followed by non-radiative deactivation, leading to mark self-quenching of fluorescence (Figure 3-9 (a)). This situation was confirmed by the reduction of a CB-loading. On the other hand, CB units on a CB-SiMe2 plate lie on a polar silica surface.

When a CB-CRA plate is exposed to cyclohexane, the CB suffers from a reorientational change as a result of interactions with cyclohexane molecules, which exhibit a dilution effect on the CB packing state so that a partial recovery of fluorescence is generated (Figure 3-9 (b)). In the case of a CB-SiMe2 plate, no orientational alteration of CB is induced even upon exposure to cyclohexane, probably because its interactions with less polar solvent is suppressed owing to relatively high polarity of CB unit.

The orientational transformation of CB residues on a CB-CRA is also induced by wetting with a nematic liquid crystal, reflecting intimate interactions of the mesogenic CB moiety with liquid crystal molecules (Figure 3-9 (c)). The wetting of a surface of a CB-SiMe2 plate with a liquid crystal causes also the reorientation of the CB, though a rate and a level of the orientational change is much slower than those for a CB-CRA plate. This is probably due to a low compatibility of a CB molecular layer with the liquid crystal because of the following reasons. First, the CB on a CB-SiMe2 is densely packed in a molecular layer, while a free space is ensured for CB units on a CB-CRA plate since the packing density of the adsorbate is determined specifically by the CRA moiety. It follows that the penetration of liquid crystal molecules into a CB-CRA layer occurs more when compared with a CB-SiMe2 molecular layer. The difference in this kind of situation results in the efficiencies of alignment of the liquid crystal filled in cells surface-modified with CB layers.
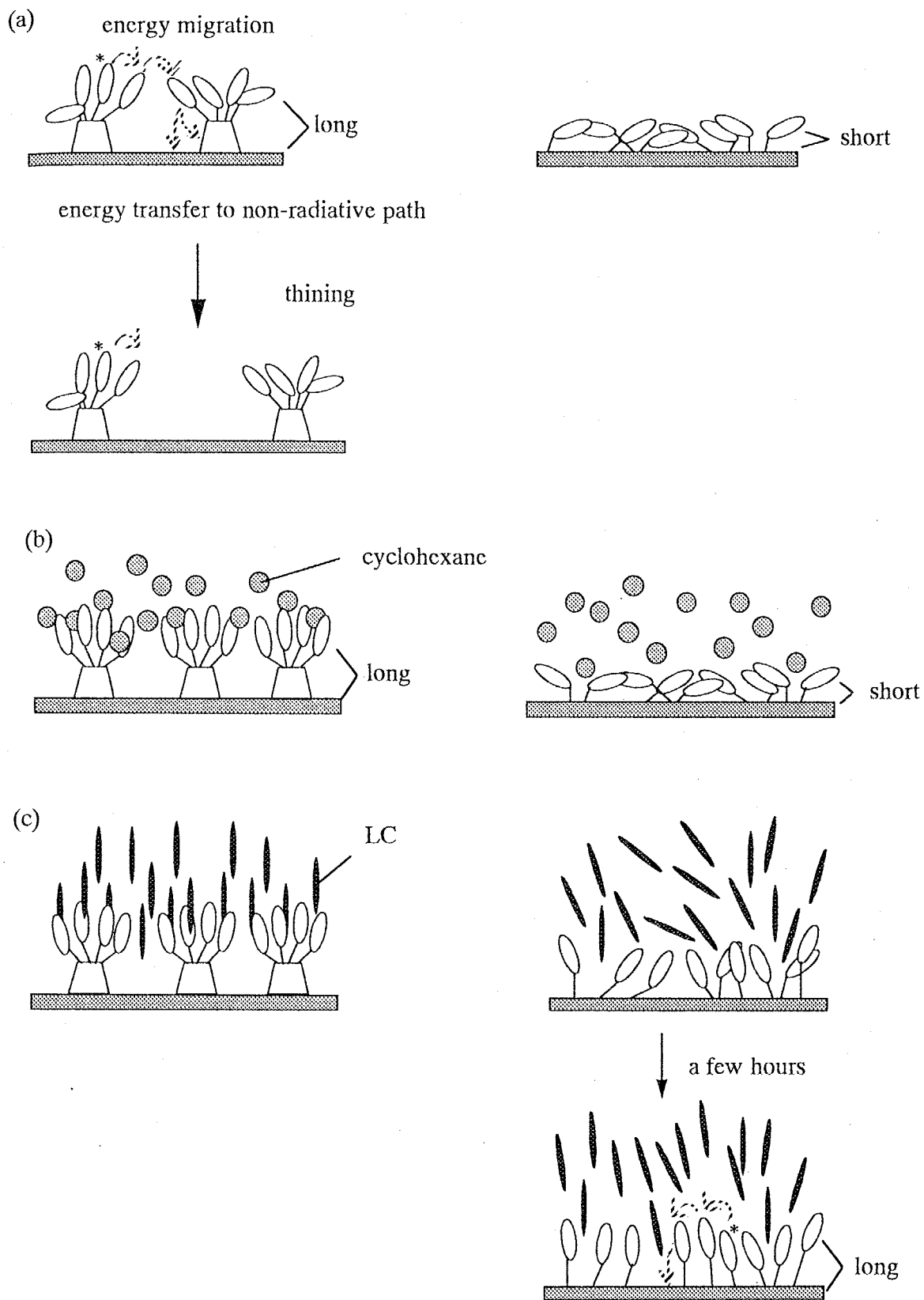
Figure 3-9 Microenvironments of CB moeties at the interface of CB-CRA plate
(right) and CB-SiMe2 plate (left) and (a) air atmosphere, (b) cyclohexane and (c)
the liquid crystal

3-4. Conclusions

Comparative studies on fluorescence behavior of CB units were performed by the preparation of molecular films through the surface adsorption of a CRA derivative to give a CB-CRA plate and the silylation of a CB derivative to prepare a CB-SiMe2 to extract effects of the linkage of the fluorescent probe to a silica surface. A calix[4]resorcinarene with four CB units at the lower rim (CB-CRA) showed excimer emission at long wavelength not only in a less polar solvent, but also in a polar solvent, meaning that the CB units are faced closely to each other because of the rigidity of the macrocyclic skeleton. The CB-CRA substituted with eight COOH groups at the upper rim forms densely packed SAM on a silica plate from its dilute THF solution owing to multi-site adsorptivity. The self-assembled CB units introduced to a silica surface using CB-CRA exhibits a marked self-quenching of fluorescence, when compared with the emission of the CB tethered to a silica surface through the silylation. This situation may arise from efficient energy migration among excited singlet state CB molecules in a CB-CRA monolayer owing to the dense packing leading to non-radiative deactivation.

When a CB-CRA plate is immersed in cyclohexane, fluorescence of the CB is partially recovered, whereas no change in both fluorescence intensity and spectral shape is induced for a CB- upon even exposure to the solvent. The difference in such emission behavior between the two kinds of plates is ascribable to difference in compatibility of molecular films with cyclohexane. A CB layer derived from CB-CRA possesses a free space since the packing density is specifically determined by the CRA moiety so that the reorientation of CB moieties is caused as a result of a dilution effect of the solvent. On the other hand, a CB molecular film chemisorbed on a CB-SiMe2 is so densely packed that relatively polar CB residues exhibit less compatibility with less polar cyclohexane.

The level of molecular interactions of the CB with a less polar liquid crystal is also influenced crucially by the method of surface modification. The wetting of a C plate with the liquid crystal induces gradual decrease in fluorescence intensity of the CB, while no modification is observed for a CB-CRA plate. This kind of the different behavior of the fluorescent probe suggests also that intimate interactions are affected by the methods of attachment of the CB. This situation was confirmed the observation that a CB-CRA plate brings about homeotropic alignment of the liquid crystal, whereas homeotropic

alignment occurs insufficiently for a CB-SiMe2 plate.

In conclusion, fluorescence measurements of CB as an emission probe provide vivid information concerning intra- and intermolecular interaction s at interfacial regions.

References

1. K. Ichimura, *Chem. Rev.*, 2000, **100**, 1847.

2. Y. Kawanishi, T. Tamaki, M. Sakuragi, T. Seki and K. Ichimura, *Langmuir*, 1992, **8**, 2061.

3. K. Ichimura, *"Photochemical Processes in Organized Molecular Systems"* ed. by K. Honda, Elsevier, 1991, 343.

4. K. Ichimura, Y. Hayashi, H. Akiyama and N. Ishizuki, *Langmuir*, 1993, **9**, 3298.

5. K. Ichimura, Y. Hayashi, K. Goto and N. Ishizuki, *Thin Solid Films*, 1993, **235**, 101.

6. H. Akiyama, Y. Akita, K. Kudo and K. Ichimura, *Mol. Cryst. Liq. Cryst.*, 1996, **280**, 91.

7. K. Ichimura, N. Fukushima, M. Fujimaki, S. Kawahara, Y. Matsuzawa, Y. Hayashi and K. Kudo, *Langmuir*, 1997, **13**, 6780.

8. Y. Hayashi, T. Maruyama, T. Yachi, K. Kudo and K. Ichimura, *J. Chem. Soc. Perkin Trans. 2*, 1998, 981.

9. K. Ichimura, M. Fujimaki, Y. Matsuzawa, Y. Hayashi and M. Nakagawa, *Mat. Sci. Eng. C*, 1999, 353.

10. A. G. S. Hogberg, *J. Am. Chem. Soc.*, 1980, **102**, 6046

11. L. Abis, E. Dalcanale, A. Du vosel and S .Spera, *J. Org. Chem.*, 1988, **53**, 5475.

12. A. G. S. Hogberg, *J. Am. Chem. Sci.*, 1989, **111**, 5397.

13. E. Kurita, N. Fukushima, M. Fujimaki, Y. Matsuzawa, K. Kudo and K. Ichimura, *J. Mater. Chem.*, 1998, **8**, 397.

14. Y. Hayashi and K. Ichimura, K. *Langmuir*, 1996, **12**, 831.

15. L. T. Zhuravlev, *Langmuir*, 1987, **3**, 316.

16. D. W. Sindorf and G. E. Maciel, *J. Phys. Chem.*, 1982, **86**, 5219.

Chapter 4

Dicyanoanthracene as a fluorescent probe for studies on microenvironments at silica/fluid interfaces

4-1. Introduction

The major concern of this chapter is to propose a novel model for island-sea structures of polymer blends using a fluorescent probe to reveal microenvironments at interfaces between two different solid phases.   The system dealt with here consists of a polymer with phenanthryl (Phe) side chains and a silica surface-modified with 9,10-dicyanoanthracene (DCA) as a fluorescent probe.   This combination was selected on the basis on the following conditions.   First, a silica surface modified with organic residues can be assumed to be a model for a two-dimensional surface region so that the elucidation of interfacial phenomena is simplified.   Second, the combination of DCA with Phe provides a convenient system exhibiting exciplex emission, which gives a novel approach to revealing interfacial events since this kind of emission occurs specifically in cases where the two phases is in contact to each other.   Thirdly, DCA is selectively excited even in the presence of Phe because an absorption band of Phe lies at a shorter wavelength region compared to that of DCA $S_0 \rightarrow S_1$.   In this respect, DCA was bound on a silica plate surface covalently through silylation to give a surface-modified plate, a polymethacrylate with phenanthryl side chains were prepared.   Fourthly, excimer emission from DCA is minimized by an appropriate choice of conditions for surface modification of a silica to control surface density of the strongly fluorescent probe molecules.   The other concern of this chapter is to present the usefulness of DCA moiety as a fluorescent probe to evaluate the surface nature of silica, which is exposed to various solvents.   This is because fluorescence of DCA is significantly sensitive to solvent polarity so that fluorescence λmax gives information concerning microenvironmental polarity at an interface between a silica surface and a solvent.

4-2. Experimental

4-2-1. Materials

The compounds with DCA moieties and silyl units were synthesized as shown in Scheme 4-1. The structure and synthetic route of a polymer possessing Phe is shown in Scheme 4-2. 2-Carboxyanthracene and zone-refined phenanthrene were commercially available from Tokyo Kasei Kogyo Co., Ltd. and used as received. All the solvent was of a fluorometry grade purchased from Cica-Merck and used as received.

2-Carboxy-9,10-dibromoanthracene

This was synthesized according to a literature with a slight modification.[1] A solution of 3.8 g (24 mmol) of bromine in 5 ml of glacial acetic acid was added dropwise into boiling glacial acetic acid (50 ml) containing 2.6 g (12 mmol) of 2-carboxyanthracene. After reflux for 2 hours, the mixture was cooled down to room temperature to collect a crystalline precipitate which was recrystallized from 1-butanol to give 4.1 g (90 %) of yellow needle-like crystals.

mp = 332.5 - 333.0 °C

Elemental Anal. for $C_{15}H_8O_2Br_2$: Calcd. C: 47.41, H: 2.12, Br: 42.05%.

Found C: 48.02, H: 2.50, Br: 43.32%.

Methyl 9,10-dibromoanthracene-2-carboxylate

To a benzene solution (20 ml) of 140 mg (0.37 mmol) of 2-carboxy-9,10-dibromoanthracene was added 90 mg (0.76 mmol) of thionyl chloride and a few drops of DMF, and the solution was stirred for 2 hours at 70 °C, followed by adding 5 ml of methanol at room temperature and by stirring for 1.5 hours at 56 °C. The solution was washed with water, a diluted aqueous sodium bicarbonate solution, and finally with water. The evaporation and recrystallization from benzene yielded 98 mg (67 %) of greenish yellow crystals

mp = 221.0 - 221.5 °C

Elemental Anal. for $C_{16}H_{10}O_2Br_2$: Calcd. C: 48.77, H: 2.56, Br: 40.55%.

Found C: 48.22, H: 2.41, Br: 41.25%.

Methyl 9,10-dicyanoanthracene-2-carboxylate
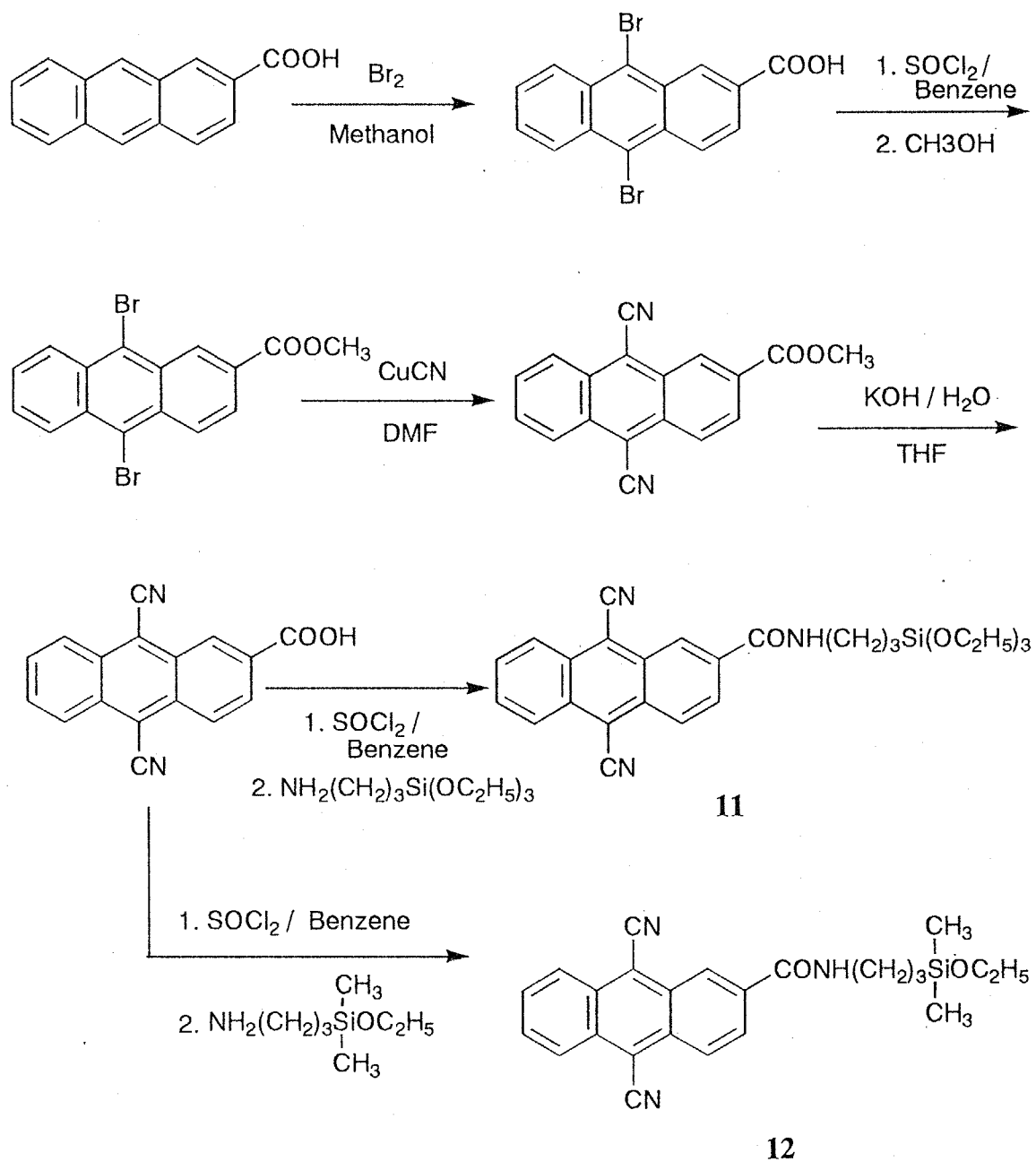
Scheme 4-1 Syntheses of **11** and **12**
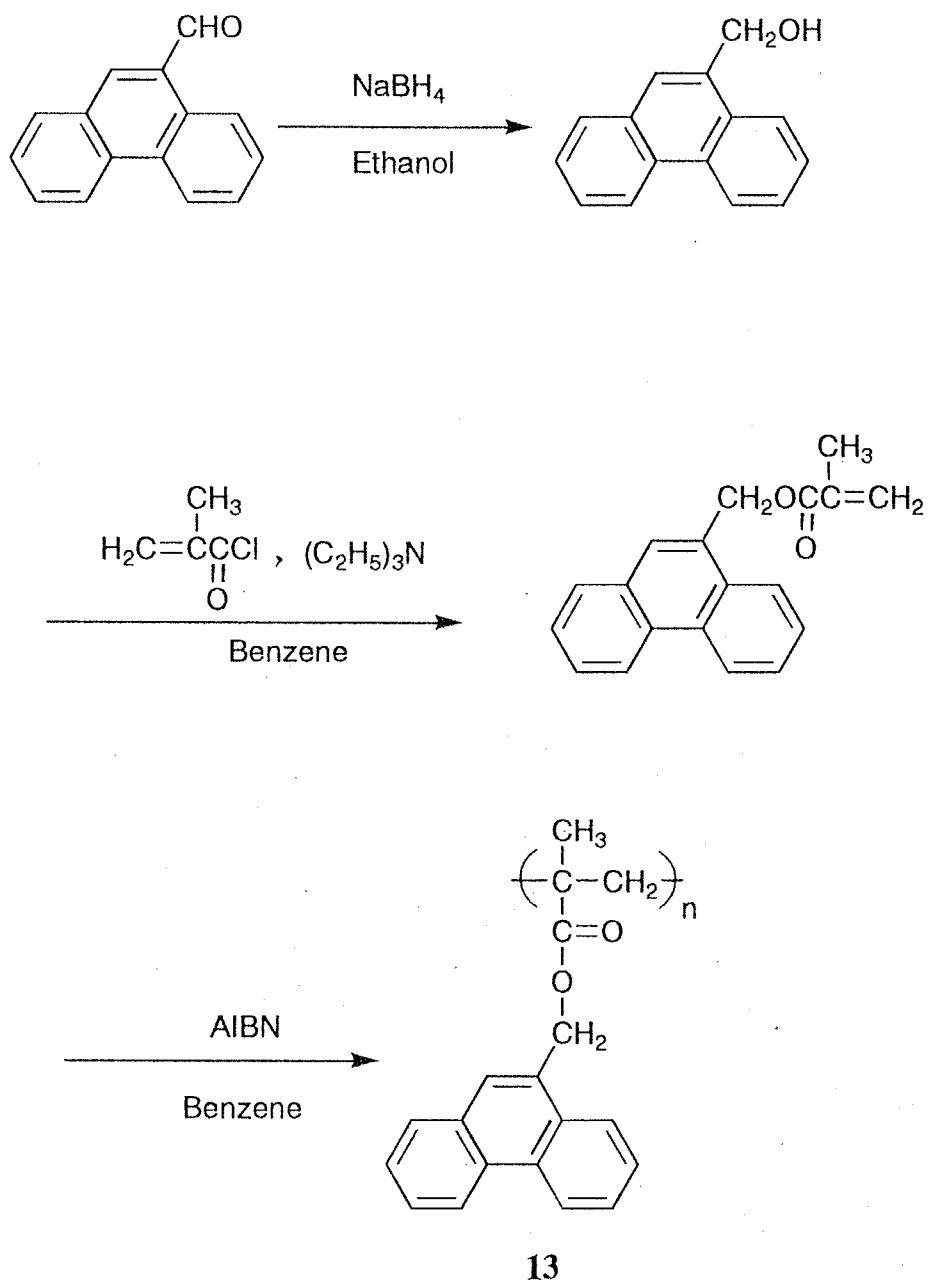
Scheme 4-2 Synthesis of **13**

A mixture of 100 mg (0.25 mmol) of methyl 9,10-dibromoanthracene-2-carboxylate and 58 mg (0.65 mmol) of CuCN in 20 ml of DMF was refluxed for 8 hours. An aqueous solution of NH_3 was added to the cooled mixture and extracted with chloroform. The extracts were washed with dilute hydrochloric acid and water and evaporated to dryness. A yellow solid product was purified by column chromatography on silica gel using benzene as an eluent, followed by recrystallization from benzene. Needle-like yellow crystals were isolated in a yield of 31 %.

mp = 247.5 - 249.0 °C

Elemental Anal. for $C_8H_{10}N_2O_2$:   Calcd. C: 75.52, H: 3.52, N: 9.79%.

Found C: 75.72, H: 3.51, N: 9.10%.

2-Carboxy-9,10-dicyanoanthracene

A mixture of a THF solution (310 ml) of methyl 9,10-dicyanoanthracene-2-carboxylate (160 mg, 0.56 mmol) and an aqueous solution (130 ml) of potassium hydroxide (180 mg, 3.2 mmol) was stirred for 4 hours at room temperature, followed by acidification with 12 N hydrochloric acid to yield yellow crystals. Recrystallization from acetone gave 120 mg needle-like yellow crystals.

mp.> 320 °C

Elemental Anal. for $C_{17}H_8N_2O_2$:   Calcd. C: 75.00, H: 2.96, N: 10.29%.

Found C: 74.53, H: 2.80, N: 10.19%.

## (N-(3-Triethoxysilylpropyl))-9,10-dicyanoanthracene-2-carboxamide (11)

To a benzene solution (10 ml) of 60 mg (0.22 mmol) of 2-carboxy-9,10-dicyanoanthracene was added 53 mg (0.45 mmol) of thionyl chloride and a few drops of DMF, and the solution was stirred for 1.5 hours at 70 °C. After an excess amount of thionyl chloride was removed under a reduced pressure, a residue was dissolved in benzene (10 ml). The solution was added dropwise to a solution of freshly distilled 3-aminopropyltriethoxysilane (50 mg, 0.22 mmol) and triethylamine (33 mg, 0.33 mmol) in 10ml benzene and stirred for 1 hour at 15°C. After evaporation of the solvent, a residual product was purified by column chromatography on silica gel with use of ethyl acetate as an eluent and recrystallized from a 10 : 1 mixture of hexane and chloroform to give 31 mg

of yellow crystals.

mp = 158 °C.

^{1}H-NMR (in CDCl$_3$):

δ(ppm) = 0.85 (t, 2H, CH$_2$Si), 1.25 (t, 9H, CH$_3$), 1.86 (m, 2H, CH$_2$CH$_2$CH$_2$), 3.60 (t, 2H, NHCH$_2$), 3.89 (q, 6H, OCH$_2$), 7.00 (br, 1H, NH), 7.85 (m, 2H, Ar), 8.25 (d, 1H, Ar), 8.55 (m, 3H, Ar), 8.80 (s, 1H, Ar)

Elemental Anal for C$_{26}$H$_{29}$N$_3$O$_4$Si,   Calcd. C: 65.66, H: 6.15, N: 8.83%.

Found C: 63.87, H: 5.66, N: 8.54%.

9-Phenanthrylmetanol

This was synthesized according to a literature.[2]   A dried methanol solution of 9-formylphenanthrene (2.5 g, 12 mmol) and NaBH$_4$ (0.23 g, 6.0 mmol) was refluxed for 1 hour.   After the solvent was evaporated, the product was recrystallized from acetone - hexane to produce 1.2 g of white needle-like crystals.

mp = 150.5 - 151.5 °C

Elemental Anal. for C$_{15}$H$_{10}$O: Calcd. C: 86.51, H: 5.81%.

Found, C: 86.36, H: 5.54%.

9-Phenanthrylmethyl methacrylate

To a cold benzene solution of 9-phenanthrylmethanol (500 mg, 2.4 mmol) and triethylamine (500 mg, 5.0 mmol), 500 mg (4.8 mmol) of methacroyl chloride was added stepwise.   After stirring for 2 hours, triethylamine chloride was removed by filteration, and the solvent was evaporated to give a solid, which was recrystallized from petroleum ether to give 330 mg of white needle-like crystals.

mp = 74.5 - 75.5 °C

^{1}H-NMR (in CDCl$_3$):

δ(ppm) = 2.00 (s, 3H, CH$_3$), 5.65 (br, s, 1H, trans-CH=), 6.15 (br, s, 1H, cis-CH=), 5.70 (s, 2H, CH$_2$), 7.7 (m, 7H, Ar), 8.7 (m, 2H, Ar)

Elemental Anal. for C$_{19}$H$_{16}$O$_2$:   Calcd. C: 82.61, H: 5.80%.

Found C: 82.36, H: 5.76%.

71

Poly(9-phenanthrylmethyl methacrylate) (13)

A 20 ml benzene solution of 9-phenanthrylmethyl methacrylate (200 mg, 0.73 mmol) and AIBN (1.0 mg, 6.1 μmol) in an ampoule was degassed, sealed and heated at 50 °C for 18 hours. The product was reprecipitated into methanol 3 times to give 150 mg of the desired.

$Mn = 4.7 \times 10^4$, $Mw = 5.6 \times 10^4$, $Mw/Mn = 1.2$

$Tg = 144 \, °C$

4-2-2. Surface modification of a silica plate

A fused silica plate (9 mm × 30 mm) was washed ultrasonically in acetone, conc. HNO_3, a saturated aqueous solution of sodium bicarbonate and water for 15 min in this sequence. The plate was immersed in a 0.05 wt% (1×10^{-3} mol/l) THF solution of (N-(3-triethoxysilylpropyl))-9,10-dicyanoanthracene-2-carboxamide (11) for 10 min and baked at 110 °C for 10 min and subjected to ultrasonical purification in THF for 10 min and in DMF for 30 min. For further treatment with trimethylchlorosilane, a surface-modified fused silica plate was immersed in a 5 wt% toluene solution of trimethylchlorosilane at 80 °C for 15 hours. The plate was washed ultrasonically in chloroform and DMF for 20 min, respectively.

4-2-3. Measurements

Absorption spectra were taken on a Hitachi UV-320 and fluorescent emission and fluorescent excitation spectra were taken on a Hitachi F-4010. Emission and excitation spectra of fused silica plates were measured with the use of an attachment for a film. The excitation wavelength for emission spectra was 385 nm due to the third peak of $S_0 \rightarrow S_1$ of the dicyanoanthracene chromophore while excitation spectra were taken by monitoring at 460 nm. All spectra of plates were corrected by that of a fused silica plate as a reference.

4-3. Results and discussions

4-3-1. Molecular design and synthesis

Fluorescent probe molecules reporting information concerning a solid/solution interface should satisfy the following conditions. First, a fluorescence quantum yield should be large because the number of molecules attached onto a solid surface is absolutely small. Second, a fluorophore should form an emissive exciplex with specific solute molecules. Thirdly, the probe molecules on a solid surface should not display excimer fluorescence because a fluorescence band of both exciplex and excimer fluorescence emerges usually at almost the same wavelength region. Fourthly, an excitation wavelength of a fluorescent probe should be well separated from an absorption wavelength region of the solute molecules. Finally, solute molecules should demonstrate no or extremely weak fluorescence compared with the probe fluorescence. These considerations had led us to select the combination of 9,10-dicyanoanthracene (DCA) as a fluorophore with phenanthrene as a solute molecule because this system satisfies the requirements stated above, as discussed below.

A fused silica plate was employed as a solid substrate here based on the following reasons. First, although specific molecular interactions between the surface photoactive units and liquid molecules play an essential role in the molecularly amplified phenomenon,[3-5] further information concerning the molecular interaction at the interface between the fused silica surface and liquid molecules are highly required to elucidate the working mechanism. Second, being different from the situation of polymer solids, the molecular motion of silica network is completely inhibited so that the aging effect due to the molecular motion of an uppermost layer of solids is thoroughly eliminated.

DCA having a carboxyl residue was prepared to condense with 3-aminopropyltriethoxysilane to afford a silylating reagent (11) for surface modification of a fused silica plate. The DCA derivative having dimethylethoxysilyl group (12), shown in Scheme 4-1, was also synthesized to attempt surface modification. The hydration and subsequent dimerization took place very rapidly, and an amount of DCA covalently bound on a fused silica plate was very small.

4-3-2. Spectra of a DCA derivative in solutions

In order to reveal spectroscopic properties of DCA, absorption and fluorescence

spectra of (N-(3-triethoxysilylpropyl))-9,10-dicyanoanthracene-2-carboxyamide (**11**) were measured in various solvents. As shown in Figure 4-1, absorption as well as emission maxima of the DCA are plotted against π^* scale expressing solvent polarity to exhibit a good linear relationship. Other solvent polarity parameters, such as dielectric constant, $E_T(30)$, donor number, acceptor number[18], displayed poor linear correlation with vmax in particular for chloroalkane solvent. The π^* scale is based on the solvatochromic effect of $p \rightarrow \pi^*$, $\pi \rightarrow \pi^*$ electronic transitions of compounds having a nitro or an amino group in solvents exhibiting no hydrogen-bond formation.[7] Negative correlation slopes for both absorption maxima and fluorescence maxima mean that DCA derivative (**11**) molecules are solvated strongly by solvents. The larger value of the correlation factor for the fluorescence implies that the solvation with larger π^* scale solvents takes place more effectively in an excited state than in the ground state.

Valley/peak values and Stokes' shifts are summarized in Table 4-1. The valley/peak value is a parameter of broadness of spectra[8] and useful when the vibrational bands are so broad that they overlap to each other. The "peak" corresponds to the height of the first vibrational band while the "valley" is defined as a minimum intensity between the first two vibrational bands. The larger the valley/peak value, the broader is the spectrum. The broadness of the absorption and emission spectra, as judged from valley/peak values, have positive correlation with π^* scale. This means that the transition energy distribution of DCA molecule becomes larger as a result of the effective solvation with solvents having larger π^* scale values. Stokes' shifts do not have good correlation with π^* scale values and can be rather classified into two groups; a smaller shift for aliphatic hydrocarbons and a larger one for the other solvents. Latter solvents have lone pairs and interact sufficiently with DCA with a strong electron acceptor character to result in a larger Frank-Condon energy.

4-3-3. DCA emission spectra on a fused silica surface

It was found that DCA emission on a fused silica plate was influenced markedly by the conditions of surface modification with **11**. The concentration of **11** and the nature of solvent played important roles in suppressing an excimer formation of DCA groups on a plate which is unfavorable for the present study on the exciplex probe technique.
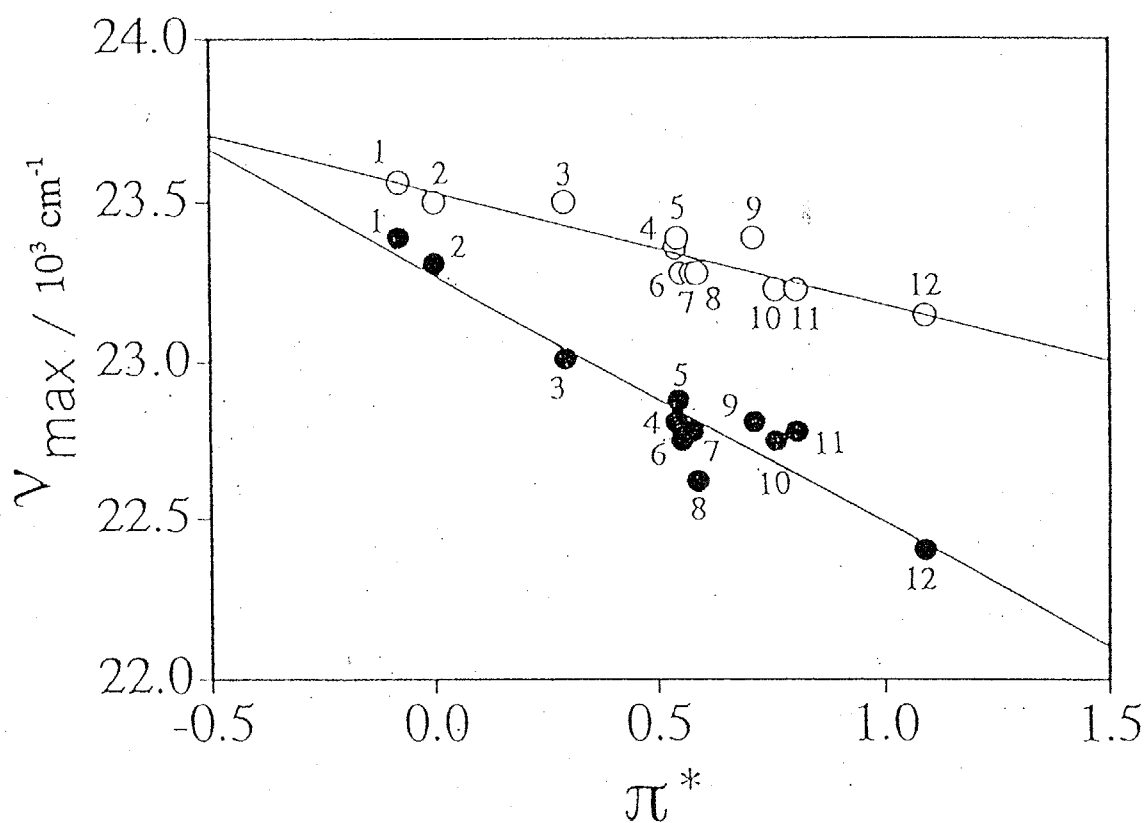
Figure 4-1. The correlation between vmax of absorption spectra (○) and fluorescence spectra (●) of **11** in solutions and π* scale values of the solvents; 1: hexane, 2: cycloh xene, 3: carbon tetrachloride, 4: ethanol, 5: ethyl acetate, 6: 1,4-dioxane, 7: tetrahydrofuran, 8: benzene, 9: acetonitrile, 10: chloroform, 11: 1,2-dichloroethane, 12: water

Table 4-1. Valley/Peak values of absorption and fluorescence spectra and Storkes' shift values

solvent	solution of 11			surface-modified quartz plate immersed in a solvent			surface-blocked quartz plate immersed in a solvent		
	Valley/Peak		Stokes' shift	Valley/Peak		Stokes' shift	Valley/Peak		Stokes' shift
	abs.	fl.	$/10^3$ cm^{-1}	ex.	fl.	$/10^3$ cm^{-1}	ex.	fl.	$/10^3$ cm^{-1}
hexane	0.4	0.32	0.17	0.62	0.79	0.5	0.6	0.74	0.35
cyclohexane	0.37	0.33	0.19	0.56	0.77	0.52	0.58	0.68	0.32
carbon tetrachloride	0.45	0.41	0.49						
ethanol	0.59	0.68	0.53	0.53	0.81	0.55	0.55	0.75	0.56
ethyl acetate	0.54	0.57	0.51	0.59	0.72	0.48	0.64	0.67	0.53
1,4-dioxane	0.61	0.62	0.53	0.55	0.72	0.55	0.52	0.67	0.42
tetrahydrofuran	0.55	0.58	0.5	0.61	0.7	0.47	0.54	0.66	0.42
benzene	0.54	0.63	0.66						
acetonitrile	0.6	0.63	0.64	0.64	0.85	0.69	0.68	0.73	0.59
chloroform	0.53	0.52	0.48	0.56	0.75	0.49	0.56	0.69	0.45
1,2-dichloroethane	0.56	0.58	0.45	0.54	0.82	0.54	0.56	0.7	0.42
water	0.65	0.87	0.75	0.59	0.92	0.95	0.61	0.83	0.67
hexamethyldisiloxane	0.44	0.41	0.19						

abs. : absorption spectrum; fl.: fluorescence spectrum; ex.: excitation spectrum

When a fused silica plate was dipped in a 1×10^{-3} mol/l THF solution of the DCA derivative (11), followed by baking at 110 °C for 10 min to lead to the covalent fixation of the fluorophore on the surface, a monomer emission of DCA was obtained, as illustrated in Figure 4-2.   Figure 4-2 shows also a broad and red-shifted spectrum of DCA bound on a fused silica plate which was immersed in a 1×10^{-3} mol/l ethanol solution, followed by heat treatment.   The same emission was observed when the plate was treated with a 1×10^{-2} mol/l THF solution.   These spectra implies that the DCA reagent was converted into siloxane oligomers before the silylation[9] to cover the surface and made crowded DCA residuals on a fused silica plate emitting excimer emission.   Fused silica plates treated with a 1×10^{-3} mol/l THF solution were used for the following experiments.   A DCA derivative (12) bearing dimethylethoxysilyl group, shown in Scheme 4-1, was also synthesized and used for surface modification.   Because of the ease of the hydrolysis and the subsequent dimerization, an amount of DCA covalently bound on a fused silica plate was too small that it was hard to obtain reliable.

The amount of DCA units attached to a silica surface was estimated spectroscopically.   Using the absorbance at 268nm of the plate and the molar absorption coefficient of 11 in THF at 268 nm ($S_0 \rightarrow S_3$ of DCA unit, $\varepsilon = 9.5\times10^4$), the average density of DCA on a fused silica plate was calculated to be about 0.17 molecule/nm^2.   Because the population of silanols on silica is around 4.5 - 5.5 per 1 nm^2,[10-13] major part of silanols remains unreacted.   Since the number of surface DCA was too small to obtain the whole absorption spectra on a plate precisely, the excitation spectra of the plate was measured in various solvents.

As shown in Figure 4-3 and Table 4-1, the DCA derivative (11) attached to a fused silica surface shows a marked red shift in both excitation and emission spectra in non-polar hydrocarbon solvents, accompanied by the increase in Stokes' shift and valley/peak values.   The comparison of Figure 4-1 with Figure 4-3 depicts clearly the anomalous behavior in aliphatic hydrocarbons.   The spectral characteristics are rather similar to those of DCA in solvents with $\pi *$ scale values larger than ca 0.5, reflecting that DCA units on the surface is surrounded by these solvent molecules.   Thus, the anomalous red shift in aliphatic hydrocarbons results from highly polar microenvironment.   This is possibly due to residual silanols and/or water molecules covering silica surfaces.[14-17]
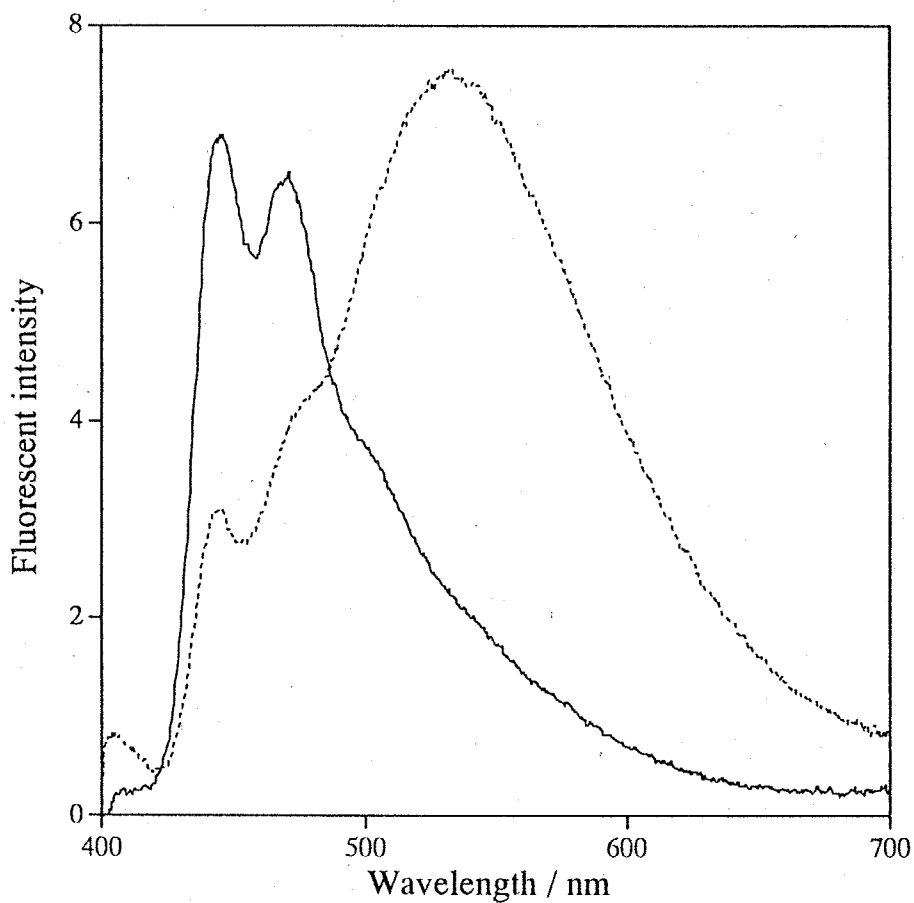
Figure 4-2. Fluorescence spectra of 11 covalently bound fused silica plates treated with a 1×10^{-3} mol/l THF solution (solid line) and a 1×10^{-3} mol/l ethanol solution (dot line) of a DCA derivative, respectively, followed by baking at 110°C.

Figure 4-3. The correlation between vmax of absorption spectra (○) and fluorescence spectra (●) of a DCA-modified fused silica plate immersed in solvents and π* scale values of the solvents; 1: hexane, 2: cycloh xene, 3: carbon tetrachloride, 4: ethanol, 5: ethyl acetate, 6: 1,4-dioxane, 7: tetrahydrofuran, 8: benzene, 9: acetonitrile, 10: chloroform, 11: 1,2-dichloroethane, 12: water. The lines are the correlation slopes for the solutions of 11 shown in Figure 4-1.

Because these non-polar solvent molecules possess no affinity to a highly polar solid surface, surface-adsorbed water molecules cannot be replaced by water-immiscible solvent molecules to give rather a polar microenvironment. These facts agree with the results reported by Lochmüller et. al. that an excimer formation of a pyrene covalently bound on a silica gel takes place more rapidly in a water-immiscible solvent like hexane than a water-miscible solvent like THF. Water molecules adsorbed on a silica gel are not expelled in hexane and accelerate the excimer formation.[18] A moderate red-shift in the excitation spectra of surface DCA in water-immiscible chloroform and 1,2-dichloroethane is caused by the same situation.

The Stokes' shifts of DCA on the surface are insensitive to the nature of solvent, in contrast to solution phase spectra; DCA dissolved in aliphatic hydrocarbons shows a very small Stokes' shift compared with the other solvents as shown in Table 4-1. Anomalous behavior at an interface with these aliphatic hydrocarbons was also observed for the valley/peak values, as summarized in Table 4-1. They are much larger than those in solutions and approximately same as those for solution of the other solvents. These all are due to that DCA residues on a fused silica surface are placed in a highly polar microenvironment, reflecting the peculiar nature of a silica surface when a surface-modified plate is immersed in aliphatic hydrocarbons.

4-3-4. Monomer emission of a surface-blocked fused silica plate

For further studies on the effect of silanols on interfacial microenvironment, a DCA-modified plate was treated with trimethylchlorosilane to reduce the number of surface silanols. A surface-modified fused silica plate was immersed in a 5 wt% toluene solution of trimethylchlorosilane at 80 °C for 15 hours. The plate was washed ultrasonically in chloroform and DMF for 20 min, respectively. Contact angle measurements supported that silanols are blocked by trimethylsilyl residues; stationary contact angles for water before and after the trimethylsilylation were 35° and 85°, respectively.

The relationship between vmax of both excitation and fluorescence spectra of the capped plate and π^* scale is illustrated in Figure 4-4. The trimethylsilylation resulted more or less in the reduction of the red shift in both spectra in all solvents. In particular,
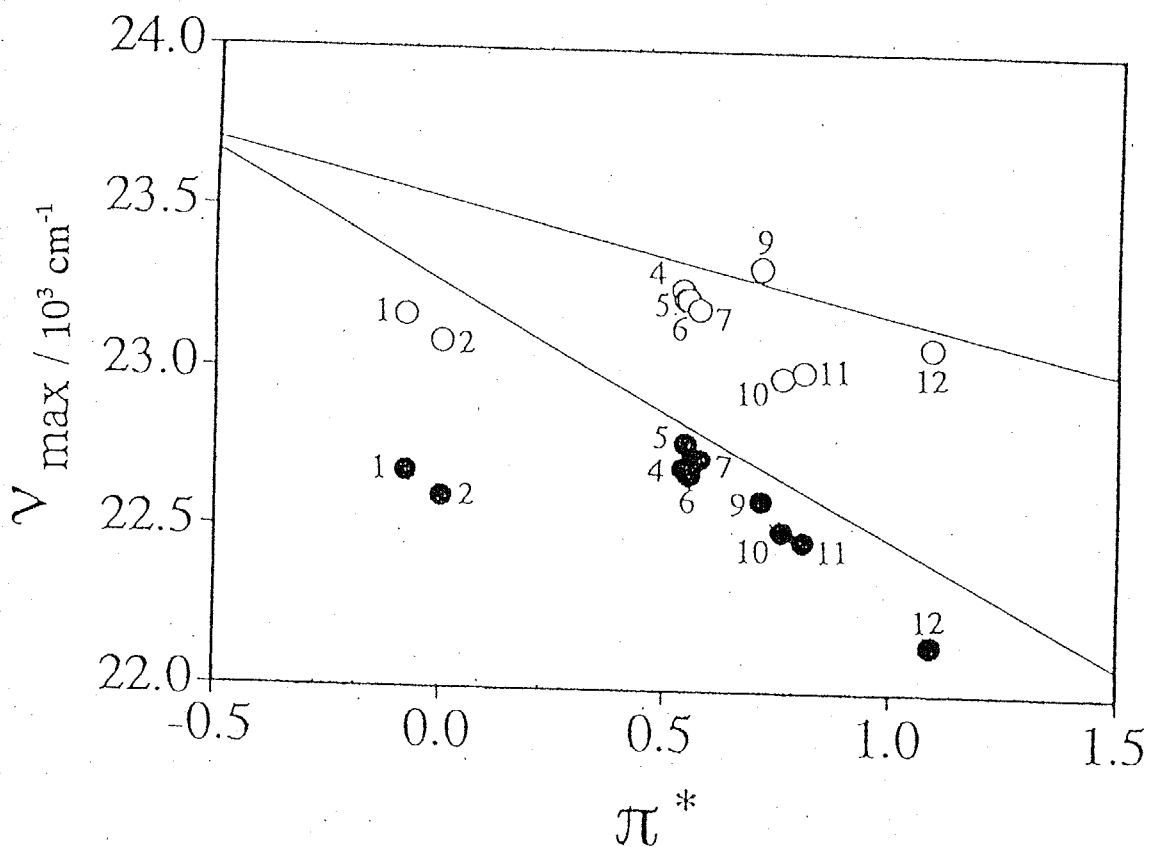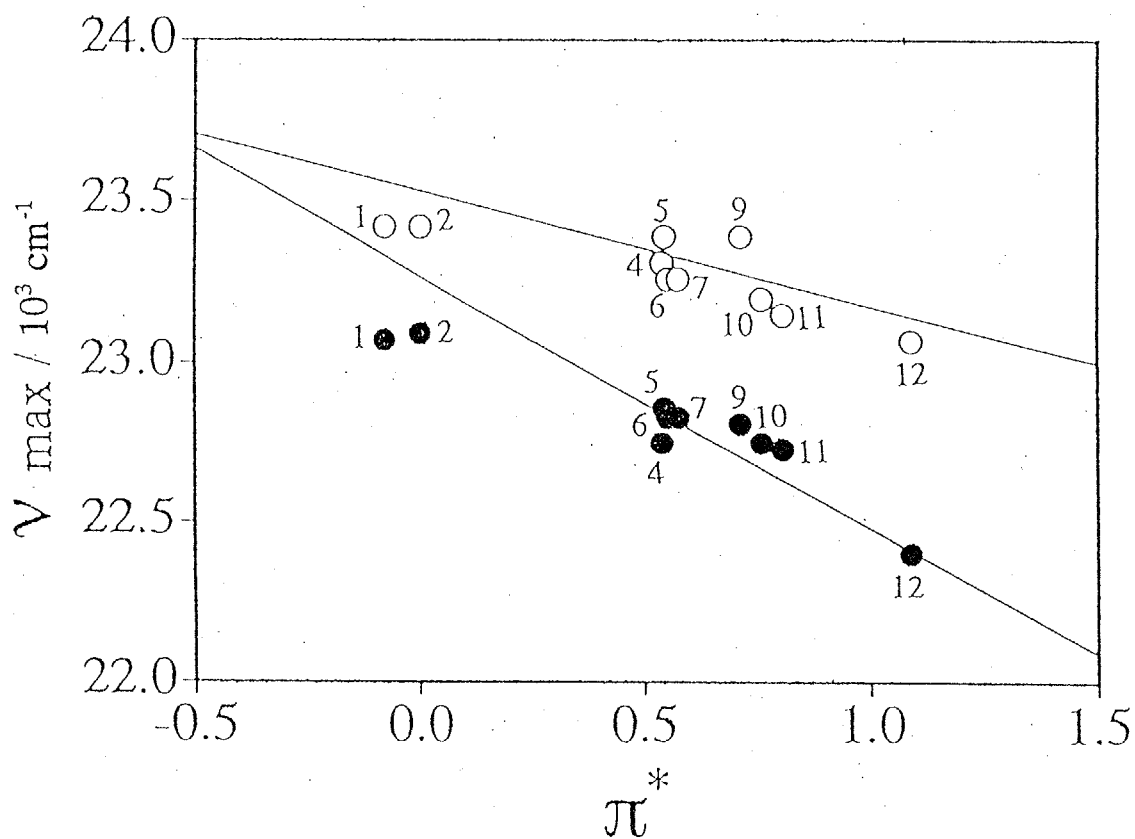
Figure 4-4. The correlation between vmax of absorption spectra (○) and fluorescence spectra (●) of a capped DCA-modified fused silica plate immersed in solvents and π^* scale values of the solvents; 1: hexane, 2: cycloh xene, 3: carbon tetrachloride, 4: ethanol, 5: ethyl acetate, 6: 1,4-dioxane, 7: tetrahydrofuran, 8: benzene, 9: acetonitrile, 10: chloroform, 11: 1,2-dichloroethane, 12: water. The lines are the correlation slopes for the solutions of 11 shown in Figure 4-1.

the red-shift decreased markedly in aliphatic hydrocarbons. This result is in a good agreement with a previous study of Lochmüller et. al. disclosing that the exciplex emission of pyrene and dimethylaniline bound on a silica gel dispersed in a water-immiscible solvent was red-shifted when the silica gel was trimethylsilylated.[19] Trimethylsilyl residues are expected to give rise to a non-polar surface as estimated by non-polar nature of hexamethyldisiloxane as a model compound; both absorption and emission maxima of 11 in hexamethyldisiloxane are the same as those in hexane, respectively. The excitation maxima as well as the emission maxima of DCA on the capped plate are still red-shifted compared with those in solutions. This situation is clearly visualized by comparing the plots for the hydrocarbon solvents with π^* value = ca. 0.0 in Figures 4-1 and 4-4. The slight red shift of DCA on the capped plate immersed in aliphatic hydrocarbon solvents may reflect the character of the trimethylsilylated surface which bears slight polarity possibly owing to Si-O bonds. The fact that λmax of DCA on the surface-blocked fused silica plate are very close to that in corresponding solutions indicates strongly that DCA residues on the capped surface are solvated with solvent molecules in a way quite similar to DCA molecules in solutions.

Other spectral properties of a surface-blocked fused silica plate are also compiled in Table 4-1. The valley/peak values of the excitation and emission spectra in aliphatic hydrocarbons are not altered by the trimethylsilylation, showing that the transition energy distribution of surface molecules is not markedly influenced by the change in surface micropolarity by the trimethylsilylation. The transition energy distribution of DCA is enhanced by binding on a solid surface and not altered by the micropolarity of a surface.

4-3-5. Exciplex emission of DCA-modified fused silica plate with phenanthrene

Prior to the exciplex observation at an interface, it was confirmed that a combination of DCA and phenanthrene fulfills the required condition for the observation of exciplex. DCA forms an exciplex with phenanthrene in a THF solution, as shown in Figure 4-5. The $S_0 \rightarrow S_1$ absorption bands of DCA lies in a wavelength region of 350 - 440 nm whereas phenanthrene absorbs light of wavelengths shorter than 350 nm. No excimer fluorescence was observed even in a 5 mmol/l saturated chloroform solution of DCA although typical polyacene derivatives show strong excimer fluorescence in this

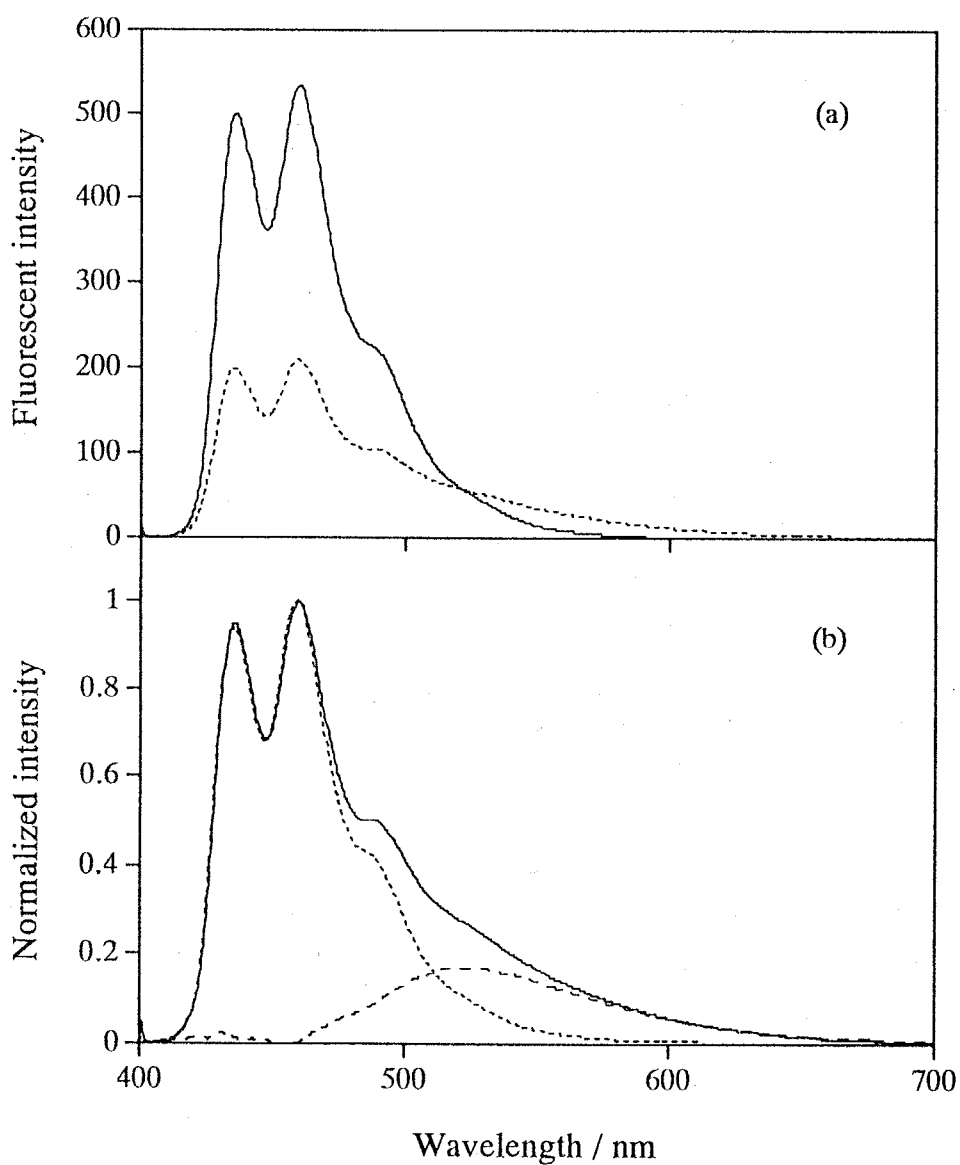Figure 4-5. (a) Fluorescence spectra of a THF solution of 1×10^{-4} mol/l 9,10-dicyanoanthracene (dot line) with and (solid line) without 1×10^{-2} mol/l phenanthrene. (b) The normalized spectra and a differential spectrum (broken line).

concentration range. These facts mean that this system is good for the requirements for the exciplex probe technique stated above.

A fluorescence spectrum of a DCA-modified fused silica plate immersed in a 1×10^{-2} mol/l phenanthrene solution of hexane has a broad shoulder at a long-wavelength region, as shown in Figure 4-6. A spectrum normalized at the monomer emission band at 446 nm and a differential spectrum is also shown in Figure 4-6. The differential spectrum is assignable to an exciplex emission between surface DCA and phenanthrene dissolved in a solution. λmax was 555 nm. To the authors' knowledge, this is the first observation of an exciplex emission emerged at a solid/fluid interface where a fluorophore is bound on a solid surface to form an exciplex with a counterpart in solution. The interfacial exciplex fluorescence displays a considerable red shift of 55nm in hexane containing 1×10^{-2} mol/l phenanthrene, as shown in Figure 4-7. This suggests strongly that the microenvironmental polarity at the interface between fused silica plate and hexane is much higher than that in bulk hexane. The exciplex emission was also detected when a DCA plate capped with trimethylsilyl chloride was immersed in a hexane solution of phenanthrene although the emission maximum appeared at 515 nm with a slight red shift (Figure 4-7). These results agree with a previous report that λmax of an exciplex of a pyrene with a dimethylaniline, both of which are covalently bound on a surface of a silica gel, is red-shifted in hexane when compared with that in a solution and that the capping with trimethylsilyl units reduces the red shift.[19] These are in line with the results observed in the effect of media on the DCA emission as mentioned above. This confirms that DCA units are surrounded by polar environment due to the residual silanols and water molecules at the interface between a fused silica plate and non-polar hexane. The intensity ratios of exciplex to monomer emission of uncapped and capped DCA plates immersed in a phenanthrene solution in hexane are reduced approximately by a half when compared with that in a homogeneous solution. This is caused by the two factors. One is the opportunity of phenanthrene molecules to approach to DCA molecules which is reduced roughly by a half when the fluorophore is bound on a silica surface plate. The other is the enhanced portion of the charge separation path ((DCA-Phe)* → DCA⁻ + Phe⁺) leading to the deactivation because the micropolarity at an interface is higher than the bulk.
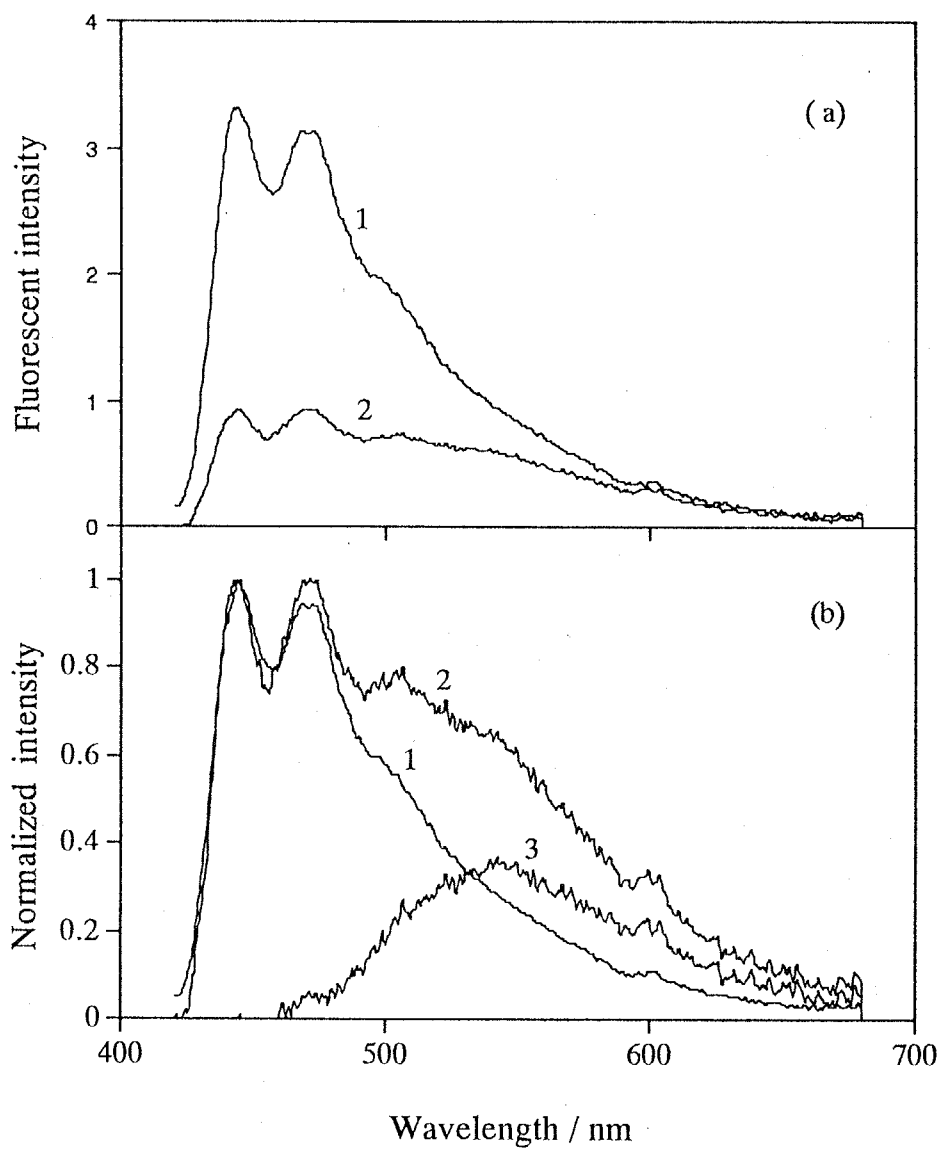
Figure 4-6. (a) Fluorescence spectra of a surface-modified fused silica plate immersed in hexane (1) and in hexane containing 1×10^{-2} mol/l phenanthrene (2). (b) The normalized spectra and a differential spectrum (3).
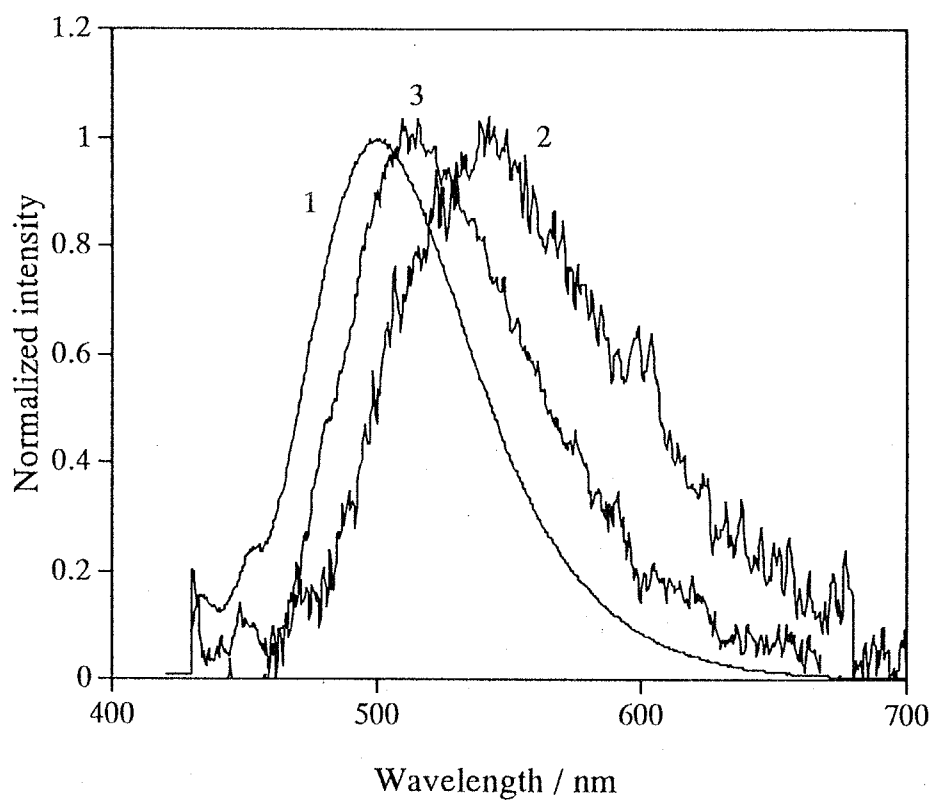
Figure 4-7. Exciplex fluorescence spectra of **11** dissolved in hexane containing 1×10^{-2} mol/l phenanthrene solution (1), a DCA-modified fused silica plate (2) and a surface-blocked DCA-fused silica plate (3) immersed in the phenanthrene solution.

The fluorescence spectrum of a DCA plate immersed in a phenanthrene solution of chloroform was also observed, which is shown in Figure 4-8. The fluorescence intensity was weakened by immersing in a phenanthrene solution of chloroform. But very weak exciplex emission was only observed as shown in the normalized spectra, Figure 4-8. This means the energy of excited DCA transferred to ground state phenanthrene. The spectra of DCA plate immersed in a phenanthrene solution of THF or ethanol displayed the same phenomena as the case of chloroform solution. In these polar solvents, the intensity ratio of the exciplex to the monomer emission is small owing to an enhanced non-radiative relaxation path to the ground state possibly through an ion pair solvated by polar solvents. Furthermore, the fluorescence itself is weak in polar solvents. These situations do not allow us to monitor microenvironmental polarity in polar solvents by means of the exciplex probe.

4-3-6. Exciplex emission between DCA bound on a fused silica and phenanthryl side chains tethered to polymethacrylate chains

A DCA-modified fused silica was immersed in a chloroform solution of poly(9-phenanthrylmethyl methacrylate) (13) to take a fluorescence spectrum of this system, and the results are shown in Figure 4-9. A distinct exciplex emission between DCA and phenanthrene unit was observed, in contrast to the case of very weak exciplex in a phenanthrene solution shown in Figure 4-8. This implies that the polar ester groups of 13 and polar silanols are interactive through hydrogen bonds to link the polymer on the silica surface.

The interaction of ester groups and silanol residuals was studied in the following ways. A DCA-modified plate was dipped in a chloroform solution of 13, followed by immersing in hexane to record fluorescence spectra. The results shown in Figure 4-10 tell significant increase in the exciplex emission. This observation suggests that the plate is adsorbed with 13 owing to efficient interactions between the ester groups and silanol groups. When another plate was immersed in the chloroform solution of 13, followed by dipping in fresh chloroform, the exciplex emission increased in intensity, as shown in Figure 4-11 (b and c). This fact shows that the polymer adsorbed on the surface is not desorbed even in chloroform and interactions of the surface DCA with adsorbed 13 are

Figure 4-8. Fluorescence spectra (above) and normalized spectra (below) of DCA-modified fused silica plate immersed in choroform (solid line) and in chloroform solution of phenanthrene (broken line)

Figure 4-9. Fluorescence spctra (above) and normalized spectra (below) of DCA-modified fused silica plate immersed in choroform (solid line) and in chloroform solution of **13** (broken line)
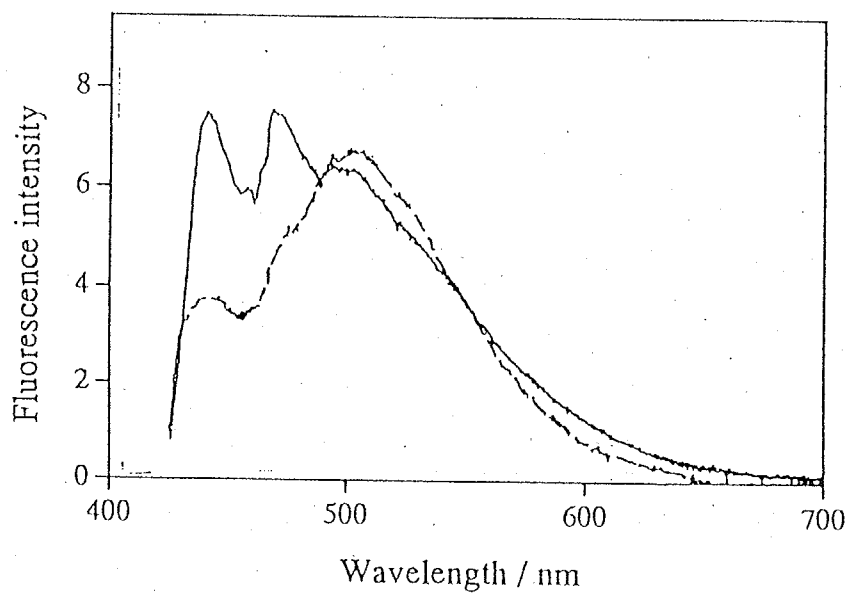
Figure 4-10   Fluorescence spectra of DCA-modified fised silica plate immersed in chloroform solution of 13 (solid line) and the plate picked up from the solution and immersed in fresh hexane (broken line).
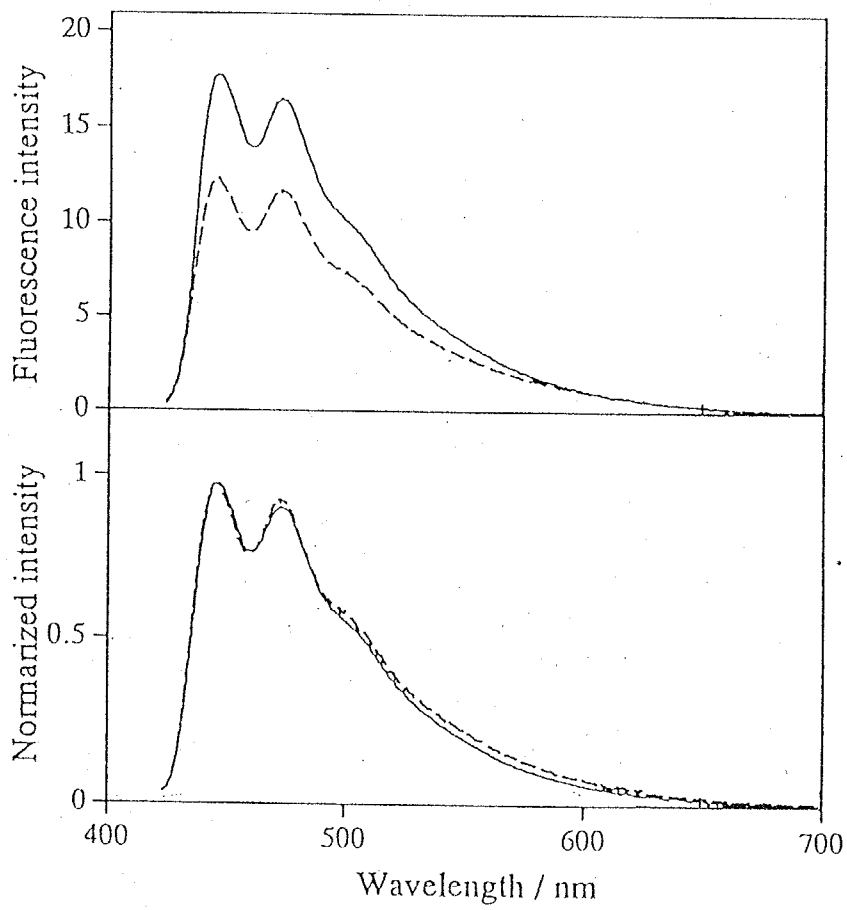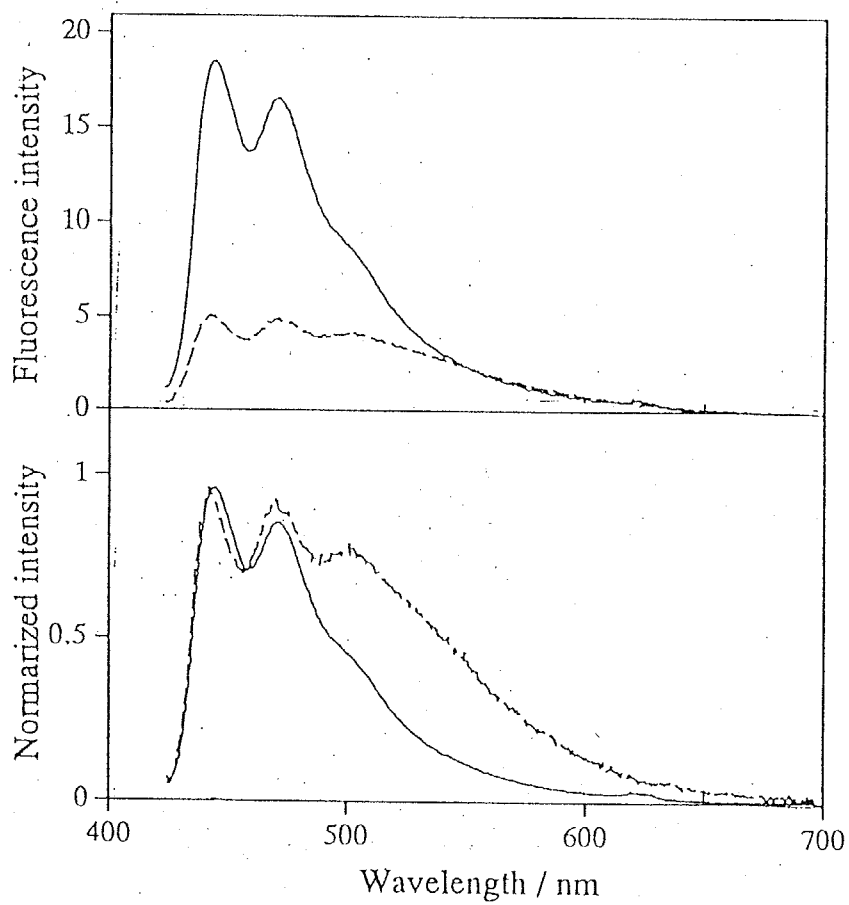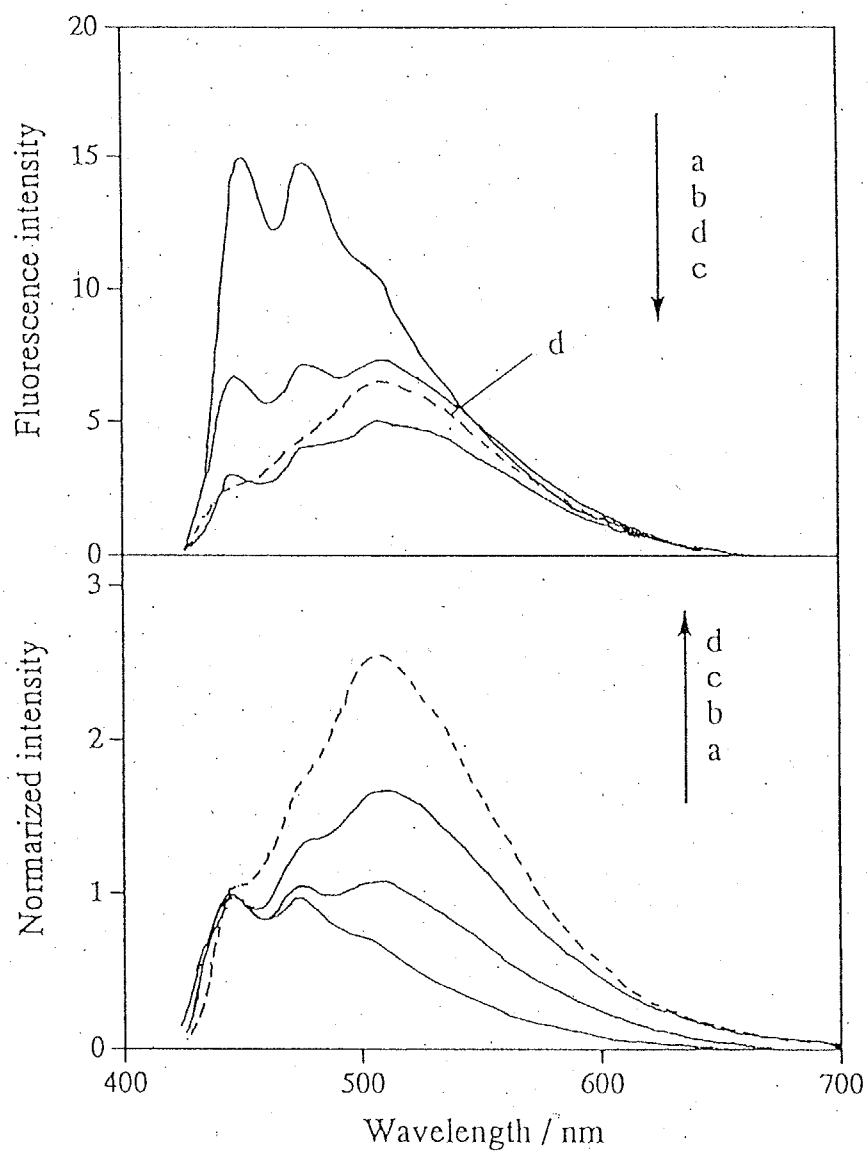
Figure 4-11   Fluorescence spectra (above) and normalized spectra (below)

a) DCA-modified fised silica plate in chloroform solution of **13**

b) the plate picked up from the solution and immersed in fresh chloroform

c) same as b) but 30 min later

d) the plate picked up from chloroform and immersed in fresh hexane

enhanced in chloroform during 30 min. As shown in Figure 4-11(d), when the plate was picked up from the chloroform and subsequently immersed in hexane again, the exciplex emission was more increased in a manner similar to the first experiment.

On the other hand, quite a contrastive observation was made when a DCA-modified plate immersed in the chloroform solution of **13** was dipped into fresh THF. Only monomer emission of DCA was observed, whereas no exciplex formation was detected. This facts mean that **13** adsorbed on the plate is desorbed readily in THF because of efficient solvation of THF to the polymethacrylates. No formation of the exciplex between DCA and Phe was confirmed by immersing the plate in hexane. Fluorescence observed was only of DCA monomer.

In order to provide an interfacial model for polymer/polymer solids, a plate dipped in the chloroform solution of **13** was dried to take fluorescent spectra. The spectra were corresponding to both of DCA monomer and DCA-Phe exciplex, whereas the spectral shape was complicated. Note that a DCA-modified silica plate spin-coated with PMMA shows a broad emission band together with DCA monomer emission, probably because of the concomitance of excimer emission of DCA. Taking notice of the fact that DCA chemisorbed on a silica displays no excimer emission in solution, a local density of DCA on the surface is increased as a result of covering with the polymer. Excimer emission was also observed for a DCA-modified plate even covered with **13**. Though the Phe group has small absorbance at the excitation wavelength of 385 nm is negligible small in solution, it could not be neglected in condensed film. The Phe moieties form excimer of Phe in a film of **13** upon excitation at 385 nm because they are locally concentrated in film. These results imply that a system consisting of DCA-modified silica plate and a film of **13** is not suitable for an interfacial model of polymer/polymer solids.

4-4. Conclusions

Appropriate choice of a solvent and a concentration of a DCA silylating reagent afforded a selective surface modification of a fused silica plate to display a monomer fluorescence of the fluorophore. Whereas both λmax of absorption and emission spectra of a DCA derivative in solutions correlated with the π^* scale expressing solvent

polarity, both spectral maxima of DCA covalently bound on a fused silica surface were anomalously red-shifted when a plate was immersed in aliphatic hydrocarbons. This arises from the fact that the micropolarity around probe molecules bound on a surface was markedly enhanced by residual silanols of silica surface and water molecules adsorbed on the surface. This was supported by the observation that the red shift in λmax of excitation and emission spectra of the surface DCA was effectively suppressed by capping residual silanols with trimethylsilyl groups. The Stokes' shifts as well as the broadness of spectral shapes of surface DCA reflects the nature of silica surfaces in a similar way.

Immersion of a DCA-modified fused silica plate in a phenanthrene solution in hexane resulted in the emergence of a fluorescence band at a red-shifted wavelength as a shoulder due to an exciplex between DCA and phenanthrene at an interface. The fluorescence maximum of the exciplex was also sensitive to the micro polarity on silica surfaces. These implied that DCA was a suitable candidate as an emission probe for elucidation of interfacial phenomena.

The exciplex emission between DCA and phenanthrene was observed when the DCA-modified plate is immersed in a poly(9-phenanthrylmethyl methacrylate) solution, followed by dipping in hexane or chloroform, providing a model system for revealing interfacial phenomena between a solid and a fluid layer. On the other hand, this system is not suitable for a model to obtain information concerning interfaces between two kinds of solids because no exciplex formation is generated when the silica plate with a **13** film.

References

1. E. de B. Barnett, J. W. Cook and H. H. Grainger, *Ber.*, 1924, **57B**, 1775.

2. S. Ito, N. Numata, H. Katayama and M. Yamamoto, *Macromolecules*, 1989, **22**, 2207.

3. K. Ichimura, Y. Hayashi and N. Ishizuki, *Chem. Lett.*, 1992, 1063.

4. K. Ichimura, Y. Hayashi, Y. Kawanishi, T. Seki, T. Tamaki and N. Ishizuki, *Langmuir*, 1993, **9**, 857.

5. K. Ichimura, Y. Hayashi, H. Akiyama, T. Ikeda and N. Ishizuki, *Appl. Phys. Lett.*, 1993, **63**, 449.

6. C. Reichardt, *"Solvents and Solvent Effects in Organic Chemistry 2nd Ed."* VCH, Weinhein, 1979

7. M. J. Karmelet, J. L. Abboud and R. W. Taft, *J. Am. Chem. Soc.*, 1977, **99**, 6027.

8. Y. Suzuki and S. Tazuke, *Macromolecules*, 1981, **14**, 1742.

9. S. R. Culler, H. Ishida and J. L. Koenig, *J. Colloid Interface Sci.*, 1985, **106**, 334.

10. L. T. Zhuravlev, *Langmuir*, 1987, **3**, 316.

11. G. Foti and E. sz. Kovats, *Langmuir*, **1989**, 5, 232.

12. A. Tuel, H. Hommel, A. P. Legrand and E. sz. Kovats, *Langmuir*, 1990, **6**, 770.

13. J. Gum, R. Iscovici and J. Sagiv, *J. Colloid Interface Sci.*, 1984, **101**, 210.

14. J. C. W. Frazer, W. A. Patrick and H. E. Smith, *J. Phys. Chem.*, 1927, **31**, 897.

15. J. H. Frazer, *Phys. Rev.*, 1929, **33**, 97.

16. R. I. Razouk and A. S. Salem, *J. Phys. Chem.*, 1948, **52**, 1208.

17. K. Klier, J. H. Shen and A. C. Zettlemoyer, *J. Phys. Chem.*, 1973, **77**, 1458.

18. C. H. Lochmüller, A. S. Colborn, M. L. Hunnicutt and J. M. Harris, *J. Am. Chem. Soc.*, 1984, **106**, 4077.

19. C. H. Lochmüller, M. T. Kersey and M. L. Hunnicutt, *Anal. Chim. Acta*, 1985, **175**, 267.

Chapter 5

Synthesis and fluorescence behavior of calix[4]resorcinarenes possessing pyrenyl group(s)

5-1. Introduction

For a model system of "island-sea structures" of polymer blends, a combination of pyrenyl groups bound on a silica surface and N,N-dimethylaniline units (DMA) linked to polymethacrylate backbones is proposed in this chapter. Pyrene and DMA forms exciplex, which emits at a longer wavelength region when compared with pyrene monomer emission so that this system is suitable for revealing microenvironments and intermolecular interactions at silica/polymer interfaces. Another advantage of this combination comes from the fact that DMA is not excited by light in a wavelength region, where the $S_0 \rightarrow S_2$ excitation of pyrene is performed. But there is a problem to be considered that pyrene forms readily excimer which emits light at the same wavelength region as that of pyrene-DMA exciplex. In order to overcome this situation, the reduction of surface density of pyrene moieties as a fluorescent probe is a convenient way to suppress the formation of excimer. On account of a high fluorescence quantum yield and a long fluorescence lifetime of pyrene,[1] it may possible to detect the emission from a pyrene tethered to solid surface even in a low density. The use of a calix[4]resorcinarene having eight carboxymethoxy groups (CRA) as an anchoring unit to tether pyrenyl groups to a silica surface not only because of the rigidity of the CRA skeleton, but also because the distance among pyrenyl groups can be made large enough to suppress the excimer formation by the reduction of the number of pyrene units introduced to a CRA skeleton. Since an occupied area of CRA is about 2.0 nm^2, a distance among CRA molecules substituted with a single pyrenyl residue, for instance, is estimated to larger than 0.8 nm in average so that the excimer formation is sufficiently suppressed. In this context, the preparation of CRA derivative substituted with different numbers of pyrenyl groups is the major target of this chapter.

Though CRA originally have been attracting current interest from a viewpoint of

achieving the molecular design for molecular receptors recognizing guest molecules,[2-7] some studies which used CRA derivatives with various functional groups as self-assembled monolayers have been reported.[8-10] When a self-assembled monolayer of CRA derivatives is formed, the distance of the functional group was constant which is determined by an occupied area of CRA. The purpose of this chapter is to establish a synthetic route of CRA substituted with various numbers of pyrene residues. Whereas some reports described the stepwise synthesis of calixarene derivatives possessing pyrenyl groups starting from monophenols,[11-13] there has been no work dealing with the synthesis of CRAs substituted with pyrene derived from resorcinol.

5-2. Experimental

5-2-1. Materials

Calix[4]resorcinarenes possessing pyrenyl group(s) were synthesized as shown in Scheme 5-1. 1-Pyrenylaldehyde and diethylphosphonoacetic acid ethyl ester were used as received commercially. A toluene solution of diisobutylaluminum hydride was obtained from Aldrich Chemical Co., Inc.

Ethyl 3-(1-pyrenyl)-2-propenate.

Diethyl phosphonoacetate (15.2 g, 67.8 mmol) was added dropwise to a benzene suspension (30 ml) of sodium hydride (2.7 g, 113 mmol). After stirring for 1 hour at room temperature, a benzene solution of 1-pyrenylaldehyde (12.4 g, 53.7 mmol) was added dropwise and stirred for a few hours at 15 − 20 °C, followed by the removal of the solvent under a reduced pressure. A yellow solid residue was purified by recrystallization from benzene to give yellow needles in a yield of 84 %.

mp = 111 - 112 °C

Elemental Anal. for $C_{21}H_{16}O_2$:   Calcd. C: 83.98, H: 5.37%.

Found C: 83.52, H: 5.29%.

Ethyl 3-(1-pyrenyl)-2-propanate

-CHO

$(C_2H_5O)_2\overset{\overset{O}{\|}}{P}CH_2\overset{\overset{O}{\|}}{C}OC_2H_5$

NaH / benzene

OC_2H_5

Pd / C, H$_2$

ethanol

-C$_2$H$_5$COOC$_2$H$_5$

(iso-C$_3$H$_7$)$_2$AlH

-C$_2$H$_5$CHO

m -C$_2$H$_5$CHO

+ (4-m) C$_3$H$_7$CHO + 4 HO OH

HCl

ethanol or

2-methoxyethanol

$\left(\begin{array}{c}C_2H_4Py\\ \\HO\quad OH\end{array}\right)_n$ $\left(\begin{array}{c}C_3H_7\\ \\HO\quad OH\end{array}\right)_{4-n}$

Py =

$\overset{\overset{O}{\|}\ \overset{O}{\|}}{CH_3COCCH_3}$

Pyridine

$\left(\begin{array}{c}C_2H_4Py\\ \\CH_3CO\quad CH_3C\\ \overset{\|}{O}\quad\ \overset{\|}{O}\end{array}\right)_n$ $\left(\begin{array}{c}C_3H_7\\ \\O\quad OCCH_3\\ \overset{\|}{O}\ \ \ \ \overset{\|}{O}\end{array}\right)_{4-n}$

n = 0   **14**

n = 1~3   CRA-Py(n)

n = 4   **15**
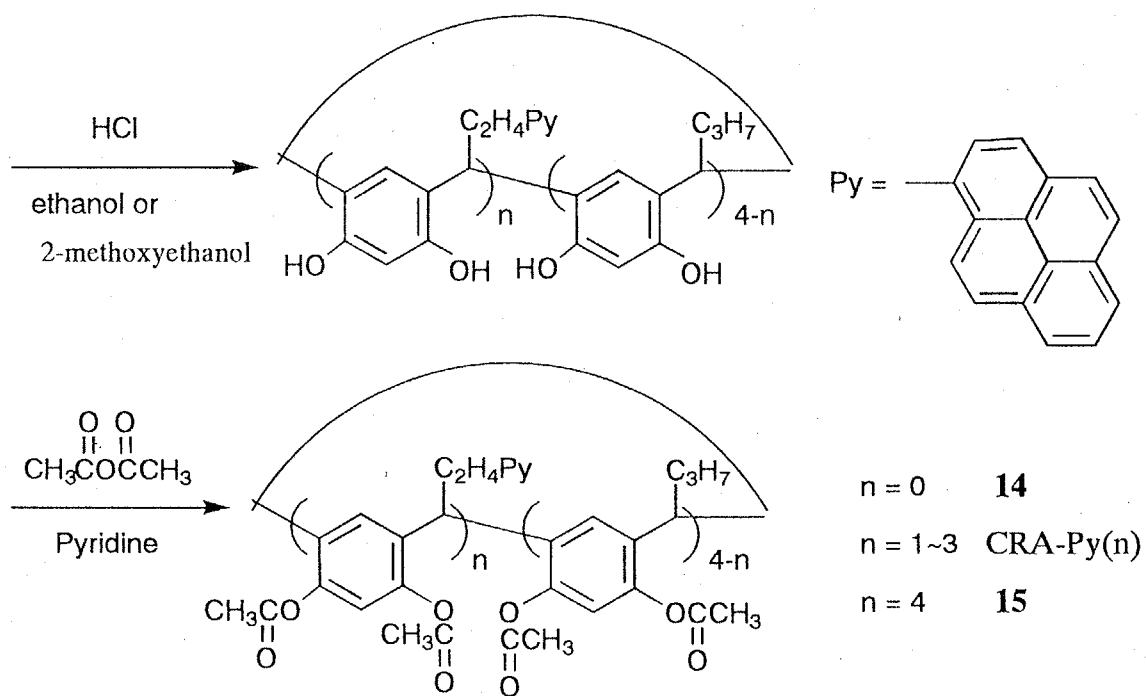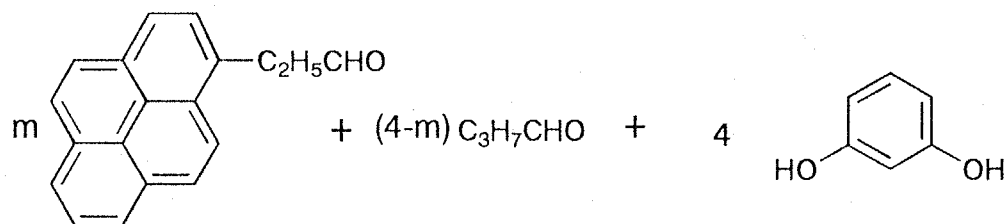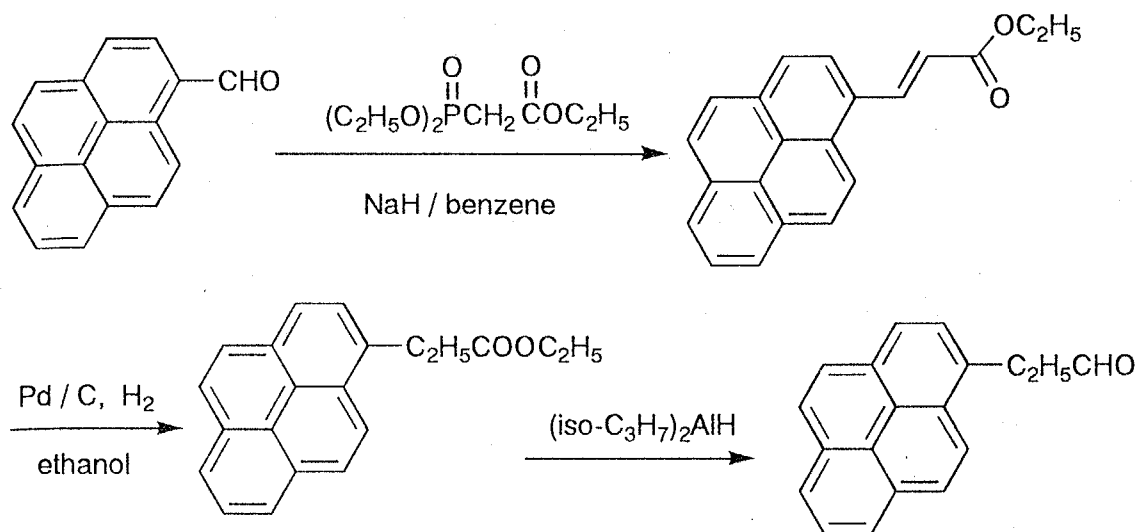
Scheme 5-1 Syntheses of **14**, **15** and CRA-Py(n)

97

Ethyl 3-(1-pyrenyl)-2-propenate (13.0 g, 43.3 mmol) was dissolved in a mixed solvent of ethanol and ethyl acetate. The solution was stirred under hydrogen in the presence of palladium charcoal at room temperature overnight. After the catalyst was filtered out, the solvent was evaporated. White crystals were recrystallized from benzene-methanol in a yield of 58 %.

mp = 65 - 67 °C

Elemental Anal. for $C_{21}H_{18}O_2$:   Calcd. C: 83.42, H: 6.00%.

Found C: 82.47, H: 6.75%.

3-(1-Pyrenyl)propanal

To a dichloromethane solution of ethyl 3-(1-pyrenyl)-2-propanate (1.00 g, 3.3 mmol) was added dropwise a 1.0 mol/l toluene solution of diisobutylaluminum hydride (3.4 ml, 3.4 mmol), and the mixture was stirred for 20 min at dry ice-methanol temperature. After adding 0.5 ml of methanol, it was stirred for 30 min, and precipitates were removed by filtration, followed by evaporation of the solvent. A solid residue was purified by column chromatography on silica gel using a mixed solvent of ethyl acetate and hexane (1:3) as an eluent, followed by recrystallization from ethanol. White crystals were isolated in a yield of 64 %.

mp = 74 - 75 °C

Elemental Anal. for $C_{19}H_{14}O$:   Calcd. C: 88.34, H: 5.46%.

Found C: 87.78, H: 5.38%.

Octaacetylated tetrapropylcalix[4]resorcinarene (14)

The preparation of tetrapropylcalix[4]resorcinarene will be shown elsewhere.[8] Tetrapropylcalix[4]resorcinarene was dissolved in a mixture of acetic anhydride and pyridine, and 3-dimethylaminopyridine was added. The solution was stirred for 13 hours at 80 °C. After water was added to the solution, the product was extracted with ethyl acetate to be subjected to purification with a mixture of acetone and hexane. White crystals of mp > 300 °C were isolated. The yield of acetylation was 65 %.

Elemental Anal. for $C_{56}H_{64}O_{16}$:   Calcd. C: 67.73, H: 6.50%.

Found C: 67.64, H: 6.49%.

Octaacetylated tetra(1-pyrenyl)ethylcalix[4]resorcinarene (15).

3-(1-Pyrenyl)propanal (24.2 mg, 93.7 mmol) and 10.4 g of resorcinol (94.5 mmol) were dissolved in 50 ml of 2-methoxyethanol, and the solution was stirred at 80 °C for 12 hours and subsequently at 120 °C for 5 hours. After the solution was cooled, water was added, and the precipitates were filtered and washed with water until the washing became pH = ca. 7. To 30ml of acetic anhydride and 10ml of pyridine dissolving the crude CRA was added 10mg of 3-dimethylaminopyridine, and the solution was stirred at 80 °C for 20 min and subsequently at room temperature overnight. After work-up with water, the product was extracted with diethyl ether and purified with column chromatography on silica gel using a 1:5 (v/v) mixture of ethyl acetate and chloroform as an eluent. The octaacetylated pyrene CRA was obtained in a 28 % yield.

mp = 173 - 176 °C

Elemental Anal. for $C_{116}H_{88}O_{16}$:   Calcd. C: 80.17, H: 5.10%.

Found C: 79.46, H: 5.15%.

Octaacetylated CRAs substituted with different numbers of pyrene (CRA-Py(n)).

CRA-Py(n)s were prepared twice with slight modification of reaction conditions. In the first run, an ethanol (30 ml) solution containing 0.70 g of 3-(1-pyrenyl)propanal (2.7 mmol), 0.58 g of butanal (8.1 mmol) and 1.19 g of resorcinol (10.8 mmol) was refluxed for 8 hours. The product was extracted with ethyl acetate after work-up with water. After evaporating the solvent, a residual solid was dissolved in 20 ml of pyridine, 10 ml of acetic anhydride and 2 mg of 3-dimethylaminopyridine, the solution were stirred at 50 °C for 5 hours. The product was extracted with diethyl ether after work-up with water and purified by column chromatography on silica gel using a 1: 5 (v/v) solvent of ethyl acetate and chloroform. Yield was 23 % by weight.

In the second run, 0.66 g of 3-(1-pyrenyl)propanal (2.6 mmol), 0.19 g of butanal (2.6 mmol) and 0.57 g of resorcinol (5.2 mmol) were heated in 2-methoxyethanol (30 ml) at 120 °C for 15 hours. The subsequent procedures were the same as the first run. Yield was 48 % by weight. The products of both runs were subjected to preparative HPLC to isolate octaacetylated CRA with different numbers of pyrene in the conditions stated as below.

99

5-2-2. Analytical methods

Reversed phase silica gel columns, JASCO Crestpak C18S and MERCK LiChrispher 100 RP-18, were used as an analytical HPLC column and a preparative HPLC column, respectively. The ratio of mixed solvents of methanol/water as an eluent was 90 : 10 for first 5 min, graduated to 100 % of methanol during the following 25 min and finally 100 % of methanol. A flow rate was 1 ml/min or 4 ml/min for analysis or preparative HPLC, respectively. The detection was made at the wavelength of 274 nm.

5-2-3. Physical measurements

NMR spectra were taken on a JEOL EX500 at room temperature. Absorption and fluorescence spectra were obtained with HITACHI UV320 spectrometer and F4000 fluorospectrometer, respectively. The excitation wavelength of fluorescence spectra was 345nm. Fluorescence decay times were determined using a PRA time-correlated single photon counting system equipped with a multichannel analyzer (NORLAND IT-5300). As an excitation source, a deuterium-filled (0.5 atm) flash lamp (PRA model 510) was used, operating at 30 kHz. The half-width of the pulse was ca. 2 ns. The excitation light wavelength passed through a monochromator was 345 nm. A concentration of sample solutions was adjusted so that the absorbance at 345 nm was 0.2. The fluorescence of monomer and excimer was passed through glass filters which cut off light of wavelengths < 350 nm and > 420 nm (Toshiba UV-37 and UV-D33S) and a glass filter which cuts off light of wavelengths < 450 nm (Toshiba Y-47), respectively. The decay curves were deconvoluted with an iterative nonlinear least-squares method.

5-3. Results and discussions

5-3-1. Synthesis of octaacetylated CRAs possessing pyrenyl group(s) (CRA-Py(n))

CRAs were prepared by the condensation of the corresponding aldehyde with resorcinol in the presence of hydrochloric acid. In order to obtain CRAs substituted with different numbers of pyrenyl residue, resorcinol was reacted with an equimolar amount of mixtures of 3-(1-pyrenyl)propanal and butanal. Two experiments were performed with

different mixing ratios of the two aldehydes in ethanol and 2-methoxyethanol, respectively. Since the purification by column chromatography of CRAs is very hard due to the strong adsorptivity of phenolic OH groups on chromatographic carriers, the OH groups of products were acetylated to be subjected to reverse phase HPLC separation.

As shown in Figure 5-1, five definite peaks were observed for both runs performed under different ratios of the aldehydes. The elution times of the first peak and the fifth peak were in line with that of authentic samples, CRA-Py(0) **(14)** and CRA-Py(4) **(15)**. For the first run, small peaks were observed just after the definite peaks as shoulders whereas only sharp peaks were observed for the second run. There is a possibility that these shoulder peaks were due to a conformational isomer of each peak products. In references [14-17], Hogborg and Abis et. al. showed that CRAs are formed as a mixture of different conformers at an early stage of the acidolytic condensation, and after a prolonged reaction period, the predominant transformation to the most thermodynamically stable crown conformer takes place. According to these references and our experiment results that the acetylated product of another acid-catalyzed condensation, that was stopped after 4 hours instead of 8 hours, brought lager minor peaks of HPLC, the minor peaks of HPLC were assigned to be conformational isomers of CRA. Considering that the reaction underwent about for 15 hours at 120 °C in the second run whereas for 8 hours at 80°C in the first run, the product distribution of the second run is favorable for the formation of the crown conformers with different pyrene residues. In other words, the products in the first run contain mixtures of CRA conformers other than crown conformers.

Using a preparative HPLC column, the second, third and fourth fractions of the second run were collected to isolate octaacetylated CRA derivatives. The structural elucidation of each fraction was performed by NMR spectra. An NMR spectrum of the third fraction as a representative example is shown in Figure 5-2. The presence of a sharp singlet at 6.97 ppm assignable to Ha of the benzene rings confirms the crown conformation.[16] Hb of the benzene rings of octaacetylated CRA derivatives appears as a too broad signal, as described in a literature.[16] The crown conformation was also confirmed for the second and the fourth fractions in a similar way. Judging from the integral data of NMR spectra, the second fraction was identified with octaacetylated CRA possessing one pyrenylethyl and three propyl groups (CRA-Py(1)) while the third and
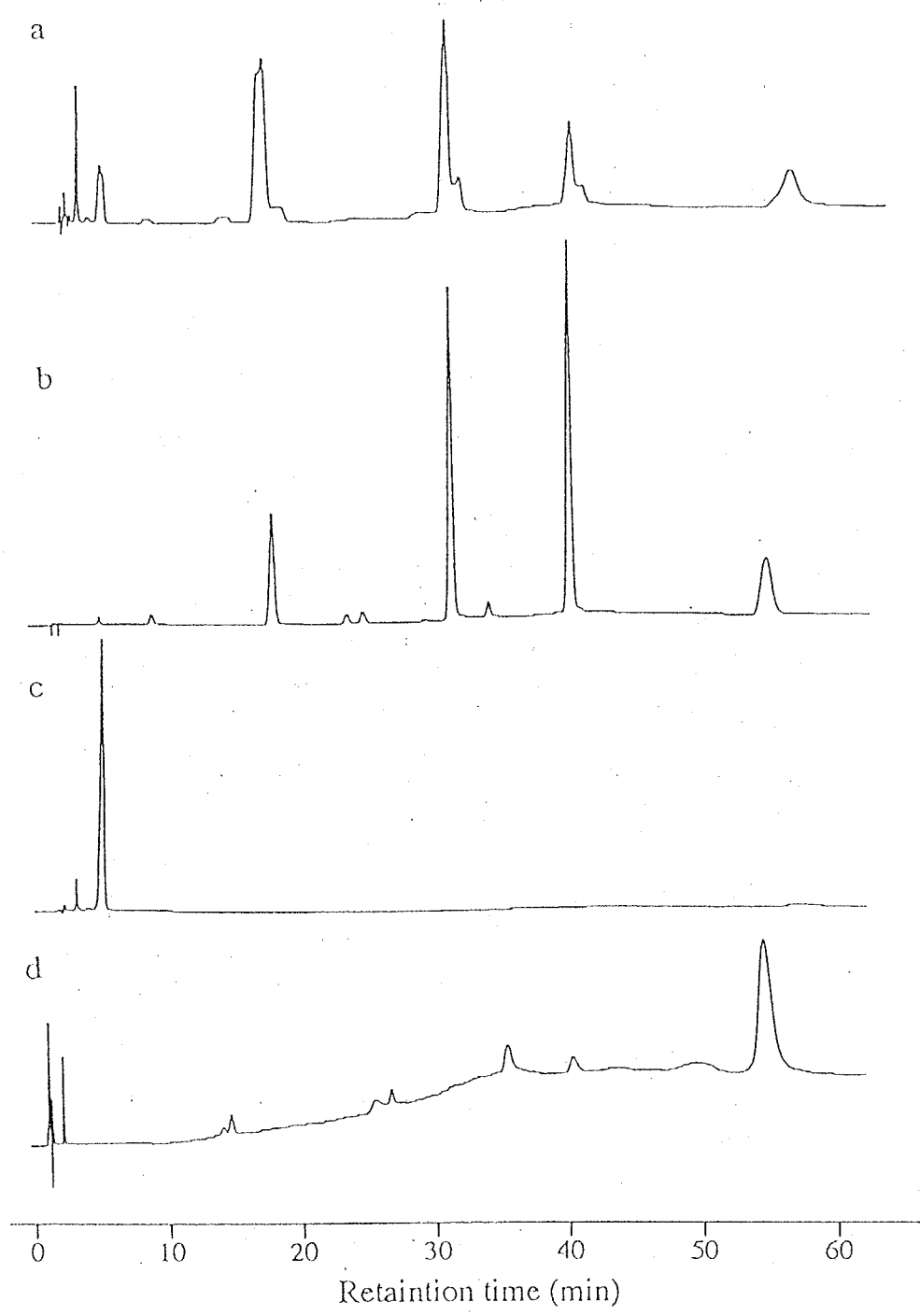
Figure 5-1 HPLC charts of CRA-Py(n) obtained (a) in the first run and (b) in the second run and of authentic samples 14(c) and 15(d).
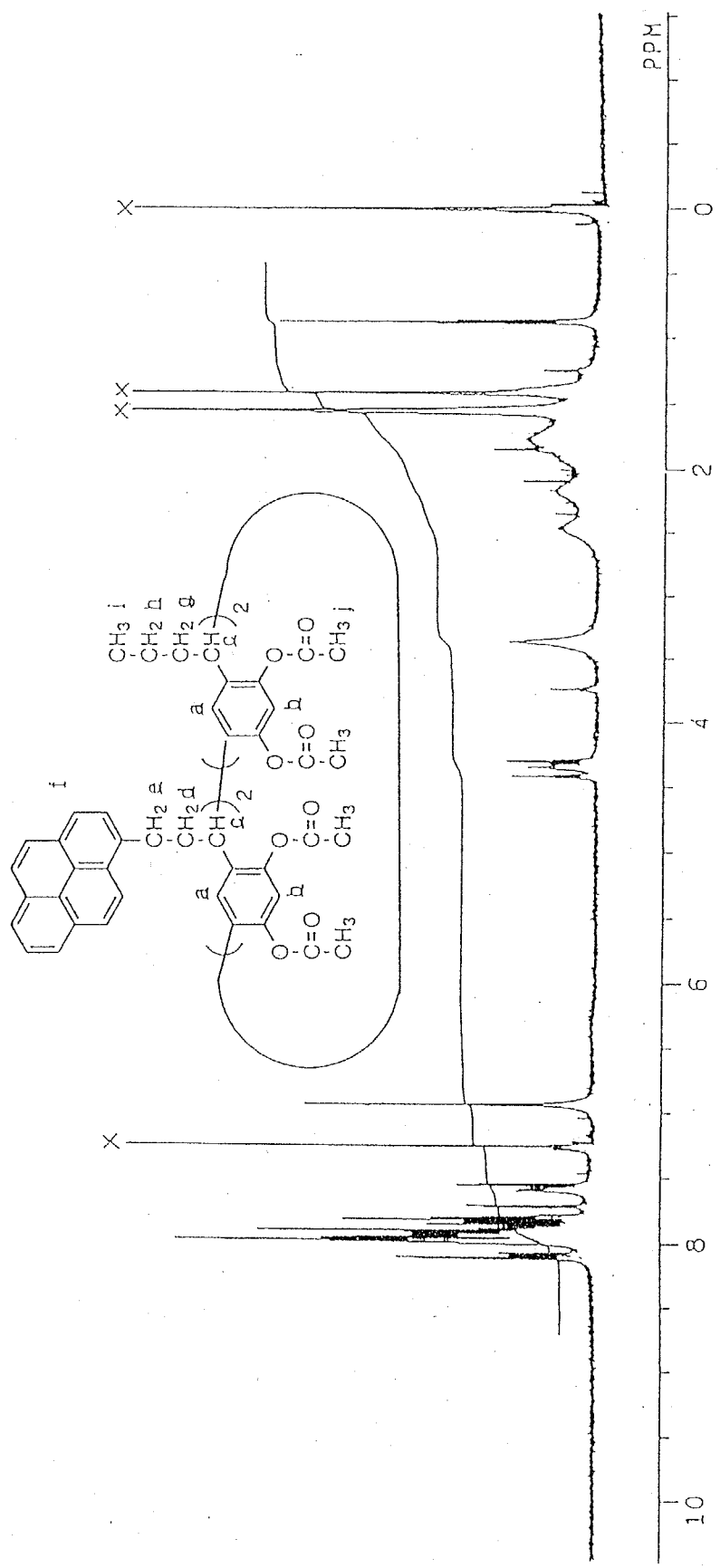
Figure 5-2 NMR spectrum of the third fraction separated by HPLC of the second run:

Hi; 0.87, Hj; 1.5-2.0, Hd, Hg, Hh; 2.0-2.6, He; 3.37, Hc; 4.2-4.5, Hb; 6-7 (not observed clearly, see text), Ha; 6.97, Hf; 7.5-8.2 ppm, ✕; solvents and TMS.

fourth ones were identified with the acetylated CRA with two pyrenylethyl and two propyl groups (CRA-Py(2)) and that with three pyrenylethyl and a propyl groups (CRA-Py(3)), respectively.   Although there should exist two structural isomers of CRA-Py(2) with two pyrenylethyl groups at the adjacent positions and the opposite positions, respectively, the separation of these isomers was unsuccessful under the present HPLC condition.   The UV absorption of CRA-Py(n) at this wavelength is due to both resorcinol moiety and pyrene chromophore.   The molar absorption coefficients at 274 nm, at which HPLC peaks were detected by UV absorption, of CRA-Py(0), CRA-Py(1), CRA-Py(2), CRA-Py(3) and CRA-Py(4) were measured in methanol to be 4.4×10^3, 4.7×10^4, 9.0×10^4, 1.3×10^5 and 1.8×10^5, respectively.   Using these absorption coefficients and the area ratio of HPLC peaks of each fraction, the product distribution of the both runs were calculated.   The ratio of produced CRA-Py(n) (n = 0 to 4) was considered to be same as the ratio of the purified CRA-Py(n) by column chromatography after acid-catalyzed condensation and acetylation, which was analyzed by HPLC, since the retention times of the column chromatography for the all fractions of CRA-Py(n) were same under used condition.   The ratio of the fractions was equal to the ratio of the concentrations of CRA-Py(n) (n = 0 to 4) in the solution used in HPLC analysis.   The each concentration was calculated by the division of the HPLC peak's area at 274 nm by the absorption coefficients (ε) at 274 nm of CRA-Py(n) (n = 0 to 4).

For the first run, the NMR areas of the small signals were summed up to the corresponding main signals.   As shown in Table 5-1, experimental values are in good agreement with calculated ones under the assumption that the condensation reactions of the two aldehydes proceed at the same rate.

5-3-2. Intramolecular interaction between pyrenyl groups

The absorption maximum at 345 nm due to pyrene moiety in chloroform is not influenced by the number of the pyrene residue.   The molar absorption coefficients of four CRAs with different numbers of pyrene at 345 nm are summarized in Table 5-2. The fact that the absorption maximum and the absorption coefficient per pyrenyl unit are not dependent on the number of pyrene substituent(s) implies that there are essentially no intramolecular interactions in the electronic ground state between pyrenyl groups.   On the

104

Table 5-1 The raito of CRA-Py(n) of synthesized octaacetylated products

Run#		x				
		0	1	2	3	4
1	Observed*	0.39	0.37	0.18	0.05	0.01
	Estimated**	0.32	0.42	0.21	0.05	0.003
2	Observed*	0.09	0.24	0.34	0.25	0.08
	Estimated**	0.06	0.25	0.38	0.25	0.06

*: calculated from HPLC area of absorption monitored at 274 nm
**: calculated with assumption that the reaction rates of two aldehyde are same

Table 5-2 Absorption molecular coefficients of CRA-Py(n) in chloroform

n	ε_{342} / l mol^{-1}cm^{-1}	ε_{342} per pyrenyl unit / l mol^{-1}cm^{-1}
1	3.3×10^4	3.3×10^4
2	6.8×10^4	3.4×10^4
3	9.8×10^4	3.2×10^4
4	1.23×10^5	3.3×10^4

other hand, NMR signals due to pyrenyl group(s) in a higher field region are quite different among the CRA derivatives, as shown in Figure 5-3. Any peaks of pyrenyl group shift to an upper field when the number of pyrenyl groups increases. This fact is interpreted in terms of the crowded conformation of pyrenyl substituents so that the ring current effect of the aromatic ring system brings about the upper field shift.

The full assignment of ^{1}H signals of the pyrene ring of CRA-Py(1) and CRA-Py(4) was performed by comparison to all ^{1}H-NMR signals of α,ω-di(1-pyrenyl)alkanes assigned in reference [11] as summarized in Table 5-3, whereas NMR spectra of CRA-Py(2) and CRA-Py(3) were too complicated to assign all of the peaks. The assigned peaks of H(2) and H(6) of CRA-Py(3) are separated into two doublets, respectively. It is noteworthy that the integral ratio of (upper field doublet)/(down field doublet) is 1/2 for the two couples (Figure 5-3). This fact shows that the ring current effect on the pyrenyl group whose both sides are pyrenyl groups is different from that of the pyrenyl group which has no neighboring pyrenyl group at an alternative side and the ratio of the population of CRA-Py(2) isomers were 2:1 for neighboring and opposite types. The extent of the ring current effect was evaluated by the difference ($\Delta\delta$) between the chemical shifts of each proton of CRA-Py(1) and CRA-Py(4). As shown in Table 5-3, H(3), H(8) and H(9) display larger $\Delta\delta$ values among all pyrene protons by stronger ring current effect, indicating that these three protons are closer to the center of another pyrenyl group compared with the other protons. This situation was proved by a space filling molecular model.

This result forms a striking contrast to the report by K. A. Zachariasse et al. They studied the relationship between NMR spectra and fluorescence properties of bichromophoric systems in which two pyrenyl residues are linked through a polymethylene spacer with variant chain lengths.[18] They showed that J values of the neighboring protons of the bipyrenyl groups are not influenced each other at all, and the proton chemical shifts are essentially identical for all of the bipyrenyl compounds. The marked ring current effect in the multi-chromophoric system in the present work is obviously due to the restricted mobility of the cyclic skeleton. In other words, the orientation of functional groups tethered to the lower rim of the cyclic CRA is forced to be restricted.

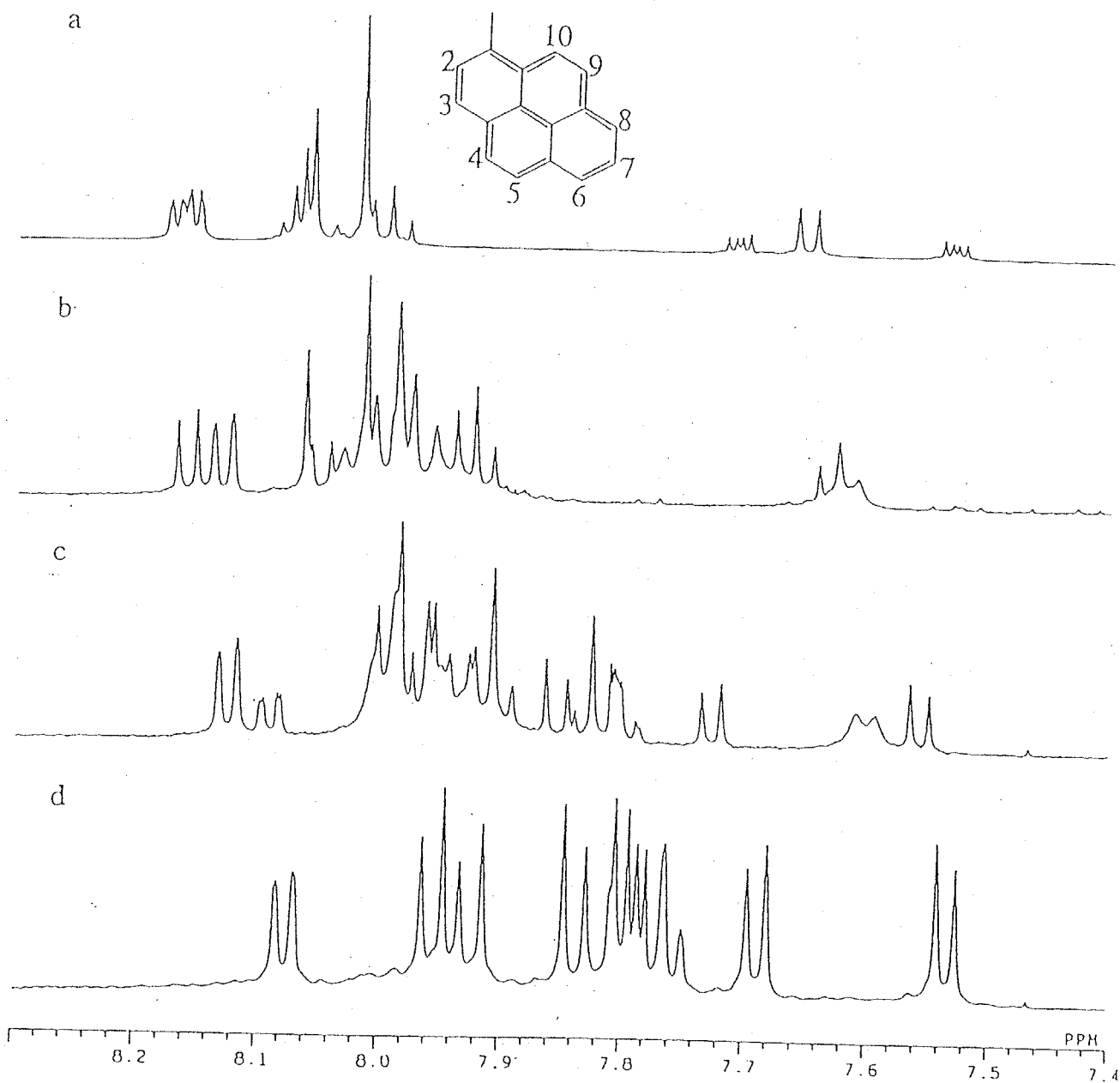5-3-3. Steady state fluorescence in solutions

Figure 5-3 NMR spectra of separated fractions of the second run in a pyrenyl proton region; CRA-Py(1) (a), CRA-Py(2) (b), CRA-Py(3) (c) and CRA-Py(4) (d).

Table 5-3 Assignment of ¹H-NMR peaks of CRA-Py(n)

¹H	CRA-Py(1)		CRA-Py(2)		CRA-Py(3)		CRA-Py(4)		Δδ(ppm) between CRA-Py(1) and CRA-Py(4)
	δ(ppm)	J(Hz)	δ(ppm)	J(Hz)	δ(ppm)	J(Hz)	δ(ppm)	J(Hz)	
H(2)	7.651		7.632		7.556 7.600 [c]		7.534		0.117
H(3)	8.064		a		7.726 b		7.688		0.376
$J_{2,3}$		7.69		7.69		8.06 7.33		7.69	
H(4)	8.016		a		b		7.954		0.062
H(5)	8.016		a		b		7.837		0.179
$J_{4,5}$		-						8.79	
H(6)	8.166		8.158		8.089 8.124 [c]		8.075		0.091
H(7)	7.992		a		b		7.793		0.199
H(8)	8.158		8.128		b		7.756		0.402
$J_{6,7}, J_{7,8}$		7.33		7.69		6.56 7.32		7.33	
H(9)	8.047		a		b		7.795		0.252
H(10)	8.073		a		b		7.922		0.151
$J_{9,10}$		9.16						9.16	

δ: ±0.0007ppm , J: ±0.37Hz,   a = 7.906~8.060,   b = 7.788~8.001,   c: integral ratio=1:2

The intramolecular interaction of pyrene residues of CRA derivatives was more clearly grasped by measuring fluorescence spectra of CRA-Py(n) in solution. As expected, the emission intensity ratio of excimer to monomer (Ie/Im) increased as the increase in the number of pyrenyl group, as presented in Figure 5-4. Note here that the difference of Ie/Im between CRA-Py(2) and CRA-Py(3) is larger than that between CRA-Py(3) and CRA-Py(4). This fact indicates that the excimer formation results from the additional attachment of a pyrenyl group to CRA-Py(2) more favorably than that to CRA-Py(3). The effects of an additional pyrene group to both of two isomers of CRA-Py(2), neighboring-type and opposite-type, for excimer formation were stronger than that to CRA-Py(3), whose pyrenyl groups were already packed enough to form excimer. The emission maximum of the excimer is not affected by the number of pyrenyl group.

When compared with intermolecular excimer emission observed in a 4.6 mmol/l solution of a monomeric ethyl 3-(1-pyrenyl)propanate (Figure 5-5), the excimer of CRA-Py(n) formed intramolecularly appears at a shorter wavelength region. This may result again from the restricted mobility of the cyclic molecular framework that leads to the formation of the intramolecular excimer with a relatively higher electronic energy in the lowest singlet state. The intramolecular excimer emission of CRA-Py(n) ($n > 2$) exhibits a slight (2 nm) blue-shift in cyclohexane irrespective of the number of pyrene when compared with that in THF as shown in Figure 5-6 whereas no solvent effect was observed for the intermolecular excimer emission from the monomer at all as shown in Figure 5-5. This means that the solvation to intramolecular excimer of CRA-Py(n) molecules depend more or less on the nature of solvents.

The structure of the intermolecular excimer of a pyrene derivative is the most stable "face-to-face" one in any solvents whose fluorescence does not depend on the solvent natures. In contrast, the intramolecular pyrene groups linking CRA can not make the most stable "face-to-face" excimer but solvated excimer and that the stronger solvation in polar THF makes the fluorescence red-shifted than in non-polar cyclohexane. It was reported that λmax of intramolecular emission of α,ω-bis-(1-pyrenyl)alkane in methylcyclohexane solution is influenced by the number of methylene groups (m) linking two pyrenyl residues; as m increases, λmax is blue-shifted from 20 kcm^{-1} (500 nm) (m = 3) to 22 kcm^{-1} (455 nm) (m = 5, 6) and then red-shifted to 20.5 kcm^{-1} (488 nm) (m = 13) and
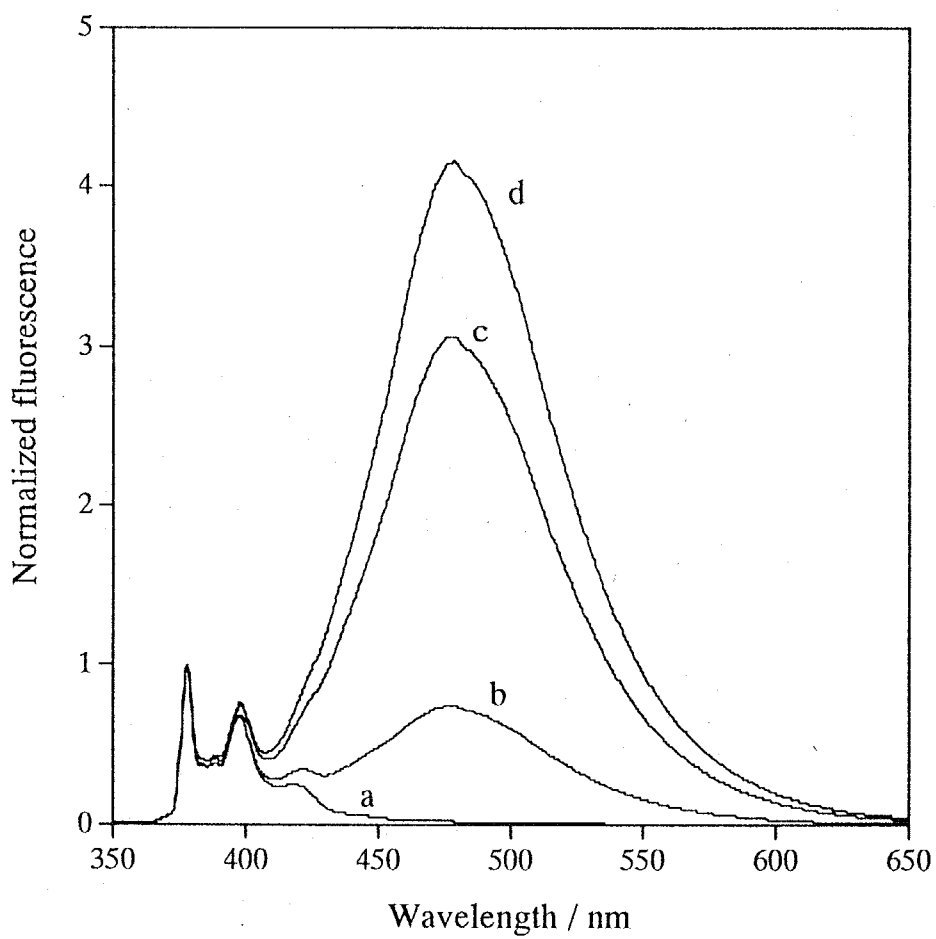
Figure 5-4 Fluorescence spectra normalized at 377.5 nm of CRA-Py(n) in
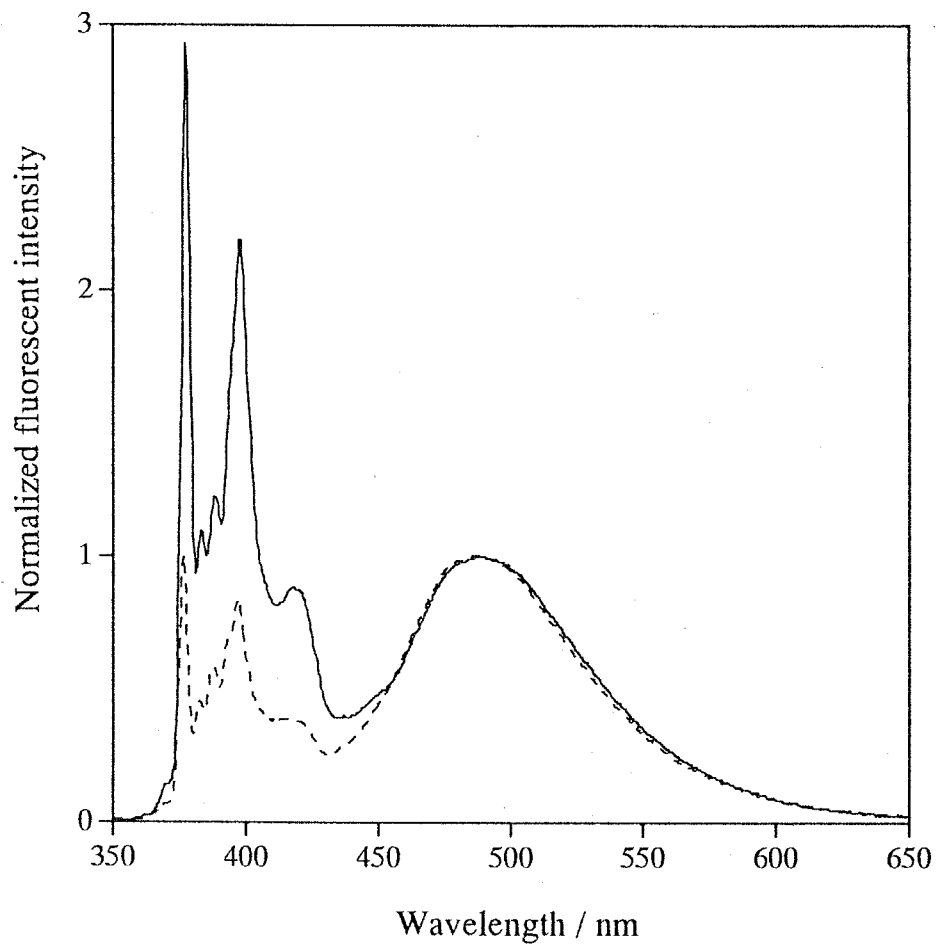THF; CRA-Py(1) (a), CRA-Py(2) (b), CRA-Py(3) (c) and CRA-Py(4) (d).

Figure 5-5   Fluorescence spectra normalized at λmax of excimer of ethyl

3-(1-pyrenyl)propanate in THF (solid line) and in cyclohexane (dot line); both

concentrations are 4.6 mmol/l.
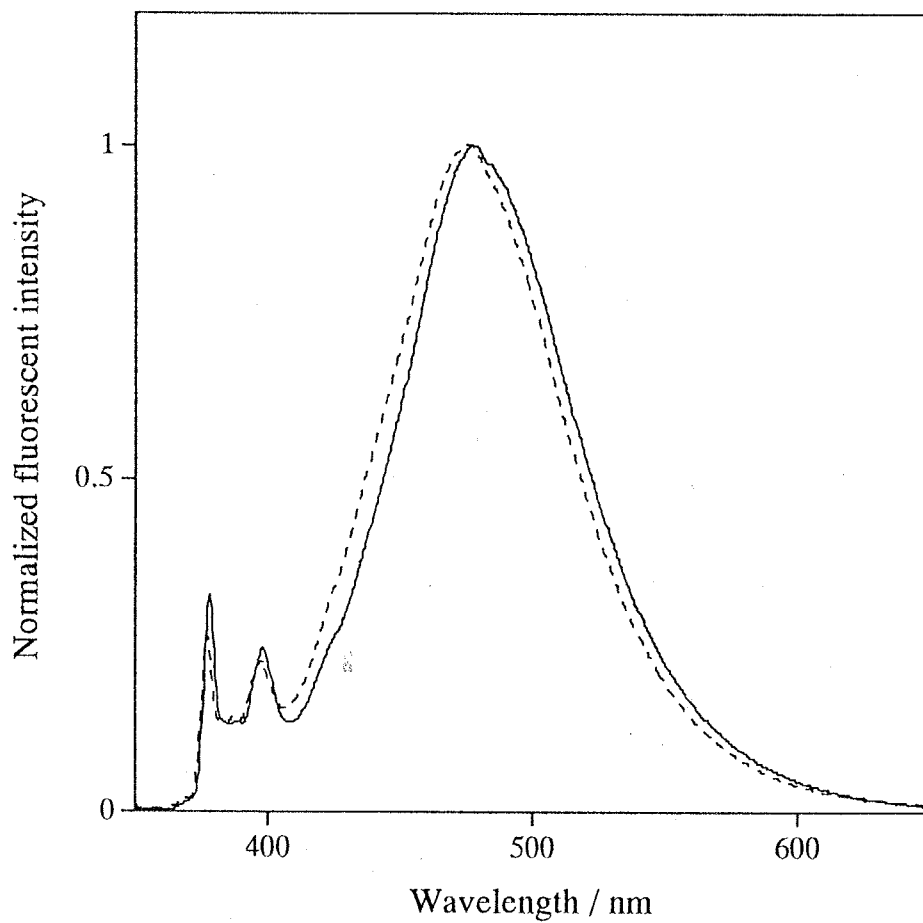
Figure 5-6 Fluorescence spectra normalized at λmax of excimer of

CRA-Py(3) in THF (solid line) and in cyclohexane (dot line).

not shifted when m is larger than 13 as a result of strained conformation of the intramolecular excimer.[19] λmax of the excimer of CRA-Py(n) (473 nm in cyclohexane) is almost the same as those of 1,4-bis-(1-pyrenyl)butane (471 nm) and 1,9-bis-(1-pyrenyl)nonane (474 nm) in methylcyclohexane. These facts suggest that the conformational strain in excimers of CRA-Py(n) series is not affected by n despite the increase in the molecular crowd with increases in n and that the extent of the strain of CRA-Py(n) is in a range similar to that of the bipyrenyl compounds with tetra- and nanomethylene spacers.

5-3-4. Fluorescence decay time in solutions

Emission decay times of CRA-Py(n) in THF or cyclohexane were measured using a single photon counting system. All the deconvoluted data were fitted well with triple exponentials as expressed in the following equations;

$$Im(t) = A_1 \exp(-t/\tau_1) + A_2 \exp(-t/\tau_2) + A_3 \exp(-t/\tau_3)$$

$$Ie(t) = B_1 \exp(-t/\tau_1) + B_2 \exp(-t/\tau_2) + B_3 \exp(-t/\tau_3)$$

where $A_1, A_2, A_3 > 0$ and $-B_1 = B_2 + B_3 > 0$.

The decay data are summarized in Table 5-4. τ_1, τ_2 and τ_3 are very close to the decay time constants of 1,3-bis-(1-pyrenyl)propane reported previously.[20-22] According to the literatures,[14,15] the above-mentioned equations were fitted within a kinetic scheme consisting of three excited species; one excited monomer and two excimers (Scheme 5-2), whereas the decay processes of 1,13-bis-(1-pyrenyl)tridecane and 1,3-(2-pyrenyl)propane were analyzed as a double exponential, respectively.[12,14-15] As shown in Table 5-4 which contains also the data for the bipyrenyl compounds, a one type excimer specifically made from 1,3-bis-(2-pyrenyl)propane has a long time decay constant while an another type excimer originated from 1,13-bis-(1-pyrenyl)tridecane has a short time decay constant. Both types of excimers are produced from 1,3-bis-(1-pyrenyl)propane and CRA-Py(n). The preexponential factors, B_2 and B_3, indicate the ratio of two types.

Though the ratios of these two excimers are different in CRA-Py(n), the fluorescence wavelength and broadness are almost same, which means the energy levels are almost same. Both excimers are fully overlapped excimers since the energy level of a partially overlapped excimer is different and the fluorescence wavelength shifts. The two
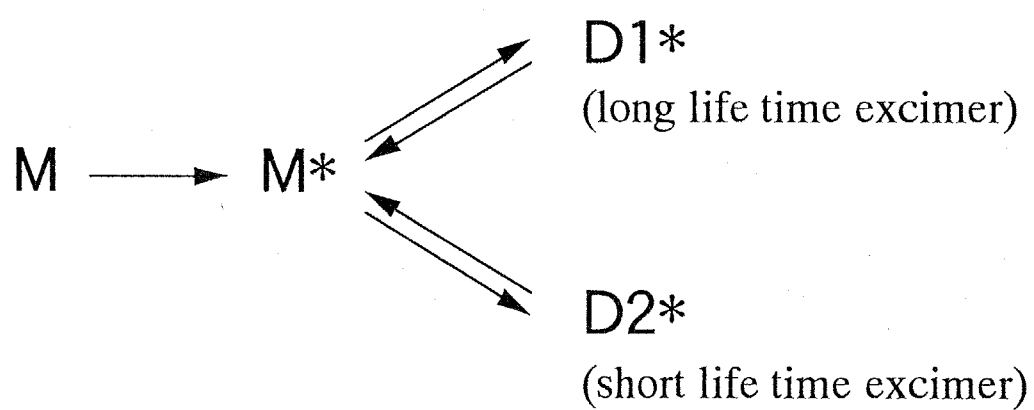
Table 5-4 Fluorescence decay time constants and preexponential factors

sample		solvent	temperature	monomer emission			excimer emission		
				τ_1/ns (A_1)	τ_2/ns A_2	τ_3/ns A_3)[a]	τ_1/ns (B_1)	τ_2/ns B_2	τ_3/ns B_3)[b]
CRA-Py(1)		tetrahydrofuran	room temp.			217			
CRA-Py(2)				4.2 (0.30)	32 0.26	121 0.44	8.8 (-0.91)	58 0.44	116 0.56
CRA-Py(3)				11 (0.65)	33 0.22	112 0.13	11 (-0.96)	39 0.63	106 0.37
CRA-Py(4)				5.8 (0.63)	22 0.26	101 0.11	7.6 (-0.90)	38 0.56	96 0.44
CRA-Py(1)		cyclohexane	room temp.			185			
CRA-Py(2)				3.5 (0.18)	27 0.25	124 0.57	9.9 (-0.85)	35 0.59	112 0.41
CRA-Py(3)				15 (0.55)	40 0.35	130 0.09	12 (-0.85)	45 0.81	120 0.19
CRA-Py(4)				5.8 (0.62)	28 0.29	111 0.09	6.7 (-0.77)	42 0.71	94 0.29
1,3-bis-(1-pyrenyl)propane	c	methylcyclohexane	40°C	5.1 (0.96)	54.6 0.036	149.9 0.0072	5.1 (-0.98)	56.5 0.67	145.2 0.33
1,3-bis-(2-pyrenyl)propane	c			5.2 (0.98)	- -	139.6 0.015	5.1 (-0.99)	- -	149.7 1.00
1,3-bis-(1-pyrenyl)propane	d	toluene	20°C	not described			8.1 (-1.00)	57.9 0.71	129.8 0.29
1,13-bis-(1-pyrenyl)tridecane	d			not described			15.7 (-1.00)	52.1 1.00	- (-)

a: An's were calculated to make $A_1+A_2+A_3=1$

b: Bn's were calculated to make $B_2+B_3=1$

c, d: data from ref.14, 10

$$M \longrightarrow M* \begin{array}{c} \nearrow \!\!\!\!\!\swarrow \quad \text{D1*} \\ \\ \searrow \!\!\!\!\!\nwarrow \quad \text{D2*} \end{array}$$

D1*
(long life time excimer)

D2*
(short life time excimer)

Scheme 5-2 A kinetic scheme for excimer formation of 1,3-bis-(1-pyrenyl)propane proposed by Zachariasse et. al.[15]

excimers must have different structures. The structure of the former type excimer, whose life time is almost same as the excimer of 1,3-bis-(2-pyrenyl)propane, must be face-to-face symmetric because 1,3-bis-(2-pyrenyl)propane has a symmetric structure itself. The other type excimer appears in 1,13-bis-(1-pyrenyl)tridecane whose decay time constant is shorter has another structure, not symmetric rather asymmetric one. It is reasonable that the ratio of symmetric type excimer to asymmetric one is larger in THF than that in cyclohexane, considering that cyclohexane is poor solvent for CRA-Py(n).

The ratio decreases markedly as n changes from 2 to 3, but increases as n changes from 3 to 4. When n = 2, pyrenyl groups are not so crowded, and symmetric type excimer whose decay time constant is long is made more easily than for CRA-Py(3) or CRA-Py(4) whose pyrenyl groups are crowded. The fact that a symmetric type excimer is made more easily in CRA-Py(4) than in CRA-Py(3) can be explained with two hypotheses that closer pyrenyl groups make symmetric type excimer easily than farther groups do and that excimers are made between closer pyrenyl groups more easily in CRA-Py(4) whose pyrenyl groups are too crowded to make excimers between farther pyrenyl groups compared with in CRA-Py(3).

5-4. Conclusions

A mixture of five species of calix[4]resorcinarene possessing variant numbers of pyrenylethyl group was synthesized by the reaction of resorcinol with a mixture of pyrenylpropanal and butanal, followed by acetylation to be subjected to HPLC separation. The analysis of the production distribution indicated that the reaction rates of two aldehydes are almost the same. The intramolecular interactions between pyrenyl groups of the crown conformer of CRAs were too weak to influence their electronic absorption spectra, but strong enough to shift NMR chemical shifts of proton peaks of pyrenyl groups markedly. The CRAs possessing pyrenylethyl groups form intramolecular excimers, and the strain of the excimers is almost the same as that of α, ω-dipyrenyl compounds with tetra- and nanomethylene spacers. The decay time data showed that CRAs substituted with pyrenyl groups form two types of intramolecular excimer just as in the case of 1,3-bis-(1-pyrenyl)propane.

References

1. J. B. Birks, "*Photophysics of Aromatic Molecules*", 1970, Wiley-Interscience (London), Chapter 4.

2. H. Schneider, D. Guttes and U. Schneider, *Angew. Chem. Int. Ed. Engl.*, 1986, **25**, 647.

3. B. Dhawan, S. I. Chen and C. D. Guttes, *Macromol. Chem.*, 1987, **188**, 921.

4. Y. Aoyama, Y. Tanaka and S. Sugahara, *J. Am. Chem. Soc.*, 1989, **111**, 5397.

5. K. Kurihara, K. Ohta, Y. Tanaka, Y. Aoyama and Y. Kunitake, *Thin Solid Films*, 1989, **179**, 21.

6. K. Kurihara, K. Ohta, Y. Tanaka, Y. Aoyama and Y. Kunitake, *J. Am. Chem. Soc.*, 1991, **113**, 444.

7. D. Cram, *Nature*, 1992, **356**, 29.

8. E. Kurita, N. Fukushima, M. Fujimaki, Y. Matsuzawa, K. Kudo and K. Ichimura, *J. Mater. Chem.*, 1998, **8**, 397.

9. M. Ueda, N. Ueda, K. Kudo and K. Ichimura, *J. Mater. Chem.*, 1997, **7**, 641.

10. K. Ichimura, N. Fukushima, M. Fujimaki, S. Kawahara, Y. Matsuzawa, Y. Hayashi and K. Kudo, *Langmuir*, 1997, **13**, 6780.

11. I. Aoki, H. Kawabata, K. Nakashima and S. Shinkai, *J. Chem. Soc. Chem. Commun.*, 1991, 1771.

12. I. Aoki, T. Sakaki and S. Shinkai, *J. Chem. Soc. Chem. Commun.*, 1992, 730.

13. M.Takeshita and S. Shinkai, *Chem. Lett.*, 1994, 125.

14. A. G. S. Hogberg, *J. Org. Chem.*, 1980, **45**, 4498.

15. A. G. S. Hogberg, *J. Am. Chem. Soc.*, 1980, **102**, 6046.

16. L. Abis, E. Dalcanale, A. Du vosel and S .Spera, *J. Org. Chem.*, 1988, **53**, 5475.

17. A. G. S. Hogberg, *J. Am. Chem. Sci.*, 1989, **111**, 5397.

18. P. Reynders, W. Kuhnle and K. A. Zachariasse, *J. Phys. Chem.* 1990, **94**, 4073.

19. K. A. Zachriasse and W. Kuhnle, *Z. Phys. Chem. Neue Folge*, 1976, **101**, 267.

20. K. A. Zachariasse, G. Duveneck and R. Busse, *J. Am. Chem. Soc.*, 1984, **106**, 1045.

21. K. A. Zachariasse, R. Busse, G. Duveneck and W. Kuhnle, *J. Photochemistry*, 1985, **28**, 237.

22. K. A. Zachariasse, G. Duveneck and W. Kuhnle, *Chem. Phys. Lett.* 1985, **113**, 337.

Chapter 6

Exciplex emission of pyrene and N,N-dimethylaniline at the interface between a silica surface and a polymer layer

6-1. Introduction

In the preceding chapter, an attempt was made to fabricate a model system for revealing microenvironmental conditions at an interface between two different kinds of phases using 9,10-dicyanoanthracene (DCA) as a fluorescent probe exhibiting exciplex emission in the presence of phenanthrene (Phe). Exciplex emission gives novel information about interfacial phenomena, because the exciplex emission is generated specifically at an interface, when each component molecule forming the exciplex is tethered to each material to be studied. Whereas the combination of DCA with Phe gives a novel system to shed light into an interface between a DCA-modified silica surface and a polymer with Phe side chains in a solution, the system was not appropriate for revealing an interfacial microenvironment between the silica surface and a polymer film, because of the emission of DCA excimer and highly condensed Phe absorbing the excitation light, which comes selectively from the silica surface.

This chapter aims at constructing another system providing information about interfacial microenvironments between silica and a polymer solid using exciplex emission, taking notice of the following conditions. 1) The system exhibits intermolecular interactions between a fluorescent probe adsorbed on a silica surface and segments of the polymer to display strong exciplex emission. 2) The fluorescent probe on a silica shows no excimer emission because usually wavelengths of an excimer and an exciplex of a fluorophore lie in the same region so that this situation makes the system so complicated for the fluorescence analysis. 3) The polymer does not fluoresce to simplify the emission system at an interface. To satisfy these conditions, the combination of pyrene and N,N-dimethyaniline (DMA) is adopted in this chapter.

There have been reports on fluorescence of pyrene adsorbed on silica gel,[1-3] self-assembled monolayers incorporating pyrene groups.[4,5] They show excimer emission so

that they are not suitable for the present study, since, as stated just above, exciplex emission with DMA will be hidden by pyrenyl excimer.[6-8] This problem can be essentially overcome by the reduction of surface density of pyrenyl groups. As a procedure for modification of a silica surface with controlled density of pyrenyl residues, calix[4]resorcinarene (CRA) was employed in this work, take note of the facts that CRA gives rise to self-assembled monomolecular films quite readily owing to its strong adsorptivity to a silica surface.[9-12] Besides, the synthesis of CRA possessing a single pyrenyl group and three alkyl chains was achieved in chapter 5. This compound is in line with the present study, as shown below. An occupied area of a CRA substituted with eight carboxymethoxy units in a self-assembled monolayer has been reported to be around 2.0 nm^2 so that a distance between the center of molecules is about 1.6 nm. In this way, when a length of a spacer between a pyrenyl group and the CRA framework is short enough, the fluorescent moieties should be well separated in the monolayer to suppress the excimer formation. Since a CPK model of the molecule indicates that a spacer with more than two methylenes is long and flexible enough to permit pyrenyl groups close to each other to form excimer on a surface even though CRA skeleton is rigid, CRA with a pyrenylmethyl group is ordered for the purpose.

In this context, fluorescence behavior of a CRA derivative possessing a single pyrene unit adsorbed on a silica surface was investigated in this chapter. Colloidal silica particles was used in this work for the adsorption of the macrocyclic compound owing to marked enlargement of a surface area of silica, leading to enhancement of emission intensity. A polymethacrylate with DMA side chains was synthesized and made it in contact with the CRA-modified silica surface to follow exciplex emission.

6-2. Experiment

6-2-1. Materials

Octacarboxymethoxylated 1-pyrenylmethyltrimethylcalix[4]resorcinarene (16) was synthesized as shown in Scheme 6-1. 1-Pyrenylacetic acid, acetaldehyde and resorcinol were commercially available and used as received. Colloidal silica was kindly donated by Nissan Chemical Industry. The structure and the synthetic route of methacrylate polymer
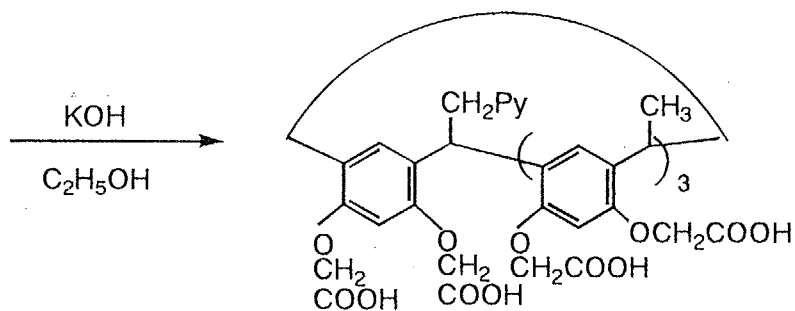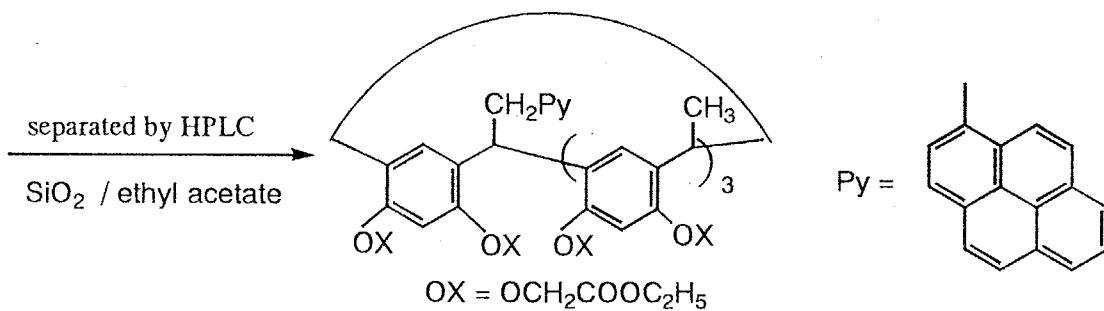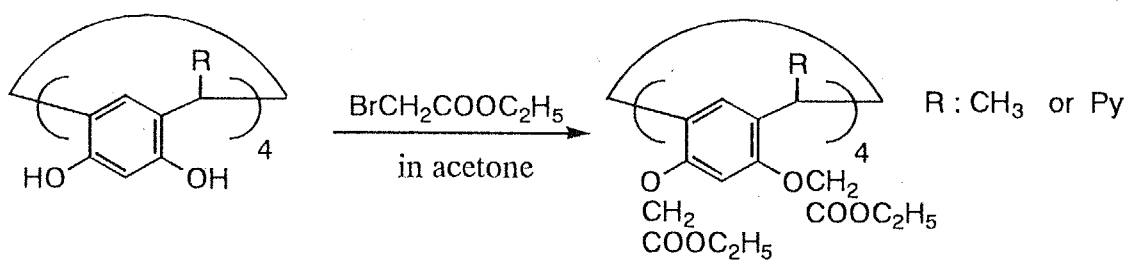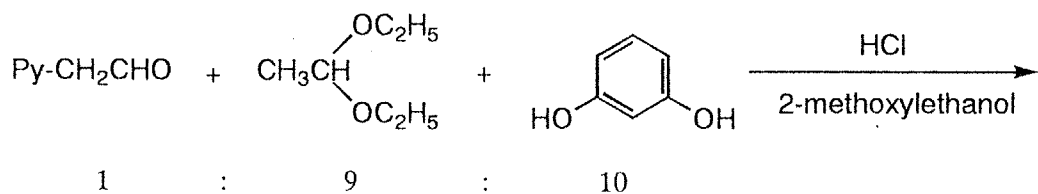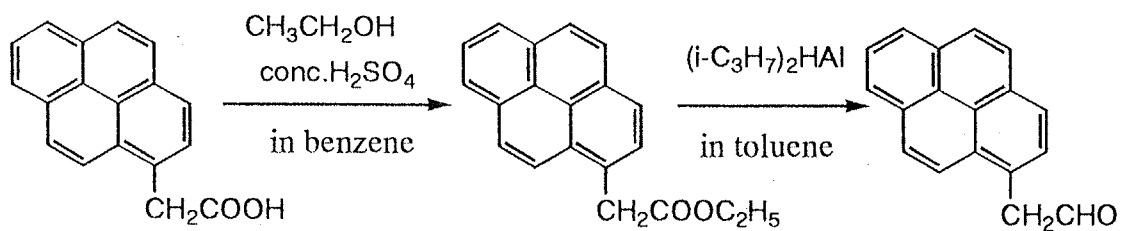
Scheme 6-1 Syntheses of 16

possessing dimethylaniline moiety (**17**) were shown in Scheme 6-2. (3-Aminopropyl)dimethylethoxysilane was purified by distillation before use.

Ethyl 1-pyrenylacetate

To a solution of 1-pyrenylacetic acid (0.94 g, 3.6 mmol) in ethanol (3 ml) was added sulfuric acid (0.2 ml) and dry benzene (15 ml) and refluxed for 3 hours. The solution was washed with a 5% sodium hydrogen carbonate aqueous solution, water, and a sodium chloride saturated aqueous solution. After drying with potassium carbonate, the solvent was removed by evaporation, and a residue was purified by column chromatography (SiO_2, ethyl acetate : hexane = 1:3) and recrystallization from ethanol to give yellow needles in a 82 % yield.

mp = 98 – 99 °C

^{1}H-NMR (in CDCl3)

δ (ppm) = 1.22 (t, 3H, J=7.1Hz), 4.17 (q, 2H, J=7.1Hz), 4.34 (s, 1H), 7.9 - 8.4 (m, 9H)

1-Pyrenylacetaldehyde [13]

A solution of ethyl 1-pyrenylacetate (0.83 g, 3.2 mmol) dissolved in dry toluene (20 ml) was stirred at -78 °C under nitrogen stream, followed by addition of a hexane solution of 1 mol/l diisobutylaluminum hydride (2 ml) and stirring for 2 hours at -78 °C. The addition of hydrochloric acid (0.5 ml) and tetrahydrofuran (4.5 ml) to the reaction mixture at -78 °C under stirring resulted in the precipitation of a pale yellow solid, which was collected by filtration and recrystallized from a mixture of acetate and hexane. Yield 82 %.

mp = 137 - 138 °C,

^{1}H-NMR (in CDCl3)

δ (ppm) = 4.39 (d, 2H, J=2.3Hz), 7.8 - 8.3 (m, 9H), 9.89 (t, 1H, J=2.3Hz)

Calix[4]resorcinarenes with 1-pyrenylmetyl and methyl groups

A 2-methoxyethanol (30 ml) solution containing 0.59g (2.4 mmol) of 1-pyrenylacetaldehyde, 2.11 g (17.9 mmol) of acetaldehyde, 2.23 g (20.3 mmol) of resorcinol and a few drops of hydrochloric acid was refluxed for 14 hours. The crude product was
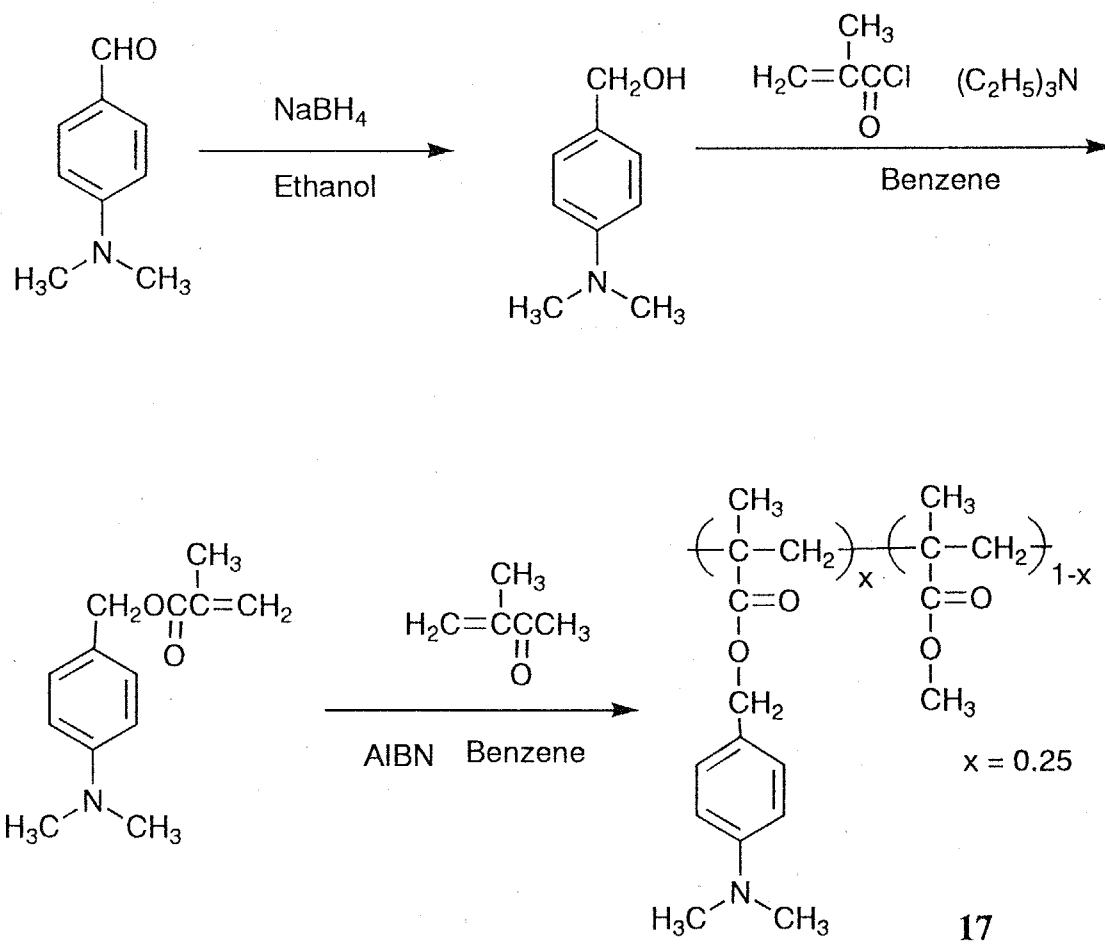
Scheme 6-2 Synthesis of **17**

extracted with ethyl acetate after work-up with water and subjected to separation with column chromatography (SiO_2, ethyl acetate) to isolate a mixture of calix[4]resorcinarenes with 1-pyrenylmetyl groups and methyl groups. Yield was 26 % by weight.

^{1}H-NMR ($CDCl_3$)

δ (ppm) = 1.28 (d, 22.5H, J=6.9Hz), 2.52 (s, 2H), 4.3 - 4.7 (m, 8.5H), 6.14(s, 8.5H), 6.76(s, 8.5H), 7.8 - 8.3 (m, 9H), 8.3-9.4 (br, 17H, disappeared when D_2O was added)

Octaethyl carboxylate of 1-pyrenylmethyltrimethylcalix[4]resorcinarene

A mixture of calix[4]resorcinarenes with 1-pyrenylmethyl and methyl groups (0.85 g) was dissolved in dry acetone, and ethyl bromoacetate (3.0 g) and K_2CO_3 (ground, 3.0 g) were added to the solution. After the solution was stirred for 66 hours at room temperature, the solid was removed by filtration, followed by evaporation of the solvent to give a yellow oil of a mixture of octaethoxycarbonylmethoxylated CRAs. The separation of the mixture was performed by HPLC (column : SiO_2 (Crestpak-SIL (JASCO)), eluent : ethyl acetate, detector : UV). The first fraction was octaethylcarbonylmethoxylated CRA with four methyl groups, which was not detected with 345 nm light. The second fraction was octaethylcarbonylmethoxylated CRA with one pyrenylmethyl group and three methyl groups, which was sensitive to 345 nm light. The second fraction was collected to give 0.82 g of a yellow solid.

mp = 85 - 86 °C

^{1}H-NMR (in CDCl3)

δ (ppm) = 1.21 (t, 24H, J=7.0Hz) 1.54 (d, 9H, J=9.0Hz), 2.32 (s, 2H), 4.21 (q, 16H , J=7.0Hz), 4.27 (s, 16H) 4.4-4.7 (m, 4H), 6.25 (s, 4H), 7.16 (s, 4H), 7.7-8.3 (m, 9H)

Elemental Anal. for $C_{80}H_{88}O_{24}$: Calcd. C: 67.03, H: 6.19%.

Found C: 67.29, H: 5.98%.

Octacarboxymethoxylated 1-pyrenylmethyltrimethylcalix[4]resorcinarene (16)

The separated octaethylester of the CRA (0.82 g) was dissolved in methanol containing KOH. After stirring for 30 minutes at room temperature, chloroform and water were added

to the solution. An aqueous layer was separated and treated with HCl and extracted by a mixture of acetone and chloroform. Yield was 93%.

mp > 300 °C (decomp.)

^{1}H-NMR (DMSO-d6)

δ (ppm) = 1.46 (d, 9H, J=9.0Hz), 2.24 (s, 2H), 4.38 (s, 16H), 4.4-4.6 (m, 4H), 6.46 (s, 4H), 7.13 (s, 4H), 7.5-8.2 (m, 9H)

Elemental Anal. for $C_{64}H_{56}O_{24}\cdot4H_2O$: Calcd. C: 60.00, H: 5.04%.

Found C: 60.27, H: 4.81%.

4-Dimethylaminobenzyl alcohol

Sodium borohydride (1.0 g, 26 mmol) was added to an ethanol solution of p-dimethylaminobenzaldehyde (5.07 g, 34.0 mmol), and the solution was refluxed for 3 hours. After extracting with diethyl ether and purification by column chromatography (SiO2, acetone : hexane = 1:4), the product was obtained as an oily substance in a 97 % yield.

^{1}H-NMR (in $CDCl_3$)

δ (ppm) = 1.68 (t, 1H, J=4.5Hz), 2.90 (s, 6H), 4.49 (d, 2H , J=4.5Hz), 6.69 (d, 2H, J=9.0Hz), 7.21 (d, 2H, J=9.0Hz)

4-Dimethylaminobenzyl methacrylate

4-Dimethylaminobenzyl alcohol (1.42 g, 9.42 mmol) and triethylamine (2.0 2g, 20.0 mmol) were dissolved in benzene. Methacryloyl chloride (2.09 g, 20.0 mmol) was added to the solution in an ice bath. After stirring for 2 hours in an ice bath, followed by filtration and washing with water, the product was purified by column chromatography (SiO$_2$, acetone : hexane = 1:20) and recrystallization from petroleum ether. Yield was 32 %.

mp = 40 - 41 °C

^{1}H-NMR (CDCl3)

δ (ppm) = 1.95 (d, 3H, J=1.1Hz), 2.96 (s, 6H), 5.11 (s, 2H), 5.55 (t, 1H, J=1.1Hz), 6.15 (s, 1H), 6.75 (d, 2H, J=9.0Hz), 7.31 (d, 2H, J=9.0Hz)

Elemental Anal. for $C_{13}H_{17}NO_2$: Calcd. C: 71.21, H: 7.81, N: 6.38%.

Found C: 71.46, H: 7.90, N: 6.11%.

Poly(4-dimethylaminobenzyl methacrylate-*co*- methyl methacrylate)   (17)

0.27 g (1.2 mmol) of 4-dimethylaminobenzyl methacrylate, 0.32 g (3.2 mmol) of methyl methacrylate and 0.011 g (0.067 mmol) of azobisisobutylonitrile were dissolved in 15 ml benzene. The solution was placed in an ampoule, degassed by freeze-pump-thaw method and sealed. After heating at 65 $^{\circ}$C for 24 hours, a viscous solution was poured into methanol to isolate the copolymer, which was purified by reprecipitation from THF solution into methanol. Yield was 73% by weight. The copolymer ratio was calculated with ^{1}H-NMR and elemental analysis data.

$Mn = 4.9 \times 10^3$, $Mw = 2.3 \times 10^4$

dimethylaminobenzyl:methyl = 1:3.0

$Tg = 107\,^{\circ}C$

Elemental Anal. for $(C_{13}H_{17}NO_2)(C_5H_8O_2)_{3.0}$:   Calcd. C 64.71, H 7.96, N 2.69%.

Found C 64.47, H 7.72, N 2.94%.

6-2-2. CRA-modification of colloidal silica

Colloidal silica of a 73 nm diameter without surface pores was washed ultrasonically in acetone, an aqueous NaOH solution, a HNO_3 solution and finally in water. The colloidal silica was put in a toluene solution of aminopropyldimethylethoxysilane (10 vol%), and the suspension was refluxed for 1 hour, followed by centrifugal separation, washing in toluene ultrasonically. The particles were suspended in toluene again, separated and dried. The density of the amino group on the silica particles was estimated to be 1.7 groups/nm^2 by the following elemental analysis data on the assumption that a particle is a sphere of a density of 2.3 g/cm^3.

Elemental Anal. for the modified colloidal silica: Found C: 0.62, H: 0.48, N: 0.14%.

The aminated colloidal silica was put in a THF solution of **16** (1×10^{-4} mol/l) and stirred for 30 min at room temperature. After stirring, the colloidal silica was isolated by centrifugal separation. The yellow color of the solution became pale, while the modified colloidal silica turned from white to yellowish brown in color, suggesting the adsorption of **16** on the colloidal silica. The colloidal silica was washed in pure acetone ultrasonically,

precipitated by centrifugal separation and dried. The density of pyrenyl group on the silica was calculated as 0.22 groups/nm^2 by the following elemental analysis data. The reacted colloidal silica is abbreviated Py-CoSi.

Elemental Anal. for Py-CoSi: Found C: 1.49, H: 0.56, N: 0.13%.

6-2-3. Sample preparations for the interfacial studies

Py-CoSi (100 mg) was placed in a 0.5 ml THF or chloroform containing 20 mg of **17**, the suspension was shaken ultrasonically for 30 min, followed by evaporation of the solvent under atmosphere overnight and under a reduced pressure for 2 hours. Annealing samples were achieved by heating.

6-2-3. Physical measurements

The surface-modified colloidal silica covered with a polymer layer were placed in a 0.5 mm thick quartz cell, and their emission spectra were taken on a JASCO PF-777 with the use of an attachment for a film. The excitation wavelength for emission spectra was 349 nm for the first peak of $S_0 \rightarrow S_2$ of the pyrenyl chromophore. DMA unit has no absorption band at this wavelength. All spectra of plates were corrected by that of unreacted colloidal silica as a reference.

Fluorescent lifetime was measured by a single photon counting system with an excitation source of mode-locked Nd:YAG laser and dye laser (Rhodamine B) whose half-width was 0.20 ns operating at 400 kHz.

6-3. Results and discussions

6-3-1. Effect of preparative conditions on pyrene fluorescence

Schemes 6-1 and 6-2 show the synthetic route of the sample used in this chapter. Octacarboxymethoxylated CRA possessing one pyrenyl group (**16**) was synthesized and isolated by the according to the procedure described in Chapter 5. The surface modification of colloidal silica was achieved by the amination followed by adsorption of **16**. Samples (Py-CoSi/**17**) for fluorescence analysis were prepared by suspending the surface-modified

colloidal silica in a solution of the polymethacrylate with DMA side chains (**17**), followed by the removal of the solvent. For the solvent of a polymer solution, chloroform or THF was adopted. Though they are both good solvents for polymethacrylate, their solvation strengths are different as described in chapter 4. The solvation to polymethacrylate of THF was strong enough to destroy the adsorption of the polymer on a silica surface, which was caused by the interaction of carbonyl of polymer and silanol of silica surface, whereas polymethacrylate kept adsorbing on silica surface in chloroform.

Two Py-CoSi/**17** samples were prepared with chloroform solution of **17**. Py-CoSi/**17**(a) was the sample vacuumed after the solvent was evaporated under atmosphere at room temperature to remove chloroform completely. Py-CoSi/**17**(b) was without drying under vacuum, which contains remained solvent. The effect of the remained solvent would be revealed by fluorescence measurements. For comparison, a sample of the CRA-modified colloidal silica covered with a PMMA layer (Py-CoSi/PMMA) was also prepared from a chloroform solution of PMMA. On the other hand, two Py-CoSi/**17** samples were also prepared from THF solution of **17**. Py-CoSi/**17**(c) was the sample whose solvent was slowly evaporated under atmosphere at room temperature during 2 days and removed under vacuum. Py-CoSi/**17**(d) was evaporated fast under vacuum from the first. The solvent evaporating speed would influence the microenvironment at interface when the solvent was THF which solvate **17** strongly. The prepared samples are summarized in Table 6-1.

Fluorescence spectra of Py-CoSi/**17**(a), (b) and Py-CoSi/PMMA normalized at 379 nm are shown in Figure. 6-1. The samples are excited at 349 nm so that the emission comes specifically from the pyrene S_0 to S_2 region. Whereas Py-CoSi/PMMA displays only the monomer emission, a broad emission at a long wavelength region was observed for Py-CoSi/**17**. No excimer emission was detected even for Py-CoSi/PMMA. It is very likely that the interface between a CRA-modified silica surface and a PMMA layer is reasonably considered to be not much different from that between the silica surface and a **17** layer. It follows that the emission bands at a longer wavelength region arises not from the excimer, but rather from exciplex between the surface pyrene and DMA tethered to polymer chains. This is the first observation of exciplex emission at an interface between two kinds of solids. Py-CoSi/**17**(b) without vacuum treatment showed blue-shifted exciplex emission, in contrast Py-CoSi/**17**(a), which was dried sufficiently and its intensity was a little smaller than that of

Table 6-1 Preparation of samples

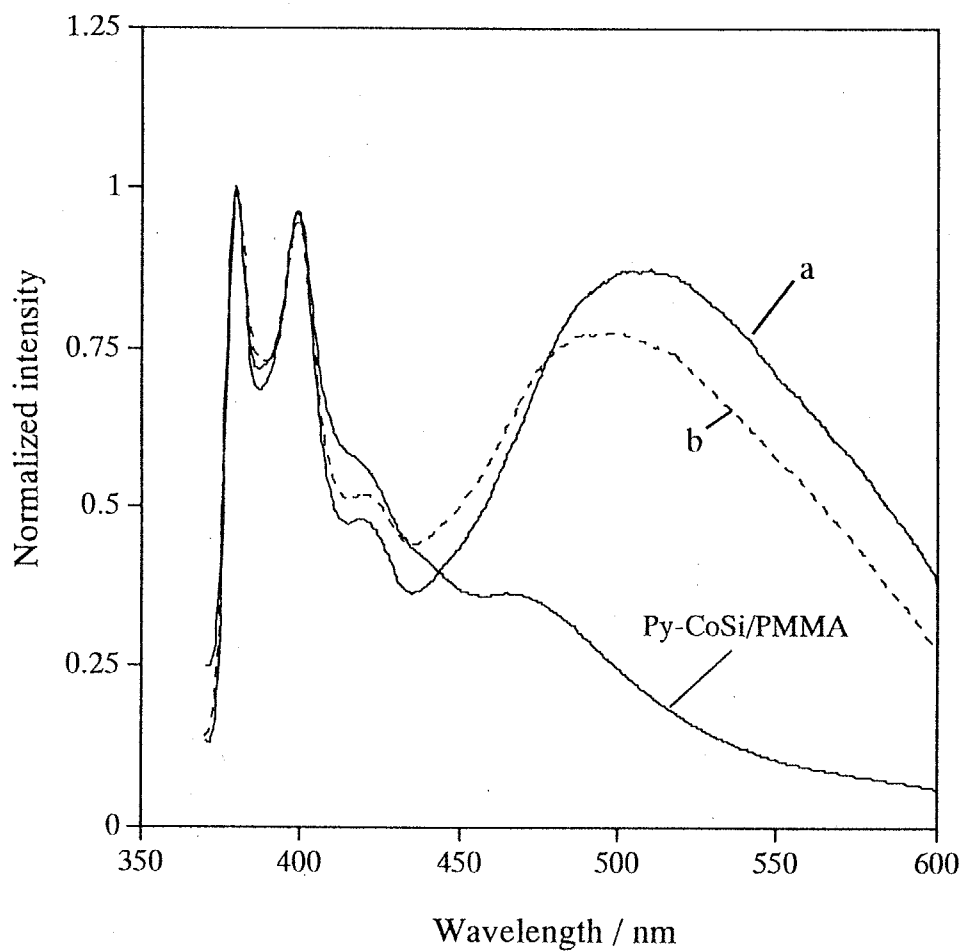|	solvent of a polymer solution	evaporation of solvent	vacuum after evaporation
Py-CoSi/**17**(a)	chloroform	under atomosphere	yes
Py-CoSi/**17**(b)	chloroform	under atomosphere	no
Py-CoSi/**17**(c)	tetrahydrofuran	under atomosphere	yes
Py-CoSi/**17**(d)	tetrahydrofuran	under vacuum	
Py-CoSi/PMMA	chloroform	under atomosphere	yes

Figure 6-1 Fluorescence spectra of Py-CoSi/17 prepared with chloroform solutions (a (solid line) and b (dot line) see Table 6-1) and Py-CoSi /PMMA nornalized at λmax of monomer emission.

Py-CoSi/17(a).

Fluorescence spectra of Py-CoSi/17(c), (d) are shown in Figure. 6-2. There are some differences between the spectra in respect with intensity ratios of exciplex emission to monomer emission (Ie/Im) and λmax of exciplex. For Py-CoSi/17(c), the emission maximum displays significant blue-shift. On the other hand, Py-CoSi/17(d) showed a red-shift and larger Ie/Im when compared with Py-CoSi/17(a). Such sensitivity of exciplex emission to the preparative conditions of the Py-CoSi/17 samples may reflect the existence more than two species in different microenvironments.

For more information on these exciplex species, fluorescence lifetimes were measured. Fluorescence lifetimes of Py-CoSi/17 at various wavelengths were summarized in Table 6-2. The monitoring wavelength was 398 nm to follow monomer fluorescence, whereas wavelengths at 480 nm and 540 nm were selected for tracing exciplex emission at a shorter and a longer wavelength of the exciplex from Py-CoSi/17. The decay curves were well analyzed as triple exponential decay components and no rise component. The fact that there is no rise lifetime indicated that exciplex did not form dynamically with movement of polymer segment after pyrene monomer became excited state by absorption of irradiated light. There must be performed ground state complexes of pyrenyl group and DMA and exciplex formed just after a pyrenyl group adsorb excited light without polymer segment movement. There was no distinct difference in the lifetimes between the samples prepared under various preparative conditions.

In contrast to Py-CoSi/PMMA, the lifetime constants of which measured at 389 nm and at 480 nm are not far from each other, and the longest lifetime (τ_3) of Py-CoSi/17 exciplex emission was longer than that of monomer emission, whereas the shortest and the middle ones (τ_1, τ_2) are almost the same. τ_3 of Py-CoSi/17 monomer emission is close to that of Py-CoSi/PMMA. The intensity ratios of τ_3 of exciplex emission are larger at 540 nm than that at 480 nm. It is assumed from these data that 11 ns and 16 ns for τ_3 are of monomer and exciplex, formed from ground state complex, respectively. On the other hand, the kinetic paths, which τ_1 and τ_2 are assigned to, cannot be made clear though they must be related to deactivation by energy transfer to polymer matrix or colloidal silica surface. On the basis of these results data, it is assumed that pyrenyl groups on a silica surface and DMA units attached to polymer backbones form ground state complexes at the silica/polymer interface,
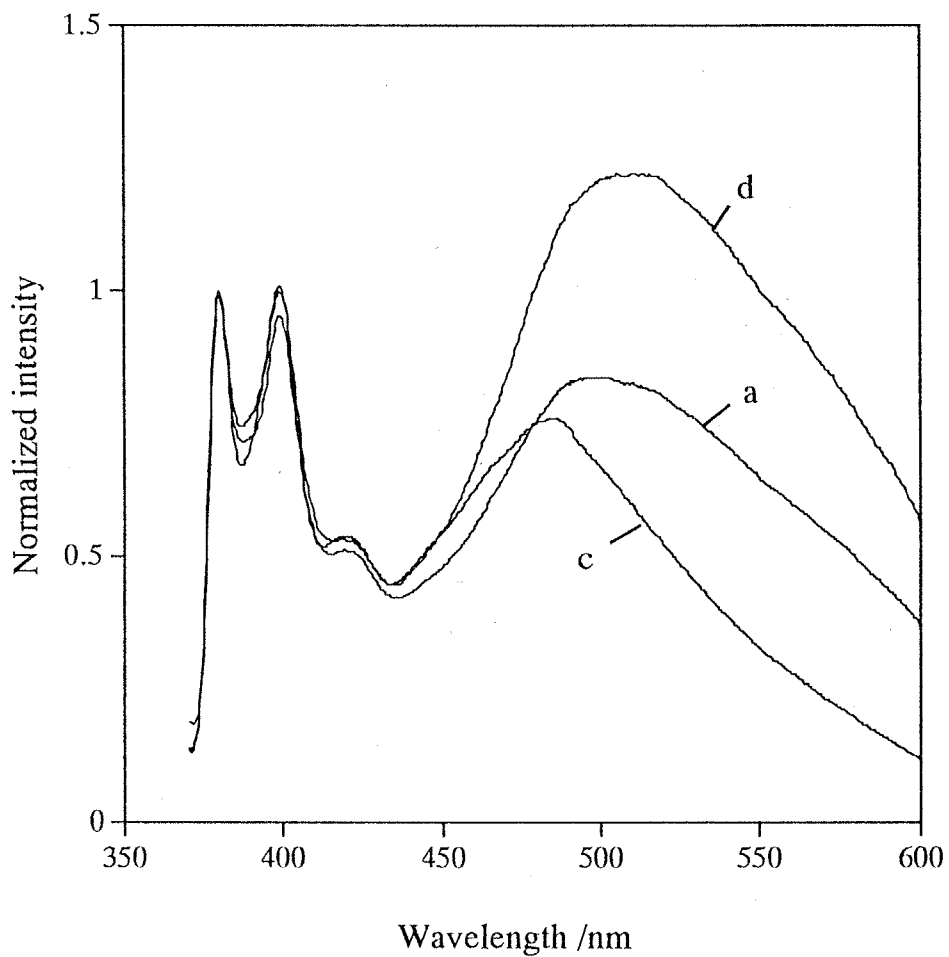
Figure 6-2 Fluorescence spectra of Py-CoSi/17 prepared with chloroform solution (a, see Table 6-1) and tetrahydrofuran solutions (c and d, see Table 6-1) nornalized at λmax of monomer emission.

Table 6-2 Fluorescence life times

λmon	398 nm			480 nm			540 nm		
	τ_1 / ns (int) [1]	τ_2 / ns (int)	τ_3 / ns (int)	τ_1 / ns (int)	τ_2 / ns (int)	τ_3 / ns (int)	τ_1 / ns (int)	τ_2 / ns (int)	τ_3 / ns (int)
Py-CoSi / **17** (a)	0.53 (0.05)	2.0 (0.26)	9.7 (0.69)	0.53 (0.17)	2.2 (0.24)	15.2 (0.59)	0.56 (0.09)	3.1 (0.18)	16.7 (0.74)
Py-CoSi / **17** (b)	0.51 (0.21)	2.6 (0.38)	12.3 (0.41)	0.56 (0.17)	2.2 (0.26)	14.7 (0.56)			
Py-CoSi / **17** (c)	0.62 (0.08)	2.8 (0.30)	11.9 (0.62)	0.50 (0.10)	2.0 (0.30)	15.6 (0.60)	0.63 (0.10)	2.4 (0.23)	17.0 (0.68)
Py-CoSi / **17** (d)	0.57 (0.05)	2.5 (0.32)	10.9 (0.63)	0.49 (0.10)	2.3 (0.22)	15.6 (0.68)	0.41 (0.05)	2.3 (0.17)	15.2 (0.78)
Py-CoSi / PMMA	0.81 (0.10)	2.6 (0.29)	12.6 (0.61)	0.68 (0.28)	1.9 (0.24)	12.7 (0.48)			

[1] int =(Amp(n) × τ_n) / Σ (Amp(i) × τ_i)

* errors : τ_1 ±0.06 ns τ_2 ±0.2 ns τ_3 ±1.9 ns

leading to the diversified distribution of energy states while their exciplex states have similar lifetimes. Exciplex originated from a ground state complex with a lower energy emits at a shorter wavelength since it deactivates to the same ground state complex because of fixed matrix.

The distributions of ground state complexes depend on preparative conditions. The difference between exciplex emission of Py-CoSi/17(a) and (b) can be explained as follows; residual chloroform molecules solvate the ground state complex to make their energy level lower to emit at a little shorter wavelength in the case of Py-CoSi/17(b). The remarkable blue-shift of exciplex emission of Py-CoSi/17(c) prepared from a THF solution compared with Py-CoSi/17 (a), which was prepared from a chloroform solution, can be explained as follows. Polymer chains of 17 may be expanded by the solvation in a THF solution to form a more stable ground state complex with pyrenyl groups on a silica than the case of a chloroform solution, because THF solvates methacrylate polymer better than chloroform does as described in chapter 4. Slow evaporation may freeze the stable complex, which has been made in a solution, at a silica/polymer interface and showed exciplex emission at shorter wavelength compared to that in a chloroform solution. Py-CoSi/17(d), which was prepared from a THF solution and subjected to fast solvent evaporation, showed stronger exciplex emission at a longer wavelength region compared to Py-CoSi/17(a)-(c), which were subjected to slow solvent evaporation. In the case of Py-CoSi/17(d), the evaporating process was too fast to solvate the side chain DMA during evaporation to left more DMA units faced at the interface to make unstable ground state complex, which showed red-shift exciplex emission. Less side chain DMA units could not get into the polymer bulk during fast evaporation. These models were described in Figure 6-3.

6-3-2. Annealing effects

The samples of Py-CoSi/17 prepared under various conditions were annealed to check the alteration of fluorescence behavior. Figure 6-4 shows fluorescence spectra of Py-CoSi/17(a) prepared from a chloroform solution. The intensity of broad emission at longer wavelength region increased and the λmax moved slightly to shorter wavelength during annealing at 105 °C, 2 °C below Tg of 17, for 30 min. But annealing at 105 °C for more than 30 min did not cause any change. These phenomena were same for Py-CoSi/17(b)

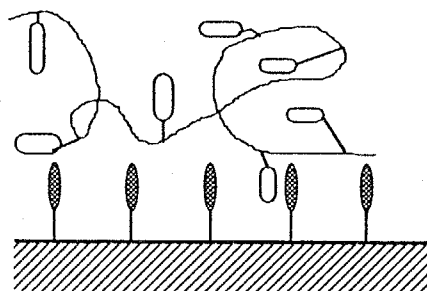<u>a</u> : solvent evaporated under
atmosphere and vacuum
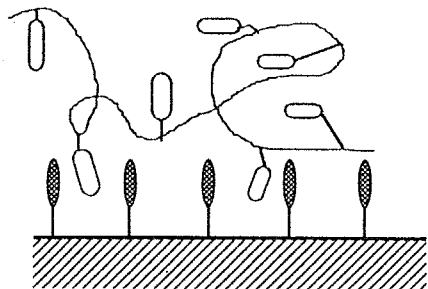
<u>b</u> : no vacuum
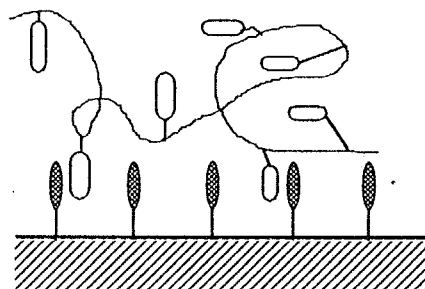
<u>c</u> : solvent evaporated under
atmosphere and vacuum
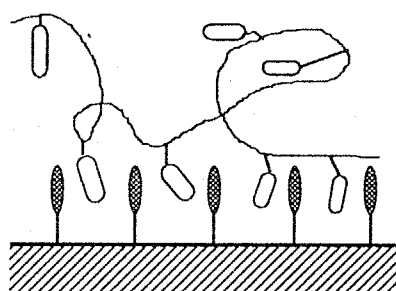
<u>d</u> : solvent evaporated under vacuum

Figure 6-3 Speculative drawings for Py-CoSi/**17** samples prepared from chloroform

solutions (<u>a</u>, <u>b</u>) and tetrahydrofuran solutions (<u>c</u>, <u>d</u>)
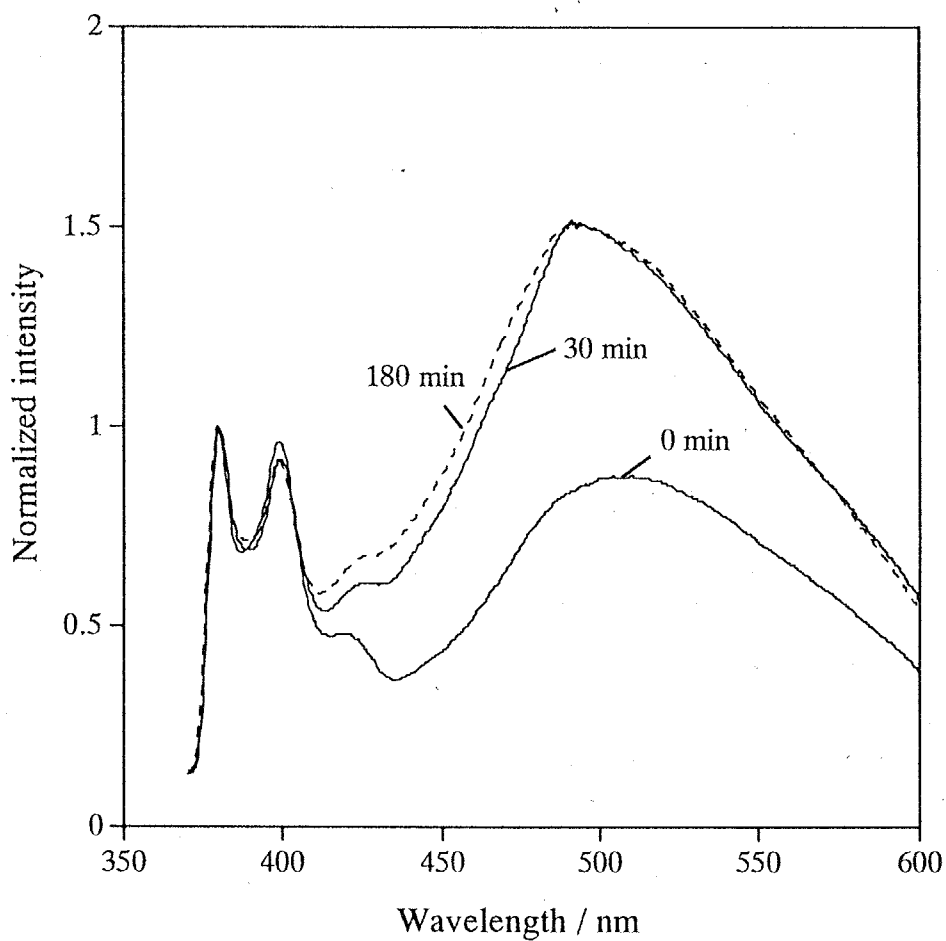
Figure 6-4   Fluorescence spectra of Py-CoSi/17(a) prepared with chloroform solutions (see Table 6-1) and annealed at 105°C for 0 min, 30 min (solid line) and 180 min (broken line) nornalized at λmax of monomer emission.

though some solvent remained at first. For comparison, Py-CoSi/PMMA and a sample that 17 coated on non-treated colloidal silica were also annealed at 105 °C. Py-CoSi/PMMA did not display any change in fluorescence behavior after annealing, implying that the increase in emission intensity at longer wavelengths of Py-CoSi/17 is not caused by interactions between pyrenyl groups themselves. It was confirmed that the emission at the longer wavelength region during annealing is not due to DMA units, since non-modified colloidal silica coated by 17 showed no spectral change during annealing. Based on these data, the broad emission at longer wavelengths can be assigned to an exciplex. Fluorescence lifetimes were not altered before and after the annealing, as shown in Table 6-3. These results suggest that the microenvironment of each ground state complex of pyrenyl groups and DMA units at Py-CoSi/17 interface does not change drastically though both the population and fraction of ground state complexes with lower energy levels increase during annealing at temperatures just below Tg. As mentioned above, the annealing leads to the thermal relaxation of polymer segments at the interface. Consequently, the DMA units of 17 are more stable at the boundary region to form a ground state complex with pyrenyl group when compared with those in a polymer bulk.

For the case that annealing temperature was 90 °C, the spectral changes were almost same as that at 105 °C as shown in Figure 6-5. But the changing process took longer time than the case of 105 °C annealing. Ie/Im increased at the initial period in 30 min and the population of exciplex that emits at shorter wavelength region increased after 30 min annealing.

In comparison with the annealing at the temperature under Tg, the annealing effect at 120 °C, which was higher than Tg by 13 °C was different as shown Figure 6-6. The increment of the Ie/Im was not saturated at 30 min and the spectrum moved shorter wavelength more than the case of 105 °C or 90 °C. The lifetimes were also changed dynamically after 210 min annealing. τ_3 became shorter and shorter during annealing to result that the fluorescence decay curves were analyzed as double exponential time constants; the longest time constant, which assigned to exciplex lifetime, and middle time constants became close and combined as τ_2. The annealing at the temperature higher than Tg for long time produced the polymer chain movement to the interfacial layer more intricate than annealing under Tg to make the population of preformed ground state sites large and their

Table 6-3 Fluorescence life times of annealed samples

	Annealing		480 nm			540 nm		
λmon	Temperature	time	τ_1 / ns (int)	τ_2 / ns (int)	τ_3 / ns (int)	τ_1 / ns (int)	τ_2 / ns (int)	τ_3 / ns (int)
Py-CoSi / 17 (a)	105 ℃	180 min	0.61 (0.14)	2.3 (0.24)	17.8 (0.62)			
Py-CoSi / 17 (a)	120 ℃	30 min	0.46 (0.09)	1.9 (0.30)	12.6 (0.61)			
Py-CoSi / 17 (a)	120 ℃	210 min	0.73 (0.28)		6.6 [*2] (0.48)	0.94 (0.20)		10.9 [*2] (0.80)
Py-CoSi / 17 (c)	105 ℃	180 min	0.57 (0.11)	2.2 (0.23)	16.1 (0.66)	0.49 (0.04)	2.2 (0.14)	16.6 (0.82)

[*1] int =(Amp(n) × τ_n) / Σ (Amp(i) × τ_i)   [*2] double exponential   * errors : τ_1 ±0.06 ns τ_2 ±0.2 ns τ_3 ±1.9 ns
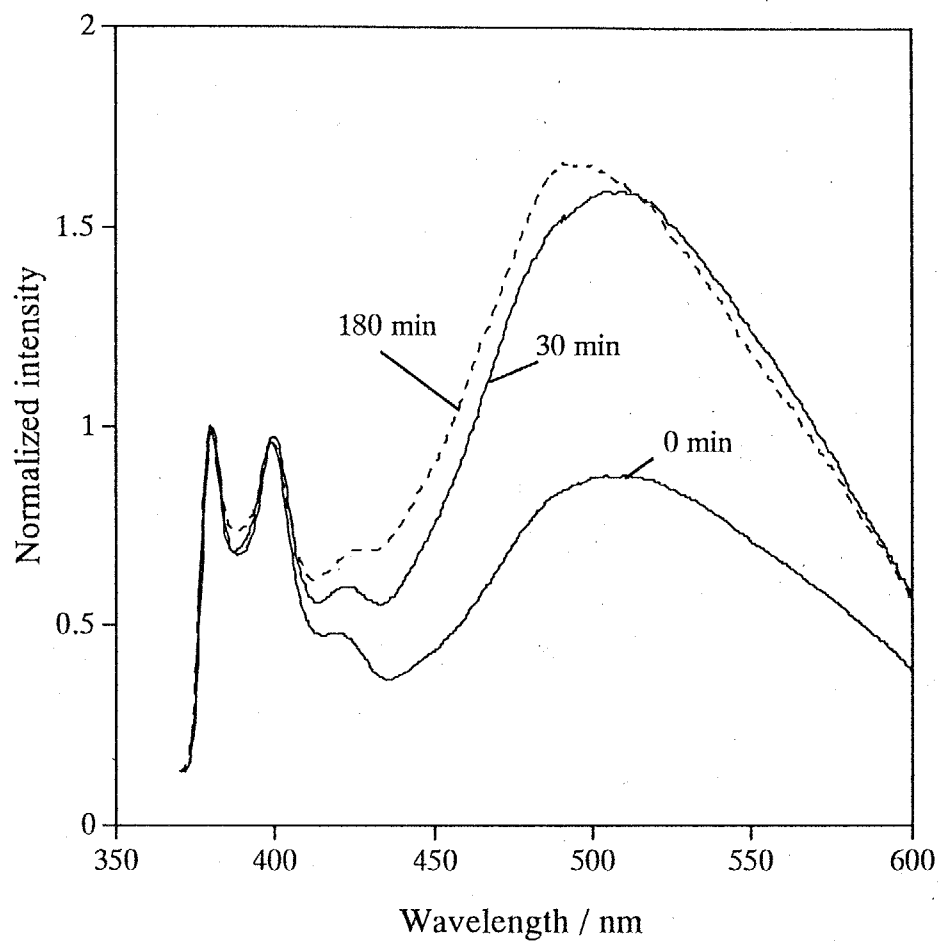
Figure 6-5 Fluorescence spectra of Py-CoSi/17(a) prepared with chloroform solutions (see Table 6-1) and annealed at 90°C for 0 min, 30 min (solid line) and 180 min (broken line) nornalized at λmax of monomer emission.
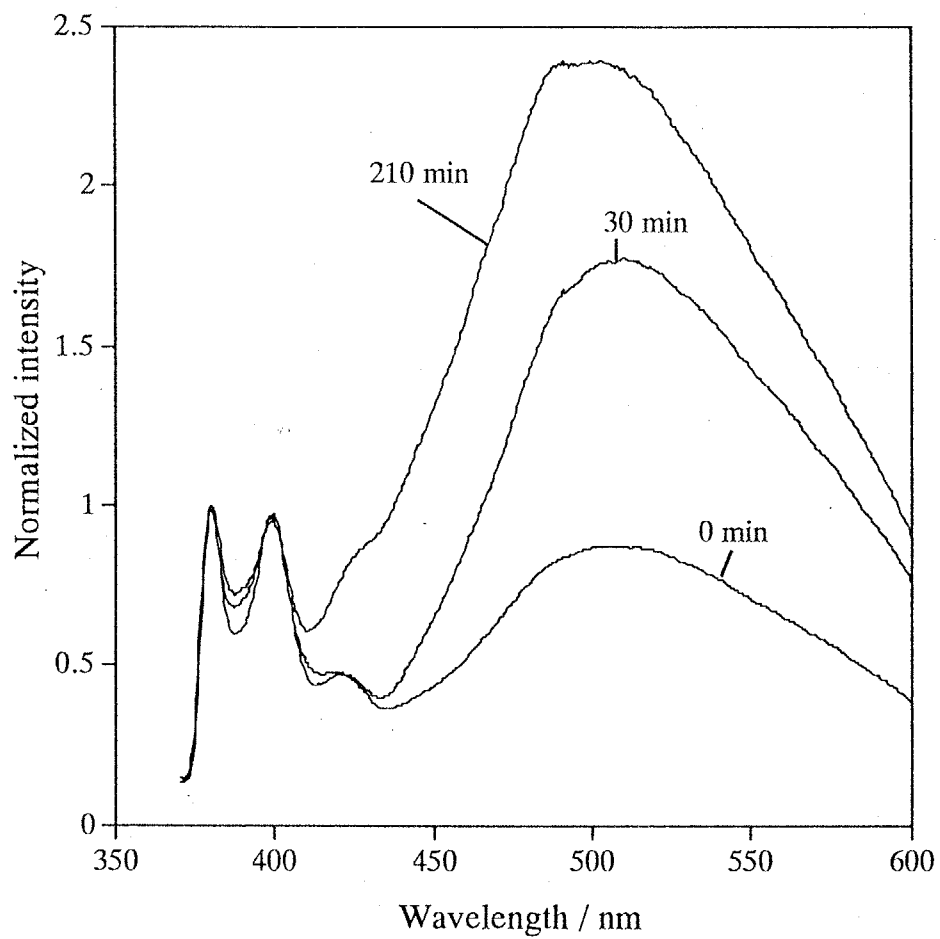
Figure 6-6   Fluorescence spectra of Py-CoSi/**17**(a) prepared with
chloroform solutions (see Table 6-1) and annealed at 120°C for 0 min, 30
min and 180 min nornalized at λmax of monomer emission.

microenvironments were ordered to be easily deactivated.

The spectra of the samples from tetrahydrofuran solution after annealing were shown in Figure 6-7 and 6-8. Annealing temperature was 105 °C, which is 2 °C lower than Tg of 17.

The annealing effect on Py-CoSi/17(c), which prepared by slowly evaporated tetrahydrofuran, enhanced the spectra intensity. But the shape of the spectrum was almost kept during annealing as shown in Figure 6-7. These effects continued for over 30 min annealing. For this sample, there was no remarkable change in fluorescence lifetimes as shown in Table 6-3. These results implied that the microenvironment of preformed ground state complexes produced just after evaporation was most stable energy level. The increment of the population of polymer side DMA units facing silica surface pyrenyl groups during annealing made the fluorescent intensity ratio (Ie/Im) larger. The spectrum at 180 min annealing was similar to that of Py-CoSi/17(a) 180 min annealing under Tg shown Figures 6-4 and 6-5.

Figure 6-8 shows that the spectra of Py-CoSi/17(d) which was fast evaporated under vacuum, moved to shorter wavelength region but Ie/Im was almost kept. Ie/Im showed the population of DMA units facing to pyrenyl groups, which was produced large enough by freezing as that with solvent during fast evaporation. Spectral movements indicated that polymer side chain DMA units moved during annealing to make the microenvironment of the complexes at silica/polymer interface became more stable. The stressed microenvironment of ground state complex sites, which was frozen under stressed condition during fast evaporation, was released during annealing. The spectrum of the sample annealed for 180 min was similar to the spectra of the other samples annealed under Tg for 180 min.

6-3-3. The most stable microenvironment at silica/polymer interface

As described in 6-3-2, the fluorescence spectral shape of all Py-CoSi/17 prepared from chloroform and THF became closer to each other by annealing. Emission spectra of Py-CoSi/17 shored at room temperature for one month were also measured. All the spectra showed the same shape and one of them is shown in Figure 6-9. λmax was around 490 nm and Ie/Im was around 1.6. Even the sample annealed at 120 °C became the same shape though its Ie/Im was larger than 2. This spectrum must be the final state of spectral changes
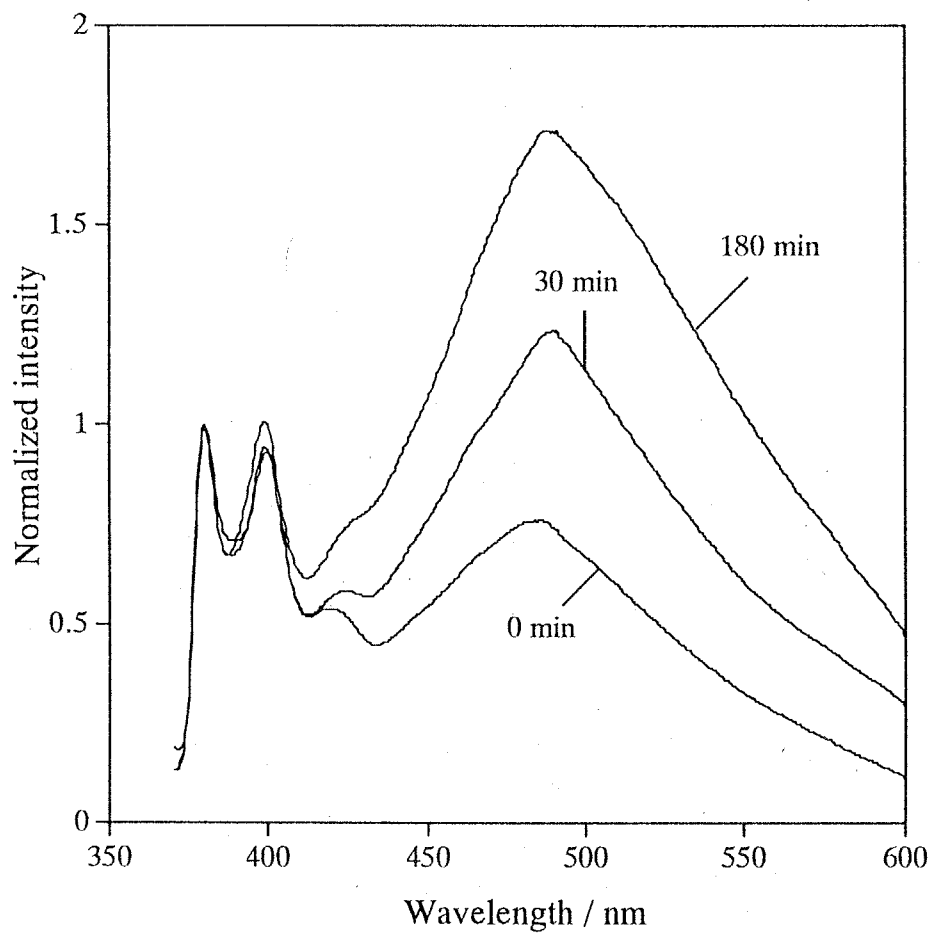
Figure 6-7   Fluorescence spectra of Py-CoSi/17(c) prepared with tetrahydrofuran solution and evaporated slowly (see Table 6-1) and annealed at 105°C for 0 min, 30 min and 180 min nornalized at λmax of monomer emission.
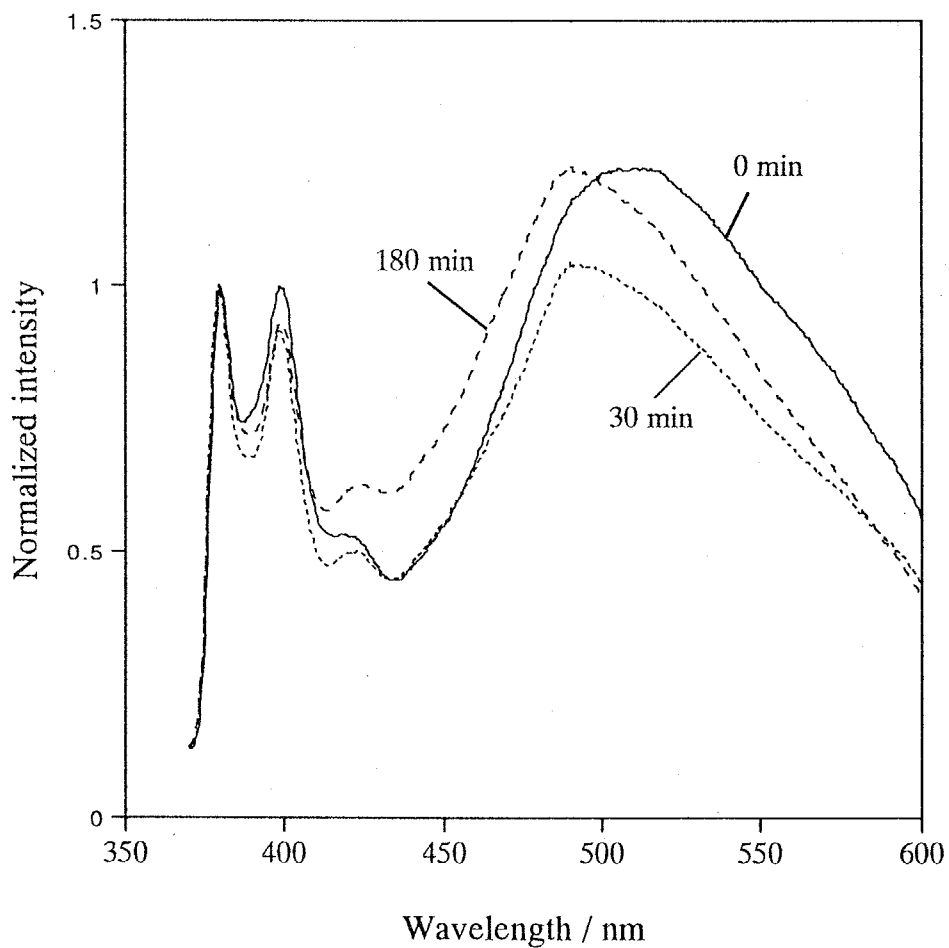
Figure 6-8   Fluorescence spectra of Py-CoSi/17(d) prepared with tetrahydrofuran solution and evaporated fast (see Table 6-1) and annealed at 105°C for 0 min (solid line), 30 min (dot line) and 180 min (broken line) nornalized at λmax of monomer emission.
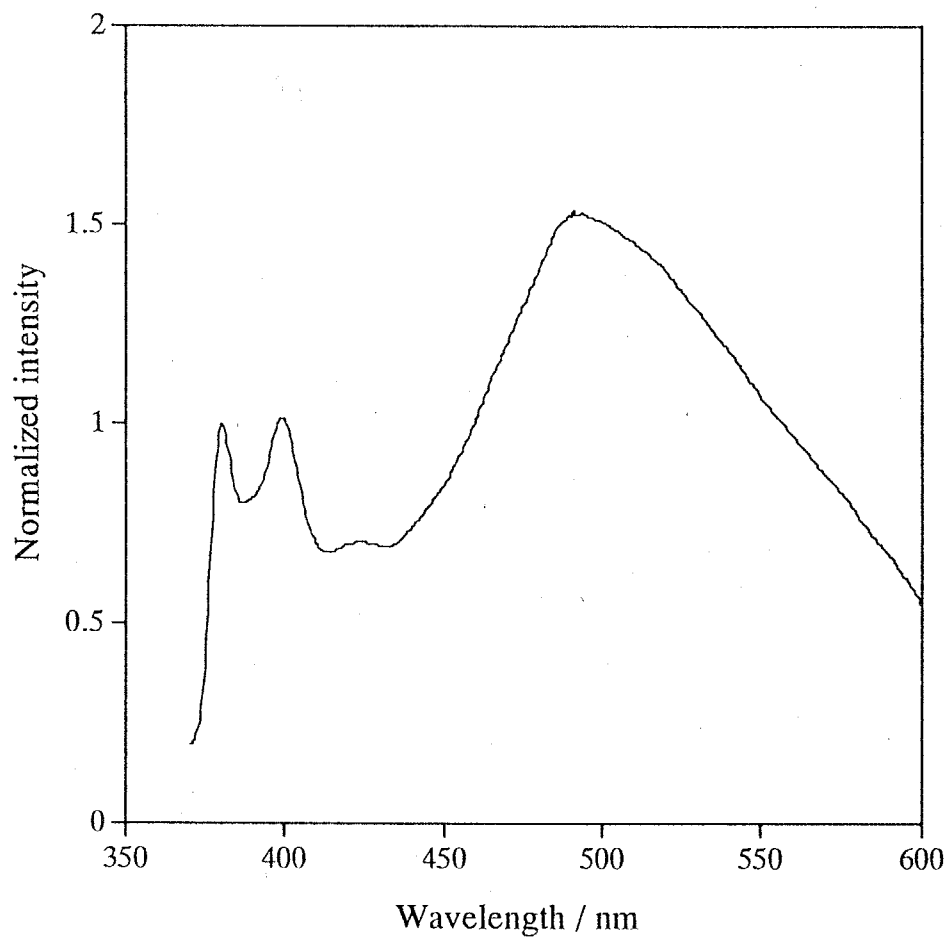
Figure 6-9 The fluorescence spectra of Py-CoSi/**17** left under atmosphere at room teperature for one month.

of all the samples whose polymer segments possessing DMA moved to the most stable position. The first state of the microenvironment of solid/polymer interface depends on the preparation condition but annealing made the interfacial microenvironment to be same state that is independent on the initial condition. It is revealed that annealing under polymer Tg in a few hours makes the microenvironment of silica/polymer interface most stable. On the other hand, annealing above Tg makes the interface layer more intricate than the most stable microenvironment and it change to the most stable one during leaving at room temperature for long time like a month.

6-4. Conclusions

Molecular interaction between a functional group modified on a silica surface and another functional group of polymer which coated on the silica, which have been prepared as a model of an interface of polymer blends, was observed with static and dynamic fluorescence measurements. Pyrene and dimethylaniline were adopted for the functional groups modified on silica and polymer respectively. Pyrene was linked to silica surface though a calix[4]resorcinarene skeleton in order to keep the distance of pyrenyl groups and avoid making excimer between them. Dimethylaniline was imported in methacrylate polymer as side chain substitute. The molecular interaction at the interface of two materials was observed as exciplex emission.

It was considered that there were several sorts of sites of the functional groups at the interface, for example, independent pyrene monomer site, independent pyrene-dimethylaniline exciplex site and the sites where exciplex could be formed by monomer and monomer could be broken up from exciplex. Just after the sample preparation, the population of each site depend on the sample preparation conditions, especially the polymer solvent and evaporation speed of the solvent.

The annealing effects were also measured. The ways of spectral change depend on the initial condition and annealing temperature. However, generally the λmax of exciplex moved to shorter wavelength and Ie/Im increased, the spectra whose movement or increase of Ie/Im had saturated did not change any more. Exciplex wavelengths indicate the difference between the energy of excited state and that of ground state. Ie/Im indicate the population of

145

sites. During annealing, the distribution of exciplex population and the microenvironment of exciplex site became the most stable ones, though the initial distribution and microenvironment depended on the sample preparation conditions.

References

1. (a) K. Hara, P. de Mayo, W. R. Ware, W. A. C. Weeden, G. S. K. Wong and K. C. Wu, *Chem. Phys. Lett.*, 1980, **69**, 105., (b) R. K. Bauer, P. de Mayo, W. R. Ware and K. C. Wu, *J. Phys. Chem.*, 1982, **86**, 3781., (c) R. K. Bauer, P. de Mayo, L. V. Natarajan and W. R. Ware, *Can. J. Chem.*, 1984, **62**, 1279., (d) P. de Mayo, L. V. Natarajan and W. R. Ware, *ACS Symp. Ser.*, 1985, **278**, 1. (chap.1)

2. (a) C. H. Lochmüller, A. S. Colborn, M. L. Hunnicutt and J. M. Harris, *Anal. Chem.*, 1983, **55**, 1344., (b) C. H. Lochmüller, A. S. Colborn, M. L. Hunnicutt and J. M.Harris, *J. Am. Chem. Soc.*, 1984, **106**, 4077., (c) C. H. Lochmüller and M. J. Hunnicutt, *J. Phys. Chem.*, 1986, **90**, 4318., (d) C. H. Lochmüller and M. T. Kersey, *Langmuir*, 1988, **4**, 572.

3. (a) P. Hite, R. Kransansky and J. K. Thomas, *J. Phys. Chem.*, 1986, **90**, 5795., (b) M. A. Marro and J. K. Thomas, J. K. *J. Photochem. Photobio.*, 1993, **A72**, 251.

4. P. Somasundaran, S. Krishnakumar and J. T. Kunjappu, *ACS symp. Ser.*, 1995, **615**, 104 (chap. 7)

5. S. H. Chen and C. W. Frank, *ACS symp. Ser.*, 1995, **615**, 217 (chap.14).

6. J. B. Birks *"Photophysics of Aromatic Molecules"*, Wiley-interscience, London, 1969, 403 (Chap 9).

7. N. Mataga, T. Okada and N. Yamamoto, *Bull. Chem. Soc. Jpn.*, 1966, **39**, 2562.

8. N. Mataga, T. Okada and N. Yamamoto, *Chem. Phys. Lett.*, 1967, **1**, 119.

9. K. Ichimura, N. Fukushima, M. Fujimaki, S. Kawahara, Y. Matsuzawa, Y. Hayashi and K. Kudo, *Langmuir*, 1997, **13**, 6780.

10. Y. Hayashi, T. Maruyama, T. Yachi, K. Kudo and K. Ichimura, *J. Chem. Soc. Perkin Trans. 2*, 1998, 981.

11. K. Ichimura, M. Fujimaki, Y. Matsuzawa, Y. Hayashi and M. Nakagawa, *Mat. Sci. Eng. C*, 1999, 353.

12. E. Kurita, N. Fukushima, M. Fujimaki, Y. Matsuzawa, K. Kudo and K. Ichimura, *J. Mater. Chem.*, 1998, **8**, 397.

13. S. E. Klassen, G. H. Daub and D. L. VanderJagt, *J. Org. Chem.*, 1983, **48**, 4361.

Chapter 7

Enhancement of desorption-resistance of adsorbed monolayers of calix[4]resorcinarenes bearing cinnamoyl residues by photodimerization

7-1. Introduction

As described in chapters 3 and 6, the major concern with the crown isomer of calix[4]resorcinarenes (CRAs) has been concentrated on their surface adsorption behavior to assemble functional monolayers on solid surfaces, taking notice of the amphiphilic characteristics of the macrocyclic skeleton which possess a unique chemical structure with hydrophobic sites and hydrophilic sites tethered to each rim of the cyclic molecular framework. The unique points of CRAs are hardly adhesion on silica surface through multi-site hydrogen bonding because of eight hydrophilic units and suitable space of hydrophobic functional groups for photoreaction because of macrocyclic skeleton. In order to extend the strategy to fabricate monolayers incorporating photofunctional moieties through the simple procedure consisting of dipping a substrate plate in a solution of a functional CRA, an essential problem is how to suppress the desorption of CRA derivatives from solid surfaces even in polar solvents since monolayer formation is achieved simply by hydrogen bond formation. It has been confirmed that CRA derivatives having phenolic hydroxyl, carboxyl and hydroxyethyl groups, respectively, adsorb on a silica surface to form monolayers by immersing silica plates in solutions of the CRAs.[1-3] It has been also reported recently that the desorption resistance of a CRA derivative with eight carboxyl groups (CRA-CM) is markedly improved by the modification of silica surface with an aminoalkyl silylating reagent to lead to the surface adsorption through the NH_2/COOH interaction[5], even though CRA-CM is most tightly adsorbed on a silica surface and hardly desorbed by ultrasonic treatment in organic solvents without a hydroxyl group, predominant part of the CRA-CM desorbed in ethanol or methanol.

An alternative method to enhance the desorption resistance by intermolecular photocycloaddition of a CRA-CM derivative bearing crosslinkable residues will be reported in this chapter. The idea is based on the fact that the increment of adsorption sites of

adsorbates leads to the increase in the adsorption strength,[6] as exemplified by the sticking of a barnacle through the enzymatic crosslinking of an adhesive protein.[7] The purpose of this report is two-fold. First, a CRA derivative with cinnamoyl residues is prepared to assemble a surface-adsorbed monolayer to show that the desorption even in alcoholic solvents is in fact suppressed by the photocycloaddition of cinnamoyl residues tethered to the upper rim of the cyclic framework. Second, a monolayer of the CRA with cinnamoyl residues on a silica plate is applied to perform the photocontrol of liquid crystal alignment in order to display the photofunctionality of the monolayer.
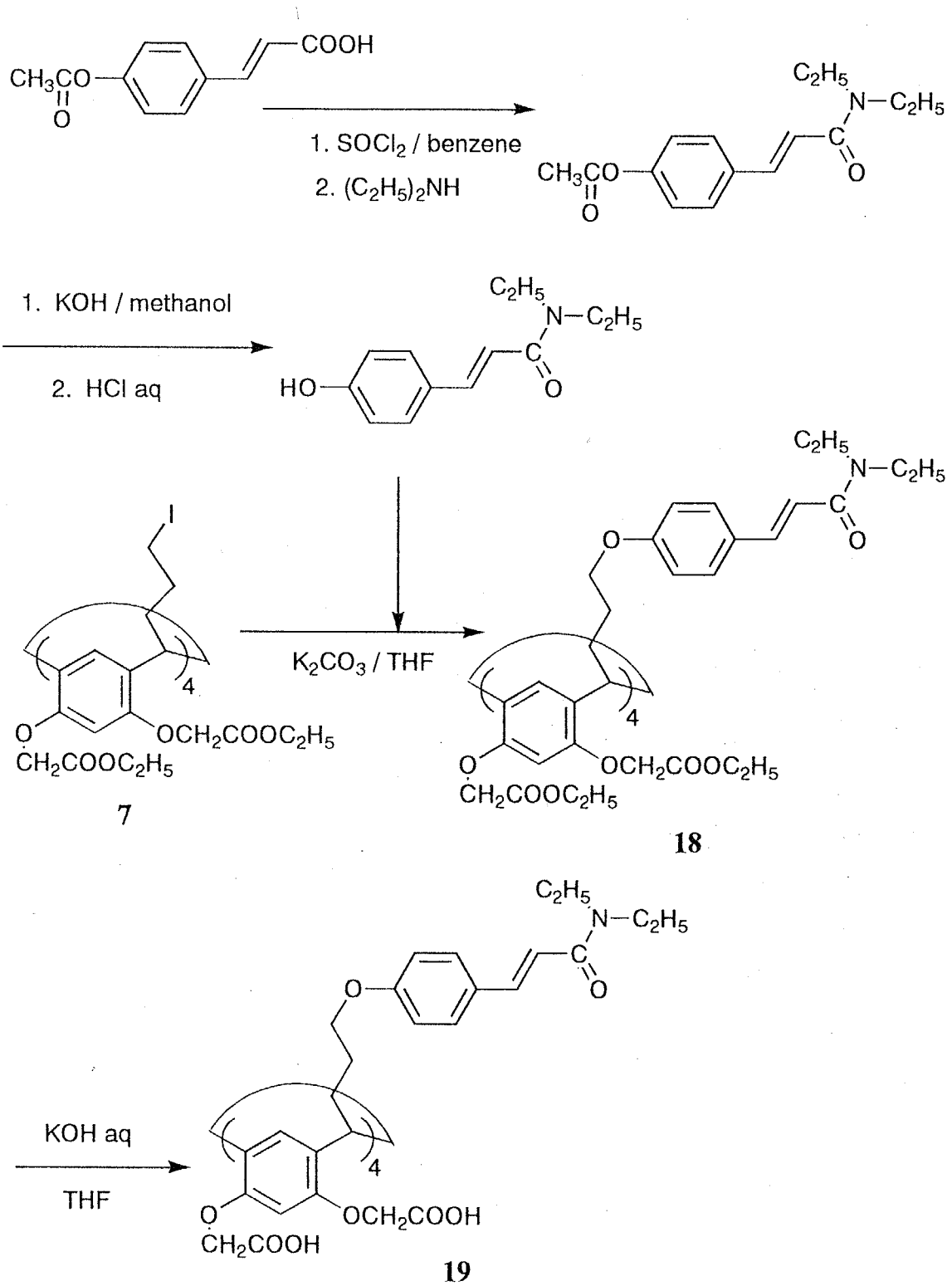
7-2. Experimental

7-2-1. Materials

The crown conformer of CRA-CM having four cinnamoyl groups (19) was prepared for the present purpose by the reaction of octaethyl ester of CRA-CM bearing four iodopropyl residues (7)[4], shown in Scheme 3-1 in chapter 3, with *N,N*-diethyl-4-hydroxycinnamoylcarboxamide, followed by the alkaline hydrolysis of the resultant octaethyl ester of 19 (18) whose synthetic route is shown in Scheme 7-1. Furthermore, as shown in Scheme 7-2, two compounds were prepared, which are *N,N*-diethyl-4-propanoyloxylcinnamoylcarboxamide as the monomer model (20) and 1,3-bis-(3-(p-(*N,N*-diethylcinnamoylcarboxamide)-oxy)-propoxy)benzene as the dimer model (21), for the studies on photochemistry in solutions.
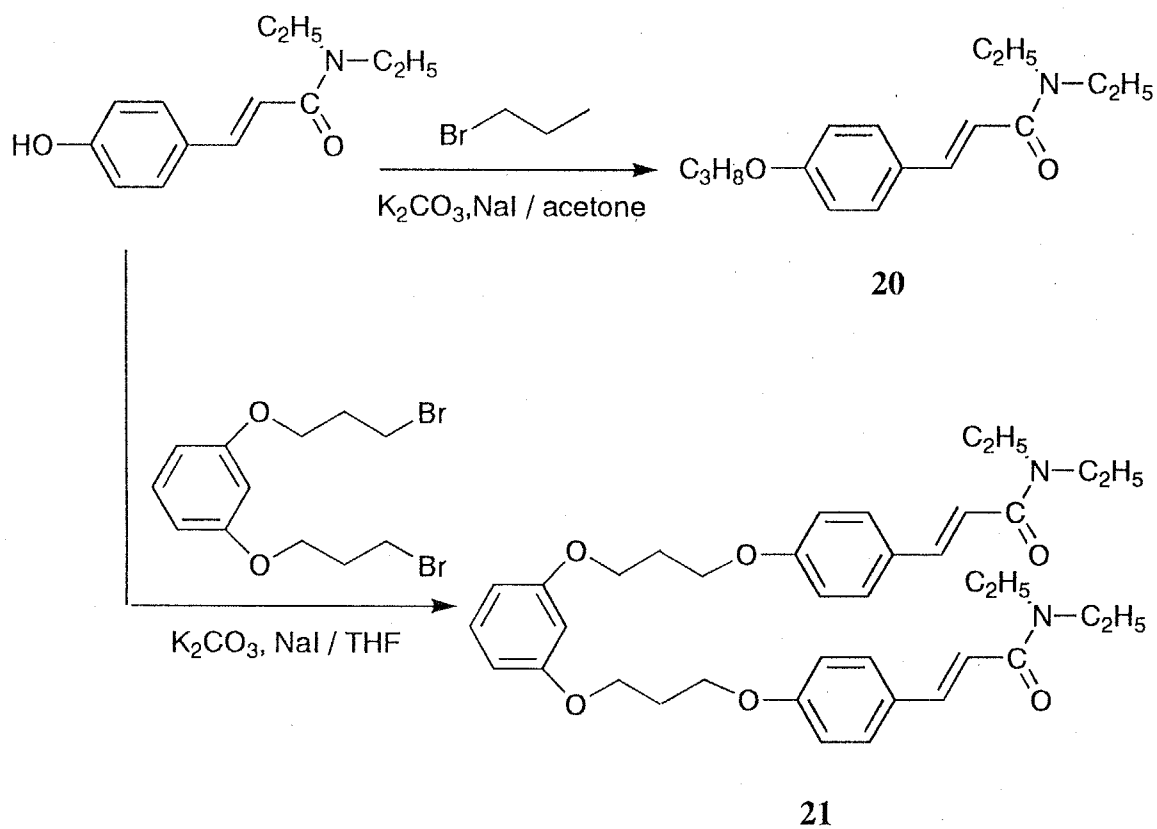
N,N-diethyl-4-hydroxycinnamoylamide

4-Acetoxylcinnamic acid (1.59 g, 7.70 mmol) was treated with 2 ml of thionyl chloride in 4 ml of benzene to give the corresponding acid chloride, which was reacted with diethylamine (1.73 g, 2.37 mmol) in benzene to produce *N,N*-diethyl-4-acetyloxycinnamoylamide. The product was purified by column chromatography on silica gel using ethyl acetate as an eluent to give a pale brown oil in a 48.6 % yields. An NMR spectrum supported the *E*-configuration.

^{1}H-NMR(in CDCl$_3$) :

COOH

CH_3CO—O— ...

1. $SOCl_2$ / benzene
2. $(C_2H_5)_2NH$

C_2H_5
N—C_2H_5
C
CH_3CO—O—
O

1. KOH / methanol

2. HCl aq

C_2H_5
N—C_2H_5
C
O
HO—

I

$OCH_2COOC_2H_5$
$CH_2COOC_2H_5$

7

K_2CO_3 / THF

C_2H_5
N—C_2H_5
C
O

$OCH_2COOC_2H_5$
$CH_2COOC_2H_5$

18

C_2H_5
N—C_2H_5
C
O

KOH aq

THF

OCH_2COOH
CH_2COOH

19

Scheme 7-1 Synthesis of **18** and **19** used in chapter 7.

Scheme 7-2 Syntheses of model compounds, **20** and **21**, used in chapter 7.

δ (ppm) = 1.18 (q, 6H, CH₃), 2.28(s, 3H, CH₃CO), 3.45 (q, 4H, NCH₂), 6.75 (d, 1H, J = 15 Hz, COCH=), 7.07 (d, 2H, J = 7 Hz, Ar-H), 7.51 (d, 2H, J = 7 Hz, Ar-H), 7.67 (d, 1H, J = 15 Hz, ArCH=)

Elemental Anal. for $C_{15}H_{19}NO_3$: Calcd. C: 68.95, H: 7.33, N: 5.36%.

Found C: 68.87, H: 7.35, N: 5.19%

N,N-Diethyl-4-acetyloxycinnamoylcarboxamide

N,N-diethyl-4-hydroxycinnamoylcarboxamide (0.97 g, 3.7 mmol) in methanol was treated with potassium hydroxide (1.57 g, 28.0 mmol) for 30 minutes at room temperature, followed by acidification with hydrochloride. After removal of the solvent, the product was extracted with ethyl acetate to give yellowish white crystals, which were purified by recrystallization with a mixture of ethyl acetate and hexane. Yield was 54 %.

mp = 169 - 170 °C

¹H-NMR(CDCl₃)

δ (ppm) = 1.21 (q, 6H, CH₃), 3.47 (q, 4H, NCH₂), 6.65 (d, 1H, J = 15 Hz, COCH=), 6.87 (d, 2H, J = 7 Hz, Ar-H), 7.38 (m, 3H, Ar-H + OH), 7.64 (d, 1H, J = 15 Hz, ArCH=)

Elemental Anal. for $C_{13}H_{17}NO_2$: Calcd. C: 71.21, H: 7.81, N: 6.38%.

Found C: 71.10, H: 7.75, N: 6.27%.

2,8,14,20-Tetra(3-(4-(N,N-diethylcinnamoylcarboxamide)-oxy)-propyl)-4,6,10,12,16,18,22,24-octa(carboxymetoxy)calix[4]resorcinarene (18)

N,N-Diethyl-4-hydroxy-cinnamoylcarboxamide (0.27 g, 1.2 mmol) and potassium carbonate (0.18 g, 1.3 mmol) were added to 15 ml of THF solution containing 7 (0.41 g, 0.22 mmol). The solution was stirred for 24 hours at room temperature. After the solvent was evaporated, the solution was diluted with ethyl acetate washed with water. CRA with four cinnamoyl residues and eight ethoxycarbonylmethoxyl residues (18) as a brown sticky oil was obtained in a 71 % yield.

¹H-NMR(in CDCl₃) :

δ (ppm) = 1.28 (m, 48H, CH₃), 1.98~2.19 (m, 32H, CH₂CH₂CH), 3.47 (m, 16H, NCH₂), 3.99 (t, 32H, ArOCH₂), 4.25 (m, 32H, OCH₂CO + COOCH₂),

4.73 (t, 4H, CH), 6.23 (s, 4H, Ar-H), 6.63 (d, 4H, J = 16 Hz, COCH=),
6.72 (s, 4H, Ar-H), 6.79 (d, 8H, J = 8 Hz, Ar-H), 7.36 (d, 8H, J = 8 Hz,
Ar-H), 7.62 (d, 4H, J = 16 Hz, Ar-CH=)

Elemental Anal. for $C_{124}H_{156}N_4O_{32}$:   Calcd. C: 67.25, H: 7.10, N: 2.53%.

Found C: 66.97, H: 7.16, N: 2.31%

2,8,14,20-Tetra(3-(4-(N,N-diethylcinnamoylcarboxamide)-oxy)-propyl)-4,6,10,12,16,18,22,24-octacarboxycalix[4]resorcinarene (19)

A potassium hydroxide aqueous solution (0.45 g (8.0 mmol) / 20 ml) was added to 50 ml THF solution of **18** (0.46 g, 0.21 mmol), and the mixture was stirred for 1 hour at room temperature, followed by acidification with hydrochloride to give a white precipitate in a 56% yield.

mp = 153-154 °C

^{1}H-NMR(in DMSO-d_6) :

δ (ppm) = 1.09 (m, 24H, CH₃), 1.69~1.9 (m, 16H, CH₂CH₂CH), 3.47 (m, 16H,
NCH₂), 3.95 (t, 32H, ArOCH₂), 4.20-4.48 (q, 32H, OCH₂CO), 4.63 (t,
4H, CH), 6.43 (s, 4H, Ar-H), 6.70 (s, 4H, Ar-H), 6.80 (d, 8H, J = 8
Hz, Ar-H), 6.87 (d, 4H, J = 16 Hz, COCH=), 7.38 (d, 4H, J = 16 Hz,
Ar-CH=), 7.51 (d, 8H, J = 8 Hz, Ar-H)

Elemental Anal. for $C_{108}H_{124}N_4O_{32}$:   Calcd. C: 65.18, H: 6.28, N: 2.81%.

Found C: 64.89, H: 6.46, N: 2.65%

N,N-Diethyl-4-propanoyloxylcinnamoylcarboxamide (20)

A mixture of 1-bromopropane (4.01g, 30.0 mmol), potassium carbonate (4.14 g, 30.0 mmol), N,N-diethyl-p-hydroxylcinnamoylcarboxamide (4.38 g, 20.0 mmol) and sodium iodide (2.0 g, 1.3 mmol) in 50 ml of acetone was refluxed for 8 hour, followed by the evaporation of the solvent.   The residue was dissolved in ethyl ether, and the solution was washed with water and evaporated to yield a pale brownish oil.

^{1}H-NMR(in CDCl₃) :

δ(ppm) = 1.03 (t, 3H, CH₃CH₂CH₂), 1.21 (m, 6H, CH₃CH₂N), 1.80 (m, 2H,
CH₃CH₂CH₂), 3.48 (m, 4H, NCH₂), 3.92 (t, 2H, OCH₂), 6.70 (d, 1H, J =

153

16 Hz, COCH=), 6.87 (d, 2H, J = 7 Hz, Ar-H), 7.45 (m, 3H, Ar-H +

OH), 7.67 (d, 1H, J = 15 Hz, ArCH=)

Elemental Anal. for $C_{16}H_{23}NO_2$:　Calcd. C: 73.53, H: 8.87, N: 5.36%.

Found C: 73.36, H: 9.09, N: 5.41%

1,3-Bis-(3-(p-(N,N-diethylcinnamoylcarboxamide)-oxy)-propoxy)benzene (21)

A solution of 1.00g of 1,2-bis(3-bromopropyloxy)benzene (2.84 mmol) which was synthesized in chapter 3 and 2.49 g of N,N-diethyl-p-hydroxylcinnamoyl-carboxamide (1.14 mmol) in 50 ml of THF was refluxed for 10 hr in the presence of 1.71 g of potassium carbonate (1.14 mmol) and 1.71 g of sodium iodide (1.14 mmol). The reaction mixture was diluted with ethyl acetate and washed with water. Evaporation of the solvent was followed by silica gel column chromatography using a 6:1(v/v) mixture of ethyl acetate and hexane as an eluent to give crystals in a 28% yield after recrystallization from benzene-hexane.

mp = 116 - 117°C

^{1}H-NMR(in CDCl$_3$) :

δ(ppm) = 1.14 (m, 12H, CH$_3$), 2.19(m, 4H, CH$_2$CH$_2$CH$_2$), 3.40 (q, 8H, NCH$_2$),

4.09 (m, 8H, OCH$_2$), 6.40~6.50 (m, 3H, Ar-H), 6.62 (d, 2H, J = 15 Hz,

COCH=), 6.83 (d, 4H, J = 9 Hz, Ar-H), 7.00~7.30 (m, 1H, Ar-H), 7.40

(d, 4H, J = 9 Hz, Ar-H), 7.60 (d, 2H, J = 15 Hz, ArCH=)

Elemental Anal. for $C_{38}H_{48}N_2O_6$:　Calcd. C: 72.59, H: 7.69, N: 4.45%.

Found C: 72.36, H: 7.66, N: 4.36%

7-2-2. Adsorption experiments

Fused silica plates were washed ultrasonically in a series of solvents in the following order; acetone, water, aqueous KOH solution, water, nitric acid, water, saturated aqueous solution of KHCO$_3$ and finally water. A fused silica plate was immersed in a THF solution of **16** (1-2 × 10^{-4} mol/l) for 10-20 min at room temperature, followed by washing in pure acetone to remove excess amount of **19**. An amount of the cyclic compound adsorbed on the plate was estimated by UV absorption spectroscopy under assumption that no modification of absorption coefficient of the cinnamoyl residue is made by surface

154

adsorption.·

7-2-3. Photochemistry

A spectroirradiator equipped with a diffraction grating and a Xe-lamp, CRM-FA (Jasco), was used for photoirradiation of **18** and model compounds in acetonitrile solutions and **19** on fused silica plates. The bandwidth of light was ± 7 nm. Acetonitrile is convenient for photoreaction study because it is transparent at >190 nm light. Solution photochemistry was followed by taking UV-visible absorption spectra on a diode array spectrometer, HP8452A (Hewlett Packerd) while UV-visible absorption spectra of surface-modified quartz plates were resorted on HITACHI UV-320.

7-2-4. Fabrication of liquid crystal cells

A fused silica plate adsorbing **19** was exposed to light in a range from 290 nm to 390 nm from a super-high pressure mercury arc (USH-500D, Ushio electronics, 1.5 mW/cm^2 at 365 nm) passed through a glass filter (UV-D35; Toshiba) and a photomask. Subsequently, a liquid crystal cell was prepared by sandwiching 4-cyano-4'-pentylbiphenyl (T_{NI} = 35.4 °C) as a nematic liquid crystal between the photoirradiated quartz plate and a quartz plate which was treated with lecithin for homeotropic alignment. Birefringent photoimages recorded in the cell were observed with a polarized microscope, OLYMPUS BH-2.

7-3. Results and discussions

7-3-1. Molecular design and synthesis

It is well-known that photoirradiation of cinnamic acid and its derivatives in solid states results in (2+2) cycloaddition which provides a convenient way to link two molecules through a covalent bond. It followed that a molecular design has been made to tether cinnamoyl groups to the methylene bridges of CRA moiety with eight carboxymethoxy groups (CRA-CM). Since alkaline hydrolysis is involved in the synthesis of CRA-CM through the corresponding octaester derivative, cinnamoylamide was employed here owing

to the resistance to alkaline media. When compared to cinnamic acids and cinnamates, little work has been done on the photodimerzation of cinnamoylamides.[8,9] As described in chapter 3, a crown conformer of a CRA substituted with four 3-iodopropyl residues at the lower rim and eight ethoxycarbonylmethoxy residues at the upper rim (7) is a convenient intermediate to introduce four photofunctional groups to the cyclic skeleton through the Williamson reaction.[4] In this way, 7 was treated with N,N-diethyl-(4-hydroxycinnamoylamide) to give 18 which was subjected to alkaline hydrolysis to yield the desired product (19). For the comparison with solution photochemistry, both of a monomer model compound (20) and a dimer model compound (21) were also synthesized. 20 has one cinnamoylamide unit with propoxy group, whereas 21 has two cinnamoylamide moieties, which are linked at the m-position of benzene ring through five chain atoms in order to resemble the partial structure of 19.

7-3-2. Solution photochemistry

It is known that cinnamoylamide isomerizes reversibly between E-isomer and Z-isomer under photoirradiation and displays no thermal isomerization.[10] This was confirmed as shown in Figure 7-1 (a). UV-irradiation of an acetonitrile solution of the model compounds 20 with 330 nm light, which was longer shoulder wavelength of E-isomer but was not absorption band of Z-isomer, induced spectral changes accompanied by the appearance of an isosbestic point at 274 nm and the blue shift of λmax from 282 nm to 268 nm due to E-to-Z photoisomerization. Exposure of the irradiated solution to 259 nm light, which is the wavelength of largest different absorbance between Z-isomer and E-isomer, recovered the spectrum due to E-isomer, holding the isosbestic point, as shown in Figure 7-1(b). 20 also showed E-to-Z photoisomerized by 300 nm, which was λmax of E-isomer. An acetonitrile solution of 6×10^{-3} mol/l of 20 was irradiated with 330 nm light for 1 hr to give a photostationary state. The solvent was removed under reduced pressure, and a residual product was subjected to ^{1}H-NMR spectrum measurement to elucidate the product distribution. ^{1}H-NMR measurement revealed that the product is assigned to be Z-isomer having doublet peaks of olefinic protons at 5.93 and 6.52 ppm ($J = 12$ Hz) while doublet peaks due to E-isomer olefinic protons appear at 6.70 and 7.67 ppm ($J = 16$ Hz). It should be stressed that chemical shifts of N-ethyl protons are quite different between E-
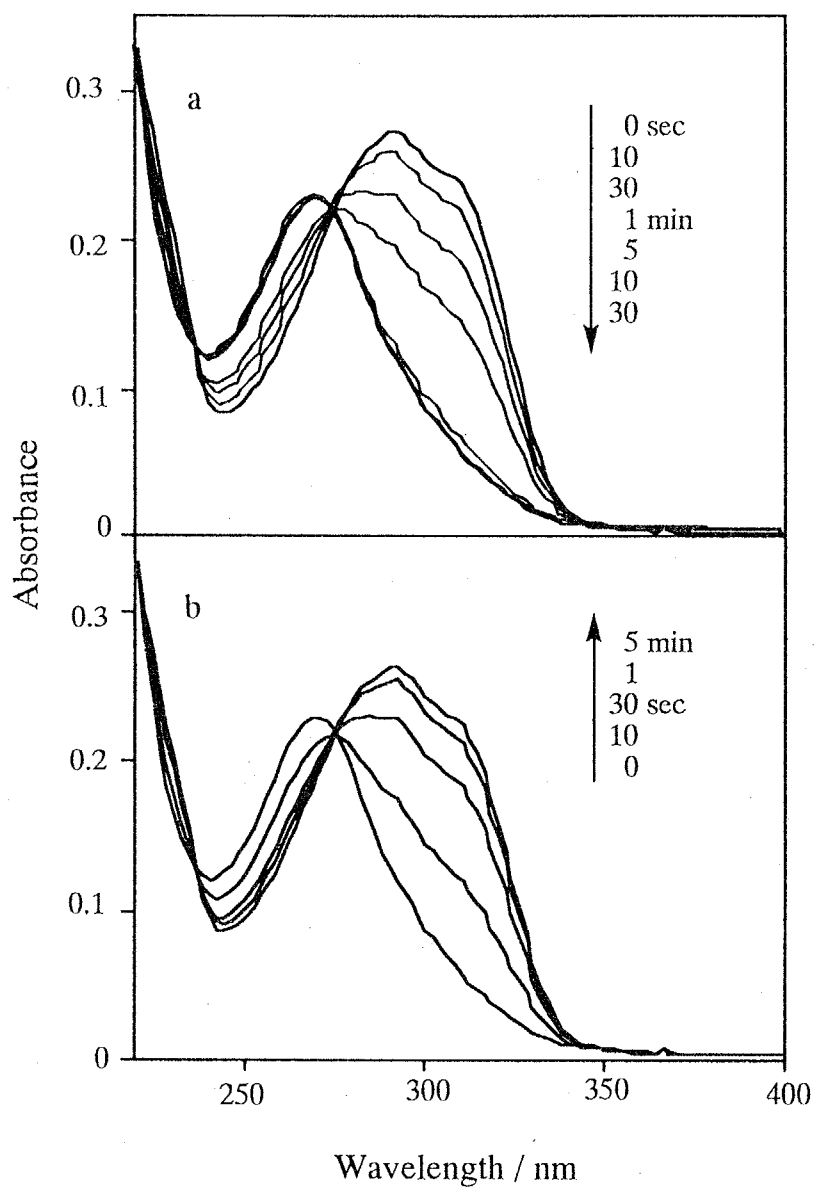
Figure 7-1. UV-visible spectral changes of **4** in acetonitrile (a) under 330 nm photoirradiation and (b) under 259 nm photoirradiation after 330 nm irradiation to give a photostationary state.

and Z-isomers. Broad peaks due to the methylene protons of E-isomer centered at 3.5 ppm is changed into two quartets at 3.29 and 3.58 ppm for Z-isomer whereas a broad peak at 1.2 ppm for six protons of E-isomer is converted into two triplet peaks at 0.99 and 1.18 ppm for Z-isomer. The environment of two ethyl groups are equivalent in E-isomer because of the easy rotation around the CO-N bond. On the other hand, two ethyl groups are not equivalent to each other for Z-isomer, since the rotation around the CO-N bond is suppressed because of a steric hindrance. These facts imply that E-isomer is s-cis while Z-isomer is s-trans. A predominant product at the photostationary state under 259 nm irradiation of **20** was identified as E-isomer by ^{1}H-NMR analysis.

Photochemical behavior of the dimer model (**21**) was slightly different from that of **20**. Irradiation of **21** in acetonitrile with 300 nm or 330 nm light brought about spectral changes quite similar to those of **20** due to exclusive E-to-Z photoisomerization to form a mixture of E- and Z-isomers. On the other hand, irradiation with 259 nm light resulted in the decrease in the absorbance at a shorter wavelength region without change in λmax at 292 nm as shown in Figure 7-2. We achieved ED-diagram analysis of the spectral changes to reveal whether any side reaction was involved upon 259 nm irradiation. ED-diagrams consist of plots of absorbance changes at arbitrary wavelengths toward those at a basis wavelength so that their linearity indicates the involvement of a single chemical reaction.[11] An ED-diagram for 259 nm irradiation shown in Figure 7-3 deviated from linearity, implying the occurrence of side reaction(s). The structural elucidation of a photoproduct other than the geometrical isomers was unsuccessful because of its minute formation, while it was anticipated that intramolecular cycloadduct(s) is formed. The photoproducts of **21** after prolonged irradiation with 259 nm light in the dilute acetonitrile solution were corrected by evaporation of solvent to identify the product(s). According to ^{1}H-NMR measurements, though it was defined that 10 % of total peak integration of double bonds reduced aside that 15% of E-isomer isomerized into Z-isomer, no new peak of evidence of photocycloaddition was appeared. These results suggest that intramolecular photocycloaddition takes place for **21** under irradiation with 259 nm light, whereas essentially no photocycloadduct is formed under irradiation with light at the longer wavelengths.

The photochemistry of **18** in a dilute acetonitrile solution consisted solely of E/Z
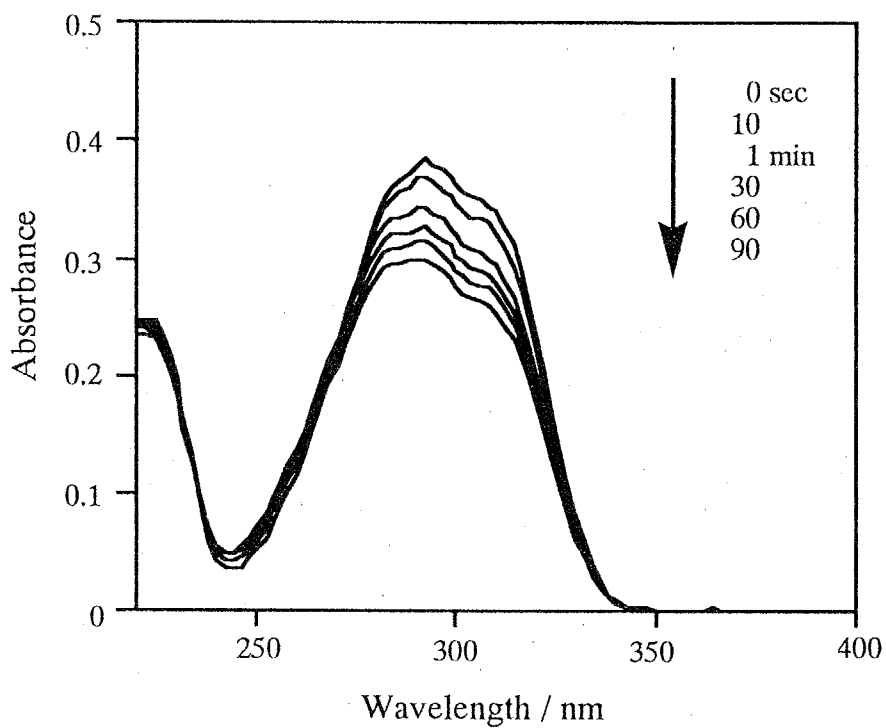
Figure 7-2 UV-vis spectra of **21** solution under 259 nm photoirradiation.
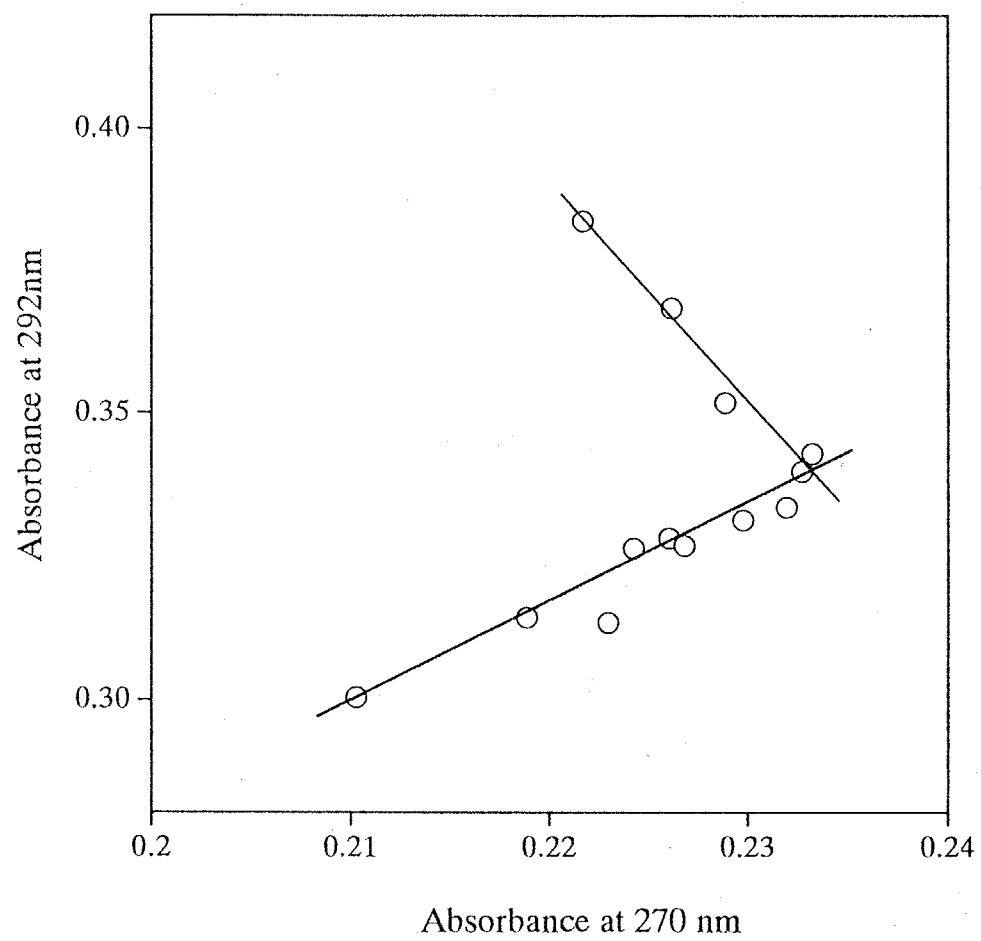
Figure 7-3 E-D diagram of **21** reacted under 259 nm light irradiation.

isomerization upon irradiation with 330 nm light, as demonstrated by the presence of an isosbestic point in spectral changes and the linearity of their ED-diagram. On the other hand, prolonged irradiation of the solution with 300 nm light induced side reaction(s), whose spectral change was shown in Figure 7-4, as confirmed by the deviation from the linearity of a ED-diagram, suggesting the occurrence of photocycloaddition. ^{1}H-NMR analysis of photoproducts showed that the intensity of olefinic protons due to the sum of *E*- and *Z*-isomers is reduced, suggesting the intramolecular cycloaddition of the cinnamoyl group.[8] Three signals appeared at 4.59 ppm, 6.13 ppm and 6.28 ppm, but their assignment failed, because peaks to be observed at 4.27 and 4.43 ppm due to cyclobutane rings derived from cinnamoyl amides[10] were not detected because of the strong peaks at 3.8 - 4.4 ppm due to OCH_2 and $COOCH_2$ of **18**. In a way similar to 300 nm light irradiation, irradiation with 259 nm light resulted in the decrease of absorbance at > 250 nm region of *E*-type **18**, that was also similar as the case of dimer model (**21**) but the decreasing rate of the chromophore absorbance was larger.

7-3-3. Adsorption on a fused silica plate

A fused silica plate was immersed in a solution of **19** in THF for 5 min to perform surface adsorption of the macrocyclic compound. The amount of **19** adsorbed on the plate surface was estimated by an absorbance due to the cinnamoylamide An occupied area was calculated to be 2.0 nm²/molecule under the assumption that the molecular coefficient (ε) of **18** is not much altered. Note that the area is slightly larger than the base area of CRA-CM derivative (1.8 nm²/molecule) which is estimated by a molecular model and π-A isotherms measurements,[6] indicating that **19** forms a densely packed SAM though the molecule possesses the complicated chemical structure.

7-3-4. Photoreaction on a fused silica plate

UV-visible absorption spectral changes of **19** adsorbed on the silica plate under irradiation with 300 nm light are shown in Figure 7-5. The appearance of isosbestic points at the early stage within 30 sec implies the predominant occurrence E-to-Z photoisomerization. In contrast to the solution photochemistry of **18**, prolonged irradiation resulted in the gradual disappearance of the absorption band centered at about
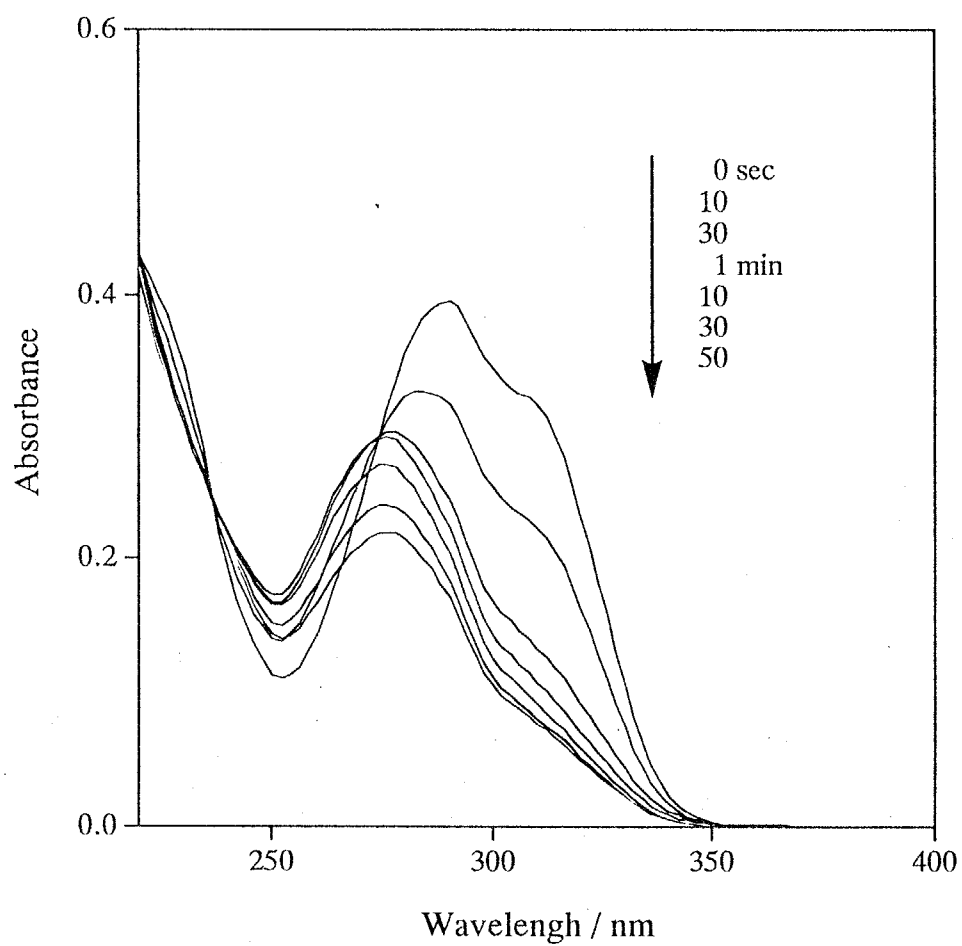
Figure 7-4 . UV-visible specrta of **18** in acetonitrile under 300 nm
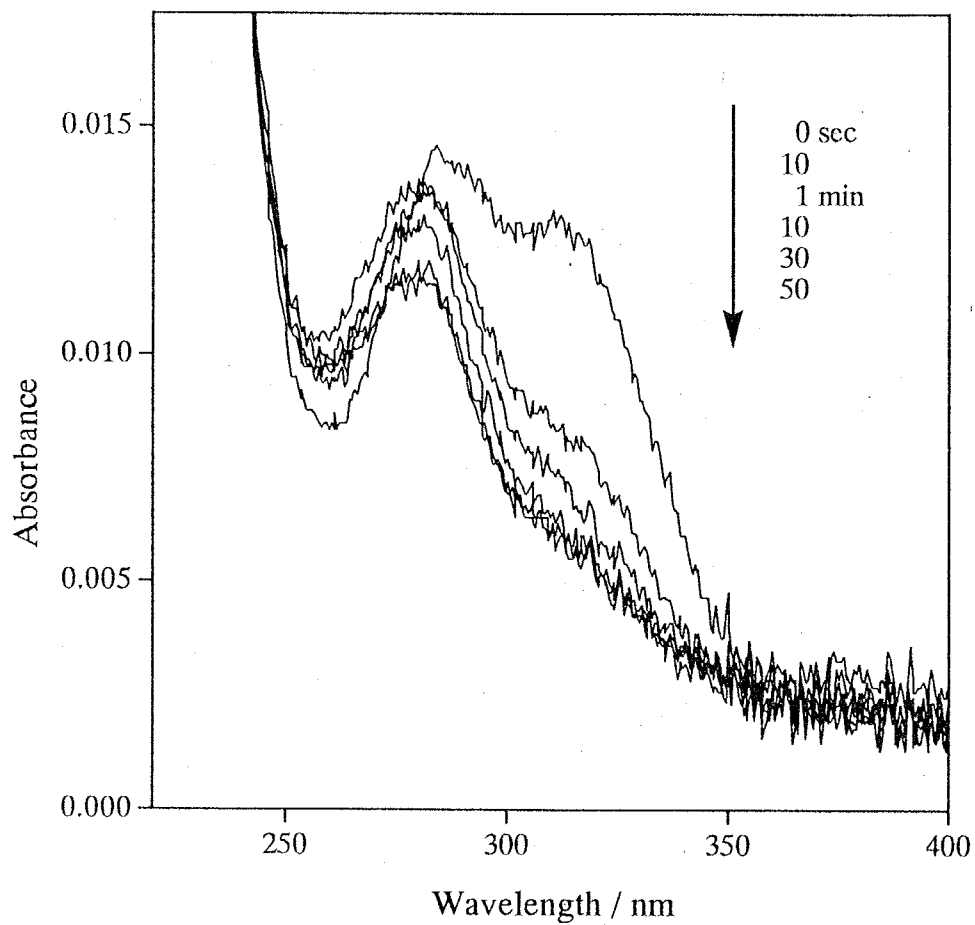
photoirradiation .

Figure 7-5 Absorption spectra of **19** adsorbed on a fused silica plate under 300 nm light irradiation.

300 nm due to Z-isomer, suggesting that the chromophores suffer from photodimerization. Irradiation with 330 nm light caused also the gradual disappearance of the band, though the rate was much slower when compared with the 300 nm irradiation. This is probably because the photodimerization proceeds more efficiently upon excitation with 300 nm light. The involvement of the two photoreactions, photoisomerization and photodimerization, was confirmed by ED-diagram analysis of the spectral changes. This situation is supported also by the fact that spectral changes of the monolayer are quite similar to those of **18** in solution shown in Figure 7-4 It is reasonable to assume that the photo cycloaddition occurs in the SAM not only intramolecularly, but also intermolecularly on account of the dense packing of the macrocyclic compound.

7-3-5. Desorption from a fused silica plate

Desorption of **19** from silica plates before and after photoirradiation was followed by monitoring absorbances at λmax of the cinnamoyl after rinsing silica plates in ethanol ultrasonically. Figure 7-6 shows spectral alterations of the plates exposed to 300 nm light before and after rinsing with ethanol as a function of exposure period. The results show essentially no change in spectral shapes before and ultrasonical treatment in ethanol, suggesting that the chemical structure is not much different between adsorbed and desorbed molecules. Desorption behavior of **19** was also examined after irradiation with light at 259 nm and 330 nm, respectively. Table 7-1 summarizes fractions of desorbed of **19** under various irradiation conditions. The fact that 67 % of **19** is not desorbed even after the rinsing in ethanol arises from the multi-site adsorptivity of the CRA-CM compounds, as discussed in our previous paper. No effect of photoirradiation on enhanced desorption resistance was observed by photoirradiation for 1 min, irrespective of excitation wavelengths. Note here that, as seen in Figure 7-6, the irradiation for 1 min results in marked reduction of the absorption band of E-isomer owing to photoisomerization and gives rise to no significant decrease of absorbances at about 270 nm due to Z-isomer. These facts imply that the desorption is not influenced by the isomerism of the cinnamoyl group of **19** because the adsorptivity is determined specifically by the carboxyl residues as polar heads. Consequently, the photoirradiation for 1 min does not display any suppressive effect on the desorption. When surface-modified plates were exposed to 259
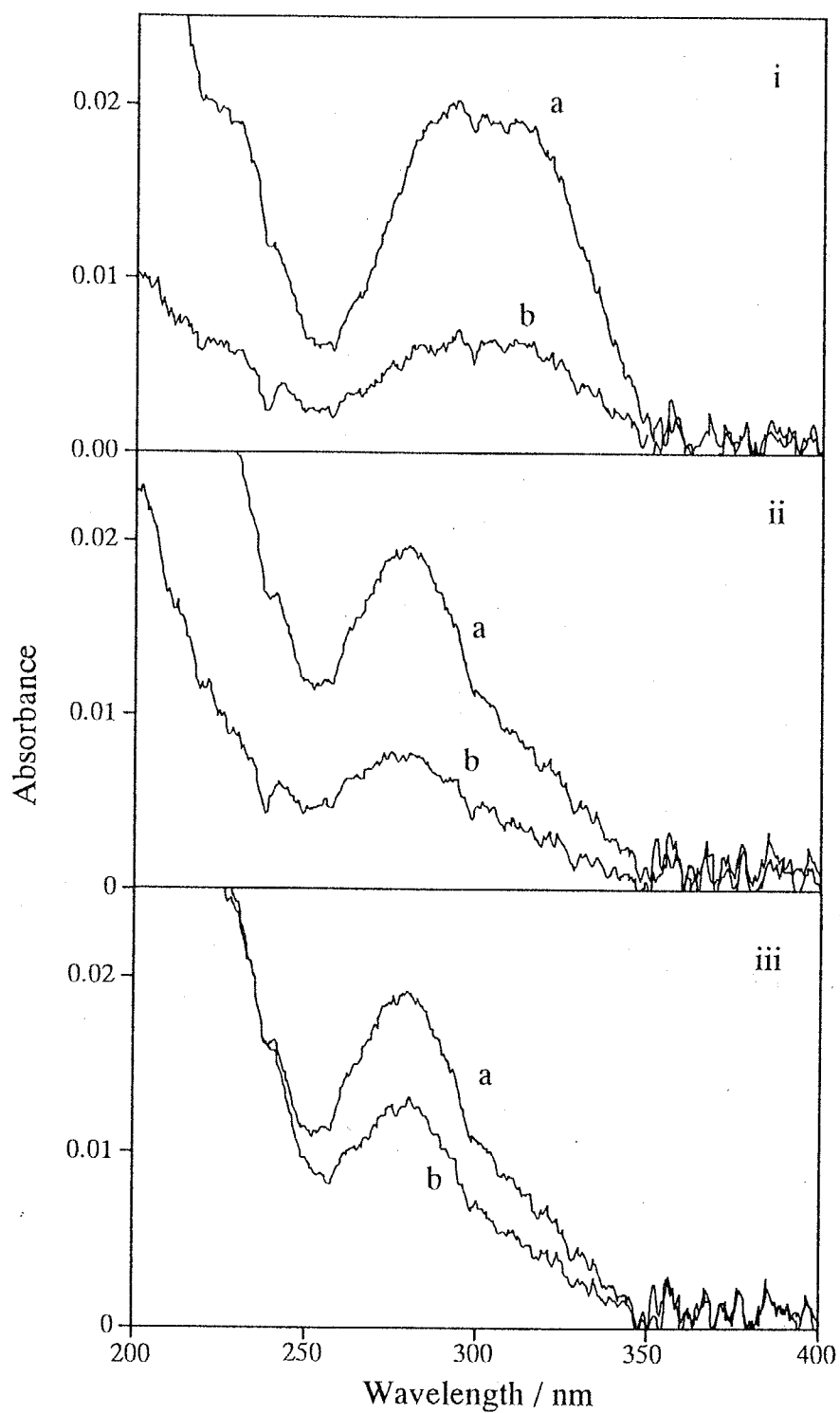
164

Figure 7-6. UV-visible spectra of a fused silica plate adsorbing **19**, which was irradiated with 300 nm light for (i) 0 min, (ii) 1 min and (iii) 30 min (a) before and (b) after ultrasonic treatment in ethanol.

Table 7-1. The level of desorption of **19** in ethanol

λirr	irradiation time / min		
	0	1	30
	67 %		
259 nm		59 %	17 %
300		66 %	19 %
330		75 %	55 %

nm or 300 nm light for 30 min, the desorption was sufficiently suppressed, whereas prolonged irradiation with 330 nm light exhibited a scarce effect on the desorption resistance. As stated above, 330 nm excitation leads hardly photodimerization, which occurs efficiently when irradiation is made at shorter wavelengths of 259 nm and 300 nm, respectively. These results indicate that the desorption resistance comes from the intermolecular photodimerization of the cinnamoyl residues to enhance molecular weights of adsorbed molecules so that the number of adsorption sites increases significantly. The possibility that the enhanced desorption resistance arises from intramolecular photocycloaddition of the double bonds may not be accepted because of the following results. A dilute THF solution of **19** was exposed to 300 nm light for 30 min in advance for intramolecular photodimerization, followed by the adsorption experiments to prepare a silica plate modified with the macrocyclic compound. As shown in Figure 7-7, an absorption spectrum of the plate is quite similar to that of **19**, which was irradiated in the SAM (Figure 7-6(iii)), The immersion of the plate in ethanol resulted in the desorption of 68 % of the adsorbed molecules, suggesting that the intramolecular photodimerization plays no role in the enhancement of desorption resistance.

7-3-6. Photocontrol of liquid crystal alignment

Extensive studies have been carried out on command surfaces, which display the photocontrol of alignment of liquid crystal (LC) systems. It has been already reported that SAMs fabricated by the surface adsorption of photoreactive molecules such as azobenzenes on silica plates through hydrogen bonds are capable of controlling LC alignment by photoirradiation.[12-14] Although the SAM preparation by means of hydrogen bonding is convenient due to the simple preparative procedures, the photoreactive monolayers deposited on substrate plates through non-covalent bonds are of insufficient reliability from practical viewpoints because of partial desorption of the photoreactive molecules, which act as contaminants. Cinnamate moieties have been employed as photoreactive units for the photocontrol of LC alignment so that they have been attached to polymer backbones to prepare thin polymeric films and tethered to a silica substrate surface through silylation. In this context, the macrocyclic compound **19** is of very interest, since photoirradiation plays dual roles in the LC photoalignment control due to the photoreactions and the
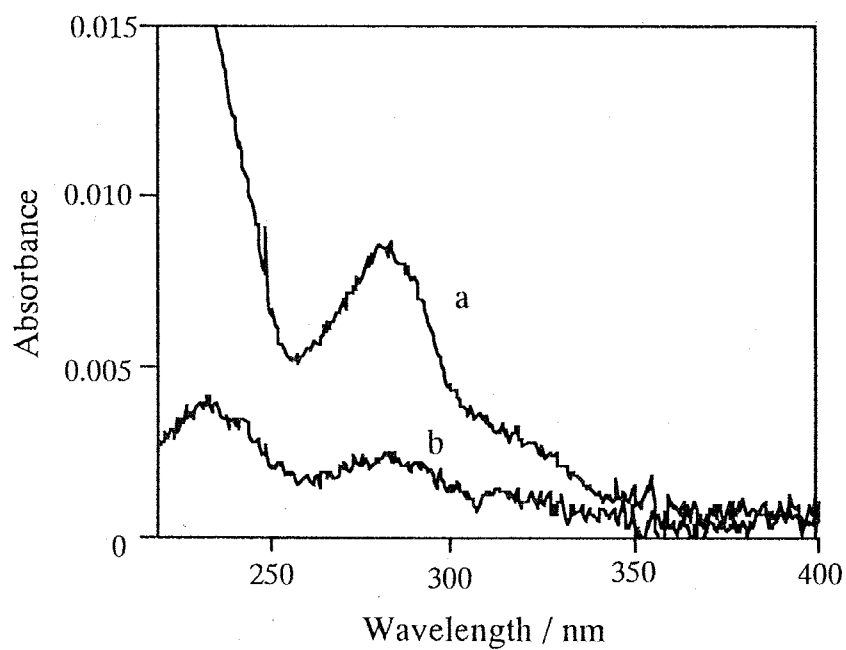
Figure 7-7. UV-visible spectra of a fused silica plate adsorbing 1, which was irradiated with 300 nm light in a dilute THF solution in advance (a) before and (b) after ultrasonic treatment in ethanol.

enhanced desorption resistance of the SAMs, which are readily prepared, as shown above. This situation led us to achieve the photoalignment control of LC by photoirradiated SAM of **19**.

Cell fabrication was made by employing a silica plate adsorbing **19** and a silica plate surface-modified with lecithin for homeotropic LC alignment. Before UV irradiation, the hybrid cell exhibited random planer alignment, indicating that the SAM of **19** induces planer alignment. When the cell was exposed to 290 -390 nm light from a super-high pressure mercury arc through a photomask for 20 min, LC alignment in photoirradiated areas became homeotropic. A polarized microscope demonstrated photopatterning as given in Figure 7-8. The photopattern was not altered at all even after heating the cell at 60 °C above the transition temperature of the LC for 2 hours. The thermostability arises not only from the photodimerization leading to the suppressive effect on orientational relaxation,[15] but also from the desorption resistance.
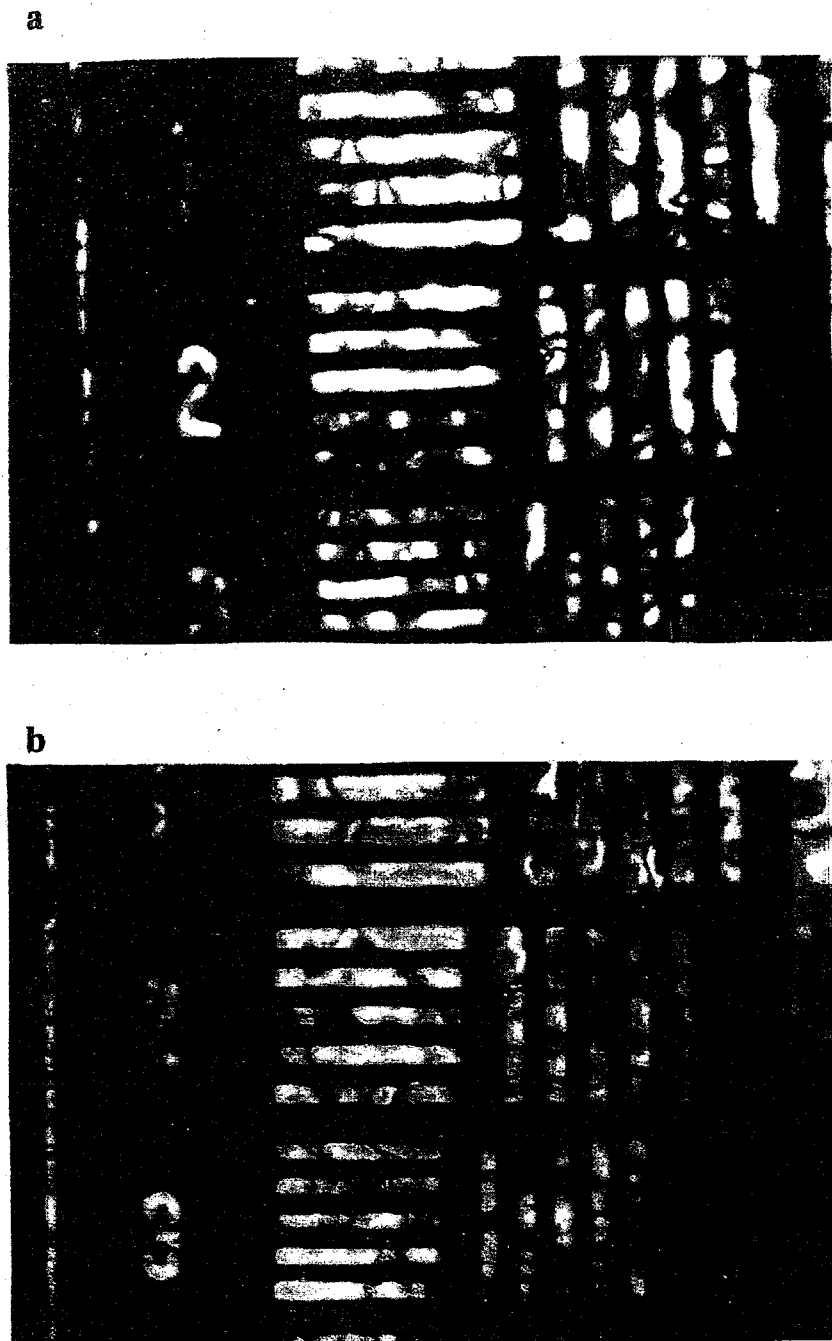
Figure 7-8 Polarized micrographs of a nematic liquid crystal cell with 19 adsorbed
fused silica plate which photoirradiated through a photomask; before heat treatment
(a) and after heating at 60 °C for 2 hours (b)

7-4. Conclusions

The cinnamoyl derivative (20) as a monomer model compound exhibits solely E/Z photoisomerization in solution in excitation wavelength range from 259 nm through 330 nm. In contrast to this, the photochemistry of a dimer model compound (21) and the octaester of 19 (18) in dilute solutions displayed marked wavelength dependence. 21 undergoes not only the photoisomerization, but also intramolecular photodimerization when irradiation of its dilute solution was made at 259 nm, whereas photodimerization occurred hardly upon irradiation with light at 300 nm and 330 nm. The octaester of 19 (18) in a dilute solution suffered also from the photoisomerization accompanied by a side reaction, which may intramolecular photodimerization, when irradiation was performed with light of a wavelength region of 259 - 300 nm and the excitation with 330 nm light caused essentially only the photoisomerization.

SAM of 19 with a relatively dense packing was fabricated simply by immersing a fused silica plate in a dilute solution of 19. In contrast to the photochemistry of 18 in dilute solution, irradiation of the SAM of 19 with light not only in the range of 259 nm - 300 nm, but also at 330 nm resulted in the concurrence of a side reaction, which is likely to be intra- and intermolecular photodimerization. The desorption behavior of the SAM from the silica plate was examined before and after photoirradiation to reveal that the desorption resistance is markedly enhanced by photoirradiation because of the intermolecular photodimerization of the cinnamoyl units to increase molecular weights of the adsorbate. The effect of intermolecular photodimerization on the enhancement of desorption resistance was confirmed by the facts that no enhancement of desorption resistance was obtained when the SAM preparation was achieved after photoirradiation of a dilute solution of 19 to cause intramolecular photodimerization along with photoisomerization.

The present procedure for the preparation of SAMs having the photodimerizable units was applied to photocontrol of LC alignment. Photoirradiation resulted in transformation of LC alignment from homeotropic into planar orientation, and the LC photoalignment exhibited reasonable thermostability probably due to the photoisomerization leading to the desorption resistance.

References

1. M. Ueda, N. Fukushima and K. Ichimura, *J. Mater. Chem.*, 1995, **5**, 1007.

2. M. Ueda, N. Fukushima and K. Ichimura, *J. Mater. Chem.*, 1997, **7**, 641.

3. E. Kurita, N. Fukushima, M. Fujimaki, Y. Matsuzawa, K. Kudo and K. Ichimura, *J. Mater. Chem.*, 1998, **8**, 397.

4. K. Ichimura, N. Fukushima, M. Fujimaki, S. Kawahara, Y. Matsuzawa, Y. Hayashi and K. Kudo, *Langmuir*, 1997, **13**, 6780.

5. S.-K. Oh, M. Nakagawa and K. Ichimura, *Chem. Lett.*, 1999, 349.

6. G. J. Fleer and J. Lyklema, *"Adsorption from Solution at the Solid/Liquid Interface"*, ed. G. D. Parfitt and C. H. Rochester, Academic Press, New York, 1983

7. E. Lindner and C. A. Dooley, *Proc. Int. Biodegradation Symp. 3rd,* 1976, 465.

8. S. Akabori, T. Kumagai, Y. Habana and S. Satou, *J. Chem. Sci. Perkin Trans. 1*, 1989, 1497.

9. L. Leiserowitz and G. M. Schmidt, *J. Chem. Sci. A*, 1969, 2372.

10. F. D. Lewis, J. E. Elbert, A. L. Upthagrove and P. Hale, *J. Org. Chem.* 1991, **56**, 553.

11. G. Gauglitz, *"Studies in organic chemistry 40: Photochromism, Molecules and Systems"*, ed. H. Dürr and H. Bouas-Laurent, Elsevier, Amsterdam 1990

12. K. Ichimura, "Photochromic polymers, Polymers as electrooptical and photooptical active media" ed. by V. Shibaev, Springer-Verlag, 1996, 138.

13. K. Ichimura, Y. Suzuki, T. Seki, A. Hosoki and K. Aoki, *Langmuir,* 1988, **4**, 1214.

14. Y. Kawanishi, T. Tamaki, M. Sakuragi, T. Seki and K. Ichimura, *Langmuir*, 1992, **8**, 2061.

15. K. Ichimura, Y. Akita, H. Akiyama, Y. Hayashi and K. Kudo, *Jpn. J. Appl. Phys., Part 2*, 1996, **35**, L992.

Chapter 8

Summary

The major purpose of this thesis is to present novel approaches to elucidate microenvironments and molecular interactions at interfaces between a solid and a fluid or between two kinds of solids using fluorescent probes. Silica is used as a solid, the surface of which is modified with fluorescent probe molecules. The surface modification of silica is performed by the chemisorption with silylating reagents bearing fluorescent moieties and the adsorption of calix[4]resorcinarene derivatives (CRA) substituted with fluorescent units through hydrogen bonding.

A silylating reagent having a cyanobiphenyl (CB) unit was chosen as a fluorescent probe to provide a model for a solid/liquid crystal interface, taking notice of the characteristics of CB, which is a mesogenic core and emits strong monomer and excimer fluorescence sensitive to environmental polarity. Fluorescence behavior of CB chemisorbed on a silica plate was markedly altered by the contact with a fluid layer to give information about microenvironmental conditions at an interface between a silica plate and a fluid layer. A significant red shift of the fluorescence maximum of the CB was generated at a silica/air interface when compared with that in solution. This reflects the high polarity of a silica surface. The red shift was reduced by the contact with cyclohexane, suggesting interactions of the surface CB with less polar solvent molecules, whereas the reduction of the red shift occurred more significantly upon contact with a nematic liquid crystal with a polarity similar to cyclohexane. These results imply the involvement of specific interactions of the CB with liquid crystal molecules owing to the mesogenic nature of the CB. This situation is also supported by the observation that excimer emission of the CB on a silica plate at a longer wavelength region disappears completely to give monomer emission upon contact with the liquid crystal. The fluorescence of the CB in the presence of the liquid crystal was not altered at elevated temperatures resulting in isotropic phase of the liquid crystal, suggesting molecular interactions at the interface is not influenced by the phase change of a bulk liquid crystal.

It was also revealed by fluorescence measurements that the structure of spacers tethering CB to a silica surface affects prominently molecular interactions between the CB and fluid molecules by comparing the ways for surface modification involving the silylation and the adsorption of calix[4]resorcinarene bearing CB units (CRA-CB). A plate modified with CRA-CM exhibited a markedly low fluorescent intensity and a blue shift in the air when compared with a plate CB-modified by the silylation. The results arise from a difference in the rigidity of the spacer chains. Owing to the restricted conformation of the CB attached through the rigid CRA framework, CB units are stretched out from the silica surface, whereas the CB units attached by the silylation are rather closely packed and lie on a polar silica surface because of the flexibility of the spacer chain. The fluorescence intensity of the CB-CRA was partially enhanced by the contact with cyclohexane and a less polar nematic liquid crystal, suggesting specific interactions of the CB units on the surfaces with fluid molecules. Fluorescence spectra of the CB were also influenced by the attachment methods of the fluorescent probe, indicating that excimer formation occurs hardly on a CB-CRA plate. This is due to the fact that the CB moiety adsorbed through the CRA orients perpendicularly to the silica surface, in particular, in the presence of a less polar solvent or a liquid crystal, showing again the dilution effect of these fluid molecules at the interface. Specific interactions between the surface CB and a liquid crystal were monitored also by changes of alignment of the liquid crystal after cell assembly; homeotropic alignment was generated immediately on a CB-CRA plate, whereas incomplete homeotropic alignment was observed on a plate modified by the CB-silylation even after a few hours.

It was shown that 9,10-dicyanoanthryl (DCA) unit is an effective fluorescent probe for studies on interfaces because the fluorescence is sensitive to polarity whereas the fluorophore forms an excimer and an exciplex with phenanthrene. DCA units were introduced to a silica surface through silylation to study the interplay with solvent molecules and a polymethacrylate with phenanthryl side chains. Whereas spectral maxima (vmax) of both absorption and fluorescence spectra of a DCA derivative in solution are correlated with the π^* scale expressing solvent polarity in a linear manner, maximum wavelengths (λmax) of both spectra of the DCA on a silica surface were anomalously red-shifted when a DCA-modified plate was immersed in aliphatic

hydrocarbons. These results reveal that a micropolarity around the DCA molecules on a surface is markedly enhanced by residual silanols on a silica surface and water molecules adsorbed on the surface. The samples with residual silanols capped with trimethylsilyl groups were also studied. A blue shift was observed for both excitation and emission spectra of the capped DCA-modified plate, supporting the reduction of micropolarity on the modified silica surface. Furthermore, exciplex emission was observed at an interface between a DCA-modified plate and a solution containing phenanthrene or the polymer having phenanthryl side chains. The fluorescence maximum of the exciplex was also sensitive to the micro polarity on silica surfaces.

Aiming at preparing novel fluorescent probe molecules, a mixture of five species of calix[4]resorcinarene possessing variant numbers of pyrenyl group was synthesized by the reaction of resorcinol with a mixture of pyrenylpropanal and butanal, followed by acetylation to be subjected to HPLC separation. Intramolecular interactions between the pyrenyl units of the crown conformer of CRAs were investigated. NMR proton peaks of the pyrene were shifted markedly to higher magnetic field by increasing pyrenyl groups because the pyrenyl groups existed at "face-to-face" positions to produce ring current effect even in solution. Fluorescence spectra and decay time data showed that the strain of the excimers are almost the same as that of α, ω-bipyrenyl compounds with tetra- and nanomethylene spacers and that two types of intramolecular excimers exist just as in the case of 1,3-bis-(1-pyrenyl)propane.

Pyrene as a fluorescent probe was linked to a surface of colloidal silica though a calix[4]resorcinarene skeleton to study interfacial interactions with a polymethacrylate with N,N-dimethylaniline side chains, which can form an exciplex with pyrene. The surface-modified colloidal silica covered with the polymer with N,N-dimethylaniline side chains displayed exciplex emission. A broadness of the emission suggests that exciplex species are localized at an interface with various microenvironments altering energy level of the molecules in ground state as well as in excited singlet state. A ratio of excimer to monomer emission of the pyrene gives also novel information about a local density of the fluorophore on silica. Since this system provides a model for the two kinds of solids, annealing effect on the fluorescence of the pyrene on colloidal silica was studied in more detail. On one hand, fluorescence of the samples was influenced more or less by a solvent

175

dissolving the polymer and evaporation conditions of the solvent. On the other hand, heat treatment of the sample above the glass transition temperature of the polymer or prolonged storage at room temperature leads finally to the same fluorescent spectra, irrespective of preparative conditions of the samples. These results indicate that the reorientation of segments of the polymer occurs at the interface to give rise to thermodynamically the most stable state. Consequently, it can be say that monitoring exciplex emission at interfaces provides a effective way to approach to study on interfacial phenomena.

A novel way to enhance the desorption resistance of adsorbed monolayers of CRA derivatives was investigated. A key compound is a CRA with four cinnamoyl units, which was adsorbed on a silica plate to form a self-assembled monolayer with dense packing. The cinnamoyl residues underwent both E/Z isomerization and intramolecular photodimerization in solution. Compared with solution photochemistry of the compounds displaying the photoisomerization as a major photochemical event, UV-irradiation of the self-assembled monolayer resulted in photodimerization. The UV-irradiated monolayer exhibited marked desorption resistance even in a polar solvent, suggesting that intermolecular photodimerization of the cinnamoyl residues takes place to result in stepwise photopolymerization, which enhance the desorption resistance due to an increase in molecular weights of the adsorbed molecules.

List of publications

Relative to the thesis

1. Shigeo Tazuke, Yuko Higuchi, Nobuyuki Tamai, Noboru Kitamura, Naoto Tamai and Iwao Yamazaki, "Formation and relaxation of an excited complex in a polymer", *Macromolecules*, 1986, **19**, 603-606.

2. Kunihiro Ichimura, Yuko Hayashi and Norio Ishizuki, "Photocontrol of in-plane alignment of a nematic liquid crystal by a photochromic spiropyran monolayer absorbing linearly polarized light", *Chem. Lett.*, 1992, 1063-1066.

3. Kunihiro Ichimura, Yuko Hayashi, Yuji Kawanishi, Takahiro Seki, Takashi Tamaki and Norio Ishizuki, "p-Cyanoazobenzene as a command molecule for azimuthal anisotropy regulation of a nematic liquid crystal upon exposure to linearly polarized visible light", *Langmuir*, 1993, **9**, 857-860.

4. Kunihiro Ichimura, Yuko Hayashi, Haruhisa Akiyama, Tomiki Ikeda and Norio Ishizuki, "Photo-optical liquid crystal cells driven by molecular rotors", *Appl. Phys. Lett.*, 1993, **63**, 449-451.

5. Kunihiro Ichimura, Yuko Hayashi, Tomiki Ikeda and Norio Ishizuki, "Regulation of azimuthal anisotropy of nematic liquid crystals by azobenzene monolayers absorbing linearly polarized visible light", *Chem. Funct. Dyes, Proc. Int. Symp., 2nd*, 1993, 359-364.

6. Yuko Hayashi, Yoshihiro Kawada and Kunihiro Ichimura, "Dicyanoanthracene as a fluorescence probe for studies on silica surfaces", *Langmuir*, 1995, **11**, 2077-2082.

7. Yuko Hayashi and Kunihiro Ichimura, "Fluorescence studies on intermolecular interactions of cyanobiphenyl groups chemisorbed on a quartz surface with liquid crystals", *Langmuir*, 1996, **12**, 831-835.

8. Seiji Akimoto, Hideyuki Nishizawa, Tomoko Yamazaki, Iwao Yamazaki, Yuko Hayashi, Masanori Fujimaki and Kunihiro Ichimura, "Excimer formation of cyanobiphenyls in calix[4]resorecinarene derivative probed by picosecond time-resolved fluorescence spectroscopy", *Chem. Phys. Lett.*, 1997, **276**, 405-410.

9. Yuko Hayashi, Tsuyashi Maruyama, Tadayoshi Yachi, Kazuaki Kudo and Kunihiro Ichimura, "Synthesis and fluorescence behavior of calix[4]resorcinarenes possessing pyrenyl group(s)", *Perkin Transaction 2*, 1998, 981-987.

10. Yuko Hayashi, Shintaro Suzuki and Kunihiro Ichimura, "Enhancement of desorption-resistance of adsorbed monolayers of calix[4]resorcinarenes by photocycloaddition" *J. Mater. Chem.* accepted

11. Yuko Hayashi, Masanori Fujimaki and Kunihiro Ichimura, "Comparison of fluorescence behaviors of cyanobiphenyl unit modified on a fused silica plate through calix[4]resorcinarenes or alkylsiliates", submitted

12. Yuko Hayashi and Kunihiro Ichimura, "Exciplex emission between pyrene adsorbed on colloidal silica and dimethylaniline at polymer side chain", submitted

Others

13. Hiroshi Masuhara, Jun A. Tanaka, Noboru Mataga, Yuko Higuchi and Tazuke, Shigeo, "Intrapolymer charge separation induced by picosecond multiphoton excitation: polyesters with pendant 1-pyrenyl groups in DMF", *Chem. Phys. Lett.*, 1986, **125**, 246-250.

14. Tomiki Ikeda, Hiroyuki Mochizuki, Yuko Hayashi, Masahiko Sisido and Tomoyoshi Sasakawa, "Hole transport in liquid-crystalline media. I. Effect of matrices on hole drift mobilities of 1,2-trans-bis(9H-carbazol-9-yl)-cyclobutane doped in polymer liquid crystals", *J. Appl. Phys.*, 1991, **70**, 3689-3695.

15. Tomiki Ikeda, Hiroyuki Mochizuki, Yuko Hayashi, Masahiko Sisido and Tomoyoshi Sasakawa, "Hole transport in liquid crystalline media. II. Hole drift mobilities of copolymers of acrylates with side-chain mesogens and dimeric carbazoles", *J. Appl. Phys.*, 1991, **70**, 3696-3702.

16. Mao Peng Lin, Yuko Hayashi, Tomiki Ikeda and Takeshi Endo, "Photocrosslinking of polymers initiated by benzylsulfonium salts as cationic initiators. Part I. Poly(ethylene-co-glycidyl methacrylate)", J. Mater. Sci., 1992, **27**, 2896-2901.

17. Mao Peng Lin, Yuko Hayashi, Tomiki Ikeda and Takeshi Endo,"Photocrosslinking of polymers initiated by benzylsulfonium salts as cationic initiators. Part II. Poly(1,3-dioxolane-4-methyl methacrylate) and copolymers with methyl methacrylate", *J. Mater. Sci.*, 1992, **27**, 2902-2907.

18. Kunihiro Ichimura, Yuko Hayashi, Kouhei Goto and Norio Ishizuki, "Photocontrol of in-plane alignment of a nematic liquid crystal by a photochromic spiropyran molecular layer", *Thin Solid Films*, 1993, **235**, 101-107.

19. Kunihiro Ichimura, Yuko Hayashi, Haruhisa Akiyama and Norio Ishizuki, "Photoregulation of in-plane reorientation of liquid crystals by azobenzenes laterally attached to substrate surfaces", *Langmuir*, 1993, **9**, 3298-3304.

20. Haruhisa Akiyama, Kazuaki Kudo, Yuko Hayashi and Ichimura, Kunihiro, "Photocontrol of azimuthal orientation of nematic liquid crystals by surface-modified poly(vinyl alcohol) thin films", *J. Photopolym. Sci. Technol.*, 1994, **7**, 129-132.

21. Yasuhiro Akita, Haruhisa Akiyama, Kazuaki Kudo, Yuko Hayashi and Kunihiro Ichimura, "Photoregulation of in-plane alignment of nematic liquid crystals by cinnamate pendant polymer films", *J. Photopolym. Sci. Technol.*, 1995, **8**, 75-78.

22. Suh Dong Hae, Yuko Hayashi, Kazuaki Kudo and Kunihiro Ichimura, "Photosensitive characteristics of poly(methacrylates) containing benzylidenephthalimidine moieties on the side chain", *Mol. Cryst. Liq. Cryst. Sci. Technol., Sect. A*, 1996, **280**, 97-102.

23. Kunihiro Ichimura, Yasuhiro Akita, Haruhisa Akiyama, Yuko Hayashi and Kazuaki Kudo, "Role of E/Z photoisomerization of cinnamate side chains attached to polymer backbones in the alignment photoregulation of nematic liquid crystals", *Jpn. J. Appl. Phys., Part 2*, 1996, **35**, L992-L995.

24. Hironori Ohmori, Koji Arimitsu, Kazuaki Kudo, Yuko Hayashi and Kunihiro Ichimura, "Acid-catalyzed rearrangement for monitoring the migration of acids in polymer films", *J. Photopolym. Sci. Technol.*, 1996, **9**, 25-28.

25. Koji Arimitsu, Kazuaki Kudo, Yuko Hayashi and Kunihiro Ichimura, "Effect of phenolic hydroxyl residues on the improvement of acid-proliferation-type photoimaging materials", *J. Photopolym. Sci. Technol.*, 1996, **9**, 29-30.

26. Yasuhiro Akita, Haruhisa Akiyama, Kazuaki Kudo, Yuko Hayashi and Kunihiro Ichimura, "Relationship between photoreactivity and ability to regulate liquid crystal alignment of polymers with cinnamate side chains", *J. Photopolym. Sci. Technol.*, 1996, **9**, 41-48.

27. Haruhisa Akiyama, Kazuaki Kudo, Yuko Hayashi and Kunihiro Ichimura, "Liquid crystal alignment regulation using photocrosslinkable polymers with azide residues", *J. Photopolym. Sci. Technol.*, 1996, **9**, 49-52.

28. Dong Hae Suh, Kazuaki Kudo, Yuko Hayashi and Ichimura, Kunihiro, "Photopolymers having benzylidenepgthalimide side chain", *J. Photopolym. Sci. Technol.*, 1996, **9**, 53-56.

29. Kunihiro Ichimura, Yasuhiro Akita, Haruhisa Akiyama, Kazuaki; Kudo and Yuko Hayashi, "Photoreactivity of polymers with regioisomeric cinnamate side chains and their ability to regulate liquid crystal alignment", *Macromolecules*, 1997, **30**, 903-911.

30. Takahiro Seki, Hidehiko Sekizawa, Kazuaki Kudo, Yuko Hayashi and Kunihiro Ichimura, "Morphological observation of photoisomerizable monolayers of azobenzene on water surface", *Mol. Cryst. Liq. Creat.*, 1997, **294/295**, 47-50.

31. Kunihiro Ichimura, Noriaki Fukushima, Masanori Fujimaki, Sumie Kawahara, Yoko Matsuzawa, Yuko Hayashi and Kazuaki Kudo, "Macrocyclic amphiphiles 1. Properties of calix[4]resorcinarene derivatives substituted with azobenzenes in solutions and monolayers" *Langmuir*, 1997, **13**, 6780-6783.

32. Masanori Fujimaki, Yoko Matsuzawa, Yuko Hayashi and Kunihiro Ichimura, "Monolayers of calix[4]resorcinarene with azobenzene residues exhibiting efficient photoisomerizability" *Chem. Lett.* 1998 165-166.

33. Dong Hae Suh, Yuko Hayashi and Kunihiro Ichimura, "Polymethacrylates with benzylidenphthalimidine side chains, 1 Photochemical characteristics of model compounds and polymers", *Macromol. Chem. Phys.* 1998 **199**, 363-373.

34. Masanori Fujimaki, Sumie Kawahara, Yoko Matsuzawa, Eiichi Kurita, Yuko Hayashi and Kunihiro Ichimura, "Macrocyclic amphiphiles 3. Monolayers of o-octacarboxymethoxylated calix[4]resorcinarene with azobenzene residuals exhibitung efficient photoisomerizability", *Langmuir*, 1998, **14**, 4495-4498.

35. Kunihiro Ichimura, Shin'ya Morino, Yuko Hayashi and Masaru Nakagawa, "Preparation and photofunctionalization of self-assembled monolayers derived from macrocyclic amphiphiles", *Mol. Superstructure Dye. Creat. Colect. Papers*, 1998, 41.

36. Kunihiro Ichimura, Masanori Fujimaki, Yoko Matsuzawa, Yuko Hayashi and Masaru Nakagawa, "Characteristics of monolayers of calix[4]resorcinarenes derivatives having azobenzene chromophores", *Mater. Sci. Eng.*, 1999, **C8-9**, 353-359.

Acknowledgments